

Optimal Meter Placement in Active Distribution System State Estimation using New Hybrid Multi-Objective Evolutionary Algorithms

Thesis

Submitted in partial fulfillment of the requirements
for the award of the degree of

Doctor of Philosophy

in

Electrical Engineering

By

Bhanu Prasad Chintala

(Roll No. 717115)

Supervisor

Dr. D. M. Vinod Kumar

Professor (HAG)



**Department of Electrical Engineering
National Institute of Technology Warangal
(An Institute of National Importance)**

Warangal-506004, Telangana State, India

December-2021

APPROVAL SHEET

This thesis entitled “Optimal Meter Placement in Active Distribution System State Estimation using New Hybrid Multi-Objective Evolutionary Algorithms” by **Mr. Bhanu Prasad Chintala** is approved for the degree of Doctor of Philosophy in Electrical Engineering

Examiners

Supervisor

Dr. D. M. Vinod Kumar

Professor (HAG)

EED, NIT Warangal

Chairman

Dr. S. Srinivasa Rao

Professor

EED, NIT Warangal

Date: _____

**DEPARTMENT OF ELECTRICAL ENGINEERING
NATIONAL INSTITUTE OF TECHNOLOGY WARANGAL
WARANGAL - 506004**

**DEPARTMENT OF ELECTRICAL ENGINEERING
NATIONAL INSTITUTE OF TECHNOLOGY WARANGAL**



CERTIFICATE

This is to certify that the thesis entitled "**Optimal Meter Placement in Active Distribution System State Estimation using New Hybrid Multi-Objective Evolutionary Algorithms**", which is being submitted by **Mr. Bhanu Prasad Chintala** (Roll No. 717115), is a bonafide work submitted to National Institute of Technology Warangal in partial fulfillment of the requirements for the award of the degree of **Doctor of Philosophy** in Electrical Engineering. To the best of my knowledge, the work incorporated in this thesis has not been submitted elsewhere for the award of any degree.

Date: 20-Decemeber-2021
Place: Warangal



20/12/2021

Dr. D. M. Vinod Kumar
(Thesis Supervisor)
Professor (HAG)

Department of Electrical Engineering
National Institute of Technology Warangal
Warangal - 506004

DECLARATION

This is to certify that the work presented in the thesis entitled "**Optimal Meter Placement in Active Distribution System State Estimation using New Hybrid Multi-Objective Evolutionary Algorithms**", is a bonafide work done by me under the supervision of Dr. D.M. Vinod Kumar, Professor (HAG), Department of Electrical Engineering, National Institute of Technology Warangal, India and was not submitted elsewhere for the award of any degree.

I declare that this written submission represents my ideas in my own words and where others' ideas or words have been included; I have adequately cited and referenced the original sources. I also declare that I have adhered to all principles of academic honesty and integrity and have not misrepresented or fabricated or falsified any idea/date/fact/source in my submission. I understand that any violation of the above will be a cause for disciplinary action by the institute and can also evoke penal action from the sources which have thus not been properly cited or from whom proper permission has not been taken when needed.

Date:20-December-2021
Place: Warangal



Bhanu Prasad Chintala
(Roll No: 717115)

ACKNOWLEDGEMENT

I am glad to express my deep sense of gratitude and thanks to my supervisor **Dr. D. M. Vinod Kumar**, Professor (HAG), Department of Electrical Engineering, National Institute of Technology Warangal, for his continuous support, guidance, and valuable suggestions. I am grateful to him for having faith in me throughout my Ph.D. studies. His knowledge, expertise, and experience helped me to perform extensive research.

I am very much thankful to **Dr. S. Srinivasa Rao**, Chairman of Doctoral Scrutiny Committee, and Professor, Department of Electrical Engineering for his continuous support, encouragement, and suggestions.

I am very much thankful to **Dr. Sailaja Kumari M**, Head, Department of Electrical Engineering for his continuous support, encouragement, and suggestions.

I take this privilege to thank my Doctoral Scrutiny Committee members, **Dr. Chintam Venkaiah**, Associate professor, Department of Electrical Engineering, **Dr. B. L. Narasimharaju**, Associate professor, Department of Electrical Engineering, **Dr. G. Rajesh Kumar**, Professor, Department of Civil Engineering, for their detailed review, constructive suggestions, and excellent advice during the process of this research work. I would like to thank **Dr. M. Raja Vishwanathan**, Assistant Professor, department of humanities and social science for his valuable suggestions, continuous support, and cooperation.

I would like to thank the teaching, non-teaching members, and fraternity of the Department of Electrical Engineering of NIT Warangal for their support and encouragement.

I wish to express my sincere thanks to **Prof. N. V. Ramana Rao**, Director, NIT Warangal for his official support and encouragement.

I would like to express my gratitude to **Dr. Chintam Venkaiah**, Associate professor, Department of Electrical Engineering for having faith in me and his constant motivation, support.

I would like to take this opportunity to thank my seniors Sachidananda Prasad, Ratna Rahul, fellow scholars Ravi, Sandeep, Hemakumar, and Ramesh for their support and encouragement.

I would like to thank all my teachers, colleagues, and seniors at various places for their support and encouragement.

I would like to express my deep sense of gratitude to my parents **Ramkishan Prasad**, **Sujatha** for their support and blessing. Without their sacrifice, constant encouragement, and moral support, this research work would not have been possible. I would like to thank my wife **Bhavana** and my son **Kalyana Krishna** for being a constant inspiration and support. I take this opportunity to thank all my family members and my well-wishers for their understanding, support, and encouragement during this research work. I would like to thank all those who helped me directly and indirectly at various stages of this work.

Bhanu Prasad Chintala

ABSTRACT

The penetration of renewable energy sources into distribution system has been increasing due to environmental concerns. Because of the uncertainty and unpredictability of renewable energy sources, distribution system operation has become complex and dynamic. Therefore, monitoring and control of the distribution system became necessary for it to operate reliably and effectively. But, monitoring of distribution system became difficult with limited metering infrastructure. As a result, the additional meters must be installed optimally and cost-effectively. In practical planning studies, trade-off solutions of multiple objectives can assist the operator to make a better decision in meter allocation in distribution system. Therefore, the meter placement problem is designed as a multi-objective optimization problem. Thus, the overall objective of the thesis is to provide optimal meter placement using new multi-objective evolutionary algorithms for improving the performance and accuracy of distribution system state estimation as well as monitoring and controlling the active distribution system.

There are many multi-objective optimization models are proposed in the literature, as all different types of multi-objective problems cannot be solved by a single optimization method. The multi-objective evolutionary algorithms (MOEAs) are classified into four categories: i) Pareto dominance based ii) decomposition based iii) indicator based and iv) model based MOEAs. Therefore, in this thesis an attempt has been made to compute an optimal locations of meters using different types of hybrid multi-objective evolutionary algorithms.

The contributions of this thesis are as follows:

- A new hybrid multi-objective evolutionary optimization algorithm based on decomposition and local dominance method is proposed for meter placement in distribution system state estimation. The meter placement is designed as a trade-off between three objectives, which are minimizing the cost of the meters, average relative percentage error of voltage magnitude, and voltage angle. As the meter placement problem is a combinatorial optimization, the Binomial distribution-based Monte Carlo method is utilized to initialize the population, which aims to improve the diversity, as a consequence it improves the convergence.
- A new indicator-based multi-objective evolutionary algorithm (MOEA) using the objective discretization method is proposed for meter placement in an active distribution system. As the meter placement problem is a combinatorial optimization, a combination of measurement sets produces a discrete objective space. Therefore, the

objective discretization method has been adopted to improve the performance of MOEA. As the performance of MOEA mostly depends on the Pareto front shape. Therefore, the proposed method employs an adaptive reference point approach to follow the shape of the Pareto front.

- A new inverse model-based multi-objective evolutionary algorithm is proposed for meter placement in active distribution system state estimation. The inverse model maps the non-dominated solution from objective space to decision space and is realized using multi-label Gaussian classification. The inverse model is used as a reproduction operator to generate additional candidate solutions from the estimated conditional probability of decision variables for given solutions. The additional solutions are generated by sampling from the inverse model, which improves the search efficiency and diversity of Pareto front solutions.
- The last contribution of the thesis is, a many-objective evolutionary optimization is proposed for meter placement in an active distribution system based on numerical observability. The addition of Pseudo measurements improves the convergence of state estimation and ensures the observability of the network. Whereas, the huge errors associated with Pseudo measurements deteriorate the performance of state estimation. For the first time in the meter placement problem, a numerical observability-based meter placement problem is proposed, which is used to select the minimum number of Pseudo measurements to ensure the observability and to improve the accuracy of the state estimation for a given set of real measurement combinations. The meter placement problem is designed as many-objective evolutionary optimization with four objectives as i) cost of distribution level Phasor measurement units (D-PMUs), ii) cost of intelligent electronic devices (IEDs), iii) root mean square error of voltage magnitude, and iv) root mean square error of voltage angle.

Contents

ACKNOWLEDGEMENT.....	i
ABSTRACT.....	iii
List of Figures.....	viii
List of Tables	xiii
List of Abbreviations	xvi
List of Symbols	xvii
Chapter 1	1
Introduction.....	1
1.1 Distribution System Overview	2
1.2 State Estimation.....	3
1.3 Weighted Least Square (WLS) based State Estimation	6
1.4 Differences between Distribution System and Transmission System.....	7
1.5 Branch Current based Distribution System State Estimation (BC-DSSE)	9
1.5.1 Jacobian Matrix Formulation $H(x)$:	9
1.5.2 Step by Step Procedure of BC-DSSE Algorithm.....	11
1.6 DSSE based on Meter Placement.....	12
1.7 Evolutionary Optimization Algorithms.....	13
1.8 Multi-Objective Evolutionary Algorithms	14
1.9 Combinatorial Nature of Meter Placement Problem.....	15
Chapter 2	18
Literature Review	18
2.1. General Overview	18
2.1.1 Node Voltage based DSSE	18
2.1.2 Branch Current based DSSE	19
2.2 Meter Placement Problem	19
2.3 Multi-Objective Evolutionary Algorithms	21
2.4 Meter Placement Problem using Multi-Objective Evolutionary Algorithms.....	23
2.5 Aims and Objectives:	24
2.6 Motivation	26
2.7 Contributions.....	28
2.8 Thesis Organization.....	30
2.9 Summary	32
Chapter 3	36

Multi-Objective Meter Placement in Distribution System State Estimation Using Hybrid Decomposition and Local Dominance Method.....	36
3.1 Introduction	36
3.2 Problem Formulation.....	37
3.3 Methodology	38
3.4 The Proposed Algorithm	39
3.5 The Binomial Distribution based Monte Carlo Method for Population Initialization	
40	
3.6 Simulation and Test Conditions	47
3.7 Results and Discussions	49
3.7.1 PG&E 69-bus Distribution System.....	49
3.7.2 Indian Practical 85-bus Distribution System	55
3.8 Summary	60
Chapter 4	63
Multi-Objective Meter Placement in Active Distribution System State Estimation using Objective Discretization and Indicator-Based Algorithm with Adaptive Reference Point Method	63
4.1 Introduction	63
4.2 Problem Formulation.....	65
4.3 Methodology	66
4.4 The Proposed Indicator based Multi-Objective Evolutionary Algorithm with Adaptive Reference Point Method Stage 1	67
Step-by-Step Process of the Proposed Algorithm Stage-1	68
4.5 Stage 2 of the Proposed Algorithm with Objective Discretization	72
4.6 Simulation and Test Conditions	75
4.7 Results and Discussions	76
4.7.1 PG&E 69-bus Distribution System.....	77
4.7.2 Indian Practical 85-bus Distribution System	87
4.8 Summary	97
Chapter 5	100
Multi-Objective Meter Placement in Active Distribution System State Estimation using Inverse Modeling based on Multi-label Gaussian Process Classification Algorithm with Adaptive Reference Point Method	100
5.1 Introduction	100
5.2 Problem Formulation:	101
5.3 Methodology:	102
5.4 Stage wise Process of the Proposed Algorithm:	108

5.5	Simulation and Test Conditions:	111
5.6	Results and Discussions	112
5.6.1	PG&E 69-bus Distribution System.....	112
5.6.2	Indian Practical 85-bus distribution system.....	122
5.7	Summary	132
Chapter 6	135
Many Objective Meter Placement in Active Distribution System State Estimation based on Numerical Observability Method.....		135
6.1	Introduction	135
6.2	Problem Formulation:	136
6.3	Numerical Observability Method:.....	137
6.4	Many-Objective Evolutionary Optimization using Inverse Model:.....	138
6.5	Simulation and Test Conditions:	141
6.6	Results and Discussion:.....	141
6.6.1	PG&E 69-bus Distribution System:.....	142
6.6.2	Indian Practical 85-bus Distribution System:	148
6.7	The Comparision of Proposed Methods.....	154
6.7.1	PG&E 69-bus Distribution System	154
6.7.2	Indian Practical 85-bus Distribution System	157
6.8	Summary	160
Chapter 7	162
Conclusions.....		162
7.1	General	162
7.2	Summary of Important Findings:	162
7.3	Scope of the Future Work	165
References.....	166
Appendix-A.....		177
Appendix-B.....		181
Publications		186
Curriculum-Vitae.....		187

List of Figures

Figure 1.1:	State estimation typical functional diagram.....	4
Figure 1.2:	Functional diagram of SCADA/DMS.....	5
Figure 3.1:	Indian Practical 85-bus distribution system: The performance characteristics with and without the Binomial Distribution based Monte Carlo simulation method.....	40
Figure 3.2:	Flowchart of the proposed algorithm.....	47
Figure 3.3	PG&E 69-bus distribution system optimal Pareto-front plots: Real measurements with an accuracy of 1% and Pseudo measurements with an accuracy of 50%.....	46
Figure 3.4:	PG&E 69-bus distribution system optimal Pareto-front plots: Real measurements with an accuracy of 3% and Pseudo measurements with an accuracy of 50%.....	52
Figure 3.5:	PG&E 69-bus distribution system optimal Pareto-front plots: Real measurements with an accuracy of 5% and Pseudo measurements with an accuracy of 50%.....	53
Figure 3.6:	Indian Practical 85-bus distribution system optimal Pareto-front plots: Real measurements with an accuracy of 1% and Pseudo measurements with an accuracy of 50%.....	56
Figure 3.7:	Indian Practical 85-bus distribution system optimal Pareto-front plots: Real measurements with an accuracy of 3% and Pseudo measurements with an accuracy of 50%.....	57
Figure 3.8:	Indian Practical 85-bus distribution system optimal Pareto-front plots: Real measurements with an accuracy of 5% and Pseudo measurements with an accuracy of 50%.....	58
Figure 4.1:	Flowchart of stage 1 of the proposed algorithm.....	72

Figure 4.2:	Flowchart of stage 2 of the proposed algorithm.....	73
Figure 4.3:	Indian Practical 85-bus distribution system: The convergence and diversity measure with and without the objective discretization method.	74
Figure 4.4:	PG&E 69-bus distribution system optimal Pareto-front plots: Real measurements with an accuracy of 1% and Pseudo measurements with an accuracy of 50% without DG (OD- Objective Discretization method)	78
Figure 4.5:	PG&E 69-bus distribution system optimal Pareto-front plots: Real measurements with an accuracy of 5% and Pseudo measurements with an accuracy of 50% without DG (OD- Objective Discretization method)	79
Figure 4.6:	PG&E 69-bus distribution system optimal Pareto-front plots: Real measurements with an accuracy of 1% and Pseudo measurements with an accuracy of 50% with DG Type-1 (P) (OD- Objective Discretization method)	81
Figure 4.7:	PG&E 69-bus distribution system optimal Pareto-front plots: Real measurements with an accuracy of 5% and Pseudo measurements with an accuracy of 50% with DG Type-1 (P) (OD- Objective Discretization method)	82
Figure 4.8:	PG&E 69-bus distribution system optimal Pareto-front plots: Real measurements with an accuracy of 1% and Pseudo measurements with an accuracy of 50% with DG Type-2 (P+jQ) (OD- Objective Discretization method)	84
Figure 4.9:	PG&E 69-bus distribution system optimal Pareto-front plots: Real measurements with an accuracy of 1% and Pseudo measurements with an accuracy of 50% with DG Type-3 (P+jQ) (OD- Objective Discretization method)	85
Figure 4.10:	Indian Practical 85-bus active distribution system optimal Pareto-front plots: 1% error in real measurements and 50% error in Pseudo measurements without DG (OD- Objective Discretization method)	88
Figure 4.11:	Indian Practical 85-bus active distribution system optimal Pareto-front plots: 5% error in real measurements and 50% error in Pseudo measurements without DG (OD- Objective Discretization method).....	89
Figure 4.12:	Indian Practical 85-bus active distribution system optimal Pareto-front plots: 1% error in real measurements and 50% error in Pseudo measurements with DG Type-1 (P) (OD- Objective Discretization method)	91
Figure 4.13:	Indian Practical 85-bus active distribution system optimal Pareto-front plots: 5% error in real measurements and 50% error in Pseudo	

measurements with DG Type-1 (P) (OD- Objective Discretization method)	92
Figure 4.14: Indian Practical 85-bus active distribution system optimal Pareto-front plots: 1% error in real measurements and 50% error in Pseudo measurements with DG Type-2 (P+jQ) (OD- Objective Discretization method)	94
Figure 4.15: Indian Practical 85-bus active distribution system optimal Pareto-front plots: 1% error in real measurements and 50% error in Pseudo measurements with DG Type-3 (P+jQ) (OD- Objective Discretization method)	95
Figure 5.1: Flowchart of the proposed algorithm.....	110
Figure 5.2: PG&E 69-bus distribution system optimal Pareto-front plots: under 1% uncertainty in real measurements 50% uncertainty in Pseudo measurements for without DG (AR – Adaptive reference point method)	114
Figure 5.3: PG&E 69-bus distribution system optimal Pareto-front plots: under 5% uncertainty in real measurements 50% uncertainty in Pseudo measurements without DG (AR – Adaptive reference point method). .	115
Figure 5.4: PG&E 69-bus distribution system optimal Pareto-front plots: under 1% uncertainty in real measurements 50% uncertainty in Pseudo measurements with DG Type-1 (P) (AR – Adaptive reference point method)	117
Figure 5.5: PG&E 69-bus distribution system optimal Pareto-front plots: under 5% uncertainty in real measurements 50% uncertainty in Pseudo measurements with DG Type-1 (P) (AR – Adaptive reference point method)	118
Figure 5.6: PG&E 69-bus distribution system optimal Pareto-front plots: under 1% uncertainty in real measurements 50% uncertainty in Pseudo measurements with DG Type-2 (P+jQ) (AR – Adaptive reference point method)	119
Figure 5.7: PG&E 69-bus distribution system optimal Pareto-front plots: under 1% uncertainty in real measurements 50% uncertainty in Pseudo measurements with DG Type-3 (P+jQ) (AR – Adaptive reference point method)	121
Figure 5.8: Indian Practical 85-bus active distribution system optimal Pareto-front plots: Real measurements with an accuracy of 1% and Pseudo measurements with an accuracy of 50% without DG (AR – Adaptive reference point method)	123

Figure 5.9:	Indian Practical 85-bus active distribution system optimal Pareto-front plots: Real measurements with an accuracy of 5% and Pseudo measurements with an accuracy of 50% without DG (AR – Adaptive reference point method)	124
Figure 5.10:	Indian Practical 85-bus active distribution system optimal Pareto-front plots: Real measurements with an accuracy of 1% and Pseudo measurements with an accuracy of 50% with DG Type-1 (P) (AR – Adaptive reference point method).....	126
Figure 5.11:	Indian Practical 85-bus active distribution system optimal Pareto-front plots: Real measurements with an accuracy of 5% and Pseudo measurements with an accuracy of 50% with DG Type-1 (P) (AR – Adaptive reference point method).....	127
Figure 5.12:	Indian Practical 85-bus active distribution system optimal Pareto-front plots: Real measurements with an accuracy of 1% and Pseudo measurements with an accuracy of 50% with DG Type-2 (P+jQ) (AR – Adaptive reference point method).....	129
Figure 5.13:	Indian Practical 85-bus active distribution system optimal Pareto-front plots: Real measurements with an accuracy of 1% and Pseudo measurements with an accuracy of 50% with DG Type-3 (P+jQ) (AR – Adaptive reference point method).....	130
Figure 6.1:	Flow chart of the proposed method with numerical observability.....	140
Figure 6.2:	PG&E 69-bus distribution system optimal Pareto-front plots: with 1% error in real measurements and Pseudo measurements with an accuracy of 50% with DG	143
Figure 6.3:	PG&E 69-bus distribution system optimal Pareto-front plots: with 5% error in real measurements and Pseudo measurements with an accuracy of 50% with DG	144
Figure 6.4:	PG&E 69-bus distribution system optimal Pareto-front plots: with 1% error in real measurements and Pseudo measurements with an accuracy of 50% without DG	146
Figure 6.5:	PG&E 69-bus distribution system optimal Pareto-front plots: with: 5% error in real measurements and Pseudo measurements with an accuracy of 50% without DG	147
Figure 6.6:	Indian Practical 85-bus distribution system optimal Pareto-front plots: with 1% error in real measurements and Pseudo measurements with an accuracy of 50% with DG	149
Figure 6.7:	Indian Practical 85-bus distribution system optimal Pareto-front plots: with 5% error in real measurements and Pseudo measurements with an accuracy of 50% with DG	150

Figure 6.8:	Indian Practical 85-bus distribution system optimal Pareto-front plots: with 1% error in real measurements and Pseudo measurements with an accuracy of 50% without DG	152
Figure 6.9:	Indian Practical 85-bus distribution system optimal Pareto-front plots: with 5% error in real measurements and Pseudo measurements with an accuracy of 50% without DG	153

List of Tables

Table 3.1:	Parameter values of the proposed algorithm, MOEA/D, NSGA-II.....	49
Table 3.2:	PG&E 69-bus distribution system: Optimal location of the power flow meters under different metrological errors	54
Table 3.3:	Indian Practical 85-bus distribution system: Optimal location of the power flow meters under different metrological errors	59
Table 4.1:	Parameters used in the proposed algorithm and NSGA-II	76
Table 4.2:	Location and size of different types of distributed generation	77
Table 4.3:	PG&E 69-bus distribution system: Optimal location of the power flow meters under different metrological errors for without DG.....	79
Table 4.4:	PG&E 69-bus distribution system: Optimal location of the power flow meters under different metrological errors with DG Type-1(P).....	83
Table 4.5:	PG&E 69-bus distribution system: Optimal location of the power flow meters with 1% measurement uncertainty with DG Type-2(P-jQ).	86
Table 4.6:	PG&E 69-bus distribution system: Optimal location of the power flow meters with 1% measurement uncertainty with DG Type-3(P+jQ).	86
Table 4.7:	Indian Practical 85-bus distribution system: Optimal location of the power flow meters different measurement uncertainty without DG.	89
Table 4.8:	Indian Practical 85-bus distribution system: Optimal location of the power flow meters different measurement uncertainty with DG Type-1(P)....	92
Table 4.9:	Indian Practical 85-bus distribution system: Optimal location of the power flow meters with 1% measurement uncertainty for DG Type-2(P-jQ). .	95
Table 4.10:	Indian Practical 85-bus distribution system: Optimal location of the power flow meters with 1% measurement uncertainty for DG Type-3(P+jQ). .	96
Table 5.1:	Parameters of the proposed algorithm, MOEA/DLD, MOEA/D and NSGA-II	111
Table 5.2:	Distributed generation size and locations	112
Table 5.3:	P&G 69-bus distribution system: Optimal location of the power flow meters under different measurement uncertainty for without DG.....	115
Table 5.4:	P&G 69-bus distribution system: Optimal location of the power flow meters under different measurement uncertainty for DG Type-1(P). ..	118
Table 5.5:	P&G 69-bus distribution system: Optimal location of the power flow meters with 1% measurement uncertainty for DG Type-2(P-jQ).....	118

Table 5.6:	P&G 69-bus distribution system: Optimal location of the power flow meters with 1% measurement uncertainty for DG Type-3($P+jQ$).....	121
Table 5.7:	Indian Practical 85-bus distribution system: Optimal location of the power flow meters under different measurement uncertainty for without DG.	124
Table 5.8:	Indian Practical 85-bus distribution system: Optimal location of the power flow meters under different measurement uncertainty for with DG Type-1(P).	128
Table 5.9:	Indian Practical 85-bus distribution system: Optimal location of the power flow meters with 1% measurement uncertainty for with DG Type-2($P-jQ$).	130
Table 5.10:	Indian Practical 85-bus distribution system: Optimal location of the power flow meters with 1% measurement uncertainty for with DG Type-3 ($P+jQ$).	131
Table 6.1:	Distributed generation size and locations	141
Table 6.2:	PG&E 69-bus distribution system: Optimal location of the D-PMUs and IEDs under different measurement uncertainty for with DG	145
Table 6.3:	PG&E 69-bus distribution system: Optimal location of the D-PMUs and IEDs under different measurement uncertainty for without DG.	148
Table 6.4:	Indian Practical 85-bus distribution system: Optimal location of the D-PMUs and IEDs with 1% measurement uncertainty for with DG.....	151
Table 6.5:	Indian Practical 85-bus distribution system: Optimal location of the D-PMUs and IEDs under different measurement uncertainty for without DG.	154
Table 6.6:	P&G 69-bus distribution system: Summary of different proposed algorithms: Optimal location of the power flow meters under different measurement uncertainty for without DG.....	155
Table 6.7:	P&G 69-bus distribution system: Summary of different proposed algorithms: Optimal location of the power flow meters under different measurement uncertainty for DG Type-1(P).	156
Table 6.8:	P&G 69-bus distribution system: Optimal location of the power flow meters with 1% measurement uncertainty for DG Type-2($P-jQ$).....	156
Table 6.9:	P&G 69-bus distribution system: Summary of different proposed algorithms: Optimal location of the power flow meters with 1% measurement uncertainty for DG Type-3($P+jQ$).....	157
Table 6.10:	Indian Practical 85-bus distribution system: Summary of different proposed algorithms: Optimal location of the power flow meters under different measurement uncertainty for without DG.....	158
Table 6.11:	Indian Practical 85-bus distribution system: Summary of different proposed algorithms: Optimal location of the power flow meters under different measurement uncertainty for with DG Type-1(P)	159
Table 6.12:	Indian Practical 85-bus distribution system: Summary of different proposed algorithms: Optimal location of the power flow meters with 1%	

measurement uncertainty for with DG Type-2(P+jQ)	159
.....
Table 6.13: Indian Practical 85-bus distribution system: Summary of different proposed algorithms: Optimal location of the power flow meters with 1% measurement uncertainty for with DG Type-3 (P+jQ).	160
.....

List of Abbreviations

AR	Adaptive Reference Point Method
ARPE	Average Relative Percentage Error
BC-DSSE	Branch Current Based Distribution System State Estimation
DG	Distributed Generation
DMS	Distribution Management System
DP	Dynamic Programming
D-PMU	Distribution Level PMU
DSSE	Distribution System State Estimation
EDA-IPM	Multi-Objective Hybrid Estimation of Distribution Algorithm- Interior Point Method
ENS	Efficient Nondominated Sorting
IED	Intelligent Electronic Device
IGD	Inverted Generational Distance
IGD-NS	Inverted Generational Distance Indicator with Noncontributing Solution Detection
MOEA	Multi-Objective Evolutionary Algorithm
MOEA/D	MOEA Based on Decomposition
NDS	Non-Dominated Sorting
NSGA-II	Non-Dominated Sorting Genetic Algorithm-II
OD	Objective Discretization Method
OOA	Ordinal Optimization Algorithm
PBI	Penalty Based Intersection
PF	Pareto Front
PM	Power Flow Meter
PMU	Phasor Measurement Unit
PSO-KH	Multi-Objective Hybrid Particle Swarm Optimization- Krill Herd Algorithm
RTU	Remote Terminal Unit
SE	State Estimation
SSA	Systematic Sampling Approach
VMM	Voltage Magnitude Meter
WLS	Weighted Least Square Method

List of Symbols

A	Archive Population
A'	New Archive population
C_{PM}	Costs of Power Flow Measurement Devices
C_{vmm}	Costs of Voltage Magnitude Measurement Devices
$CV(x)$	Penalty Function
C_{D-PMU}	Cost Of Distribution Level PMUs
C_{IED}	Cost Of IEDs
$dis(x, y)$	Euclidean Distance Between Solutions x and y .
D	Number of Divisions Along with Each Objective Coordinate
e_j	Error Projection of J^{th} row
$G(x)$	Gain Matrix
g_1	Inequality Constraints of Relative Voltage Magnitude Limits
g_2	Inequality Constraints of Relative Voltage Angle Limits
Gp	Gaussian Process
$h(x)$	Measurement Function
h_j	J^{th} row in The Jacobian Matrix
$H(x)$	Jacobian
$J(x)$	Objective Function of WLS Method
K	Covariance Function
M	Number of Objectives
N	Size of the Population
$\mathcal{N}()$	Normal Distribution
p	Probability of Success
P_c	Crossover Rate
P_m	Mutation Rate

P_{D-PMU}	Location of D-PMUs
P_{IED}	Location of IEDs
P_t	Old Population
$p(\cdot)$	Projection Operator
Q_t	New Population
R	Initial Reference Point Set
R'	Updated Reference Point Set
T	Neighborhood Size
U_{PM}	Locations of Power Flow Meters
U_{VMM}	Locations of Voltage Magnitude Measurement Meters
V	Linearly Independent Vectors
V^t	True Value of Voltage Magnitude
\hat{V}	Estimated Voltage Magnitude
w	Weight Vector
Z	Measurements From the Meters
δ^t	True Value of Voltage Angle
$\hat{\delta}$	Estimated Voltage Angle
$\sigma(t)$	Sigmoid Function
\otimes	Kronecker Product

Chapter 1

Introduction

Chapter 1

Introduction

1.1 Distribution System Overview

Day by day the electrical load demand is increasing, and to deliver reliable services to the increasing power consumers the new technologies are adopted in the power system. The deregulation of the power system was segregated into operation sectors of generation, transmission, and distribution. The deregulation introduced a competitive environment among different segments of the power system to provide customer-centric services. The adoption of new communication and information technologies leads to smart and intelligent grids. Among the three sectors of power system, distribution system has been embracing many technical and operational changes and also posing many challenges to the operators and researchers. Mainly, in recent years the integration of distributed generation (DG) is increased, which provided new opportunities to build energy markets with the active participation of system operators and prosumers, who are both producing the electrical energy and consuming power from the grid. These changes affected the operation of distribution system at a whole new level.

The Renewable sources, mainly wind and photovoltaic power penetration have increased into the system due to the environmental aspects to reduce the carbon emission from conventional generation. Moreover, the intermittent and unpredictable nature of renewable energy sources poses many challenges in distribution system. Previously distribution network is a passive network with loads, but with the introduction of DGs, distribution system become an active network. Previously, the power flow is from upstream (substation) to the downstream (loads), but with introducing the DGs, power may also flow from downstream to upstream. This causes the bi-directional power flow between loads and DGs, which makes the network operation more complex. When the power flows from load ends to upstream, cause voltage profile increases the fault current rating decrease. These changes were made to focus on a different control and operational functions such as voltage profile control, new protection schemes, stability of the distribution system, demand-side management, etc. Moreover, the intermittent, and unpredictable nature of renewable generation made network operation more dynamic. These reasons made to necessitate the enhancement of real-time monitoring and control of distribution system.

The monitoring and control of the network are usually managed by the energy management system, which works on top of the Supervisory Control and Data Acquisition (SCADA) system. SCADA gives the real-time status of the network by providing the measurement data such as bus voltage, line flows, the status of tie-line switches, circuit breakers. The data provided by SCADA may not be reliable as the measurement data comes with errors and telemetry, communication failures add noise to the data. This data is provided to the control actions and applications such as voltage profile control, reconfiguration, optimal power flow application, security analysis, and so on. For efficient operation and control, the input data is required to be more reliable as all the controls actions and functions depend on the data accuracy. Therefore, the data provided by the SCADA need to be filtered from the errors to get reliable data. State estimation mitigates the errors by filtering raw data from SCADA and providing the state variables. Therefore, state estimation plays a significant function as the operation and control actions depend on its estimation results.

1.2 State Estimation

State estimation provides the status of the network in terms of state variables. Generally, state estimation has typical functionalities as follows:

- 1. Topology Processing:** Topological processing updates the network connectivity from the data obtained from the SCADA system such as status information of circuit breakers, tie line switches. It provides the online network diagram.
- 2. Observability Analysis:** Observability analysis determines whether the state estimation solution is obtainable with the given set of measurements or not. When the network is unobservable it also provides the observable islands. Observability depends on the distribution of measurements in the network. If the network is unobservable with a given measurement set, using observability analysis, additional Pseudo measurements are added to the measurement set to make the network observable.
- 3. State Estimation:** State estimation provides an estimation of state variables using the topology information and measurement data. After state estimation, the state variables are supplied for various control actions and functions of energy management systems.

4. Bad Data Detection and Identification: Gross errors in the measurement set are detected, identified using the bad data process, and identified measurements are eliminated from the measurement set.

A typical power system state estimation functional diagram is presented in fig. 1.1. The four functionalities are an integral part of the state estimation, and it repeatedly executes time to time to give the real-time state of the system.

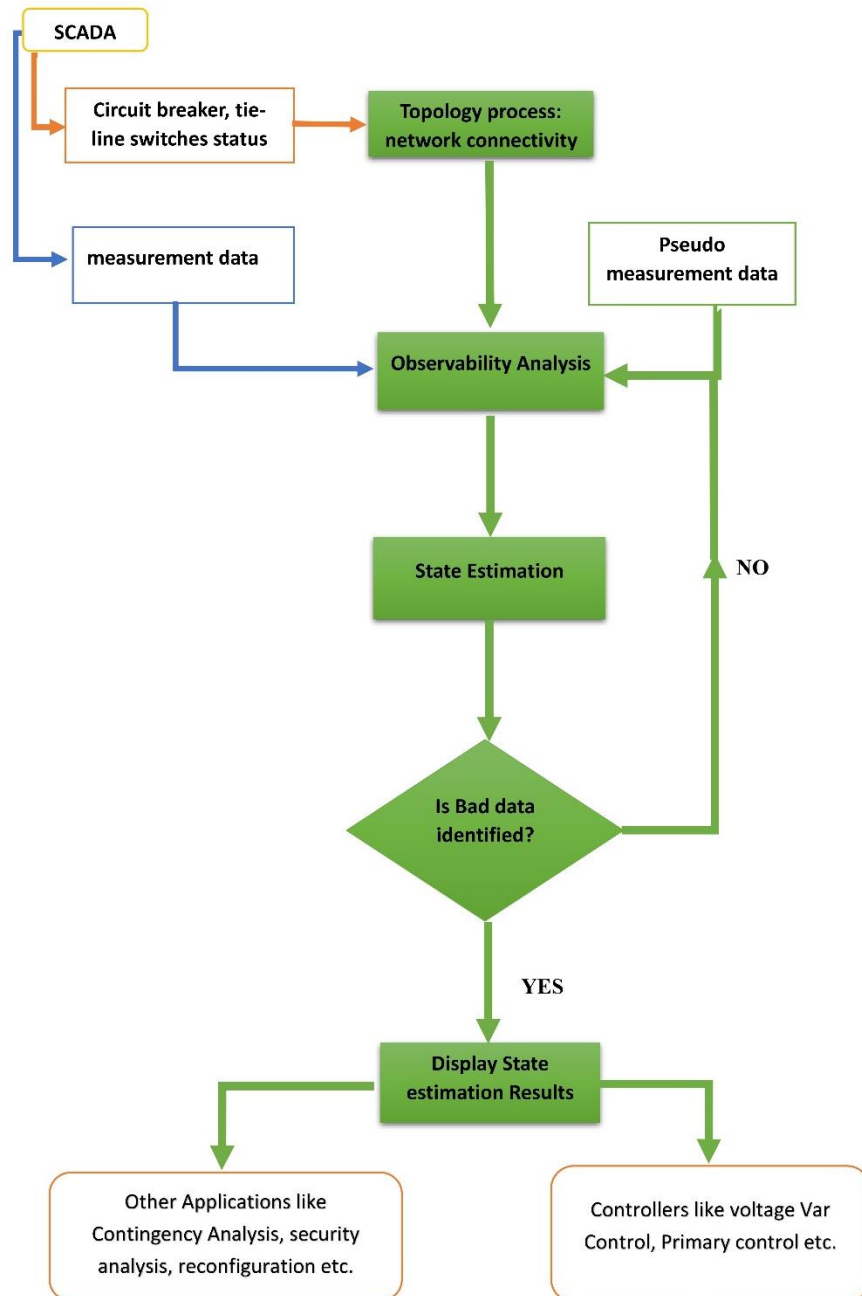


Fig. 1.1: State estimation typical functional diagram.

The measurements are collected from monitoring devices and managed by the SCADA system. The measurement devices at the substation monitor the typical electrical quantities like voltage, current, and power, etc., and the measured data is collected by Remote Terminal Units (RTUs). The different substation data is collected by corresponding RTUs and communicates the data to the SCADA system by different means of communication technologies. The Distribution Management System (DMS) will have different control and functionalities to operate the distribution system on top of the SCADA system. The data from the SCADA is processed by state estimation then the output state variables are fed to different DMS controllers like voltage regulation, automatic generation control, and fed to functions like optimal power flow, contingency analysis, etc. The functional diagram of DMS/SCADA is shown in fig. 1.2.

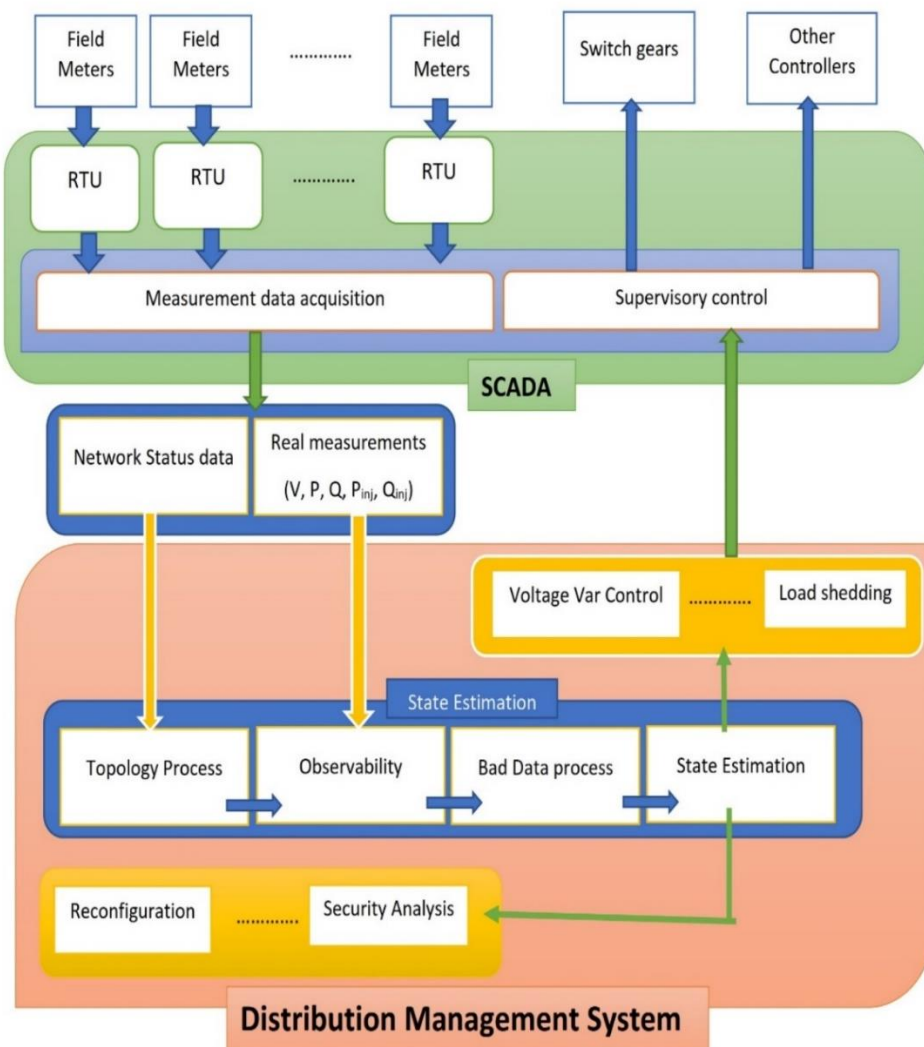


Fig. 1.2: Functional diagram of SCADA/DMS.

Many researchers are proposed different state estimation methods to achieve accurate state estimation. The state estimation function is widely used in the transmission system to estimate the state of the system. An in-depth review of transmission system state estimation is presented in [1]-[3]. Generally, the state estimation problem is formulated using the weighted least square (WLS) method. As the WLS method is susceptive to bad data, alternative to WLS, many mathematical models are proposed to formulate the state estimation to address the bad data issue [4]. The least Median of Squares (LMS), Least Trimmed Squares (LTS) methods can handle outliers in measurement data [5] and the Least Absolute Value (LAV) estimator can automatically reject the bad data [6]. However, the WLS method is the widely used approach to formulate state estimation.

1.3 Weighted Least Square (WLS) based State Estimation

The Weighted Least Square method minimizes a weighted sum of squares of state variable errors. For a given set of measurements, the measurement model is represented with a measurement function associated with noise. The measurement model is formulated as follows:

$$Z = h(x) + e \quad (1.1)$$

Where Z is $mx1$ size matrix and denotes the measurements from the meters, $h(x)$ is mxn size matrix and represents the measurement function, x is a $nx1$ size matrix and denotes set of state variables, m is the number of measurements, n is the number of state variables and e is the noise associated with the measurements. Different types of measurements are obtained from the field such as voltage, current, power injection at nodes, and power flows, these measurements set is represented by Z , which is provided as input to the state estimation. The measurements are associated with errors, which are due to ageing of meters, communication failures, device malfunction, and so on. Therefore, the measurements are modelled as functions of state variables $h(x)$, added with errors ‘ e ’. The error characteristics follows the normal distribution. Therefore, the measurements are modelled using measurement mean and meter variance parameters to represent the errors in measurements.

The errors are scalarized with corresponding measurement variance. Each meter has a specific variance (σ^2) due to the manufacturing differences and other reasons. The state estimation problem is formulated using the least squares method, which minimizes the sum of squares of errors. The objective function $J(x)$ of WLS optimization is represented as follows:

$$J(x) = [e]^T [W] [e] \quad (1.2)$$

Where, W is the weight matrix, weight is formulated by taking the reciprocal of variances of each measurement, and the weight is added to the diagonal of the weight matrix corresponding to each measurement.

The error is unknown, and it is replaced in (1.2) using (1.1), which is in the form as follows:

$$J(x) = [Z - h(x)]^T [W] [Z - h(x)] \quad (1.3)$$

The above nonlinear objective function is solved using the iterative Newton method, which gives the solution as follows:

$$\Delta x_i = (G(x))^{-1} [(H(x_i))^T [W]^{-1}] [Z - h(x)] \quad (1.4)$$

$$G(x) = (H(x))^T [W]^{-1} H(x) \quad (1.5)$$

Where, $H(x)$ is the Jacobian matrix, $G(x)$ denotes the gain matrix and 'i' is the iteration count. The Jacobian matrix $H(x)$ is formulated by differentiating measurements with respect to state variables. The solutions are iteratively updated as follows:

$$x_{i+1} = x_i + \Delta x_i \quad (1.6)$$

The state estimation is converged when the change in state variables (Δx) is smaller than a specified threshold (ϵ).

1.4 Differences between Distribution System and Transmission System

The distribution system differs in many ways from the transmission system. Both have different characteristics due to the following aspects:

1. **X/R Ratio:** Distribution system has a low X/R ratio as compared to the transmission system. The feeders in distribution system have a short length as loads are distributed around the substations, whereas the transmission system has long length lines as it connects the generation and load centers. The short feeders have less reactance as compared to the resistance and lead to a low X/R ratio.
2. **Network Topology:** Transmission system is a connected network with loops, whereas distribution system is a radial and weakly meshed network.

3. **Unbalanced Network:** Transmission system is a balanced three phase network and it is balanced using transposition of transmission lines and with aggregated loads, whereas distribution system is mostly an unbalanced system due to distributed loads on the network.
4. **Load Distribution:** Distribution system has distributed loads as the substations are near the load centers. The transmission system connects long distances between generation and load centers; therefore, the connected loads are aggregated on transmission system.
5. **Size of Network:** Distribution system has a large number of loads spread in a small area compared to transmission system. Therefore, the number of nodes in distribution system is more compared to transmission system.
6. **Metering:** As distribution system is a passive network, very few meters are sufficient to operate the network even though having a large number of nodes. Therefore, substations are installed with limited number of meters.

The transmission system and distribution system are different in characteristics; therefore, the transmission system state estimation algorithms are not directly applicable to the distribution system. Distribution system state estimation requires a large data handling capability due to a large number of nodes in the distribution system and requires it to be computationally efficient to handle the large data processing. Moreover, the state estimation accuracy is affected by an unbalanced phase network and load distribution, which introduces the nonuniform measurement distribution [7]. The large size of the network and the limited number of meters leads to the unobservability of the network. Therefore, Pseudo measurements are added to obtain the observability of the network. Whereas Pseudo measurements are generated from the historical load profiles, therefore, large errors are introduced in Pseudo measurements. Even though Pseudo measurements improve the redundancy and observability, the low accuracy of Pseudo measurements degrades the performance of state estimation. Therefore, the above reasons made to introduce specific algorithms for distribution system state estimation (DSSE) to handle the need for distribution system.

Due to the difference in basic characteristics of transmission and distribution system, DSSE formulation differs from conventional state estimation. The measurement function $h(x)$ modelling in DSSE, is mainly deviates from the transmission system state estimation. Based on the choice of state variables, measurements and representation of phases in the power flow

equation, the measurement function can have different forms. Based on the choice of state variables and formulation of measurement function the DSSE can be formulated as i) Voltage-based DSSE and ii) Branch current-based DSSE.

- **Voltage based DSSE:** In general, the voltage magnitude and voltage angle are considered state variables in transmission system state estimation. Similarly, the conventional state variables are considered in many methods to formulate the DSSE [8]- [11].
- **Branch Current based DSSE:** Branch current magnitude and current angle are used as state variables to formulate the Branch Current based DSSE (BC-DSSE). The BC-DSSE is widely used in distribution system as it provides better results compared to Voltage-based DSSE [12]-[17].

1.5 Branch Current based Distribution System State Estimation (BC-DSSE)

Baran and Kelley [12] proposed branch current based three phase distribution system state estimation, which is based on WLS method. Each phase measurement function is represented in terms of its phase currents, so it decouples three phase problem into three sub-problems. This method forms the constant gain matrix. Therefore, the method performs better in terms of convergence, computational speed and memory management compared to voltage-based-DSSE [16]. Many authors have proposed alternative BC-DSSE methods to enhance the accuracy of state estimation [12]-[17]. The branch current magnitude (i) and phase angle (α) are considered state variables in BC-DSSE. The state variable 'x' is represented as follows:

$$x = [i_1, i_2, \dots, i_{Nbr}, \alpha_1, \alpha_2, \dots, \alpha_{Nbr}] \quad (1.7)$$

In [18], the study shows that the voltage measurement at the substation affects the whole state estimation performance. Therefore, Marco Pau *et al.* [17] proposed a BC-DSSE algorithm considering the voltage magnitude at substation as a state variable to enhance the accuracy of state estimation. A general BC-DSSE algorithm is presented as follows:

1.5.1 Jacobian Matrix Formulation $H(x)$:

The Jacobean is formulated by differentiating measurement with respect to the state variables. The measurements (Z) consist of different types of measurements from the field such as voltage, current, active, and reactive power flows, node injection powers, Pseudo measurements, virtual measurements. Pseudo measurements are produced from historical data of the loads and virtual measurements are the zero injection power measurements modelled

using lower value variance in the order of 10^{-7} [19]. The Jacobian is formulated for different measurements using the following expressions:

1. Voltage Magnitude Measurement:

Suppose the voltage at p^{th} node on k^{th} branch is measured, there are n branches before the k^{th} branch to the first branch, then the voltage magnitude is given as follows:

$$V_p = V_{\text{slack}} - \sum_{i=1}^{n+1} I_{i-1,j} Z_{i-1,j} \quad (1.8)$$

Then the Jacobian matrix entries are as follows:

$$\begin{aligned} \frac{\partial V_p}{\partial I_{i-1,j}} &= -\cos \delta_p \cdot Z_{i-1,j} \cos(\alpha_{i-1,j} + \theta_{i-1,j}) \\ &\quad - \sin \delta_p \cdot Z_{i-1,j} \sin(\alpha_{i-1,j} + \theta_{i-1,j}) \end{aligned} \quad (1.9)$$

$$\begin{aligned} \frac{\partial V_p}{\partial \alpha_{i-1,j}} &= \cos \delta_p \cdot I_{i-1,j} Z_{i-1,j} \sin(\alpha_{i-1,j} + \theta_{i-1,j}) \\ &\quad - \sin \delta_p \cdot I_{i-1,j} Z_{i-1,j} \cos(\alpha_{i-1,j} + \theta_{i-1,j}) \end{aligned} \quad (1.10)$$

Where δ is angle of voltage, α is angle of current and θ is angle of impedance. When the currents are away from the path between k^{th} branch and the first branch then the Jacobian entries are equal to zero.

2. Current Magnitude Measurement:

The Jacobian entries for the current measurement of branch ‘ m ’ between nodes p, q is expressed as follows:

$$\frac{\partial I_{pq}}{\partial I_{i,j}} = \begin{cases} 1 & \text{when } (i,j) = (p,q) \\ 0 & \text{otherwise} \end{cases} \quad (1.11)$$

$$\frac{\partial I_{pq}}{\partial \alpha_{i,j}} = 0 \quad (1.12)$$

3. Power Injection Measurements:

Suppose power injection at bus k is measured and there are m buses connected to k^{th} bus and from 1 to n buses the current flow is inward to k^{th} bus, and from $n+1$ to m buses the current flow is outward to k^{th} bus, then the power injection is expressed as follows:

$$P_k + jQ_k = V_k (\sum_{i=1}^n I_{i,j} - \sum_{i=n+1}^m I_{j,i}) \quad (1.13)$$

Then the corresponding Jacobian entries are as follows:

$$\frac{\partial P_k}{\partial I_{i,j}} = V_k \cos(\delta_k - \alpha_{i,j}) \quad (1.14)$$

$$\frac{\partial P_k}{\partial \alpha_{i,j}} = V_k I_{i,j} \sin(\delta_k - \alpha_{i,j}) \quad (1.15)$$

$$\frac{\partial Q_k}{\partial I_{i,j}} = V_k \sin(\delta_k - \alpha_{i,j}) \quad (1.16)$$

$$\frac{\partial Q_k}{\partial \alpha_{i,j}} = -V_k I_{i,j} \cos(\delta_k - \alpha_{i,j}) \quad (1.17)$$

When a line is not connected to the measured injection bus, then the related entries are made zero.

4. Power Flow Measurement:

Suppose the power flow on branch k is measured, which is in between nodes p, q, then the power flow is expressed as follows:

$$P_{p,q} + jQ_{p,q} = V_p (I_{p,q})^* \quad (1.18)$$

$$P_{p,q} + jQ_{p,q} = V_p I_{p,q} (\cos(\delta_k - \alpha_{p,q}) + j \sin(\delta_k - \alpha_{p,q})) \quad (1.19)$$

The corresponding Jacobian entries are given as follows:

$$\frac{\partial P_{p,q}}{\partial I_{i,j}} = V_p \cos(\delta_p - \alpha_{p,q}) \quad (1.20)$$

$$\frac{\partial P_{p,q}}{\partial \alpha_{i,j}} = V_p I_{p,q} \sin(\delta_p - \alpha_{p,q}) \quad (1.21)$$

$$\frac{\partial Q_{p,q}}{\partial I_{i,j}} = V_p \sin(\delta_p - \alpha_{p,q}) \quad (1.22)$$

$$\frac{\partial Q_{p,q}}{\partial \alpha_{i,j}} = -V_p I_{p,q} \cos(\delta_p - \alpha_{p,q}) \quad (1.23)$$

When the state variable and the measurement branch is not in the same branch then the Jacobian entries are made zero.

1.5.2 Step by Step Procedure of BC-DSSE Algorithm

The BC-DSSE algorithm is based on the WLS method. The algorithm consists of three steps to estimate the state variables. the steps are described as follows:

- 1. Initialization:** The initial values of state variables affect greatly the performance of state estimation. Initial values are determined using two steps: i) backward approach and ii) forward approach. In the first step, in backward approach, the branch currents are calculated by setting the initial values of node voltages as one per unit and using the power injections at each node. In the second step, the branch currents calculated in backward approach are used to calculate the initial values of voltage at each node.
- 2. Update State Variables:** The residuals are calculated, and the state variables are updated using equations (1.4) and (1.6).
- 3. Update Node Voltages:** The node voltages are calculated from the state variables using the forward sweep approach.
- 4. Convergence Criteria:** If the change in the state variables is below a specified threshold limit (ϵ), then the algorithm stops and prints the results. The specified threshold limit is taken as 10^{-7} for convergence criteria.

1.6 DSSE based on Meter Placement

The network status can be monitored with the help of meters installed at different locations of the distribution network. The measurements supplied by the meters may have errors and also due to communication failure, measurement data may become erroneous. The erroneous data is filtered using the state estimation process to get the actual measurement data. Therefore, the performance of state estimation significantly influences the operation of the network as the output of state estimation is supplied to all the control actions [20]. However, the performance of the state estimation depends on the observability of the network and the redundancy of the measurements. The observability of the network depends on the distribution of meters in the network. However, the distribution network is unobservable with a limited number of meters. Therefore, additional meters are required to be installed to make the system observable. Distribution system has a large number of nodes and placing meters at each node may not be economically feasible. The network can be made numerically observable by adding Pseudo measurements [21], but the huge errors associated with Pseudo measurements deteriorates the performance of state estimation. By installing the additional real measurements at distribution network, the desired performance of state estimation can be achieved. Therefore, meters need to be placed optimally to reduce metering cost, to improve the observability and redundancy such that altogether it improves the state estimation performance.

The meter placement problem can be formulated in two ways as i) using topological observability and ii) numerical observability, by adding Pseudo measurements to additional real measurements set to improve the performance of state estimation. The topological observability is based on graph theory and whereas in second method Pseudo measurements are fixed, by taking all node injections modelled as Pseudo measurements, whereas additional real measurements are placed using an optimizing algorithm. The topological observability requires a greater number of meters to achieve observability compared to using the second method of meter placement. Moreover, the second method of meter placement ensures the desired performance of state estimation for a given set of real measurements. Therefore, this work considers the second approach of meter placement, in which all the node injections are modelled as Pseudo measurements and the real measurements are placed using the optimization technique.

The meter placement problem is formulated as an optimization problem. The optimization techniques like dynamic programming, interior point method and so on are called conventional optimization methods. Each conventional method provides better results for a specific type of optimization problem and is not suitable for other types of problems. Moreover, the conventional optimization method may not handle the mixed variable optimization problems, struck at local optima and requires existing of objective function derivative.

1.7 Evolutionary Optimization Algorithms

The limitation of conventional optimization methods can be overcome with alternative optimization techniques such as evolutionary optimization techniques, which can handle nonlinear, non-differentiable, real-world complex problems, highly constrained, high dimensionality problems, and discrete optimization problems. Evolutionary optimization algorithms are one of the branches of meta-heuristic optimization algorithms, which are inspired by the biological evolutionary theory to solve optimization problems. The evolutionary algorithms can be classified into two categories: i) population-based and ii) trajectory-based algorithms. Population-based algorithms are inspired by the biology and swarms of different species. In population-based algorithms, multiple solutions are propagated to find the optimal solution in the decision space. Genetic algorithm, Particle swarm optimization, whale optimization, and bat optimization etc., are examples of population-based algorithms. Whereas, trajectory-based algorithms are adapted from physics, in which a single solution is propagated to find the optimal solution. Tabu search, simulated annealing etc., are examples of trajectory-based algorithms. The Evolutionary optimization algorithms are best

suited to solve the meter placement problem. The meter placement can be formulated as single objective and multi-objective problems. Whereas, in practical applications of meter placement in distribution system need to consider multiple objectives instead of a single objective. The multi-objective formulation provides the trade-off solutions which are useful in making the decision of distribution system planning studies.

1.8 Multi-Objective Evolutionary Algorithms

The multi-objective meter placement can be designed using multi-objective evolutionary algorithm (MOEA). The optimization process provides the best feasible solution which is the maximum or minimum value of a given objective function. In general, the multi-objective optimization is expressed as follows:

$$\text{minimize } F(x) = (f_1(x), f_2(x), \dots, f_m(x))^T$$

subjected to constraints

Where $F(x)$ is the multi-objective function formulated from the ' m ' individual objectives $f(x)$. When $m \geq 4$ then the optimization is referred to as many-objective optimization.

Moreover, in all modern evolutionary algorithms, the balance between exploration and exploitation is a critical issue for better performance of the algorithm. Exploration refers to the global search process in objective space whereas exploitation refers to a local search around the neighbourhood of an optimal or near-optimal solution. Exhaustive exploration increases the convergence time and excessive exploitation causes the algorithm to be stuck at a local optimum point and may not reach near the global optimal solution. Therefore, the balance between exploration (global search) and exploitation (local search) is a critical issue in designing evolutionary algorithms.

In general, multi-objective evolutionary algorithms (MOEAs) are inherently designed to handle conflict goals, that minimize the distance between solutions on the Pareto front (i.e., convergence) and maximize the distribution of solutions along the Pareto front (i.e., diversity) [23]. The balance between convergence and diversity is a critical issue for obtaining qualitative and diverse trade-off solutions in MOEAs.

The multi-objective evolutionary algorithms can be divided into four categories as i) Pareto dominance based ii) decomposition based iii) indicator based and iv) model based methods. This work tried all types of multi-objective evolutionary algorithms to formulate the meter placement problem.

1. **Pareto dominance based MOEA:** The solutions are ranked based on Pareto dominance order using the non-dominated sorting method, which improves the convergence of MOEA, and the crowding distance technique is used to enhance the diversity of solutions on the Pareto front.
2. **Decomposition based MOEA:** The multi-objective problem is transformed into several single objective optimization problems. The algorithm divides the problem into subproblems using scalarization methods based on different weights. The neighbourhoods are formed based on the distance between aggregation vectors. The subproblem is simultaneously solved by exchanging information among the neighboring solutions. This improves the efficiency of searching the objective space for optimal solutions.
3. **Indicator-based MOEA:** These methods use performance indicators to guide the search process and the solutions are selected based on performance indicator value. Several types of indicator metrics are available in the literature such as hyper volume indicator, R2 indicator, inverted generational distance (IGD) and so on.
4. **Model based MOEA:** The model based MOEAs add the ability to learn from the environment in evolutionary algorithms. The traditional MOEAs such Pareto based, decomposition based, and indicator based MOEAs are designed to operate on the fixed heuristic strategies such as reproduction, selection, and variation. In the process of searching for a feasible solution, traditional MOEAs may not interact with the rapidly changing environment due to the complex properties of the problem to be solved. The model based MOEAs uses machine learning techniques to adapt to the environmental changes in the evolutionary process. The model based MOEA replaces the traditional heuristic operators such as selection, reproduction, and fitness evaluation with a machine learning model. The models use the candidate solutions as sample training data from the current generation to generate the best solutions by learning the changes in the environment.

1.9 Combinatorial Nature of Meter Placement Problem

The meter placement problem is basically a combinatorial optimization problem. The meter locations are randomly initialized at the initial stage of the evolutionary algorithm and the algorithm need to search all possible combinations of meter locations, which makes the decision space large and moreover, meter locations are represented using binary variable makes

the decision space discrete. The objective space is affected by the discrete combinatorial nature of decision space and which leads to forming a discontinuous objective space. The combinatorial optimization problems pose the challenge in searching large solution space whereas, the discontinuous objective space provides the irregular Pareto fronts, which deteriorates the performance of MOEA and reduces the diversity of the Pareto front. With the proper design of MOEAs, the issues with the combinatorial optimization problems can be addressed effectively.

Chapter 2

Literature Review

Chapter 2

Literature Review

2.1. General Overview

In recent years the availability of renewable resources in distribution system has increased, which in turn necessitates the concern for the monitoring and operation of distribution system. The uncertainty and unpredictability of renewable energy sources made the distribution system more complex to operate and control [22]. Moreover, the dynamic behavior of distribution network needs to be monitored and control to make it reliable and operate efficiently. The real-time state of the system is obtained using state estimation. The accuracy and performance of the state estimation impact the operation of distribution system as the states are used as input for control operations such as voltage stability analysis, reconfiguration, etc. [23]. The best estimation of states is obtained using state estimation (SE), which filters the errors from raw measurement data. The accuracy of the state estimation is subject to the redundancy of measurements and network observability [1]. State estimation is widely used in transmission system to determine the state of the system. whereas, due to different characteristics of distribution system, the transmission system state estimation algorithms may not be directly applicable to the distribution system. Many researchers developed specific algorithms for distribution system state estimation (DSSE). The DSSE can be formulated as i) node based DSSE and ii) branch current based DSSE.

2.1.1 Node Voltage based DSSE

Baran and Kelley [8] proposed three phase DSSE based on the WLS method with voltage magnitude and voltage angle are considered as state variables. Lu, Teng and Liu [9] proposed a DSSE algorithm by converting all the measurements into equivalent current measurements, which makes the Jacobean elements constant and equal to admittance values. The authors further extended the equivalent current based DSSE to formulate a fast decoupled method by decoupling constant gain matrix [24]. Similarly, many authors proposed node voltage based DSSE, in which node voltage magnitude and angle are considered as state variables [8]-[11].

2.1.2 Branch Current based DSSE

Baran and Kelley [12] proposed a branch current based three phase DSSE. The measurement function is expressed with phase currents to decouple the problem into three independent measurement functions. The authors showed the better results compared to node voltage based DSSE. Similarly, many branch current based DSSE techniques are proposed, which became the conventional way of designing the DSSE [12]-[17].

2.1.3. DSSE based on Meter Placement

In distribution system, the existing measurement devices are few, even though the number of nodes is very large. Therefore, with the existing inadequate measurement set, the distribution network is unobservable. To resolve this issue, Pseudo measurements are added to the measurement set in DSSE process to achieve the observability, and it improves the convergence of DSSE [21]. However, the low accuracy of Pseudo measurements propagates uncertainty in state variables. As a consequence, the accuracy of DSSE results suffer. To improve the performance of DSSE, an optimal number and appropriate type of additional real measurements are required to be deployed in distribution system.

2.2 Meter Placement Problem

Baran *et al.* [7], proposed simple rules to place the meters on the distribution system. The authors selected switching locations, which are the best locations for accurate power flow measurement, and suggested placing the meters at different locations such that the load aggregation is equal at each meter. This approach is simple and effective for the passive distribution network, whereas for active and complex distribution networks, it may not guarantee the optimal solution in terms of the number of meters and cost of the metering infrastructure.

Wang *et al.* [16], addressed impact of DSSE performance on the different type of meters and their locations. The authors concluded that power flow meters are the best among the current magnitude and voltage magnitude meters, based on the performance results of DSSE. The power flow meters and current meters improve the performance of DSSE when they are placed near the source. The voltage measurements improve the performance of DSSE when placed away from the source.

Li [25], investigated the stochastic results of DSSE and the deviation of voltage and power flow based on meter locations. The results show that the voltage deviation increase when the location of meters is away from the substation. The estimated deviation of power flow

increases once the device is far away from the substation and is also dependent on the deviation of the Pseudo measurements errors. The authors also investigated the load correlation and the results show that the higher the degree of load correlation, the lower the estimated voltage deviation will be.

The meter placement problem deals mainly with the determining of location, type, and an optimal number of meters with the desired accuracy of DSSE [26]. These three aspects are dependent on one another and also depends on the objective function, which is used to formulate the meter placement problem. Based on these aspects, different combinations of objectives have been proposed for the meter placement problem. Muscas *et al.* [27] proposed meter placement using dynamic programming based step-by-step approach for DSSE, minimization of the weighted mean value of variances of quantities is considered as an objective. Singh *et al.* [28], using an ordinal optimization algorithm (OOA), formulated a meter placement method to minimize the probability of relative state estimation errors. Likewise, several authors have attempted meter placement problem as single-objective optimization approach using conventional optimization methods [29]-[30]. The conventional optimization method may not handle the mixed variable optimization problems, struck at local optima, which requires the existing of objective function and constraint function derivatives. The limitation of conventional optimization methods can be overcome with alternative optimization techniques such as evolutionary optimization techniques, which can handle nonlinear, non-differentiable, real-world complex problems, highly constrained, high dimensionality problems, and discrete optimization problems.

In papers [31]-[33], covered an extensive review of distribution system state estimation and meter placement problem. However, much of the literature deals with single objective based optimal meter placement in distribution system state estimation. On the contrary, studies on multi-objective based optimal meter placement in distribution system have been few in literature.

In practical planning studies, while placing meters in distribution system, the decision-makers require to meet multiple objectives and the trade-off solutions among different objectives are more useful in taking a sensible decision. Therefore, meter placement is modelled as a multi-objective problem rather than single objective problem for practical applications.

Junqi Liu *et al.* [34] proposed weighted-sum-based multi-objective optimization for the trade-off between Phasor Measurement Units (PMUs) and Smart Metering (SM). In this optimization problem, the cost of PMUs and SM, relative voltage magnitude deviation, and voltage phase angle deviation are assigned with weights and then minimized the resultant weighted sum of the objective function using genetic algorithm. Linear Scalarization or Weighted-sum-based multi-objective optimization is used for solving the meter placement problem [35]-[40], in which each objective is assigned a non-negative weight, such that the sum of all the weights must become unity. However, the weighted sum based multi-objective methods fails to provide trade-off solutions. Moreover, in the case of concave Pareto fronts, weighted-sum-based multi-objective optimization gives the solutions, which are optimal in one of the objectives [41].

2.3 Multi-Objective Evolutionary Algorithms

There are many multi-objective paradigms because all different types of multi-objective problems cannot be solved by a single method [42]. The MOEAs are classified into four categories: i) Pareto dominance based ii) decomposition based iii) indicator based and iv) model based MOEAs.

1. Pareto Dominance based MOEAs: The dominance based MOEAs select the feasible solutions based on dominance order ranking. Apart from the selection of candidates, dominance methods use the secondary ranking method to improve the diversity of the Pareto front solutions. The Non-dominated Sorting Genetic Algorithm-II (NSGA-II) [43] is popular among this category. NSGA-II employs non-dominated sorting (NDS) method to identify the nondominated solutions and crowding distance is applied to preserve the population diversity. Strength Pareto evolution algorithm 2 (SPEA2) [44] and Pareto envelop-based selection algorithm-II (PESA-II) [45] are the other Pareto dominance based MOEAs. These algorithms show better performance in handling the multi-objective problems with two and three objectives. The main drawback of these methods is with increase in number of objectives the performance of MOEA deteriorates rapidly and may cause the loss of diversity in pareto front [46]. To overcome these limitations, many researchers proposed algorithms with modifications in design of Pareto based MOEA such as Grid dominance based evolutionary algorithms [47] and knee point driven evolutionary algorithm [48].

2. Weighted Sum based MOEAs: The weighted sum based MOEAs are the basic form of the decomposition based MOEAs. In these methods, the objectives are assigned with weights and

added together to form a single objective function. The sum of all the weights should equal to one, so that each objective will get its equal influence on the resultant objective value. Then the resultant objective function is solved same as the single objective optimization problem. These methods are simple in formulation of the optimization problem and converts the multi-objective problem into a single objective problem. The conventional or single objective heuristics which are useful to solve the single objective optimization problems can be directly applied to these problems. However, choosing right weight values for each objective is subject to the problem dependent. However, the limitation of these methods is that the choice of weight can influence the final optimal value of the MOEA.

3. Decomposition based MOEAs: The decomposition based MOEAs decomposes multi-objective problem into several single objective solved simultaneously. MOEA based on decomposition (MOEA/D) [49] decomposes the objective space into several sub-problems and neighborhoods defined through weight vectors. Dynamic weight based evolutionary algorithm[50], multiple single objective Pareto sampling algorithm-II [51] and multi-objective genetic local search algorithms [52] are the other methods based on decomposition. Whereas, with the uniform weight vectors these methods may not follow the shape of the Pareto front and it will adversely effect the performance of the MOEA [53].

4. Indicator based MOEAs: Indicator based MOEAs selection is guided by the performance indicator which measures the solution set performance characteristics and serves as selection criteria. Zitzler and Kunzli [54] proposed first indicator based evolutionary algorithm based on a predefined binary indicator. This method introduced the basic framework for indicator based MOEAs. Many authors proposed indicator based MOEAs such as generational distance and ϵ -dominance-based (GDE-MOEA) [55], hyper volume based MOEA [56] and R2 indicator-based many-objective metaheuristic-II (MOMBI-II) [57]. Several performance indicators are proposed through several indicator based MOEAs such as predefined binary indicator, R2 indicator, generational distance (GD) [58], inverted generational distance (IGD) [59], hyper volume (HV) indicator [60] and so on [61]- [63].

5. Model based MOEAs: The traditional MOEAs such as Pareto based, dominance based, and indicator based MOEAs are built on fixed heuristic rules. Therefore, in evolution process these MOEAs may not adapt to the changes in evolutionary environment. The model based MOEAs are designed to replace the traditional operators such as selection, reproduction, and fitness evaluations with machine learning models. This provides the ability to learn the

environment of evolutionary process by building the learning models from the candidate solutions of current generation. For training of the models, candidate solutions of the current generation in evolution process are used as sample data. The models can be replaced with the operators of traditional MOEAs such as reproduction, fitness evaluation and selection. These methos can be designed to estimate the distribution of candidate solutions. These are used as reproduction operator to generate the additional candidate solutions from the inverse model to map the objective space to decision space. when the optimization problems are computationally complex, or the fitness function is unknown then machine learning models are used as surrogate fitness functions. Bayesian multi-objective optimization algorithm (BMOA) [64], naive mixture-based multi-objective iterated density estimation evolutionary algorithm (MIDEA) [65] uses machine learning models for selections process to estimate the distribution of candidate solutions. Giagkiozis and Fleming proposed inverse-model based MOEA using Radial Basis Function Neural Networks (RBFNNs) [66] to map the objective space to decision space. Singh *et al.* proposed a surrogate-assisted simulated annealing algorithm (SASA) to evaluate the fitness function [67]. Similarly, many authors proposed model based MOEAs [68]-[70] and in-depth review can be found in [71].

Moreover, in all modern evolutionary algorithms the balance between exploration and exploitation is a critical issue for better performance of the algorithm. Exploration refers to the global search process in objective space whereas exploitation refers to a local search around the neighborhood of an optimal or near-optimal solution. Exhaustive exploration increases the convergence time and excessive exploitation causes algorithm to be struck at a local optimum point and may not reach near the global optimal solution. Therefore, proper balance is required between exploration (global search) and exploitation (local search).

In general, multi-objective evolutionary algorithms (MOEAs) are designed to handle conflict goals, that minimize the distance between solutions and Pareto front (i.e., convergence) and maximize the distribution of solutions along Pareto front (i.e., diversity) [72]. The balance between convergence and diversity is a critical issue for obtaining qualitative and diverse trade-off solutions.

2.4 Meter Placement Problem using Multi-Objective Evolutionary Algorithms

In [73], the authors proposed a Pareto-based non-dominated sorting hybrid multi-objective evolutionary optimization technique to minimize total network configuration cost, average relative percentage error of bus voltage magnitude, and voltage angle estimates. Similarly, the same authors extended their work with different objective functions using hybrid

heuristic dominance based multi-objective optimization for meter placement in distribution system state estimation [74]-[76]. However, with the increase in objectives, the objective space in size increases. Therefore, almost all solutions become non-dominated with one another. This deteriorates the selection pressure towards the set of all Pareto-optimal vectors, known as Pareto front (PF), and may even cause the loss of the population diversity in the evolutionary process to a certain extent and slows down the convergence speed of multi-objective optimization problem [77].

The shape of Pareto front of the problem to be addressed has a significant impact on MOEA's performance [78], [79]. Whereas, neither dominance-based nor decomposition-based MOEAs can handle irregular Pareto fronts. The objective values are not continuous in objective space, due to the combinatorial nature of problem [80]. As a result, objective space is discrete and Pareto front is also discontinuous in nature [81].

On the other hand, the observability analysis can be classified as i) topological observability ii) numerical observability and iii) hybrid or path-graph based observability analysis [82]. Topological observability analysis is based on graph theory, and it involves combinatorial computational complexity. Whereas the numerical observability is based on decomposing of the Jacobian matrix. If the linearly independent rows of the Jacobian matrix are equal or greater than the number of state variable, then the system is observable for a given set of measurement otherwise unobservable. In recent years, the numerical observability of distribution systems has received increased attention. Ratmir Gelagaev *et al.* [83] proposed a numerical observability analysis in distribution system by taking the X/R ratio impact on the decomposition of the Jacobian matrix. Moreover, in literature, numerical observability is not fully explored in distribution system meter placement problem.

2.5 Aims and Objectives:

The aim of the research to handle the issues with meter placement problem in the active distribution system in a multi-objective framework. The thesis addresses the issue with combinatorial optimization, discontinuous and irregular Pareto fronts, initial population diversity, search ability of the multi-objective evolutionary algorithms, and minimization of set of pseudo measurements to enhance the performance of state estimation with a set real measurement. The aims of the thesis is as follows:

- Day by day distribution system network is changing and gaining attention due to increase in addition of renewable energy sources into the system. The operation and control of distribution system became a significant area to research to address the

challenges posed by the changes in distribution network. An efficient monitoring and control algorithms need to be implemented to operate and address the challenges in distribution system.

- Distribution system as passive network, required few meter to operate the distribution system. With addition of distributed generation, the monitoring and control need to be accurate and efficient. Moreover, to monitor the active and dynamic distribution system a efficient metering infrastructure is required.
- As the meter placement problem is a offline study, the decision maker needs to inspect as many as possible trade-off solutions which are feasible in economically and technically. Therefore, a robust multi-objective solutions need to be addressed for meter placement in distribution system.
- The addition of renewable sources transform the distribution system operation and behaviour. The intermittent nature of renewable sources pose the challenges and introduces uncertainty in operation of the system. The dynamic behaviour and uncertainty of the renewable sources need to be addressed in the meter placement of distribution system.
- The distribution system need to adopt the new technology and efficient metering technologies to provide better performance. The new devices like D-PMUs and IEDs need to be considered to formulate meter placement for the distribution system and to get the improved performances of state estimation.

Objectives:

The objective of the research work is as follows:

- A new hybrid multi-objective evolutionary optimization algorithm based on decomposition and local dominance is proposed for the meter placement in distribution state estimation.
- A new indicator based multi-objective evolutionary algorithm is proposed for meter placement in active distribution system.
- A new inverse model-based multi-objective evolutionary algorithm with adaptive reference point method is proposed for meter placement in distribution system state estimation.
- The trade-off between D-PMUs and IEDs are considered to formulate the meter placement problem using inverse model-based multi-objective evolutionary

algorithm. Numerical observability method is used to minimize the number of Pseudo measurements.

2.6 Motivation

Apart from the advantages reported in the literature available, there are certain limitations. The disadvantages are listed as follows:

- In the literature, the meter placement problem is mostly formulated as a single objective optimization problem [26]-[30], whereas the practical meter placement problem deals with more than one objective, and the trade-off solutions play a significant role in taking a decision in distribution system planning.
- The weighted-sum based multi-objective approach [35]-[40] is simple to formulate and solve for the multi-objective problem. This approach transforms the multi-objective problem into a single objective problem with the aggregation of weighted objectives. Apart from the advantages, the main limitations are: (i) this approach is incapable of dealing with non-convex Pareto Front (PF). In other words, the approach provides the solutions which are optimal in one of the objectives for non-concave PF and (ii) the weight values assigned to the objective functions, largely influence the optimal solutions.
- The dominance (Pareto) based MOEAs [73]-[76] are gaining in popularity as they overcome the limitations of weighted-sum based MOEAs. The solutions are ranked based on Pareto order, instead of weighted objectives, which improves the convergence of MOEA. Then, the crowding distance method is applied to ensure the diversity of the solutions in the Pareto front. Apart from the advantages, the Pareto-based MOEAs have limitations: (i) dominance-based methods might be difficult to guarantee a measure of convergence and difficult to achieve very regular spacing of solutions in the Pareto front. (ii) With an increase in objective space, almost all solutions in a population become nondominated with one another [46]. (iii) Due to the presence of dominance resistance solutions [47], selection pressure deteriorates and may even lead to the loss of population diversity in the evolutionary process, and it deteriorates the performance of MOEA [48] and (iv) the Pareto dominance may not provide any guarantee that the solution obtained is an optimal solution, as there is no measure of performance throughout the evolutionary process.
- To overcome the issues with weighted objectives in weighted-sum-based MOEAs, in decomposition-based MOEAs the objective functions are scalarized with the weight vectors. Then, the multi-objective problem is transformed into several single objective

optimization problems [49]. The disadvantages of decomposition based MOEAs are, that (i) they require a priori knowledge of the Pareto front position in the objective space and with increase in the objective space size the number of weight vectors required might grow rapidly, even if the Pareto front is of low dimension. (ii) The weight vectors are uniformly distributed in decomposition based MOEAs. If the shape of Pareto front is irregular (disconnected, degenerated, and with sharp tails), then the best approximation of the Pareto front with uniform weight vectors cannot be obtained [53].

- Most of MOEAs use population or external archive to store non-dominated solutions obtained in each generation [84]. In general, only a limited number of diverse non-dominated solutions can be achieved in each generation, in most of population based MOEAs. However, the additional diverse solutions can be obtained by properly designing the reproduction operator in MOEA.
- Meter placement is fundamentally a combinatorial optimization problem, where the combination of meter set may not provide a continuous objective value in objective space [80]. Therefore, (i) the objective space is discrete in nature and (ii) the distribution of Pareto front is discontinuous and irregular in nature.
- The performance of MOEA strongly influences the shape of Pareto front of the problem to be solved [53], [79]. In other words, most of the MOEAs can deal with only regular Pareto front, and not just with the irregular (disconnected, degenerated, and with sharp tails) Pareto fronts.
- In distribution system, state estimation performance can be enhanced using the meter placement problem and it is handled in literature in two ways using i) topological observability and ii) numerical observability, by adding Pseudo measurements. Using topological observability-based meter placement, the total number of meters required is around one third of the number of nodes in distribution system [85]. Whereas, using the pseudo-measurement-based meter placement method the number of meters required is very less than the topological observability-based meter placement method. The advantage of a smaller number of meters is due to the additional Pseudo measurements that are supplied along with real measurements.
- However, the drawback with pseudo-measurement-based meter placement is the accuracy of state estimation suffers due to the huge error associated with Pseudo measurements. The minimum number of Pseudo measurements that are needed to be added to the measurement set is not addressed in the literature.

The research work addressed the gaps in literature and proposed new hybrid multi objective meter placement problem in distribution system to over come the limitations with single objective and weighted-sum-based MOEAs [26-40]. The work compared the different types of MOEA such as Pareto based, Dominace based, indicator based and model based MOEAs and used to formulate the meter placement problem. The thesis addresses the issue with combinatorial optimization, discontinuous and irregular Pareto fronts, initial population diversity, search ability of the multi-objective evolutionary algorithms, and minimization of set of pseudo measurements to enhance the performance of state estimation with a set real measurement.

2.7 Contributions

The objective of the thesis is to design multi-objective framework to handle the issues with the meter placement problem in distribution system.

The contributions of the thesis as follows:

- A new hybrid multi-objective evolutionary optimization algorithm based on decomposition and local dominance is proposed for the meter placement in distribution state estimation. To achieve qualitative and quantitative diverse trade-off solutions in Pareto optimal front, decomposition and dominance techniques are hybridised. In this approach, the population is initialized with the Binomial distribution-based Monte Carlo method, as the meter placement problem is a combinatorial optimization problem. Diversity improvement is the main goal of the Binomial distribution-based Monte Carlo method, as a consequence, it also improves the convergence.
- A new indicator based multi-objective evolutionary algorithm is proposed for meter placement in active distribution system. An inverted generational distance indicator with noncontributing solution detection (IGD-NS) indicator is used to evaluate the performance of the solution set and used as selection criterion. The IGD-NS indicates the diversity and convergence of the solution set and minimizes the number of solutions that have no impact on the indicator value. The objective discretization method is employed to improve the convergence and diversity of the proposed method, as each objective value spread on its own range of possible values. It enhances the search ability of MOEA and decreases the non-dominated solutions in population. The shape of the Pareto front influences the performance of a multi-objective evolutionary algorithm. Therefore, the proposed work employed a reference point method, which adaptively

update the reference points to follow the Pareto front shape. These reference points serve as priori knowledge of the approximate optimal Pareto front and in the calculation of performance indicator. The cost of meters and state estimation errors are considered as objectives to form the multi-objective optimization problem. Moreover, the impact of meter placement is investigated for various types of renewable sources and different measurement uncertainties.

- A new inverse model-based multi-objective evolutionary algorithm with adaptive reference point method is proposed for meter placement in distribution system state estimation. Inverse model generates the additional non-dominated candidate solutions by sampling the objective distribution. It improves the search efficiency and diversity of Pareto front. Meter placement is a combinatorial optimization problem consist of binary decision variables. Therefore, inverse model is realized by classification as it maps non-dominated solution from integer domain objective space to the binary domain decision space. Each meter location is represented as a label to model the binary string in decision space, as meter locations belong to multiple labels simultaneously. Therefore, inverse model is realized using multi-label Gaussian classification. The combination of meter locations may not provide continuous non-dominated solutions in Pareto front. As a consequence, discontinues Pareto front is formed. The performance of MOEA is affected by the shape of Pareto front. Therefore, adaptive reference point method is employed to follow the shape of the Pareto front. Conflicting objectives such as minimizing the cost of metering infrastructure and error in state estimates is considered, and the inverse model based multi-objective framework is used to achieve an optimal meter placement solution in an active distribution network by considering the measurement uncertainty and different types of renewable sources.
- An inverse model based many-objective evolutionary optimization is designed using four objectives as minimization of distribution level Phasor measurement units (D-PMUs) cost, minimization of intelligent electronic devices (IEDs) cost, minimization of root mean square errors of voltage magnitude and minimization of root mean square errors of voltage angle. Multi-label Gaussian classification is used to map the objective space and binary decision space in the inverse model. The trade-off between D-PMUs and IEDs are considered to formulate the meter placement problem. Numerical observability method is used to minimize the number of Pseudo measurements for a given set of real measurements, which are generated by evolutionary optimization.

2.8 Thesis Organization

The thesis is organized as follows:

Chapter 1 introduces the distribution system state estimation and its importance in monitoring and operation of the network. It briefly describes about the necessity of meter placement and the impact of renewable energy penetration in the distribution system. It describes the basics of meter placement and distribution system state estimation.

Chapter 2 provides a detailed literature review on the meter placement problem in distribution system and discusses the existing methods of the research topic. It provides various methods used to formulate the meter placement problem such as single objective and multi-objective frameworks and discusses the different optimization techniques to handle the problem.

Following an extensive literature review on the topic, the motivation of the proposed research work is presented, then objectives, contributions, and the organization of the thesis are presented.

Chapter 3 describes a new hybrid multi-objective evolutionary optimization algorithm based on decomposition and local dominance for meter placement in distribution system state estimation. The trade-off between three objectives is considered, which are minimizing the cost of the meters, average relative percentage error (ARPE) of voltage magnitude, and ARPE of voltage angle. As the meter placement problem is a combinatorial optimization, the Binomial distribution-based Monte Carlo method is utilized to initialize the population, which aims to improve the diversity, as a consequence it improves the convergence. The results of the proposed method are compared with a multi-objective evolutionary algorithm based on decomposition (MOEA/D), Non-dominated sorting genetic algorithm-II (NSGA-II) and with multi-objective hybrid particle swarm optimization- krill herd algorithm (PSO-KH), multi-objective hybrid estimation of distribution algorithm- interior point method (EDA-IPM) and demonstrated on PG&E 69-bus distribution system and Indian Practical 85-bus distribution system.

Chapter 4 presents a new indicator-based multi-objective evolutionary algorithm (MOEA) using the objective discretization method for meter placement in active distribution system. As the meter placement problem is a combinatorial optimization, a combination of measurement sets produces a discrete objective space. Therefore, the objective discretization method has been adopted to improve the performance of MOEA. The proposed MOEA is an indicator-based method based on inverted generational distance indictor with noncontributing solution

detection (IGD-NS) and with adaptive reference point method. The performance of MOEA mostly depends on the Pareto front shape, therefore the proposed method employs an adaptive reference point approach to follow the shape of the Pareto front. Moreover, the effect of distributed generation is investigated on distribution system state estimation performance for different measurement uncertainty as well as for various distributed renewable generations. The meter placement problem is modeled as a multi-objective problem with the objectives consisting of minimization of total meter cost and state estimation errors. The versatility of the proposed method is demonstrated on PG&E 69-bus distribution system and Indian Practical 85-bus distribution system. The results obtained are compared to existing MOEAs, to demonstrate the superiority of the proposed method over other methods.

Chapter 5 addresses a new inverse model-based multi-objective evolutionary algorithm for meter placement in active distribution system state estimation. The inverse model maps the non-dominated solution from objective space to decision space and is realized using multi-label Gaussian classification. The additional solutions are generated by sampling from the inverse model, which improves the search efficiency and diversity of Pareto front solutions. The combinatorial nature of the meter placement problem may produce a discontinuous Pareto front. Therefore, the adaptive reference point method is employed to adjust the reference points such that they follow the discontinuous Pareto front. The meter placement is designed as a multi-objective problem with conflict objectives such as meter cost, the estimated error of voltage magnitude, and voltage angle. The proposed method is tested under different real measurement uncertainties and for passive and active distribution networks. Different types of renewable sources are considered in the active distribution system. The superiority of the proposed method is validated by comparing it with other multi-objective evolutionary algorithms and tested on PG&E 69-bus distribution system and Indian Practical 85-bus distribution system.

Chapter 6 proposes many-objective evolutionary optimization for meter placement in active distribution system based on numerical observability. The meter placement problem can be formulated i) based on topological observability, in which the meter placement depends on the connectivity of the network, on the other hand, ii) the network can be made numerically observable by adding all node power injections as Pseudo measurements and formulated as combinatorial optimization with state estimation accuracy as an objective. The second approach is more popular as it ensures the accuracy of state estimates and requires a small number of real measurements compared to topological observability. Moreover, the addition

of Pseudo measurements improves the convergence of state estimation and ensures the observability of the network. Whereas, the huge errors associated with Pseudo measurements deteriorate the performance of state estimation. Therefore, for the first time, in the meter placement problem, numerical observability method is used to select the minimum number of Pseudo measurements to ensure the observability and improve the accuracy of the state estimation for a given set of real measurement combinations. The meter placement problem is designed as many-objective evolutionary optimization with four objectives as i) cost of D-PMUs ii) cost of IEDs iii) root mean square error of voltage magnitude and iv) root mean square error of voltage angle. The proposed many-objective evolutionary optimization is utilizing the inverse model that uses multi-label Gaussian process classification as a model to generate meter locations mapped to objective space, which enhances the search ability and diversity of evolutionary optimization. The impact of distributed generation, as well as various real measurement uncertainties, are taken into account to validate the proposed method, which is tested using the PG&E 69-bus distribution system and Indian Practical 85-bus distribution systems.

Chapter 7 summarizes the research contribution, findings, and observations on the proposed research work. Then it presents the scope for the future work that can be preceded in the topic.

2.9 Summary

This chapter provides existing literature on meter placement in distribution system. With the penetration of renewable energy sources, distribution system operation becomes more challenging. The state estimation plays a vital role in distribution system operation and control. The characteristics of distribution system required to formulate the specific algorithms for distribution system state estimation (DSSE). This chapter discusses the different DSSE solutions in literature.

DSSE performance is mainly depends on redundancy of measurements and observability of the network. Current distribution network has limited number of meters in the network, in spite of having large size of the network. To make network observable additional meters need to be placed optimally with in the financial feasibility. This chapter discusses the impact of meter placement due to different factors such as type of meters, location of meters and so on. This chapter provides multi-objective meter placement problem related existing research and presents the discussion on various types of multi-objective evolutionary

algorithms. Furthermore, motivation, contributions and organization of thesis are presented in this chapter.

Chapter 3

Multi-Objective Meter Placement in Distribution System State Estimation Using Hybrid Decomposition and Local Dominance Method

Published in

Bhanu Prasad Chintala, D. M. Vinod Kumar, “Multi-Objective Hybrid Decomposition and Local Dominance based Meter Placement for Distribution System State Estimation” **IET Generation, Transmission and Distribution**, Vol. 14, No. 20, pp. 4416-4425, September 2020.

Chapter 3

Multi-Objective Meter Placement in Distribution System State Estimation Using Hybrid Decomposition and Local Dominance Method

3.1 Introduction

In recent years, the distribution system is adopting changes and advancements of smart grid technologies and becoming more dynamic in behavior as it is changing from passive to an active network, due to the penetration of Distributed Generation (DG). These changes are necessary to enhance the real-time monitoring and control actions of the distribution system. The network states are required to be monitored and accurately estimated as they are fed as input to different control functions such as network reconfiguration, volt-var control, restoration so on. The best estimate of states is obtained using state estimation (SE), which filters the errors from raw measurement data. The accuracy of the state estimation is subject to the redundancy of measurements and the network observability. In distribution system, the existing measurement devices are few as the number of nodes is very large. Therefore, with the existing inadequate measurement set, the distribution network is unobservable. To resolve this issue, Pseudo measurements are added to the measurement set in Distribution System State Estimation (DSSE) process to achieve the observability, and it improves the convergence of DSSE. However, the low accuracy of Pseudo measurements propagates uncertainty in state variables. As a consequence, the accuracy of DSSE results suffer. Therefore, to improve the performance of DSSE, an appropriate number and type of additional real measurements are required to be deployed in distribution system at proper nodes.

This chapter proposed the meter placement problem in distribution system state estimation with a multi-objective evolutionary optimization algorithm based on decomposition and local dominance. The proposed optimal meter placement problem considered the allocation of power flow meter (PM) and Voltage magnitude meter (VMM) devices, as they are economical and readily available compared to Phasor Measurement Units (PMU) and Distribution level Phasor Measurement Units (D-PMUs). The meter placement is mainly a combinatorial optimization problem, with an increase in distribution network size, the placement locations increase, because of which individual candidate solution (chromosome) size also increases. Therefore, the diversity of the initial population may not be assured with a long binary chromosome. The work utilizes the Binary distribution-based Monte Carlo method to initialize the population with better distribution, which improves diversity, therefore it

improves the convergence, which is a by-product of this method. The main contributions of the work are as follows:

- i. A new hybrid multi-objective evolutionary optimization algorithm based on decomposition and local dominance is proposed for the meter placement in distribution state estimation.
- ii. To achieve qualitative and quantitative diverse trade-off solutions in Pareto optimal front, decomposition and dominance techniques are hybridized.
- iii. The proposed work initializes the population with the Binomial distribution-based Monte Carlo method, as the meter placement problem is a combinatorial optimization problem. Diversity improvement is the main goal of the Binomial distribution-based Monte Carlo method; therefore, it improves the convergence, which is a by-product of this method.

3.2 Problem Formulation

The proposed multi-objective evolutionary algorithm based meter placement problem considered the minimization of three objective functions: i) total cost of measurement devices (J_1) ii) the average relative percentage error (ARPE) of voltage magnitude (J_2) and iii) the average relative percentage error (ARPE) of voltage angle (J_3). The objectives that were considered can be described as follows:

$$\text{Min } J_1 = \sum_{i=1}^{nl} C_{PM,i} \cdot U_{PM,i} + \sum_{j=1}^n C_{VMM,j} \cdot U_{VMM,j} = X \cdot C^T$$

Where $X = [U_{PM}, U_{VMM}]$ and $C = [C_{PM}, C_{VMM}]$

(3.1)

$$\text{Min } J_2 = \frac{1}{m} \sum_m \frac{1}{n} \left(\sum_{i=1}^n \frac{V_i^t - \hat{V}_i}{V_i^t} \right) \times 100$$

(3.2)

$$\text{Min } J_3 = \frac{1}{m} \sum_m \frac{1}{n} \left(\sum_{i=1}^n \frac{\delta_i^t - \hat{\delta}_i}{\delta_i^t} \right) \times 100$$

(3.3)

Subjected to constraints of prespecified limits of voltage magnitude and voltage angle relative deviation as 1% and 5%, respectively for 95% of simulated cases [30]. The constraints are expressed as follows

$$g_1 = \left| \frac{V_i^t - \hat{V}_i}{V_i^t} \right| < 1\% \quad (3.4)$$

$$g_2 = \left| \frac{\delta_i^t - \hat{\delta}_i}{\delta_i^t} \right| < 5\% \quad (3.5)$$

Where J_1, J_2, J_3 are three objective functions, n, nl are the number of nodes and lines in distribution system, m is the scenarios considered for Monte Carlo simulation, C_{PM}, C_{VMM} represents the relative normalized costs of power flow measurement and voltage magnitude measurement devices. The proposed work is considered VMM as a default measurement. Therefore, the normalized cost of VMM and PM are considered the same per unit device and considered normalized cost as 1 per unit device. U_{PM} and U_{VMM} indicate the locations of power flow meter represented as '1' in case of a device placed at a particular node or line and described as '0' otherwise. Where, g_1 and g_2 are inequality constraints of relative voltage magnitude and voltage angle limits, V^t, \hat{V}, δ^t and $\hat{\delta}$ are the true value of voltage magnitude, estimated voltage magnitude, the true value of voltage angle, and estimated voltage angle, respectively. Branch current based distribution system state estimation (BC-DSSE) algorithm is used to estimate the state variables such as branch current magnitude and angle along with slack bus voltage magnitude and slack bus voltage angle [16]-[17].

The next section describes the solution methodology of the proposed hybrid multi-objective evolutionary algorithm based on decomposition and local dominance method for meter placement in distribution system state estimation.

3.3 Methodology

The proposed multi-objective evolutionary algorithm (MOEA) combines the decomposition and non-dominance sorting techniques for the selection of local solutions [49], [86]. The non-dominance sorting and decomposition techniques are adopted from NSGA-II [43], MOEA/D [49] algorithms and combined to exploit their advantages and to balance between convergence and diversity of solutions in Pareto Front.

The MOEAs give trade-off solutions in objective space and are distributed on the Pareto front. The NSGA-II ranks each solution using non-dominated sorting based on the Pareto dominance order. Whereas decomposition based MOEA (MOEA/D) employs weight vectors to decompose the multi-objective optimization problem into several subproblems. Then optimize the subproblems simultaneously. The neighborhoods are formed based on the distance between weight vectors. The neighborhood information is used to select the solutions in each population evolution. Penalty based intersection (PBI) method is used to assign each solution a relative fitness value [49]. The PBI is expressed as follows:

$$PBI(X|w, z^*) = \text{minimise } g^{bip}(X|w, z^*) = d_1 + \theta d_2$$

$$\text{where } d_1 = \frac{\|(z^* - F(X)^T \cdot w)\|}{\|w\|}$$

$$d_2 = \|F(X) - (z^* - d_1 \cdot w)\|$$

Where $X = [U_{pf}, U_{VMM}]$ and $F(X) = [J_1, J_2, J_3]$

(3.6)

Where z^* is the ideal point, w is the weight vector associated with solution X , θ is the penalty factor. The combined PBI method and dominance are used to select the local solutions of neighborhood defined by a weight vector.

3.4 The Proposed Algorithm

The proposed algorithm generates an initial population randomly of size 'N,' with binary strings indicating the locations of power flow measurements on each line. The uniformly distributed weight vectors are generated using a systematic sampling approach (SSA) [87]. Each individual in the population is assigned weight vectors and attached to a neighborhood. Then the mating parents are chosen from the neighboring region with a selection probability of ' δ ' using the minimum angle criteria. The value of selection probability ' δ ' typically assigned as 0.8. The angle criterion is used to find the nearest neighbors of weight vectors. The closest neighbors are selected with a minimum value of the angle between the weight vectors. Each weight vector is assigned with a neighborhood-based on the angle. For each weight vector, a pair of mating parents are selected from neighborhood-based on associated weight vectors, in the mating procedure. If there is no individual in the selected nearby region, then the mating parent is chosen from the whole population. The angle criteria used to select

the neighboring subregion for each weight vector [86]. The angle criteria are expressed as follows:

$$\tan \varphi = \frac{d_2}{d_1}$$

where $d_1 = \frac{\|w_i^T \cdot w_j\|}{\|w_j\|}$

and $d_2 = \left\| w_i - d_1 \frac{w_j}{\|w_j\|} \right\|$

where $i, j = 1, 2, \dots, N$ and $i \neq j$

(3.7)

Where w is the weight vector, φ is the angle between d_1 and d_2 , N is the size of the population and equal to the number of weight vectors.

The genetic operators such as two-point crossover and mutation are applied to reproduce the new offspring population. Old and new populations are combined and divided into ‘N’ subpopulation by comparing each solution using PBI method (3.6) and non-dominated sorting method for local solutions of neighborhood defined by a weight vector. Then the elitist selection process is applied to ‘N’ subpopulations to choose competent individuals. This process is repeated until the termination criterion is met. This method used a maximum number of generations as termination criteria. A fuzzy min-max method is used to determine the optimal solution from the final Pareto optimal front [88].

3.5 The Binomial Distribution based Monte Carlo Method for Population Initialization

The meter placement problem is a combinatorial optimization problem. A better-distributed combination of meter locations in the initial population improves the diversity of solutions in the objective space. The diversity of the initial population improves the searching operation of the problem; therefore, convergence improves; this is a by-product of the Binomial distribution-based Monte Carlo method. The authors in [89], initialized the population using a normal distribution with upper and lower limits as probability scaling parameters. However, in this combinatorial optimization problem, the normal distribution is not appropriate to generate the initial population. The distribution with continuous variables can be expressed using a normal distribution. However, the meter placement problem is basically a combinatorial

optimization problem. The placement of measurement devices is represented with binary variables ($X = [U_{pf}, U_{VMM}]$) as specified in equation (3.1). Where, X indicates the meter placement in a binary variable as '1' when the meter is placed in a specific location, otherwise with '0'. Thus, the Binomial distribution is suitable to represent the binary variables. Therefore, the proposed method utilized Binomial distribution to generate an initial population. The Binomial distribution models the trials of repeated experiments with a constant probability of success of each trial. The Binomial distribution is expressed as follows:

$$f(l|N, p) = \binom{N}{l} p^l (1-p)^{l}; \quad (3.8)$$

Where l is equal to the length of X , and **where** $X = [U_{pf}, U_{VMM}]$, l is the number of outcomes in 'n' trials of a Bernoulli process with a probability of success 'p.'

The meter placement problem is a combinatorial optimization; therefore, each meter placement can be considered as one trial in Binomial distribution. The set of measurements obtained from each chromosome can be represented in the binary string as 'X' vector in objective (3.1). The length of the binary string depends on the size of the distribution network. Therefore, the length of 'X' vector in (3.1) is treated as a total number of trials in the Binomial distribution. However, in distribution system, the increase in the number of meters, the accuracy of DSSE increases. But, at the same time, a large number of meter installation may not be a solution, as it increases the cost. The proposed multi-objective algorithm aims to find optimal solutions; the combination of initial meters affects the quality of solution and convergence. The combination of meters should be better distributed in the initial population so that the diversity of individuals improves. Therefore, the Binomial distribution models the combination of meters, with better distribution of the initial population through Monte Carlo simulation.

To model binomial distribution, the probability of success 'p' needs to be defined. In [85] suggested that the number of meters required for a distribution system to be topologically observable is one third (33%) of the distribution network size. The authors have also shown that, with Pseudo measurements, only 20% of meters are required for numerical observability. Thus, in this work, the population is initialized with 15% extra meters with topological observability, that is, 48% of network size, is considered as an initial number of meters. These number of meters were distributed in the initial population with Binomial distribution with the probability of success 'p' being 48%.

The multi-objective evolutionary algorithms (MOEAs) are inherently designed to handle conflict goals, that minimize the distance between solutions and Pareto front (i.e., convergence) and maximize the distribution of solutions along Pareto front (i.e., diversity). The balance between convergence and diversity is a critical issue for obtaining qualitative and diverse trade-off solutions.

Diversity is the main goal of the Binomial distribution-based Monte Carlo method. This improvement in diversity arises a question of balance between diversity and convergence, to examine the same, this work investigated the convergence and diversity improvement in MOEA. The proposed algorithm with the Binomial distribution-based Monte Carlo method improved diversity and convergence compared to the conventional proposed method. The algorithm was run several times to test performance characteristics with the initial population generated by the Binomial distribution-based Monte Carlo method. To show the versatility of the proposed Binomial distribution-based Monte Carlo method, the performance (diversity and convergence) characteristics are investigated, which is based on the performance metric Inverted Generational Distance (IGD). The definition of IGD [59], [90] is as follows:

$$IGD(P, P^*) = \frac{\sum_{x \in P^*} \min_{y \in P} dis(x, y)}{|P^*|} \quad (3.9)$$

Where P is objective function values of non-dominated solutions, P^* is the set of uniformly distributed weight vectors sampled from the Pareto optimal front and $dis(x, y)$ represents the Euclidean distance between solutions x and y . IGD metric calculates the average minimum distance from each weight in P^* to those in P , which measures the convergence and diversity of solution set P . A small value of IGD indicates a better convergence and diversity of solution set P .

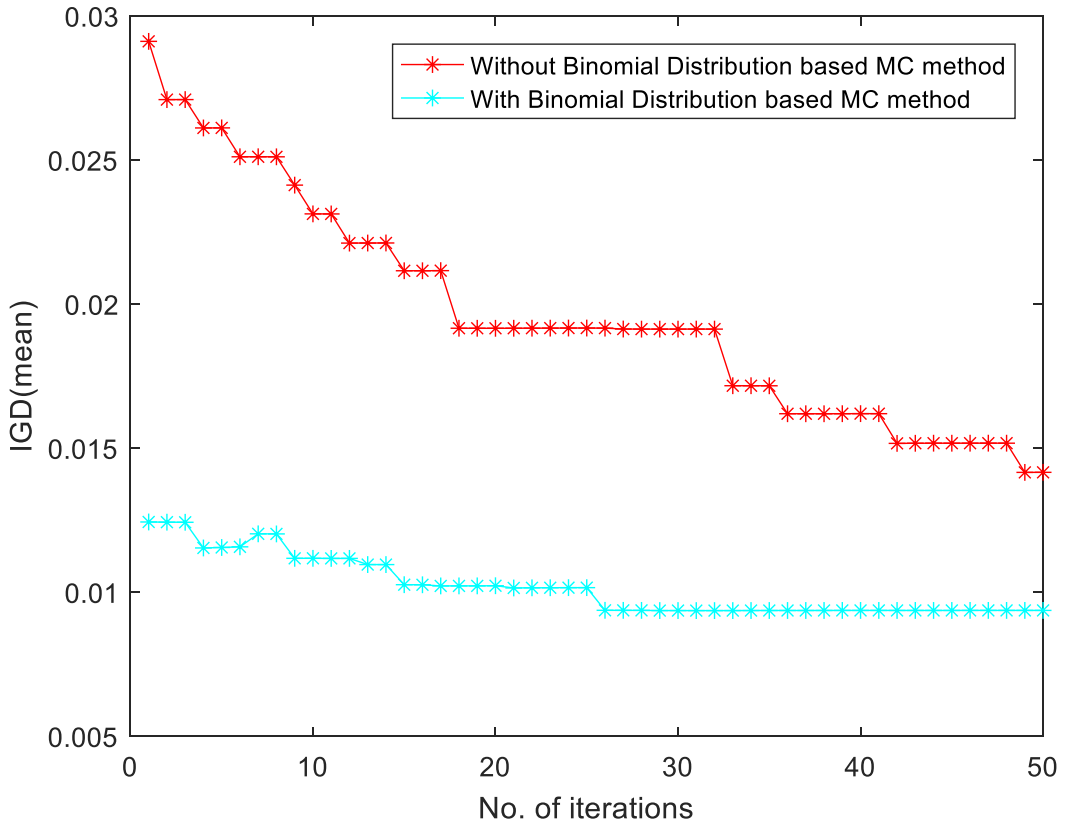


Fig. 3.1: Indian Practical 85-bus distribution system: The performance characteristics with and without the Binomial Distribution based Monte Carlo simulation method.

The performance characteristics of the proposed algorithm for a typical trial are shown in fig. 3.1. The IGD performance metric measures the diversity and convergence of the proposed MOEA. It is observed from fig. 3.1 that, the proposed MOEA with Binomial distribution-based Monte Carlo simulation yield better convergence and diversity compared to without Binomial distribution-based Monte Carlo simulation.

The pseudo-code of the proposed hybrid multi-objective evolutionary algorithm-based decomposition and local dominance method as follows:

Initialization: Generate initial population (P_t) with size N . Each candidate of the population generates the random number of power flow measurement devices and their location. Generate the uniformly distributed weight vectors using SSA [87], and the number of weight vectors using SSA is calculated as follows:

$$N(D, M) = \binom{D + M - 1}{M - 1} \text{ for } D > 0 \quad (3.10)$$

Where D is the number of divisions along with each objective coordinate, and M is the number of objectives.

Then find the objective values for each population candidate by running DSSE and check the violation of constraints (3.4) and (3.5). If any objective is violating the constraints, then the objective is added with a penalty ($CV(x)$) as follows:

$$CV(x) = \sum_{j=1}^J \langle g_j(x) \rangle \quad (3.11)$$

Where $g_j(x)$ are inequality constraints, $\langle g_j(x) \rangle$ takes absolute values of $g_j(x)$ if $g_j(x) < 0$, and '0' otherwise.

Then find neighbors with minimum angles for each weight vector using angle criteria (3.7) and find the minimum values for all the objectives to form the current ideal point.

Check for Stopping Criteria and continue for further steps.

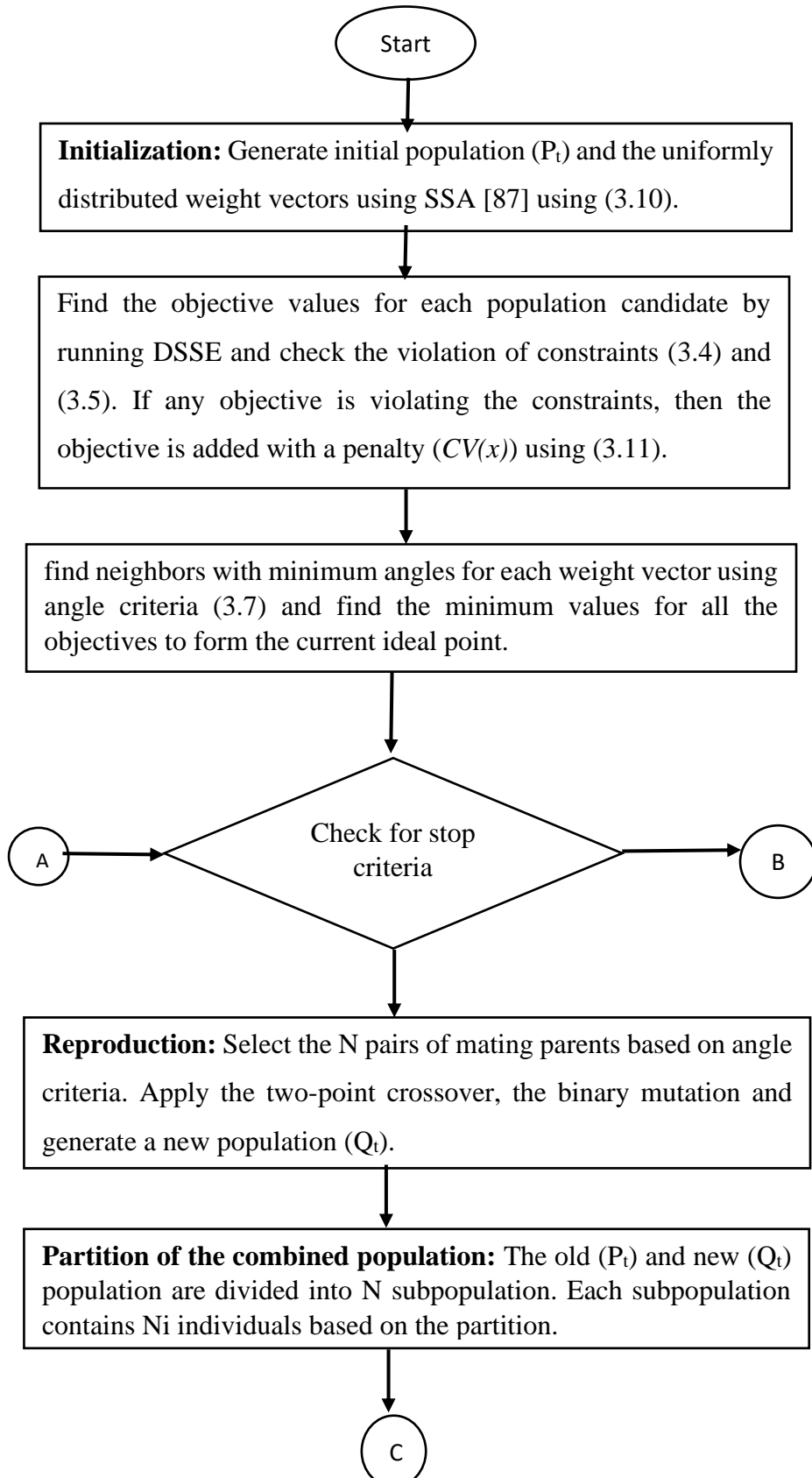
Reproduction: Select the N pairs of mating parents based on angle criteria. For each weight vector, a pair of mating parents are chosen with a probability of δ . Apply the two-point crossover for N pairs of mating parents. Apply the binary mutation to generate a new population (Q_t).

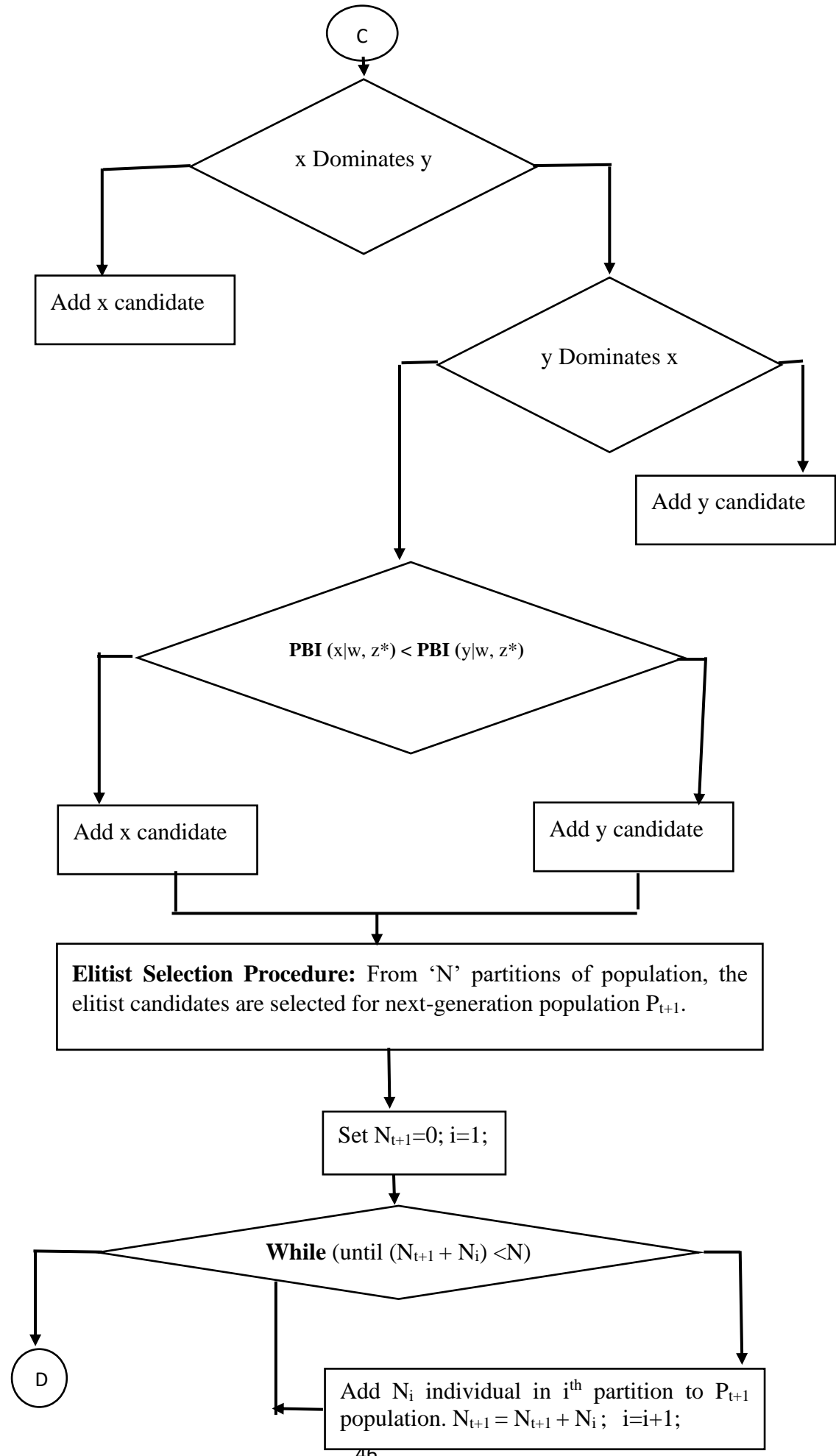
Partition of the combined population: The old (P_t) and new (Q_t) population are divided into N subpopulation. Each subpopulation contains N_i individuals based on the partition. The partition is dividing using comparing the candidates using PBI value.

Compare two individuals x and y, which are closest with associated weight vectors to divide into N subpopulations. If x dominates y return true else false otherwise compare PBI of both candidates and return the minimum PBI value candidate.

Elitist Selection Procedure: From 'N' partitions of population, the elitist candidates are selected for next-generation population P_{t+1} . Select the individual from each partition of the population until it does not exceed the population size 'N.' If the population size is less than 'N,' then chose randomly from the partitioned population.

Apply the fuzzy min-max method [88] for the final Pareto front and print the results.





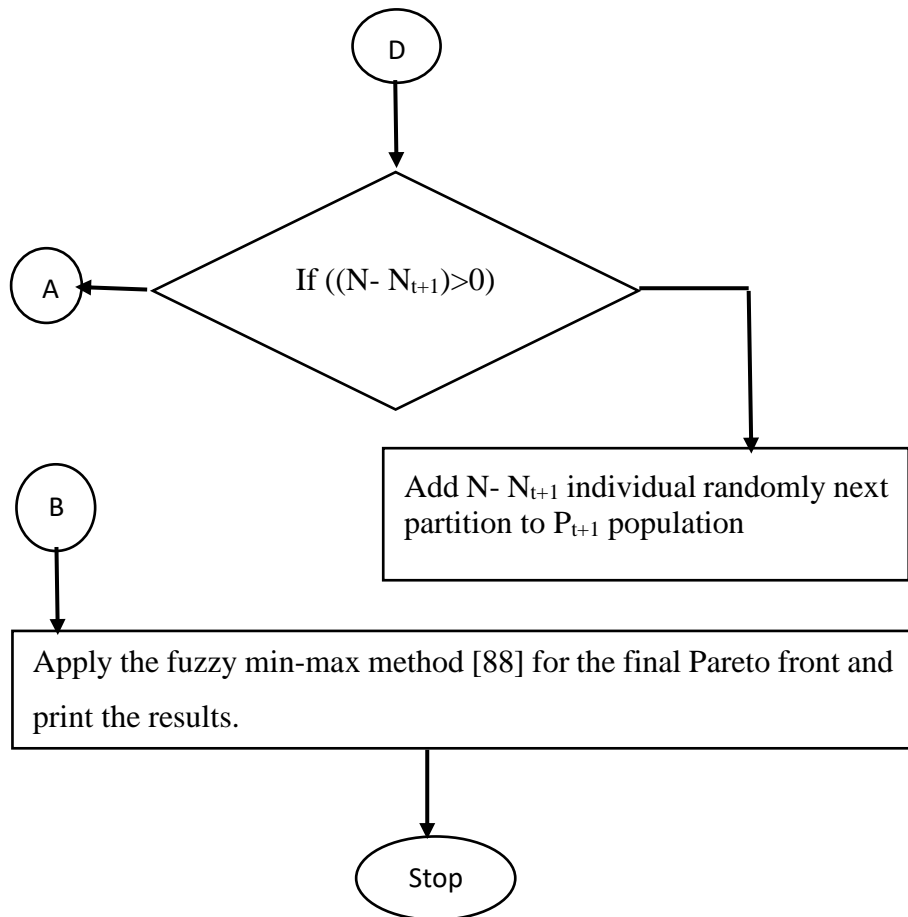


Fig. 3.2: Flowchart of proposed algorithm.

3.6 Simulation and Test Conditions

The proposed method is simulated by placing the power flow measurement devices and voltage magnitude meter. Voltage magnitude measurement device is considered as default measurement and the main aim of the proposed work is to place power flow measurements in distribution system. The active and reactive power is assumed to be obtained from a single power flow meter. In this study, a voltage magnitude meter (VMM) is placed at the substation and considered as default measurements. For SE, BC-DSSE [16]-[17] algorithm is used to estimate the states of the system for each set of measurements from the proposed algorithm. For different measurement uncertainties, Monte Carlo simulations assess the satisfactory performance of SE in terms of voltage magnitude and voltage angle, with prespecified limits of 1% and 5%, respectively, within 95% simulation cases. If the prespecified limits are violated, then the corresponding objective function is added with a penalty. In this work, 100 different network operating scenarios are considered, and each scenario is simulated for 1000 Monte Carlo trials with normally distributed measurement uncertainties to check the voltage

magnitude and angle constraint violations. Further, the following assumptions are considered for the proposed method:

- i. Voltage magnitude measurement at the slack bus and one power flow meter at the first line are considered as default measurements, and it is supplied with 1% accuracy.
- ii. Virtual measurements, on the other hand, are zero bus injection measurements, which are supplied by the operator [26]. The virtual measurements are considered as the measurements with no error [19]. These are the measurements at the nodes such as switching stations, where the power injection is equal to zero. These are treated as very accurate measurements that are no need to be measured physically. These measurements are virtually treated as measurements with no error that are supplied with low variance value. Virtual measurements are provided with a small value of standard deviation in the order of 10^{-8} [26].
- iii. To test the performance of the algorithm with large errors, Pseudo measurements are provided with a maximum error of 50% [91].
- iv. The proposed algorithm is tested for various measurement uncertainty levels by considering the real measurements with varied accuracy of 1%, 3%, and 5%.
- v. To check the voltage magnitude and angle constraint violations (4) and (5), 1000 Monte Carlo trials are carried out for different load conditions of 100 scenarios [73].

Furthermore, the parameters used for the proposed algorithm, MOEA/D, and NSGA-II are tabulated in Table-3.1. Different population sizes are tested, and it is observed that for 3 objectives, the population size with 100, is suitable to get the near-optimal solutions. The population size is considered as 100, whereas for decomposition-based methods the population size is decided based on the weight vectors, which are generated from the Systematic Sampling Approach (SSA) [87]. For the proposed method and MOEA/D, with three objectives, the population size is chosen 91 after the SSA. The number of divisions along each objective coordinate chosen as 12 ($D=12$), whereas the neighborhood size is chosen as 20 ($T=20$). The neighborhood size is chosen as 20% of the population size [49]. Divisions along each objective coordinate are chosen based on Das and Dennis Systematic Sampling Approach (SSA) [87] for the given population size and the number of objectives. With three objectives, D becomes 12 for the population size of 91 as
$$\binom{12 + 3 - 1}{3 - 1} = 91$$
 from (3.10).

Different Crossover and Mutation rates are tested and chosen Crossover rate (Pc) is 1.0, Mutation rate (Pm) is 0.05 for which it gives the better performance of the MOEA.

Table 3.1: Parameter values of the proposed algorithm, MOEA/D, NSGA-II

Algorithm	Control Parameters
The Proposed algorithm	Number of objectives (M) =3, Population size after SSA =91, the number of divisions along with each objective coordinates D=12, the neighborhood size T=20, Crossover rate (Pc)=1.0, Mutation rate (Pm)=0.05, the maximum number of generations=50
MOEA/D[49]	Number of objectives (M) =3, Population size after SSA =91, the number of divisions along with each objective coordinates D=12, the neighborhoods size T=20, Crossover rate (Pc)=1.0, Mutation rate (Pm)=0.05, the maximum number of generations=50
NSGA-II[43]	Number of objectives (M) =3, Population size =100, Crossover rate (Pc)=0.8, Mutation rate (Pm)=0.01, maximum number of generations=50

The real measurements have errors in the range of 1-5%. Pseudo measurements are based on historical data or provided by the operator based on experience. Therefore, Pseudo measurements are associated with huge errors in the range of 20- 50%. This proposed work assumed Pseudo measurements are with maximum value as 50% accuracy and real measurements are varied with 1%, 3% and 5% of the error to test the versatility of the proposed algorithm for different measurement uncertainties.

3.7 Results and Discussions

The performance of the proposed hybrid multi-objective evolutionary algorithm is verified on PG&E 69-bus distribution system and Indian Practical 85-bus distribution system.

For all figs. 3.2 to 3.7 the repeating captions are specified as given here: *(a) objective- J_2 average relative percentage error (ARPE) of voltage magnitude Vs. objective- J_3 average relative percentage error (ARPE) of voltage angle. (b) objective- J_2 average relative percentage error (ARPE) of voltage magnitude Vs. the number of power flow meters (c), objective- J_3 average relative percentage error (ARPE) of voltage angle Vs. the number of power flow meters.*

3.7.1 PG&E 69-bus Distribution System

The proposed algorithm has been tested on PG&E 69-bus distribution system [92], which has 68 lines, 21 zero bus injection nodes, and total real and reactive power load of 3.802 MW, 2.692 MVAR, respectively. The zero bus injections are modeled as virtual measurements, and

one VMM and one PM devices are considered as default measurements on the slack bus and first-line, respectively.

The performance of the proposed algorithm is tested by varying the measurement uncertainty of real meters with an accuracy of 1%, 3%, and 5%. The results are tabulated in Table-3.2, and the corresponding comparative plots of objectives are shown in figs. 3.3, 3.4, and 3.5. The results show that, with 1% accuracy of real measurements, for the proposed algorithm, the total number of measurements required is 6, including default measurements, the average relative percentage error of voltage magnitude is 0.0014%, and the average relative percentage error of voltage angle is 0.4547%. For MOEA/D, NSGA-II algorithms, including default measurements, a total of 8 and 9 meters were needed, respectively. The average relative percentage error of voltage magnitude, the average relative percentage error of voltage angle for MOEA/D, NSGA-II is 0.0019%, 0.6025%, and 0.0038%, 1.6474%, respectively. Similarly, for 3% and 5% of measurement uncertainty, the proposed algorithm performed better than MOEA/D and NSGA-II. The proposed method was compared with algorithms in the literature, PSO-KH, EDA-IPM. For PSO-KH, EDA-IPM with 1% measurement accuracy, the number of meters required is 6 and 6, respectively. The proposed method also required the same number of meters, that is, 6, but when compared with the average relative percentage error of voltage magnitude and the average relative percentage error of voltage angle, the proposed method gives better performance. The proposed algorithm also yielded better performance with 3% and 5% of metrological uncertainty when compared to PSO-KH, EDA-IPM. The numerical results, as shown in Table-3.2.

When the Pareto fronts are observed from figs. 3.3, 3.4, and 3.5, real measurement accuracy with 1%, 3%, and 5%, the proposed algorithm performed better than MOEA/D and NSGA-II, in terms of convergence and diversity of candidate solutions in the Pareto optimal front. However, MOEA/D converges better than NSGA-II, but the diversity in Pareto front is lower as it converges to the best candidates of repeated solutions. The Non-dominated sorting and dominance are combined in the proposed algorithm, it converged quickly, and the candidate solution quality is also improved as it was evident from the results shown in figs. 3.3, 3.4 and 3.5.

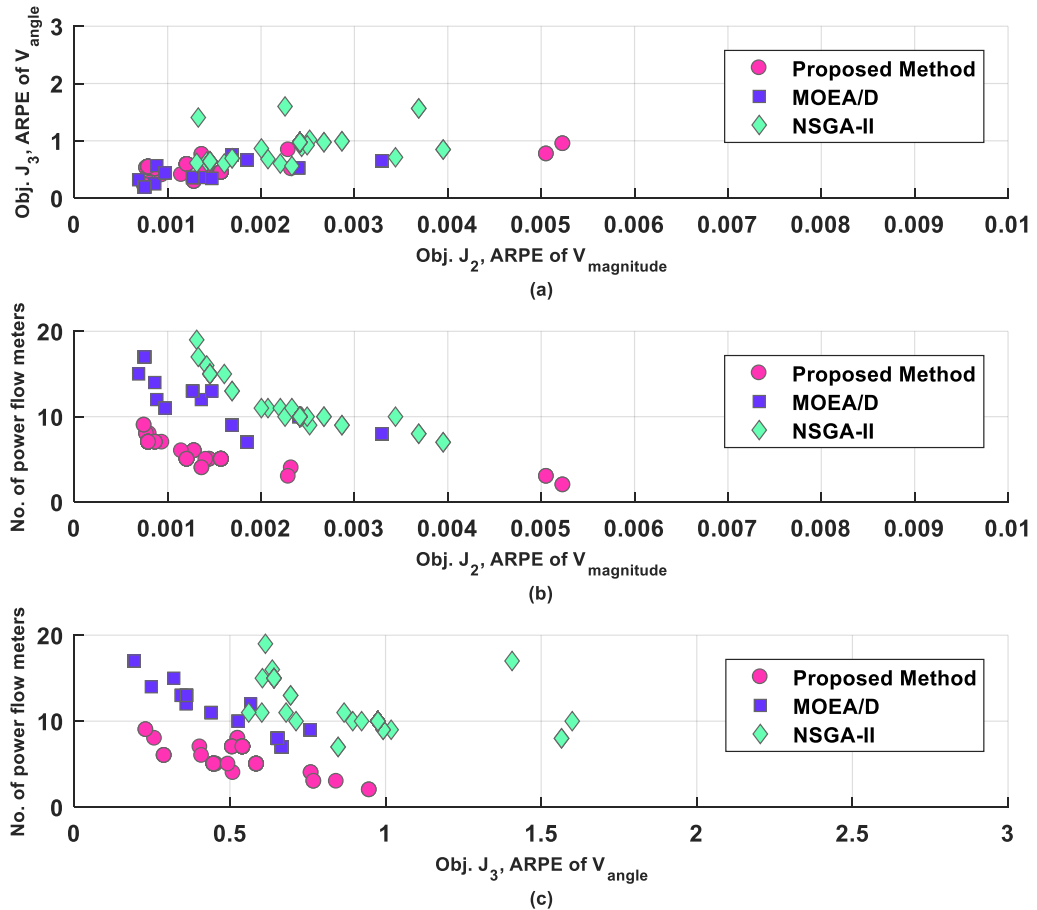


Fig. 3.3: PG&E 69-bus distribution system optimal Pareto-front plots: Real measurements with an accuracy of 1% and Pseudo measurements with an accuracy of 50%.

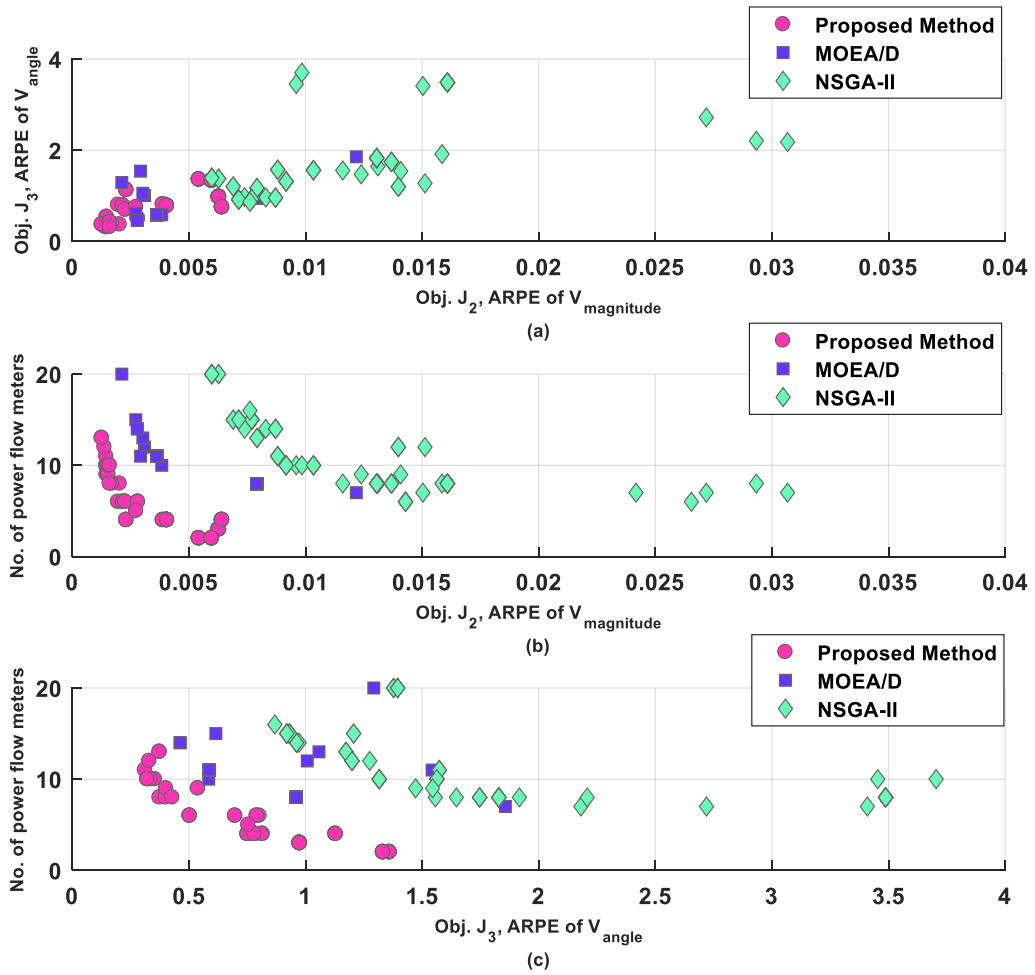


Fig. 3.4: PG&E 69-bus distribution system optimal Pareto-front plots: Real measurements with an accuracy of 3% and Pseudo measurements with an accuracy of 50%.

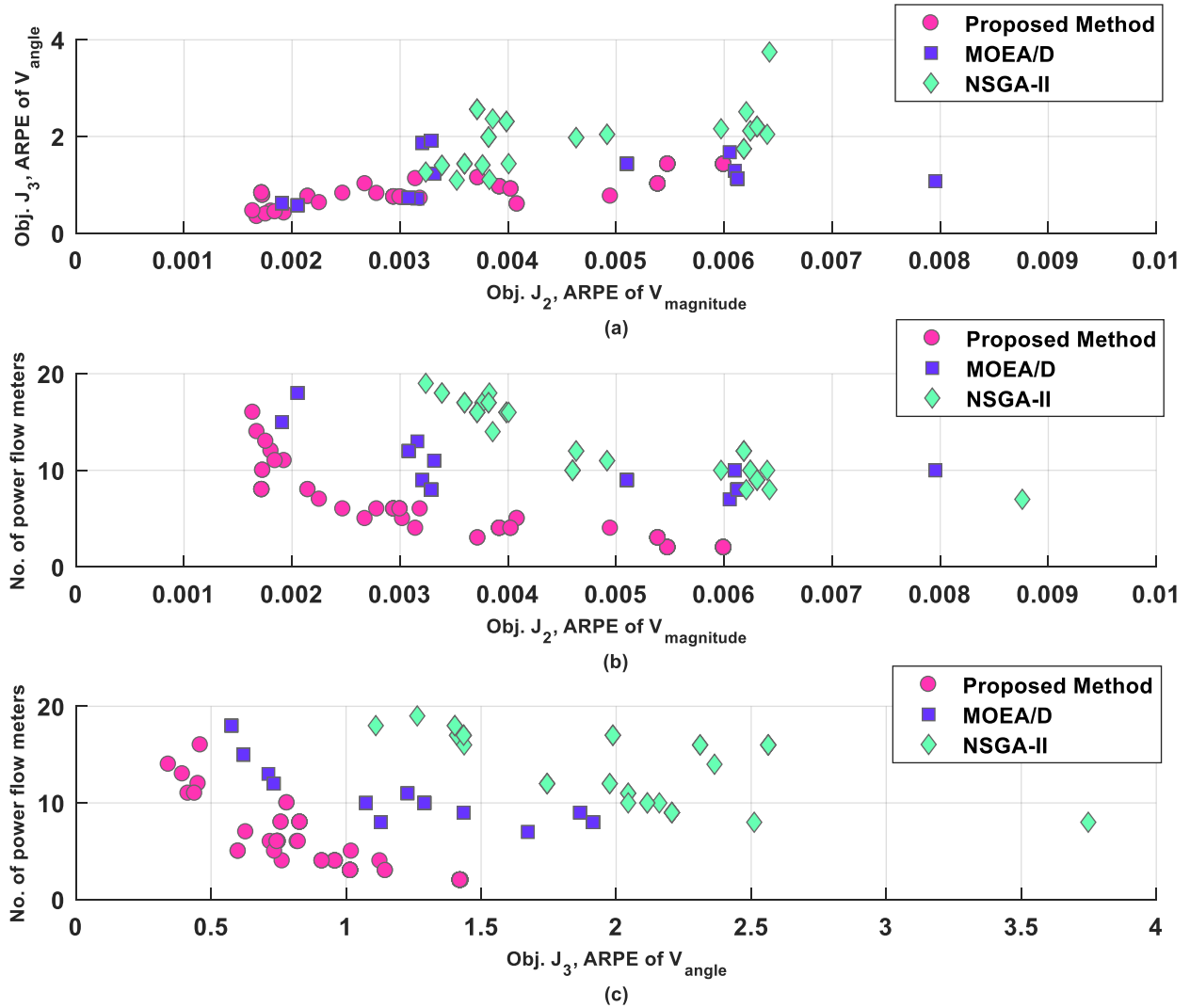


Fig. 3.5: PG&E 69-bus distribution system optimal Pareto-front plots: Real measurements with an accuracy of 5% and Pseudo measurements with an accuracy of 50%.

Table 3.2: PG&E 69-bus distribution system: Optimal location of the power flow meters under different metrological errors

Metrological error (in %)	Algorithm	Location of Power flow meters (Line numbers)	Number of power flow meters	Objective function values			Maximum error in Voltage Magnitude (in %)	Maximum error in Voltage angle (in %)
				J_1 Cost of meters (1 per unit device)	J_2 ARPE of voltage magnitude	J_3 ARPE of voltage angle		
1	Proposed algorithm	1,5,13,30,54	5	6	0.0014	0.4547	0.0158	5.1732
	MOEA/D [49]	1,6,11,28,43,53, 62	7	8	0.0019	0.6025	0.0388	5.8273
	NSGA-II [43]	1,4,10,11,12,42, 55,68	8	9	0.0038	1.6474	0.0523	6.8294
	PSO-KH [73]	1, 7, 24, 54, 66	5	6	0.0028	0.4947	0.0381	5.7922
	EDA-IPM [75]	1, 3, 7, 24, 51	5	6	0.0025	0.4821	0.0201	5.2137
3	Proposed algorithm	1,10,14,17,37, 56	6	7	0.0017	0.4906	0.0289	5.5293
	MOEA/D [49]	1,9,13,26,37,46, 59, 64	8	9	0.0055	0.9750	0.0411	5.9032
	NSGA-II [43]	1,7,14,29,32,47, 53,60	8	9	0.0118	1.5566	0.0612	7.3214
	PSO-KH [73]	1, 11, 18, 43, 52	5	6	0.0053	0.9782	0.0417	5.9154
	EDA-IPM [75]	1, 11, 19, 43, 52	5	6	0.0051	0.9657	0.0317	5.7321
5	Proposed algorithm	1,9,13, 26, 31, 46, 60	7	8	0.0023	0.6288	0.0476	5.7682
	MOEA/D [49]	1,9,13,19,30,34, 47, 63	8	9	0.0032	1.2314	0.0547	6.3262
	NSGA-II [43]	1,3,8, 14, 29, 36, 39, 45, 53, 60, 63, 66	12	13	0.0049	1.7634	0.0645	9.2437
	PSO-KH [73]	1, 7, 14, 21, 28, 33, 49, 53, 61	9	10	0.0058	1.1491	0.0523	6.3172
	EDA-IPM [75]	1, 7, 14, 19, 28, 33, 47, 53, 61	9	10	0.0056	1.1273	0.0513	6.2379

3.7.2 Indian Practical 85-bus Distribution System

The proposed method has also been investigated on Indian Practical 85-bus distribution system [93], which has 84 lines, 26 zero injection nodes, and a total load of real and reactive power of 2.574 MW and 2.622 MVAR, respectively. The zero bus injections are modeled as virtual measurements, and one VMM and one PM devices are considered as default measurements on the slack bus and first-line, respectively.

The proposed algorithm is simulated by placing the power flow meters with accuracies of 1%, 3%, and 5%, and the results are tabulated in Table-3.3. The corresponding comparative plots of objectives are shown in figs. 3.6, 3.7, and 3.8. The proposed algorithm required a total of 7 meters, including default measurements, whereas MOEA/D and NSGA-II required 10 and 11 meters, respectively. The average relative percentage error of voltage magnitude, the average relative percentage error of voltage angle for the proposed method, MOEA/D, NSGA-II is 0.0337%, 0.0385%, 0.0338%, and 0.7153%, 1.2964%, 0.8526%, respectively. In all cases of meter uncertainty with 1%, 3%, and 5%, the proposed algorithm performed better compared to MOEA/D and NSGA-II. For PSO-KH and EDA-IPM with 1% measurement accuracy, the number of meters required is 8. The proposed method only needed 7 meters, and when compared with average relative percentage error of voltage magnitude and average relative percentage error of voltage angle, the proposed method gives better performance even with 3% and 5% uncertainty cases. The results are shown in Table-3.3.

When the Pareto fronts were observed from figs. 3.6, 3.7, and 3.8 for meter accuracy with 1%, 3% and 5%, the proposed algorithm performs better than MOEA/D and NSGA-II, in terms of convergence and diversity of candidate solutions in Pareto optimal front. From the results, it is observed that with an increase in uncertainty of real measurements, the number of meters required increased, to get the satisfactory performance of DSSE in terms of voltage magnitude and voltage angle limits.

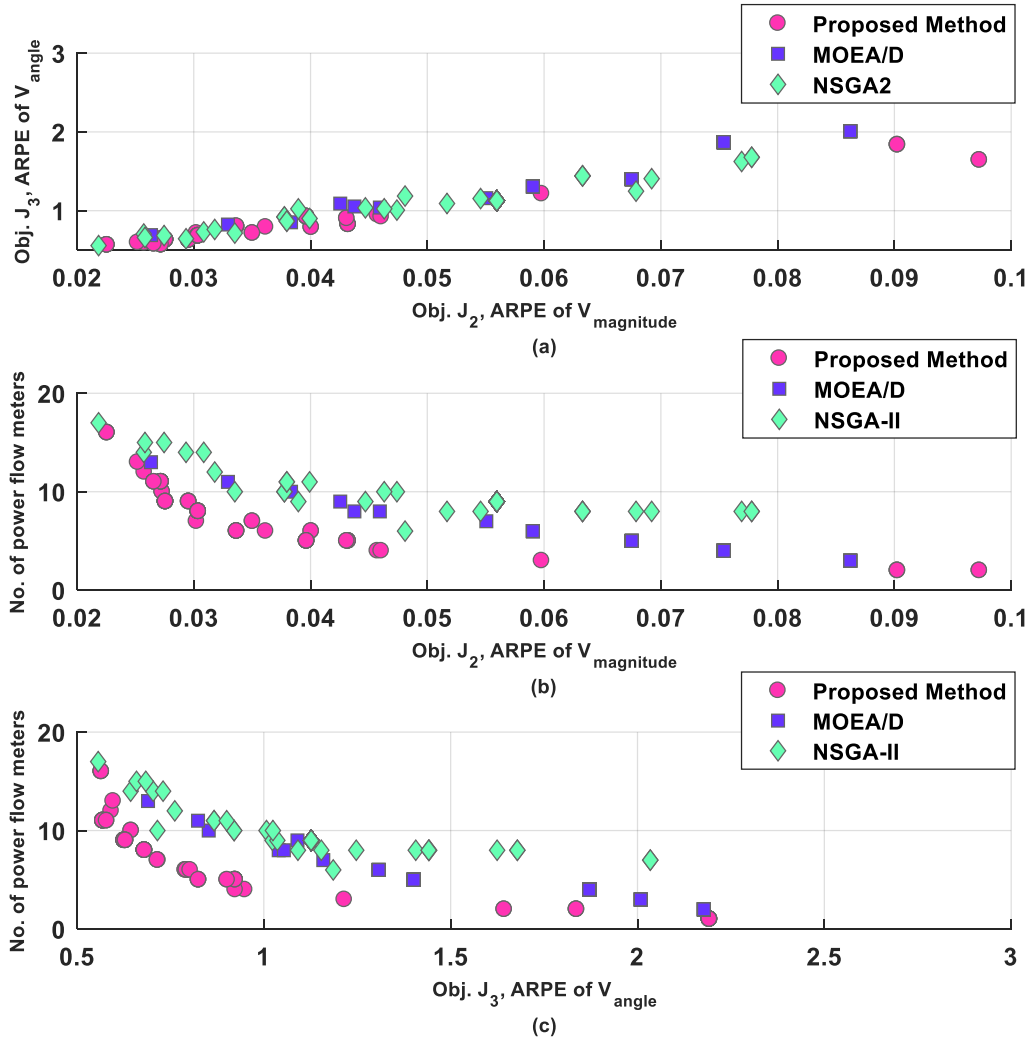


Fig. 3.6: Indian Practical 85-bus distribution system optimal Pareto-front plots: Real measurements with an accuracy of 1% and Pseudo measurements with an accuracy of 50%.

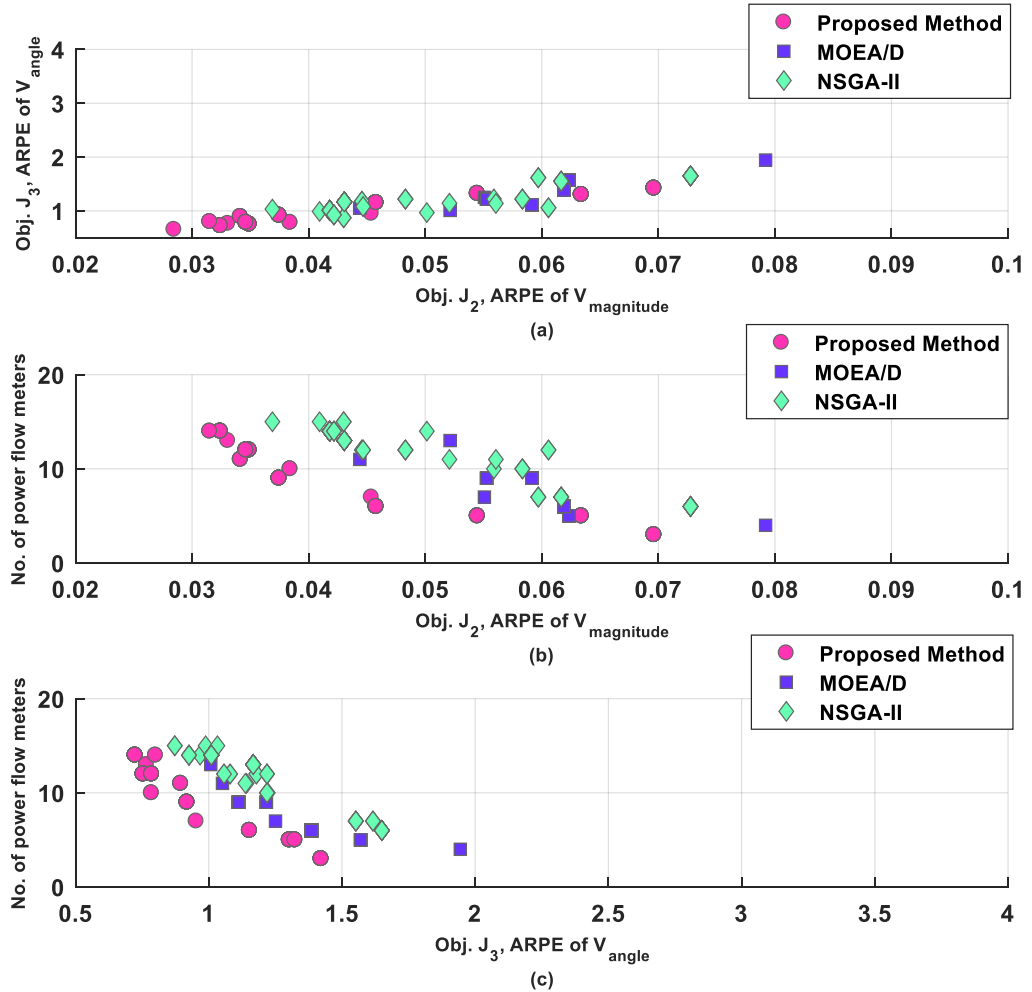


Fig. 3.7: Indian Practical 85-bus distribution system optimal Pareto-front plots: Real measurements with an accuracy of 3% and Pseudo measurements with an accuracy of 50%.

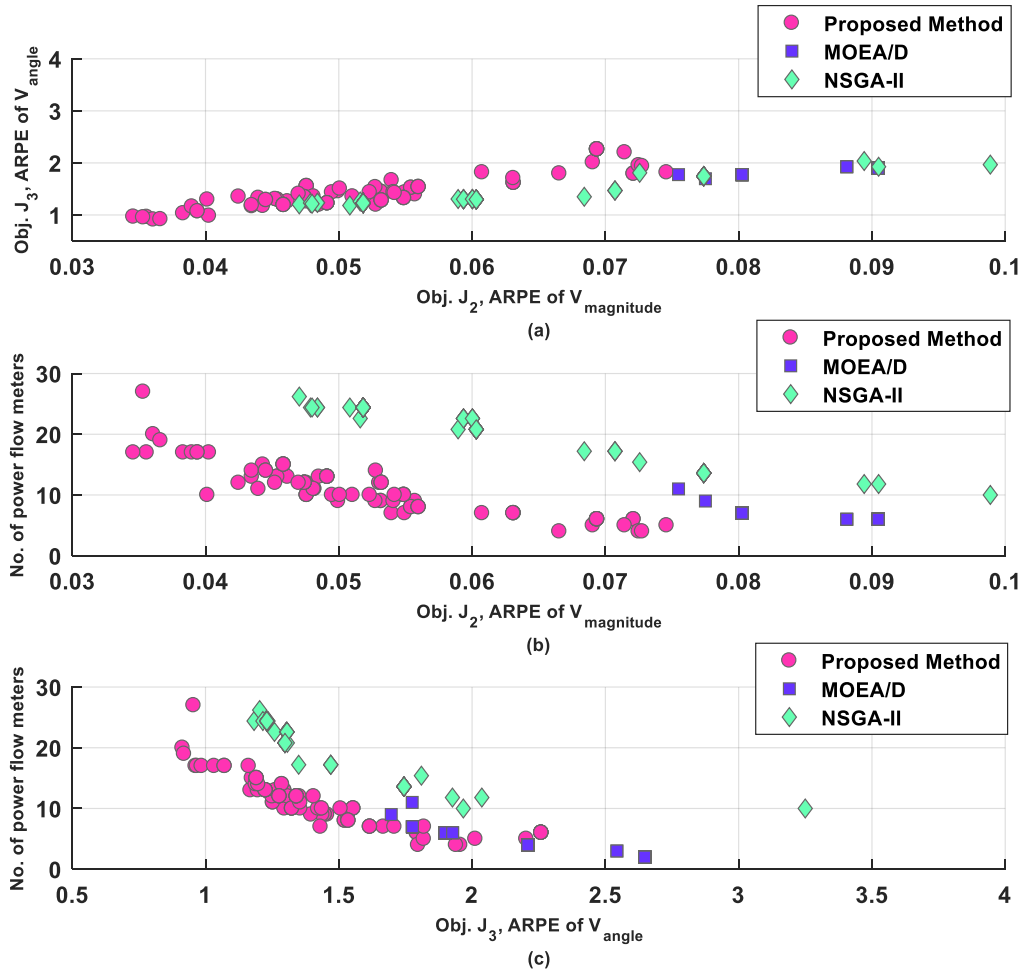


Fig. 3.8: Indian Practical 85-bus distribution system optimal Pareto-front plots: Real measurements with an accuracy of 5% and Pseudo measurements with an accuracy of 50%.

Ke Li [35] investigated the change in real-time measurement accuracy influences the results of estimation, it is evident that the effect is different for different locations. The effect will depend on the network structure. Therefore, the change in metrological error percentage has a different effect on different locations. Consequently, the meter location varies with change in real measurement accuracy. Haibin Wong *et al.* [36] also examined the issue of measurement error impact on the location of meters. The authors had shown that with the change in measurement error for different locations, based on meter type, the accuracy of distribution system state estimation varies. The same can be observed from the results, with a change in effect the location of the measurements. It is obvious that the device measurement uncertainties are specified by manufacturers. Whereas the proposed work investigated the impact of meter placement for different measurement uncertainties.

When the results of PG&E 69-bus distribution system and Indian Practical 85-bus distribution system are observed, the proposed algorithm performed better than decomposition-

based algorithm MOEA/D, Non-dominated Sorting based NSGA-II, and apart from that, it showed better results compared with other algorithms in the literature, such as PSO-KH and EDA-IPM MOEAs in terms of convergence and diversity of Pareto front as well as in the quality of solutions.

Table 3.3: Indian Practical 85-bus distribution system: Optimal location of the power flow meters under different metrological errors

Metrological error (in %)	Algorithm	Location of Power flow meters (Line numbers)	Number of power flow meters	Objective function values			Maximum error in Voltage Magnitude (in %)	Maximum error in Voltage angle (in %)
				J ₁ Cost of meters (1 per unit device)	J ₂ ARPE of voltage magnitude	J ₃ ARPE of voltage angle		
1	Proposed algorithm	1,6,11,26,30,63	6	7	0.0337	0.7153	0.1534	5.0432
	MOEA/D [49]	1,7, 16, 19, 27, 30, 47, 59, 72	9	10	0.0385	1.2964	0.1673	5.1723
	NSGA-II [43]	1,6, 7, 18, 23, 33, 35, 56, 67, 69	10	11	0.0338	0.8526	0.2089	6.1247
	PSO-KH [73]	1, 13, 18, 26, 75, 79, 84	7	8	0.0385	1.1737	0.1853	5.1722
	EDA-IPM [75]	1, 13, 19, 25, 75, 78, 84	7	8	0.0383	1.0952	0.1692	5.0660
3	Proposed algorithm	1,2, 5, 10, 30, 56, 67	7	8	0.0448	0.9184	1.7034	5.1763
	MOEA/D [49]	1,8, 16, 17, 24, 28, 33, 62, 65	9	10	0.0551	1.2506	0.2322	5.6224
	NSGA-II [43]	1,4, 8, 15, 25, 32, 54, 55, 66, 74, 84	11	12	0.0522	1.3259	0.2650	7.4781
	PSO-KH [73]	1, 17, 22, 30, 36, 73, 81	7	8	0.0438	1.3355	0.2347	5.5217
	EDA-IPM [75]	1, 34, 40, 46, 52, 53, 67, 69	8	9	0.0427	1.0433	0.2117	5.2365
5	Proposed algorithm	1,7, 26, 32, 39, 45, 57, 79, 84	9	10	0.0492	1.4288	0.2431	5.3256
	MOEA/D [49]	1,6, 8, 26, 32, 44, 54, 55, 69, 74, 83	11	12	0.0783	1.7764	0.3011	5.8867
	NSGA-II [43]	1,4, 6, 9, 26, 30, 49, 59, 63, 71, 80	11	12	0.0884	1.7494	0.3297	8.1215
	PSO-KH [73]	1, 16, 21, 24, 33, 69, 77, 79	8	9	0.0439	1.2855	0.2896	5.9407
	EDA-IPM [75]	1, 12, 20, 43, 50, 68, 75, 83	8	9	0.0464	1.4298	0.2896	5.4821

3.8 Summary

An optimal meter placement in distribution system state estimation using a new hybrid multi-objective evolutionary algorithm based on decomposition and local dominance is proposed in this chapter. Minimizing the cost of measurement devices, average relative percentage error of voltage magnitude and average relative percentage error of voltage angle are the three objectives, that are considered to evaluate the proposed algorithm. The hybridization of decomposition and dominance techniques improved the convergence and diversity of solutions in the Pareto front. As the meter placement is a combinatorial optimization problem, the population of the proposed algorithm is initialized using the Binomial distribution-based Monte Carlo method, which improved the diversity of Pareto front. Diversity improvement is the main goal of the Binomial distribution-based Monte Carlo method; therefore, it improves the convergence, which is a by-product of this method. The competent results of the proposed algorithm compared with algorithms such as MOEA/D, NSGA-II, PSO-KH, and EDA-IPM for various load demands and uncertainty of measurement devices.

The Pareto dominance and decomposition based MOEAs may not provide any guarantee that the obtained solution is an optimal, as there is no measure of performance throughout the evolutionary process. Whereas, in indicator based MOEAs, performance metric measures the performance (convergence and diversity) of a solution set and serves as selection criterion. The indicator based MOEAs overcomes the limitation of Pareto based MOEAs and decomposition based MOEAs. Therefore, chapter 4 proposes an indicator based MOEA for meter placement in active distribution system.

Chapter 4

Multi-Objective Meter Placement in Active Distribution System State Estimation using Objective Discretization and Indicator-Based Algorithm with Adaptive Reference Point Method

Published in

Bhanu Prasad Chintala, D. M. Vinod Kumar, “Meter placement in active distribution system state estimation using indicator based multi-objective evolutionary algorithm with adaptive reference point method”, accepted for publication in **Journal of Institution of Engineers (India): Series-B**, Springer Nature.

Chapter 4

Multi-Objective Meter Placement in Active Distribution System State Estimation using Objective Discretization and Indicator-Based Algorithm with Adaptive Reference Point Method

4.1 Introduction

Pareto dominance-based MOEAs are designed to address the drawbacks of weighted-sum MOEAs. The solutions are ranked based on Pareto order, which improves the convergence of MOEA, and the crowding distance approach is used to assure that the solutions are diverse. Besides the advantages, drawback of Pareto-based MOEAs is that the increase in objectives deteriorates the selection pressure and may cause a reduction in population diversity and convergence. Whereas, in decomposition-based MOEAs, the multi-objective problem is transformed into several single objective optimization problems. The drawbacks of decomposition-based MOEAs are: (i) The weight vectors are uniformly distributed in decomposition-based MOEAs. With uniformly distributed weight vectors the best approximated Pareto solutions may not be obtained for irregular (degenerated, disconnected, and with sharp tails) shape Pareto front. (ii) Even if the Pareto front is of low dimension, the number of weight vectors may rise exponentially with the objective space size. Moreover, Pareto dominance and decomposition based MOEAs may not provide any guarantee that the solution obtained is an optimal solution, as there is no measure of performance throughout the evolutionary process.

This chapter proposes a method with objective discretization and indicator-based multi-objective optimization to overcome the above drawbacks. The combination of meter set in each generation of evolution algorithm results in a discrete objective space. Therefore, the proposed method utilizes the objective discretization method, which improves the performance (convergence and diversity) of MOEA. In combinatorial multi objective optimization problem, a large possible combination of solutions in decision space is mapped to the different ranges of objective values. It means that different objective functions have different granularities (width of discretization intervals). The discretization of objective space improves the performance of combinatorial multi-objective evolutionary algorithm, as it improves the search ability of

MOEA and reduces the non-dominated solutions in population. The indicator measures the performance of a solution set and serves as selection criterion. The indicator based MOEAs overcomes the limitation of Pareto based MOEAs, because they improve the selection pressure. As the evolution process is guided by a performance indicator, it ensures that the best solutions are found throughout the evolutionary process. The proposed method is based on inverted generational distance indicator with noncontributing solution detection (IGD-NS) performance metric, which indicates the performance of solution set in terms of convergence and diversity, while also minimizing the number of noncontributing solutions in population. The noncontributing solutions are the nondominated solutions, which are away from any reference point and do not contribute to the value of the performance metric. The IGD-NS calculation requires *a priori* knowledge of approximate Pareto front. A study reveals that the shape of Pareto front, strongly influences the performance of MOEAs [53]. Therefore, the proposed method utilizes an adaptive reference point approach to follow the approximate Pareto front shape. The work has following main contributions:

- i. The objective discretization method is employed to improve the convergence and diversity of the proposed method, as each objective value spread on its own range of possible values. It enhances the search ability of MOEA and decreases the non-dominated solutions in population.
- ii. A new indicator based multi-objective evolutionary algorithm is proposed for meter placement in active distribution system. An inverted generational distance indicator with noncontributing solution detection (IGD-NS) indicator is used to evaluate the performance of the solution set and used as selection criterion. The IGD-NS indicates the diversity and convergence of the solution set and minimizes the number of solutions that have no impact on the indicator value.
- iii. The shape of the Pareto front influences the performance of a multi-objective evolutionary algorithm. Therefore, the proposed work employed a reference point method, which adaptively update the reference points to follow the Pareto front shape. These reference points serve as *a priori* knowledge of the approximate optimal Pareto front in the calculation of performance indicator.
- iv. The cost of meters and state estimation errors are considered as objectives to form the multi-objective optimization problem. Moreover, the impact of meter placement is

investigated for various types of renewable sources and different measurement uncertainties.

4.2 Problem Formulation

The multi-objective meter placement problem is formulated using three objectives: i) minimizing the cost of meters (J_1) ii) minimizing the average relative percentage error (ARPE) of voltage magnitude (J_2) and iii) minimizing the average relative percentage error (ARPE) of voltage angle (J_3). The objectives are given as follows:

$$\text{Min } J_1 = \sum_{i=1}^{nl} C_{PM,i} \cdot U_{PM,i} + \sum_{j=1}^n C_{VMM,j} \cdot U_{VMM,j} \quad (4.1)$$

$$\text{Min } J_2 = \frac{1}{m} \sum_m \frac{1}{n} \left(\sum_{i=1}^n \frac{V_i^t - \hat{V}_i}{V_i^t} \right) \times 100 \quad (4.2)$$

$$\text{Min } J_3 = \frac{1}{m} \sum_m \frac{1}{n} \left(\sum_{i=1}^n \frac{\delta_i^t - \hat{\delta}_i}{\delta_i^t} \right) \times 100 \quad (4.3)$$

The constraints considered are voltage angle relative deviation and voltage magnitude relative deviation. The boundaries are one percentage and five percentage for voltage magnitude and angle, respectively. The constraints violations are calculated for 95 percentage of simulated scenarios [30]. The following are the constraints:

$$g_1 = \left| \frac{V_i^t - \hat{V}_i}{V_i^t} \right| < 1\% \quad (4.4)$$

$$g_2 = \left| \frac{\delta_i^t - \hat{\delta}_i}{\delta_i^t} \right| < 5\% \quad (4.5)$$

4.3 Methodology

Indicator based MOEAs use an indicator to measure the performance of a solution set to guide the search process. An enhanced inverted generational distance with noncontributing solution detection (IGD-NS) indicator is used to assess the convergence and diversity of the MOEA. The proposed MOEA is based on IGD-NS with adaptive reference point method [94]. There are several performance indices in literature such as hypervolume (HV) [60], R2 indicator [61], generational distance (GD) indicator and inverted generational distance (IGD) indicator [59] so on. These indicators are used to measure the performance of a solution set and adapted as selection criteria in MOEAs.

Inverted generational distance (IGD) [59] metric indicates the convergence and diversity of a solution set. Some of the nondominated solutions, which do not have any nearest neighboring reference points, are always ignored in the calculation of the IGD metric. These omitted non-dominated solutions do not contribute to the value of the IGD metric. Therefore, these are called noncontributing solutions in non-dominated solutions of the Pareto optimal front solution set. Considering the noncontributing solutions, the inverted generational distance with noncontributing solution detection (IGD-NS) [94] is expressed as follows:

$$IGD - NS(P, P^*) = \sum_{x \in P^*} \min_{y \in P} dis(x, y) + \sum_{y' \in P'} \min_{x \in P^*} dis(x, y')$$

(4.6)

Where P' is the set of noncontributing solutions in population P , which is not closest to any reference point P^* . The first term in equation (4.6) is identical to IGD metric, which assesses the diversity and convergence of solution set P . Apart from that, the second term in equation (4.6), is an addition of the minimum distance from each noncontributing solution to the reference point P^* . This indicator decreases the number of noncontributing solutions in P' . A set of reference points, sampled from the Pareto front, are used in the calculation of IGD-NS metric. These reference points serve the purpose of a priori knowledge of approximate Pareto front. The reference points are adaptively updated as per the approximate Pareto front shape obtained in each generation. Thus, the adaptive reference points reflect the shape, irrespective of the regularity or discontinuity of Pareto front shape. The reference points are added or removed to preserve the diversity of candidate solutions. The proposed algorithm is discussed in the next section.

4.4 The Proposed Indicator based Multi-Objective Evolutionary Algorithm with Adaptive Reference Point Method Stage 1

The proposed algorithm is based on enhanced inverted generational distance indicator (IGD-NS), which is a measure of the diversity and convergence of candidate solution set, minimizing the noncontributing candidate solutions in the nondominated solutions. The proposed approach updates the reference points adaptively to track the Pareto front. For each generation, the two reference point sets and two solution sets are preserved and updated. The reference point sets contain initial reference point set (R) and updated reference point set (R') and population sets comprise of the present population (P) and the solution set of contributing nondominated solution of Archive population (A).

Initial population is randomly generated with a size of ‘N’, as a binary string indicating the meter locations. Systematic Sampling Approach is used to obtain uniformly distributed reference points (R) [87].

The mating pool is selected from the population based on tournament selection using the IGD-NS metric as fitness. Then the reference points (R) and current population (P) and archive population (A) are normalized to bring them into the same range so that the uniformly distributed reference points generate uniformly distributed solutions irrespective of the range of different objective values [95].

The crossover is applied to generate the offspring from mating parents. Binary mutation operator is used to preserve the diversity of the population.

The solutions are stored in archive populations (A), and repeated and dominated solutions are removed from it. Then the reference points are updated using angle criteria. The extreme solutions are preserved in archive population to uphold the diversity of population. The location of reference points near the extreme points are adjusted using minimum value of product of ideal point and reference point ($\overrightarrow{Z^*r}$). At least one reference point is discovered closest to the solutions then the identified reference points are transferred to a new archive population (A'). Remaining solutions are filled until the minimum size of ($|R|, |A|$) reaches the size of new archive population. Then again, the reference points are updated using minimum angle criteria using the current population.

Finally, the environmental selection is based on the elitist strategy applied to the combined population of off-springs and parent population. First, the combined population is sorted using

efficient nondominated sorting (ENS) [96]. Then the all the candidate solutions in the (k-1) fronts are directly selected for next-generation (Q), and the IGD-NS indicator is used to select the candidate solutions from the k_{th} front. Where k is the minimum number fronts such that the number of candidate solutions up to k_{th} front is less than or equal to the size of the population (N). For each candidate solution in front-k, the performance metric IGD-NS value is obtained using (4.6), and the candidate with the minimum value of IGD-NS is deleted from the front-k. Then the IGD-NS value is again calculated for the remaining candidate solutions in front-k until the remaining solutions reach the size of (N-Q).

Step-by-Step Process of the Proposed Algorithm Stage-1

Algorithm 1: The stage-1 of the proposed algorithm using indicator based multi-objective evolutionary algorithm with adaptive reference point method:

1 // Initialization //

Step 1: Initialize the population randomly of size ‘N’ as binary string representing the placement of power flow meter location on the distribution system. Systematic Sampling Approach (SSA) [87] used to produce uniformly distributed reference points (R) as follows:

$$N(D, M) = \binom{D + M - 1}{M - 1} \text{ for } D > 0$$

Where D is the number of divisions per objective coordinate, and M denotes the number of objectives.

2 Initialize solution sets P, A' and reference point sets R, R' . Copy solution sets and reference sets as follows:

$$A' \leftarrow P; \quad R' \leftarrow R;$$

Step 3:

3 **While** (“Stopping Criteria”) **do**

4 // Mating Pool Selection //

5 **for** $i = 1$ to M // M is number of objectives

6 | $f_i(p) = f_i(p) - \min_{q \in P} f_i(q), \quad \forall p \in P$
7 | // $f_i(p)$ i^{th} objective value of p

8 **End for**

9 Calculate the fitness of each candidate solution using (4.6)

10 Fitness = **IGD-NS** (P, R)

11 Initialize the selected population (S), select the mating parents based on tournament selection

12 **for** $i = 1$ to N

13 | Randomly select p, q from population P

14 | | **if** Fitness (p) > Fitness (q)

15 | | | S = S U P(p)

16 | | **Else**

17 | | | S = S U P(q)

18 | | **End if**

19 **End for**

16 **Step 4.** Two-point crossover is applied to generate offspring from mating parents. Then, binary mutation is used to produce a new population (Q).
 Combined archive population with new offspring population
 $A = A \cup Q$

17 // **Reference point Adaptation//**
Step 5: // the reference point set, archive population (A), current population (P) and are normalized

18 **for** i= 1 to M

19 $z_i^* = \min_{p \in P} f_i(p)$
 $z_i^{nad} = \max_{p \in P} f_i(p)$
 $f_i(p) = f_i(p) - z_i^*, \forall p \in A \cup P$
 $R_i^j = R_i^j * (z_i^{nad} - z_i^*), \forall j \in \{1, \dots, |R|\}$

20 **End for**

21 **Step 6:** // Archive population (A) updation //
 from 'A' remove the repeated and dominated solutions

22 **Step 7:** // To preserve the extreme end solutions in Pareto front, reference points near extreme solutions are adjusted //
 Initialize R'

23 **For** r $\in R$

24 $p = \operatorname{argmin}_{p \in A} \|F(p)\| \sin(\overrightarrow{z^*r}, F(p))$
 $r'_i = \frac{r_i}{\|r\|} \cdot \|F(p)\| \cos(\overrightarrow{Z^*r}, F(p)), \forall i \in \{1, 2, \dots, M\}$
 $R' \leftarrow R' \cup \{r'\}$

25 **End for**

26 **Step 8:**
 Initialize empty archive population A' and contributing solution A^{con}
 $A^{con} = \{p \in A \mid \exists r \in R: \operatorname{dis}(r, F(p)) = \min_{q \in A} \operatorname{dis}(r, F(q))\}$
 $A' = A' \cup A^{con}$

27 **Step 9:** // fill A' from A and A' //
 //fill remaining space until the size less than minimum size of R or A//

28 **While** (A' size < min (R or A size)) **do**

29 $R' = R' \cup (\operatorname{argmax}_{p \in (A' \setminus R')} \min_{r \in R'} \arccos(r, F(p)))$

30 **End while**

31 Determine the closest reference points to the contributing solutions (A^{con}). Make a copy in R' .
 $R' = R' \cup \{r \in R \mid \exists p \in A^{con} : \operatorname{dis}(r, F(p)) = \min_{s \in R} (s, F(p))\}$
 Remaining space in R' copied with candidate solutions from the new archive A' until the minimum of ($|R'|, |A'|$) size is reached, with reference points being in R' , having a maximum of minimum acute angel between reference values and corresponding objective value of R' and A' , respectively.

32 **While** (size (R') < min(size(R), size (A'))) **do**

33 $R' = R' \cup (\operatorname{argmax}_{p \in (A' \setminus R')} \min_{r \in R'} \arccos(r, F(p)))$

```

34   End while
35   Step 10: // preserve the extreme end solutions //  

36   Initialize the empty  $R'$ 
37   for  $r \in R$ 
38      $p = \operatorname{argmin}_{p \in P} \|F(p)\| \sin(\overrightarrow{z^*r}, F(p))$ 
39      $r'_i = \frac{r_i}{\|r\|} \cdot \|F(p)\| \cos(\overrightarrow{z^*r}, F(p)), \forall i \in \{1, 2, \dots, M\}$ 
40      $R' \leftarrow R' \cup \{r'\}$ 
41   End for
42   // Environmental Selection//  

43   Step 11: combine the population P and offspring population Q,  

44   apply elitist selection.
45    $P = P \cup Q$ 
46   for  $i = 1$  to  $M$ 
47      $f_i(p) = f_i(p) - \min_{q \in P} f_i(q), \forall p \in P$ 
48   End for
49   Step 12: sort the combined population using efficient  

50   nondominated sorting (ENS) [96].
51   Step 13: choose the number of fronts such that it satisfies the  

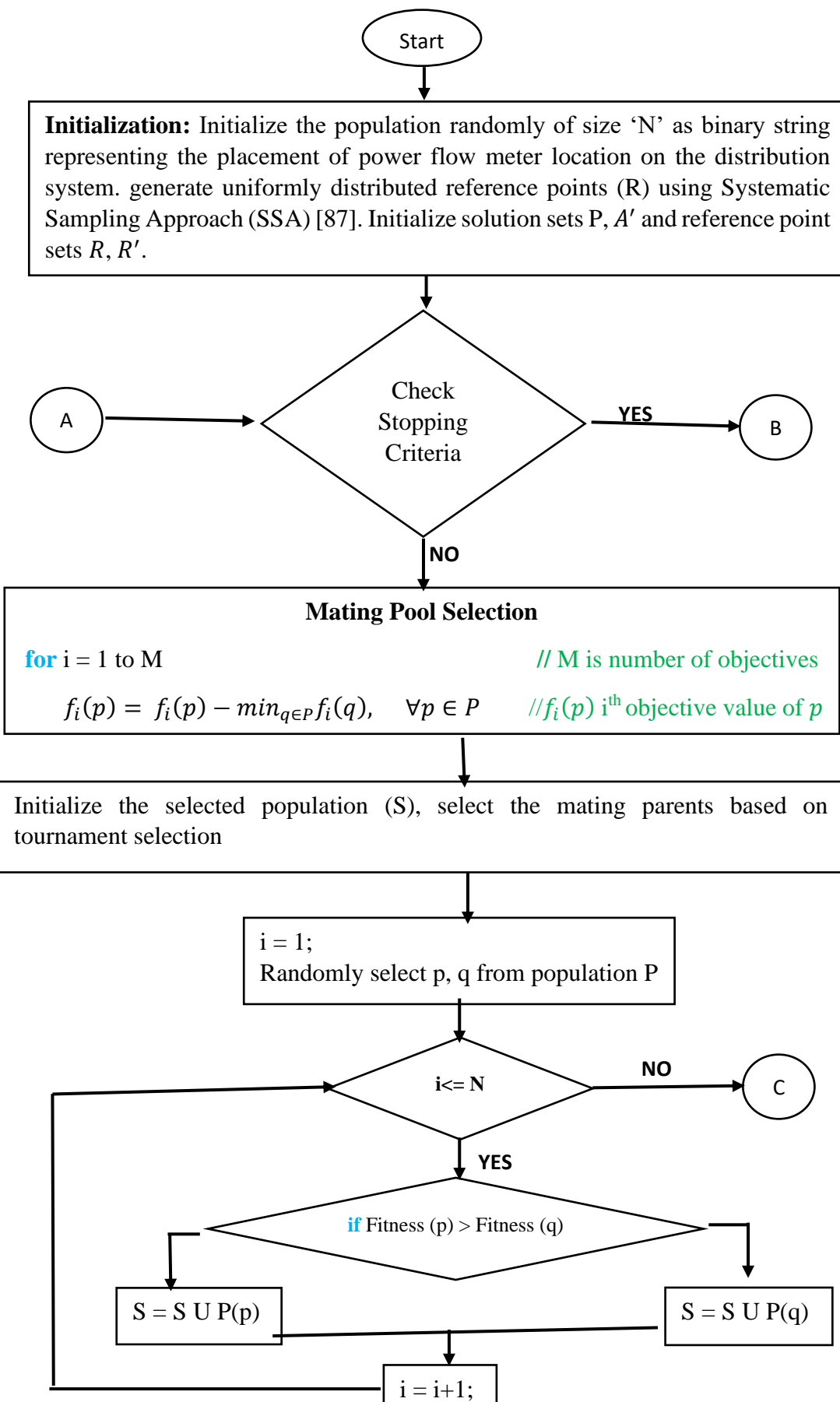
52   condition  $k = |\bigcup_{i=1}^k \text{Front}_i| \geq N$ 
53   Step 14: copy all the  $(k-1)$  fronts candidate solutions into  

54   population 'O'
55   Step 15: choose the remaining solutions from the  $k^{\text{th}}$  front until  

56   the population size reaches the size 'N' using the performance  

57   metric IGD-NS (4.6)
58   While size(Front) >  $N - \text{size}(O)$ 
59     identify the solution p with
60     minimum value of IGD - NS value
61      $p = \operatorname{argmin}_{p \in \text{Front}_k} \text{IGD-NS}(\text{Front}_k \setminus \{p\}, R')$ 
62     Delete the p solution from the Front
63   End while
64    $O = O \cup \text{Front}_k$ 
65   Assign the current population with 'O';  $P = O$ 
66 End while

```



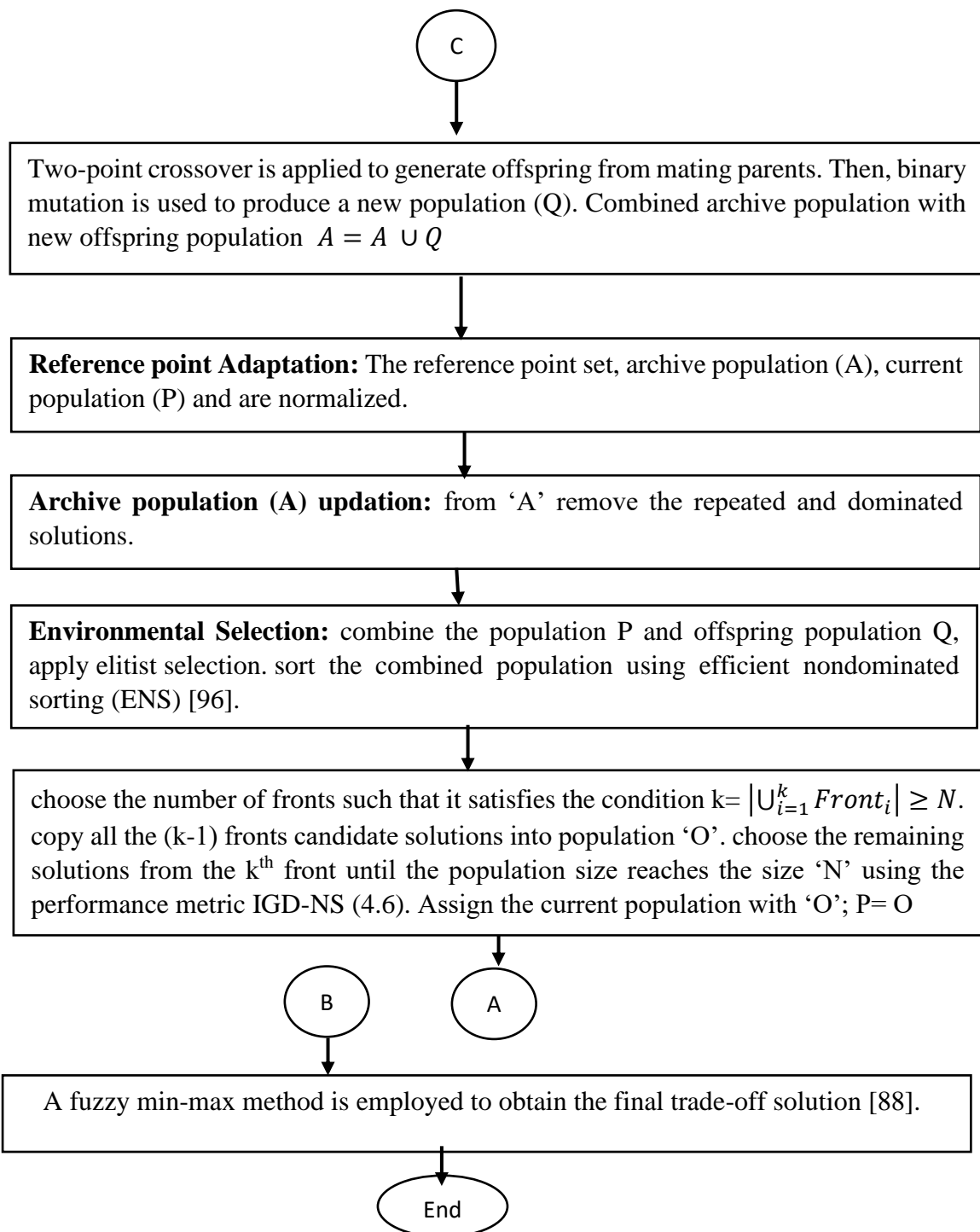


Fig. 4.1: Flow chart of stage 1 of the proposed algorithm

4.5 Stage 2 of the Proposed Algorithm with Objective Discretization

The meter placement method is generally designed as combinatorial optimization problem. The objective function values of combinatorial optimization problem are discrete in nature, due to the large possible combination of solutions in decision space being mapped to the small possible values in objective space. In multi objective problems, each objective function has a

different possible range of values. That means some objective functions have different granularity or width of discretization interval. The appropriate granularity or discretization of objective space improves the performance of combinatorial multi-objective evolutionary algorithm [80]. It also improves the search ability of MOEA and reduces the non-dominated solution in the population [81].

The objective space discretization is performed before an efficient nondominated sorting (ENS) method in environmental selection in the proposed method (stage 1). The efficient nondominated sorting (ENS) method is modified with strong Pareto dominance for ranking the solutions. Before the discretization, the objective values are normalized to an interval [0,1]. The different granularities are tested to choose the resolution of decimal places of normalized objective values and reserved for four decimal (granularity) values for objectives of the average relative error percentage (AREP) of voltage magnitude (J_2) and the average relative error percentage (AREP) of voltage angle (J_3). Whereas, the first objective (J_1), number of meters is an integer value, therefore no discretization is applied. The pseudo code of the proposed algorithm stage 2 is given as follows:

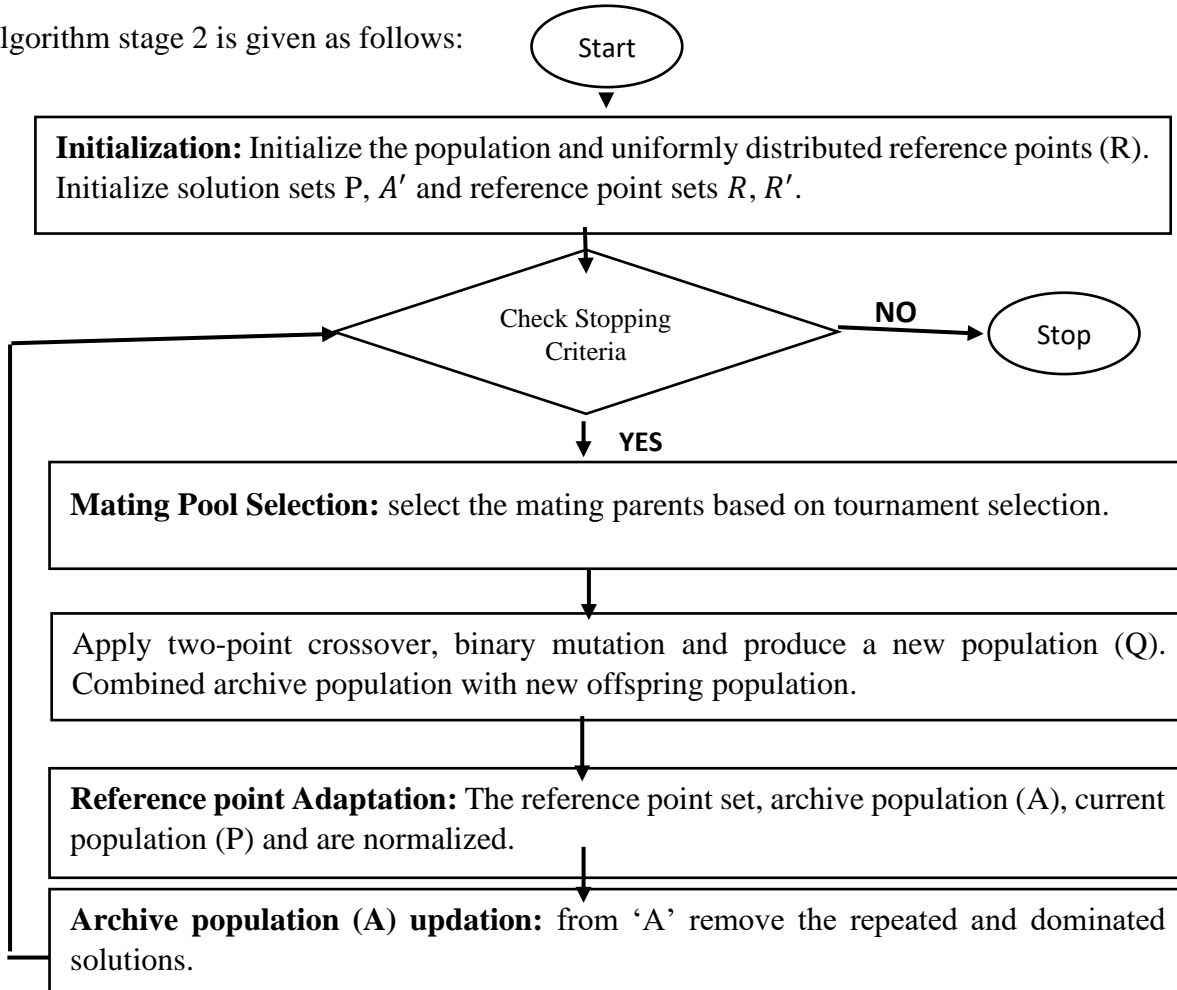


Fig. 4.2. Flow chart of stage of the proposed algorithms

The main aim of MOEA is to balance between the convergence and diversity, which are conflict objectives. To show the versatility of the proposed method with objective discretization, the performance (convergence and diversity) characteristics are investigated using inverted generational distance (IGD) performance indicator. The IGD indicator [59] is defined as follows:

$$IGD(P, P^*) = \frac{\sum_{x \in P^*} \min_{y \in P} \text{dis}(x, y)}{|P^*|} \quad (4.7)$$

Where P is the objective values of non-dominated solutions, P^* denotes the collection of uniformly distributed reference points taken from the Pareto optimum front, and the Euclidean distance between solutions x and y is denoted by $\text{dis}(x, y)$. IGD metric calculates the average minimum distance from each reference point in P^* to those in P , which measures the convergence and diversity of solution set P . A lower IGD value indicates that the higher the convergence and diversity of solution set P .

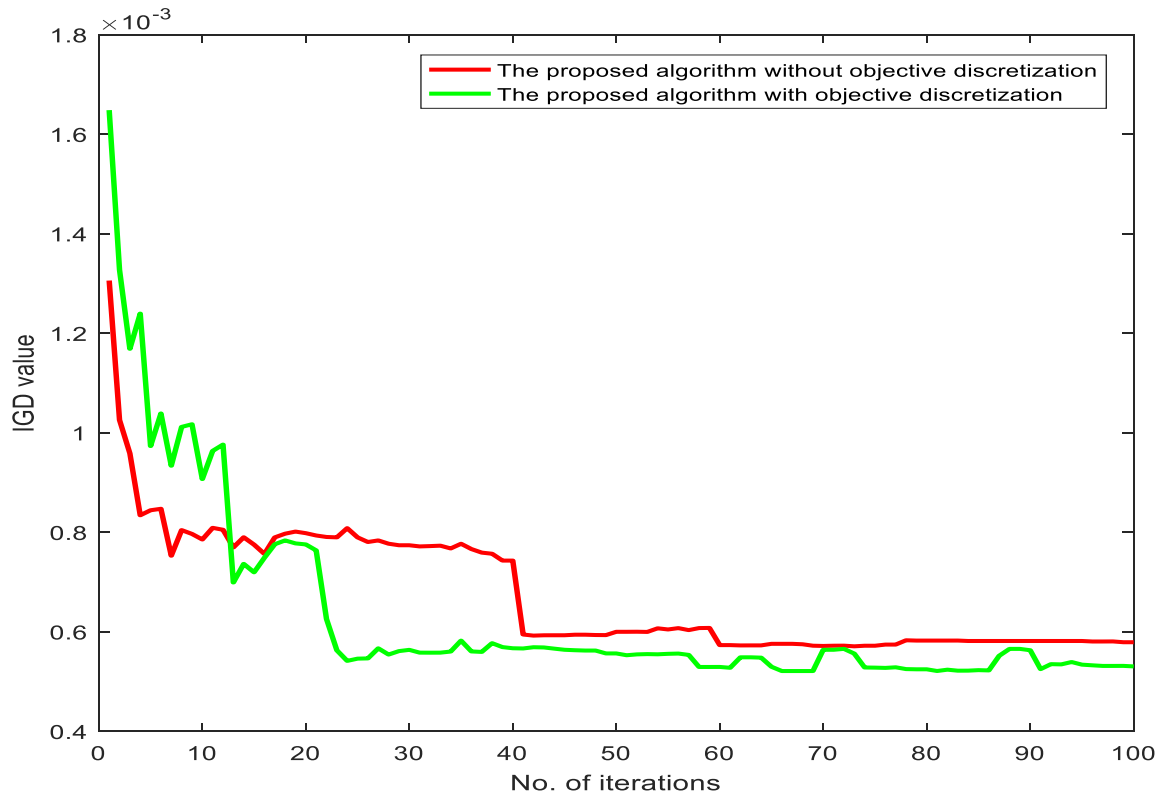


Fig. 4.3: Indian Practical 85-bus distribution system: The convergence and diversity measure with and without the objective discretization method.

The IGD performance indicator assesses the performance characteristics of the proposed algorithm. Fig. 4.3 depicts the convergence and divergence characteristics for a typical trial of the proposed algorithm. The proposed method with objective discretization method provides better performance characteristics compared to without objective discretization method, as shown in fig. 4.1. The enhancement in performance characteristics is due to the improvement in the search ability of MOEA and reduction the non-dominated solutions in population, caused by the discretization of objective values.

4.6 Simulation and Test Conditions

One power flow meter (PM) and a voltage magnitude meter (VMM) is located on the first line and at the slack bus, respectively. These meters are considered as default measurements. The active and reactive power flows are assumed to be acquired from a single PM. The proposed method is simulated by deploying PM meters at different locations on distribution network. The BC-DSSE [16]-[17] method is used to estimate the states for meter locations, which are generated by the proposed method. Monte Carlo simulation evaluate the acceptable performance of state estimation in terms of voltage magnitude and voltage angle for different measurement uncertainties, with prespecified state estimation error limitations of 1% and 5%, respectively, within 95 percent simulated scenarios. If the predefined limitations are exceeded, a penalty is applied to the corresponding objective function. voltage magnitude and angle constraint violations are evaluated by considering 100 different network operating scenarios, each of which is simulated for 1000 Monte Carlo trials with normally distributed measurement errors. In addition, the following assumptions are considered:

- i. The default measurements are provided with 1% measurement uncertainty.
- ii. Standard deviation of virtual measurements (zero bus injections) is considered in the order of 10^{-8} .
- iv. Pseudo measurements with a maximum error of 50% are supplied to test the efficacy of proposed method with huge errors.
- v. The population size is considered to be 100 for NSGA-II, whereas for the proposed method with and without discretization, the population size is obtained using the Systematic Sampling Approach (SSA), which generates uniformly distributed reference points. In addition, Table-4.1 gives the parameters that are used in the proposed algorithm, and NSGA-II [43].

Different population sizes are tested, and it is observed that for 3 objectives, the population size with 100, is suitable to get the near-optimal solutions. Therefore, population size is considered as 100, whereas for indicator-based methods the population size is decided based on the weight vectors, which are generated from the Systematic Sampling Approach (SSA) [87]. Different Crossover and Mutation rates are tested and chosen Crossover rate (Pc) is 1.0, Mutation rate (Pm) is 0.05 for which it gives the better performance of the MOEA.

Table 4.1: Parameters used in the proposed algorithm and NSGA-II

Algorithm	Control Parameters
The Proposed algorithm with and without objective discretization	Number of objectives (M) are three, Population size after SSA is 91, the neighborhood size T is 20, the number of divisions per objective coordinates D is 12, maximum number of generations are 100, Crossover rate (Pc) is 1.0, Mutation rate (Pm) is 0.05.
NSGA-II [43]	total objectives (M) are 3, size of population is 100, Crossover rate (Pc) is 0.8, Mutation rate (Pm) is 0.01, maximum number of generations are 100.

4.7 Results and Discussions

By evaluating different network scenarios, this work explores the effect of meter placement on distribution network. In addition, various types of renewable energy sources had been investigated. Table-4.2 provides the size and location of different types of renewable energy sources such as DG generating only active power, DG generating active power and absorbing reactive power from the network, and DG generating both active and reactive power. In this work, DGs are modelled as a dispatchable generation. The position of DGs is determined based on minimum voltage deviation and power loss in the network [73]. The effectiveness of the proposed algorithm is verified on PG&E 69-bus distribution system and Indian Practical 85-bus distribution system. The obtained results are compared to NSGA-II [43], and other methods such as with multi-objective hybrid PSO Krill herd algorithm (PSO-KH) [73], multi-objective hybrid estimation of distribution algorithm- interior point method (EDA-IPM) [75], dynamic programming (DP) [38] and ordinal optimization algorithm (OOA) [28].

Table 4.2: Location and size of different types of distributed generation

Test System	Bus Number	DG type and Capacity (MW) base value		
		Type-1 (P)	Type-2 (P+jQ)	Type-3 (P+jQ)
PG&E 69-bus Distribution System	50	0.180	0.180-j 0.087	0.180+j 0.087
	61	0.270	0.270-j0.130	0.270+j0.130
Indian Practical 85-bus Distribution System	45	0.277	0.235-j 0.145	0.235+j0.145
	61	0.290	0.246-j0.152	0.246+j0.152

For all figs. 4.3 to 4.13 the repeating captions are specified as given here: **(a)** *objective- J_2 average relative percentage error (ARPE) of voltage magnitude Vs. objective- J_3 average relative percentage error (ARPE) of voltage angle.* **(b)** *objective- J_2 average relative percentage error (ARPE) of voltage magnitude Vs. the number of power flow meters* **(c)**, *objective- J_3 average relative percentage error (ARPE) of voltage angle Vs. the number of power flow meters.*

4.7.1 PG&E 69-bus Distribution System

The proposed algorithm is tested on PG&E 69-bus distribution system [92], which has 68 lines, 21 zero bus injection nodes, and total real and reactive power load of 3.802 MW, 2.692 MVAR respectively. The zero bus injections are modeled as virtual measurements, and one VMM, one power flow meter at substation and one power flow meter is placed at each distribution generator, which are considered as default measurements.

The proposed algorithm for meter placement problem is investigated with 1%, and 5% real measurement uncertainty and optimal Pareto front plots are shown in figs. 4.4 and 4.5, respectively. The results correspond to objective values and performance of state estimation without DG, which are tabulated in Table-4.3. The proposed algorithm with objective discretization with 1% accuracy of real measurements, requires 6 meters including the default measurements, whereas the proposed algorithm without objective discretization, and NSGA-II require 6 and 9 respectively. The average relative percentage error (ARPE) of voltage magnitude and ARPE of voltage angle for the proposed method are 0.0008% and 0.2641%, respectively. Whereas, ARPE of voltage magnitude and voltage angle for NSGA-II are 0.0038% and 1.6474%, respectively. Whereas the existing method in literature such as PSO-KH, EDA-IPM requires 6 meters, same as the proposed method, whereas, DP and OOA methods require 7 and 8 meters respectively. In terms of objective values quality the proposed method shows the superiority as shown in Table-4.3.

Similarly, with 5% real measurement uncertainty the proposed method shows superiority

in terms of quality of solutions and as well as the number of meters required.

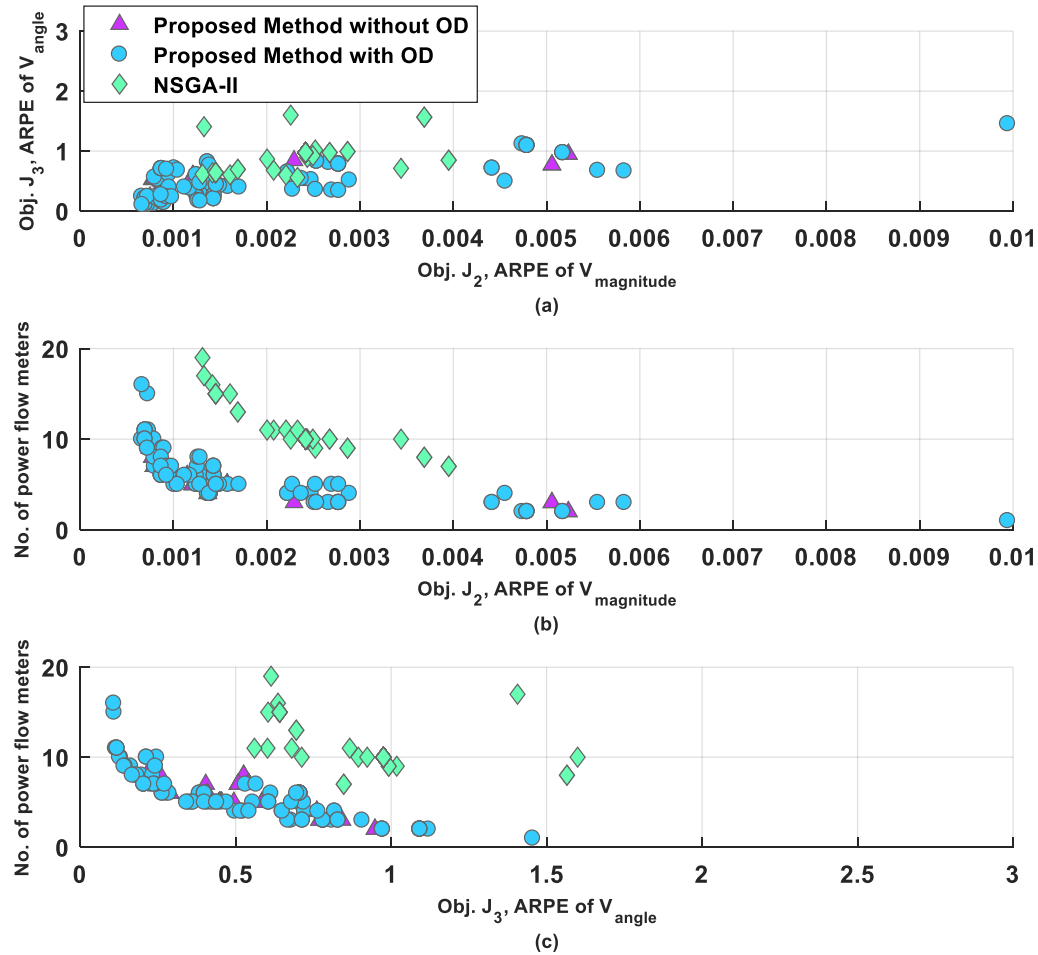


Fig. 4.4: PG&E 69-bus distribution system Optimal Pareto-front plots: Real measurements with an accuracy of 1% and Pseudo measurements with an accuracy of 50% without DG (OD-Objective Discretization method)

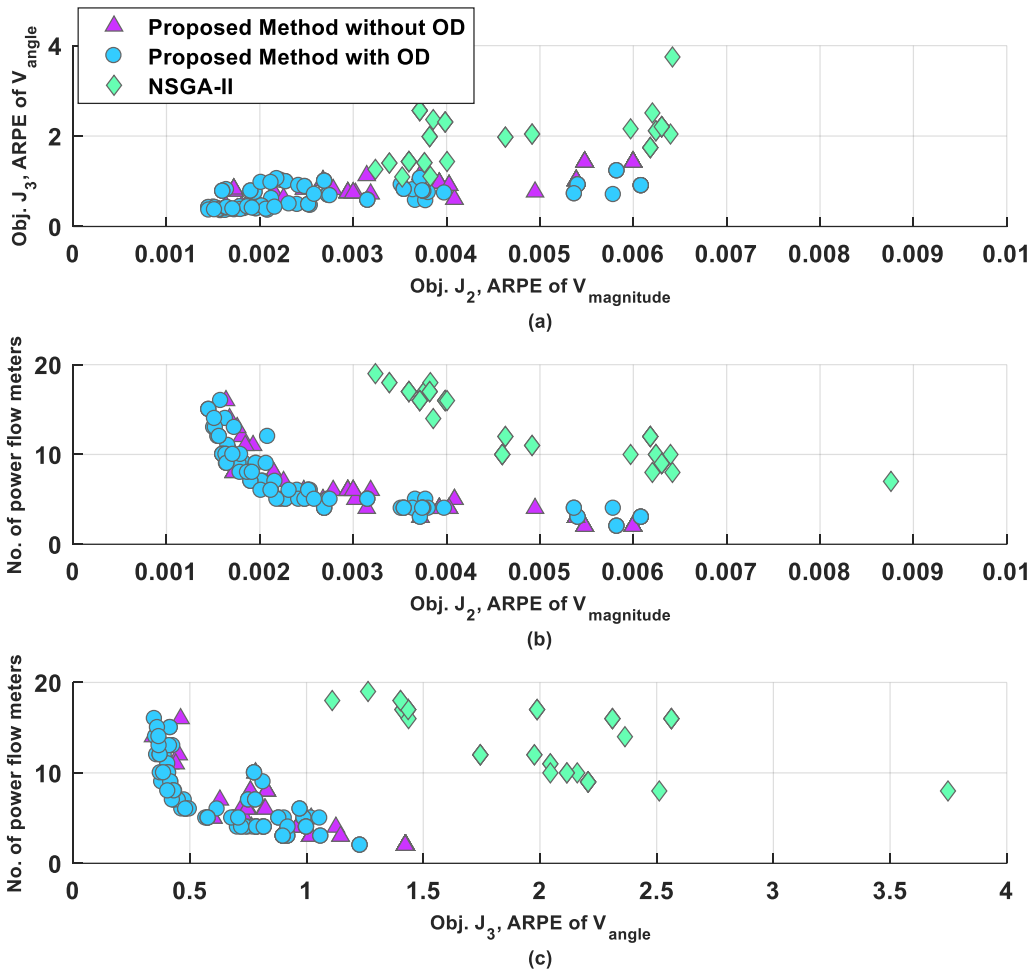


Fig. 4.5: PG&E 69-bus distribution system Optimal Pareto-front plots: Real measurements with an accuracy of 5% and Pseudo measurements with an accuracy of 50% without DG (OD-Objective Discretization method)

Table 4.3: PG&E 69-bus distribution system: Optimal location of the power flow meters under different metrological errors for without DG.

Metrological error (in %)	Algorithm	Power flow meters location(Line numbers)	Number of power flow meters	Objective function values		
				J_1 Cost of meters (1 per unit device)	J_2 ARPE of voltage magnitude	J_3 ARPE of voltage angle
1	Proposed algorithm with OD*	1, 13, 32, 43, 55	5	6	0.0008	0.2641
	Proposed algorithm without OD*	1, 5, 13, 30, 54	5	6	0.0014	0.4547
	NSGA-II [43]	1, 4, 10, 11, 12, 42, 55, 68	8	9	0.0038	1.6474

	PSO-KH [73]	1, 7, 24, 54, 66	5	6	0.0028	0.4947
	EDA-IPM [75]	1, 3, 7, 24, 51	5	6	0.0025	0.4821
	DP [38]	1, 11, 18, 33, 41, 57	6	7	0.0042	0.7861
	OOA [28]	1, 9, 17, 29, 42, 51, 57	7	8	0.0051	0.9292
5	Proposed algorithm with OD*	1, 15, 29, 40, 47, 56	6	7	0.0020	0.3458
	Proposed algorithm without OD*	1, 9, 13, 26, 31, 46, 60	7	8	0.0023	0.6288
	NSGA-II [43]	1, 3, 8, 14, 29, 36, 39, 45, 53, 60, 63, 66	12	13	0.0049	1.7634
	PSO-KH [73]	1, 7, 14, 21, 28, 33, 49, 53, 61	9	10	0.0058	1.1491
	EDA-IPM [75]	1, 7, 14, 19, 28, 33, 47, 53, 61	9	10	0.0056	1.1273
	DP [38]	1, 7, 16, 29, 34, 46, 53, 59, 61, 65	10	11	0.01512	1.8727
	OOA [28]	1, 11, 17, 26, 31, 39, 47, 53, 58, 63	10	11	0.0223	1.7821

*OD - Objective Discretization method

The proposed algorithm for meter placement problem in the active distribution system is investigated with 1%, and 5% real measurement uncertainty and the Pareto optimal plots are shown in fig. 4.6 to 4.7, respectively. The results for DG type-1 (P), are tabulated in Table-4.4. The proposed algorithm with objective discretization with 1% accuracy of real measurements, requires 8 meters including the default measurements at each DG and on the first line, whereas proposed algorithm without objective discretization, NSGA-II, PSO-KH, EDA-IPM, DP and OOA requires 9, 12, 8, 8, 9 and 11 respectively. The average relative percentage error (ARPE) of voltage magnitude and ARPE of voltage angle for proposed method are 0.0011% and 0.3122%, respectively, whereas for proposed algorithm without objective discretization, NSGA-II, PSO-KH, EDA-IPM, DP and OOA are 0.0015%, 0.0044%, 0.0011%, 0.0018%, 0.0037%, 0.0049% and 0.3458%, 0.7954%, 0.2653%, 0.3125%, 0.9127%, 0.8357% respectively. As the proposed method shows superiority with the majority of algorithms. Whereas, in the case of 5% real measurement uncertainty, when compared to all

the methods the proposed method shows superiority in terms of quality of solutions and as well as the number of meters required. Similarly, the proposed method is tested for DG type-2, type-3 and the optimal Pareto fronts are shown in fig. 4.8 and 4.9, respectively. The performance of all the algorithms is tabulated in Table 4.5 and 4.6 for DG type-2 and type-3, respectively.

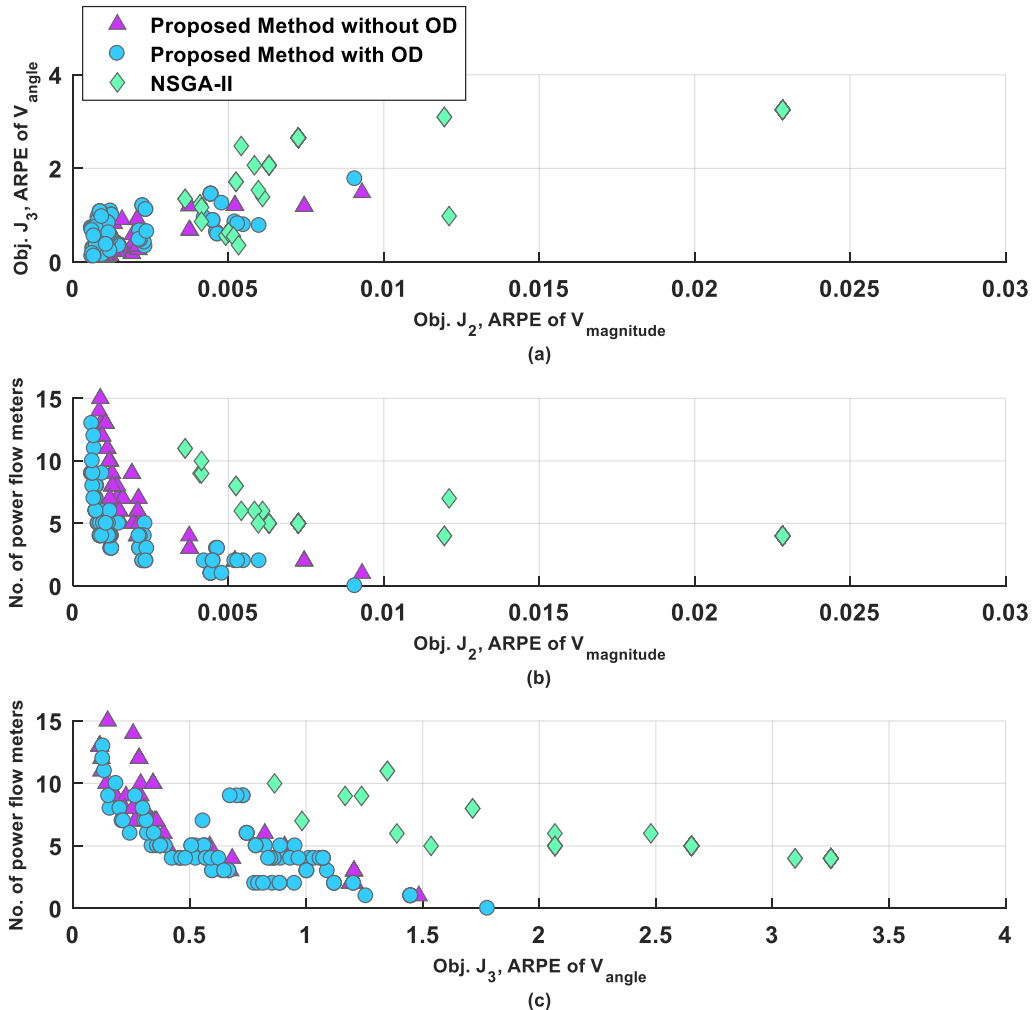


Fig. 4.6: PG&E 69-bus distribution system Optimal Pareto-front plots: Real measurements with an accuracy of 1% and Pseudo measurements with an accuracy of 50% with DG Type-1 (P) (OD- Objective Discretization method)

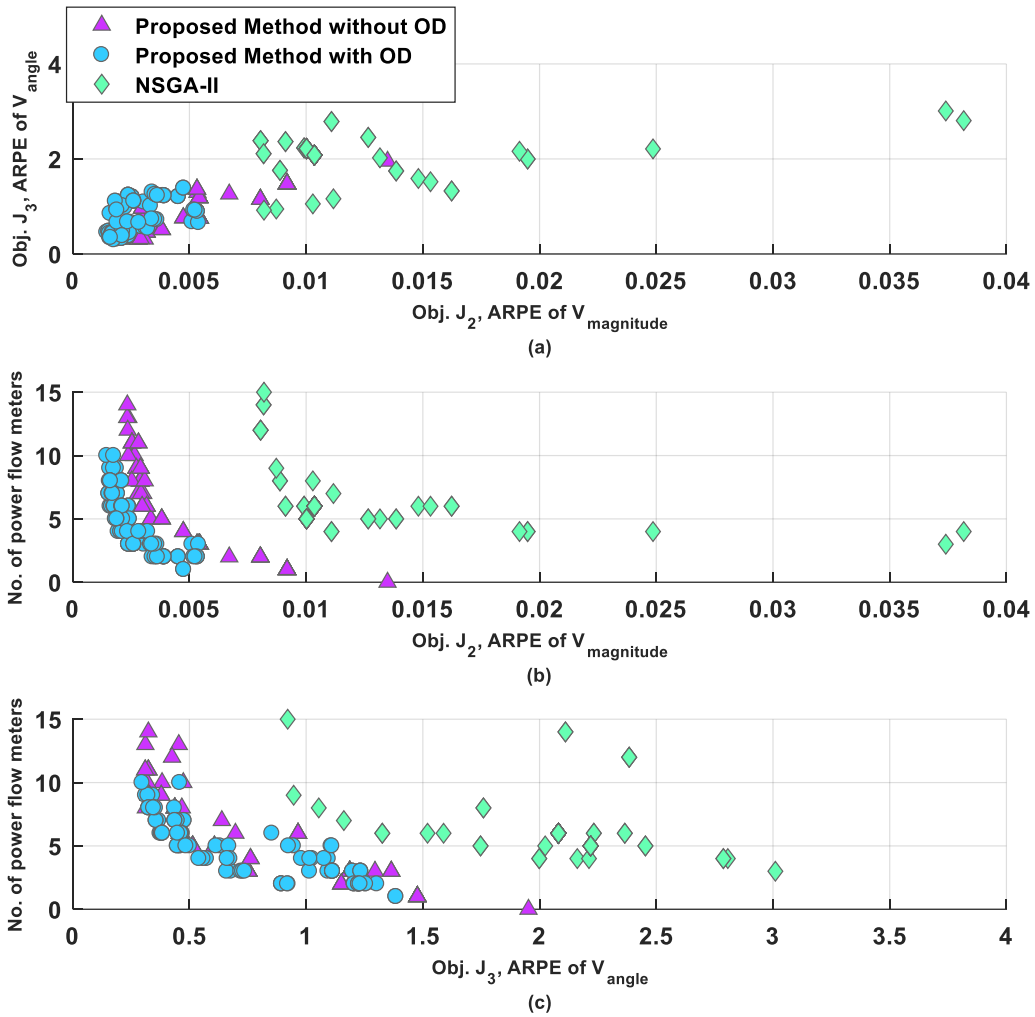


Fig. 4.7: PG&E 69-bus distribution system Optimal Pareto-front plots: Real measurements with an accuracy of 5% and Pseudo measurements with an accuracy of 50% with DG Type-1 (P) (OD- Objective Discretization method)

Table 4.4: PG&E 69-bus distribution system: Optimal location of the power flow meters under different metrological errors with DG Type-1(P)

Metrological error (in %)	Algorithm	Location of Power flow meters(Line numbers)	Number of power flow meters	Objective function values		
				J_1 Cost of meters (1 per unit device)	J_2 ARPE of voltage magnitude	J_3 ARPE of voltage angle
1	Proposed algorithm with OD*	1, 13, 30, 41, 56	5	8	0.0011	0.3122
	Proposed algorithm without OD*	1, 10, 15, 29, 44, 52	6	9	0.0015	0.3458
	NSGA-II [43]	1, 12, 18, 30, 41, 48, 52, 53, 60	9	12	0.0044	0.7954
	PSO-KH [73]	1, 49, 52, 59, 67	5	8	0.0011	0.2653
	EDA-IPM [75]	1, 49, 52, 60, 68	5	8	0.0018	0.3125
	DP [38]	1, 23, 38, 49, 51, 63	6	9	0.0037	0.9127
	OOA [28]	1, 16, 27, 33, 39, 52, 61, 63	8	11	0.0049	0.8357
5	Proposed algorithm with OD*	1, 14, 32, 42, 47, 55	6	9	0.0017	0.4698
	Proposed algorithm without OD*	1, 15, 30, 43, 47, 55	6	9	0.0031	0.4663
	NSGA-II [43]	1, 9, 15, 23, 30, 36, 43, 46, 58	9	12	0.0087	0.9465
	PSO-KH [73]	1, 3, 17, 25, 34, 42, 50, 63	8	11	0.0063	1.0587
	EDA-IPM [75]	1, 3, 17, 24, 33, 41, 50, 63	9	12	0.0051	1.1122
	DP [38]	1, 11, 14, 23, 37, 44, 59, 63, 67	9	12	0.0238	1.6345
	OOA [28]	1, 11, 19, 26, 31, 39, 49, 52, 61, 63	10	13	0.0321	1.7952

*OD - Objective Discretization method

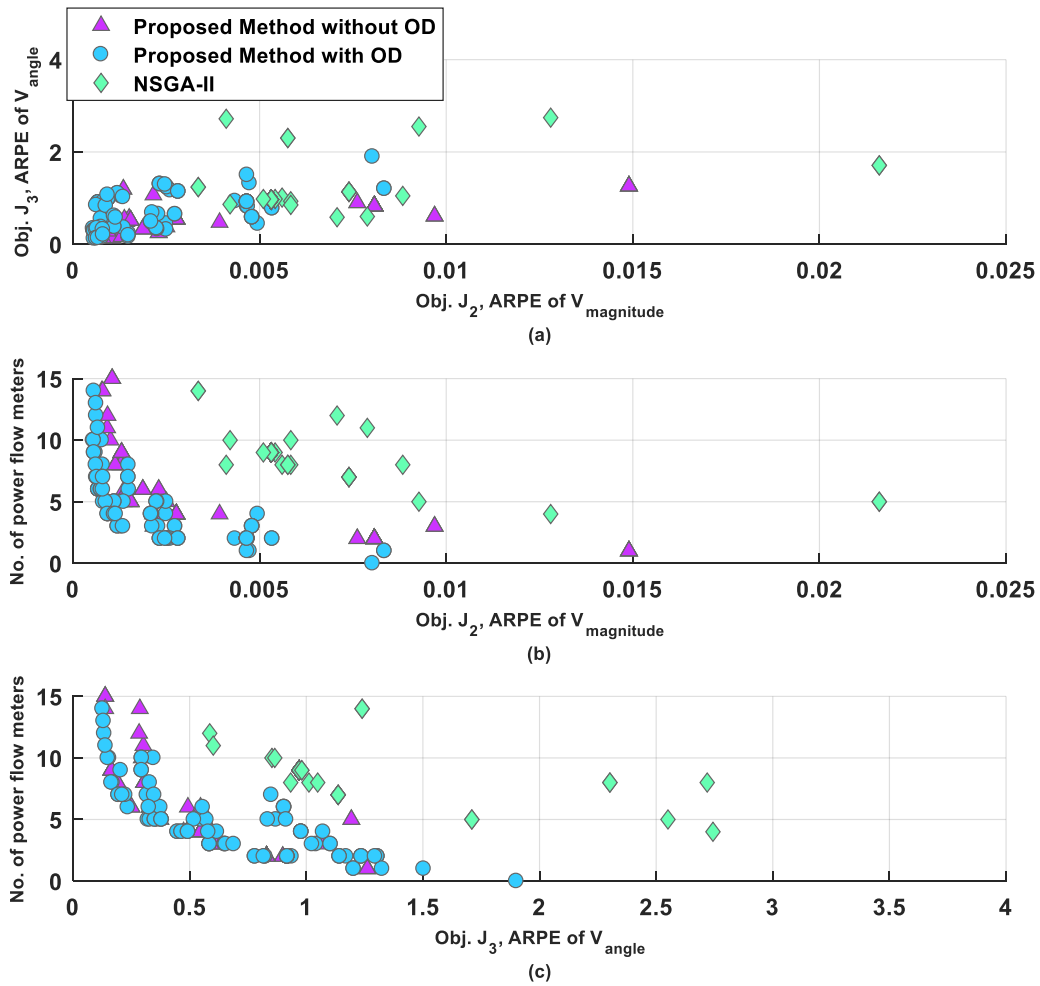


Fig. 4.8: PG&E 69-bus distribution system optimal Pareto front plots: Real measurements with an accuracy of 1% and Pseudo measurements with an accuracy of 50% with DG Type-2 (P-jQ) (OD- Objective Discretization method)

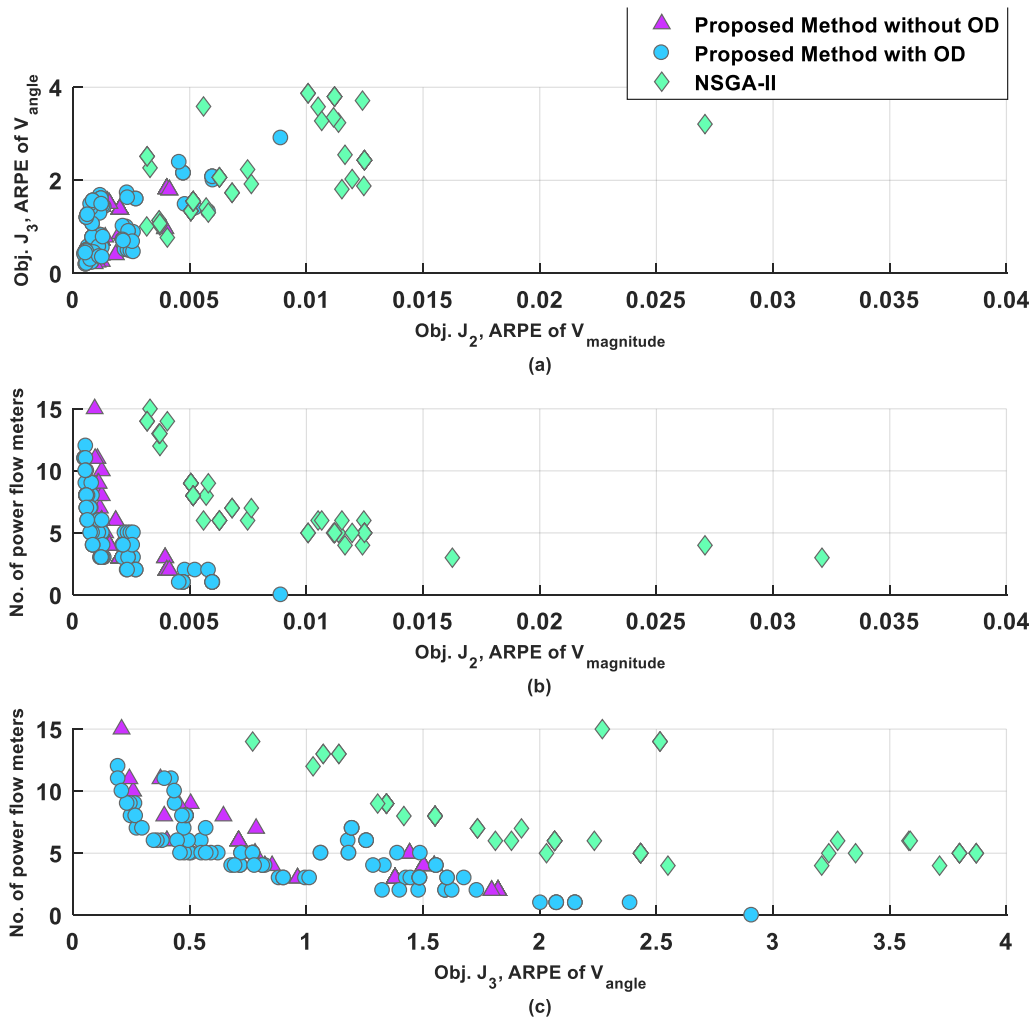


Fig. 4.9: PG&E 69-bus distribution system optimal Pareto front plots: Real measurements with an accuracy of 1% and Pseudo measurements with an accuracy of 50% with DG Type-3 (P+jQ) (OD- Objective Discretization method)

Table 4.5: PG&E 69-bus distribution system: Optimal location of the power flow meters with 1% measurement uncertainty with DG Type-2(P+jQ).

Algorithm	Location of Power flow meters(Line numbers)	Number of power flow meters	Objective function values		
			J ₁	J ₂	J ₃
Cost of meters (1 per unit device)	ARPE of voltage magnitude	ARPE of voltage angle			
Proposed algorithm with OD*	1, 14, 29, 41, 55	5	8	0.0014	0.3800
Proposed algorithm without OD*	1, 9, 12, 28, 29, 41	6	9	0.0023	0.2507
NSGA-II [43]	1, 16, 21, 31, 37, 40, 44, 58	8	11	0.0064	0.8544
EDA-IPM [75]	1, 5, 24, 37, 42	5	8	0.0069	1.1807
DP [38]	1, 7, 15, 41, 56, 66	6	9	0.0085	1.6137
OOA [28]	1, 5, 13, 14, 20, 43, 54, 56, 57	9	12	0.0088	0.9864

*OD - Objective Discretization method

Table 4.6: PG&E 69-bus distribution system: Optimal location of the power flow meters with 1% measurement uncertainty with DG Type-3(P+jQ).

Algorithm	Location of Power flow meters(Line numbers)	Number of power flow meters	Objective function values		
			J ₁	J ₂	J ₃
Cost of meters (1 per unit device)	ARPE of voltage magnitude	ARPE of voltage angle			
Proposed algorithm with OD*	1, 13, 31, 40, 58	5	8	0.0012	0.5714
Proposed algorithm without OD*	1, 9, 15, 30, 55	5	8	0.0014	0.7799
NSGA-II [43]	1, 9, 13, 22, 26, 29, 40, 55, 68	9	12	0.0039	1.2852
EDA-IPM [75]	1, 11, 32, 45, 51	5	8	0.0067	0.9864
DP [38]	1, 25, 31, 38, 65, 67, 68	7	10	0.0115	1.7095

OOA [28]	1, 6, 10, 19, 35, 45, 63, 64	8	11	0.0094	1.4584
----------	---------------------------------	---	----	--------	--------

*OD - Objective Discretization method

When the Pareto fronts in fig. 4.2 to 4.7 are observed, the proposed algorithm with objective discretization shows the evenly distributed diverse solutions as compared to proposed algorithm without objective discretization and NSGA-II. The discontinuities in Pareto fronts are clearly noticeable in all the plots in fig 4.2 to 4.7. Whereas, the irregularities in Pareto fronts are less in the proposed method Pareto fronts as compared to other methods.

4.7.2 Indian Practical 85-bus Distribution System

Indian Practical 85-bus distribution test system is used to validate the proposed method. Indian Practical 85-bus distribution system has a total load of 2.574 MW and 2.622 MVAR [93].

The effectiveness of proposed method is verified with 1%, and 5% measurement error, and the optimal Pareto fronts are given in fig 4.10 and 4.11, respectively. Table-4.7 presents the obtained results corresponding to without DG case, in terms of objective values and number of meters required. The proposed algorithm with and without the objective discretization, with 1% measurement error, both gives 7 meters including the default measurements. On the other hand, NSGA-II, EDA-IPM, PSO-KH, DP and OOA require 11, 8, 8, 9 and 10, respectively. In terms of average relative percentage error (ARPE) of voltage magnitude (J_2) and voltage angle (J_3), the proposed method with objective discretization yields better outcomes compared with the proposed method without objective discretization and the other MOEAs such as, NSGA-II, PSO-KH, EDA-IPM, DP and OOA. When compared to all the other methods, in terms of objective values and total meters the proposed method outperforms others. Furthermore, for 5% measurement error, the proposed method with objective discretization demonstrates versatility in terms of quality of solutions and total number of meters. The results show that when the real measurement uncertainty increases, the number of meters required increases.

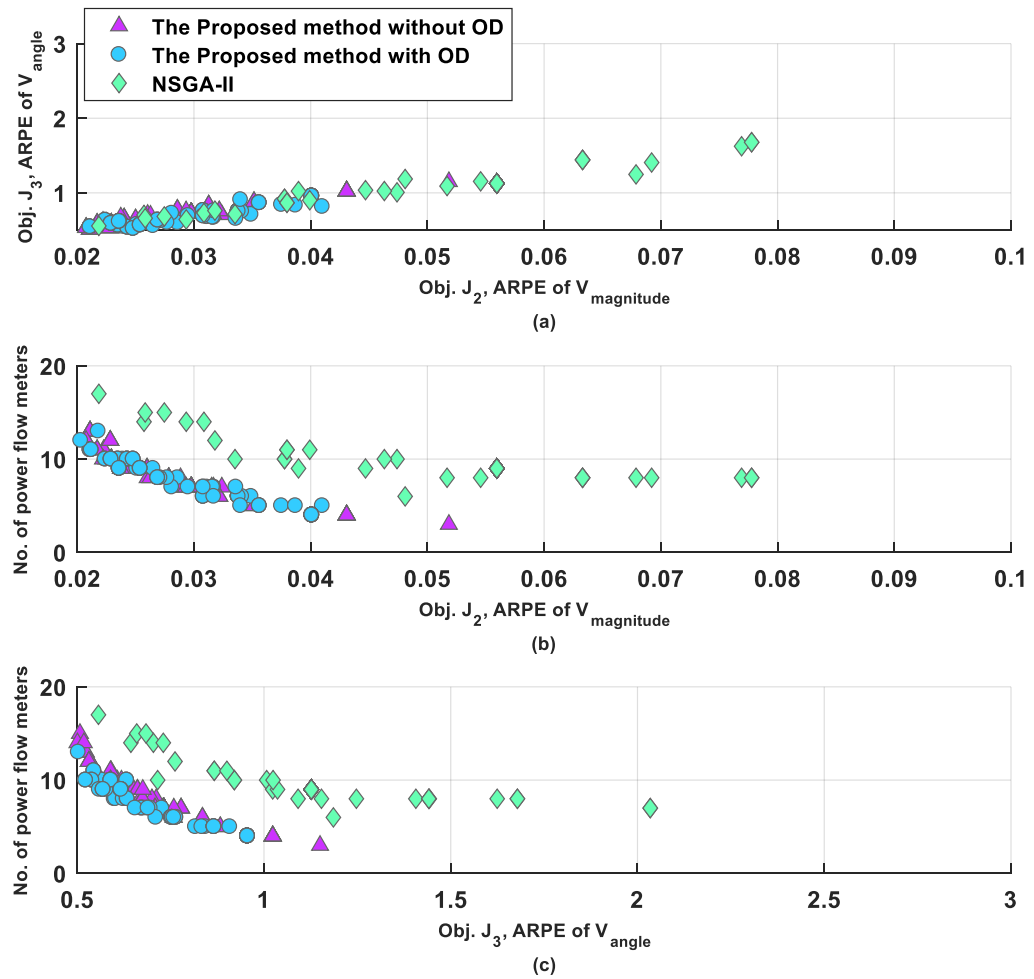


Fig. 4.10: Indian Practical 85-bus distribution system optimal Pareto-front plots: 1% error in real measurements and 50% error in Pseudo measurements without DG (OD- Objective Discretization method)

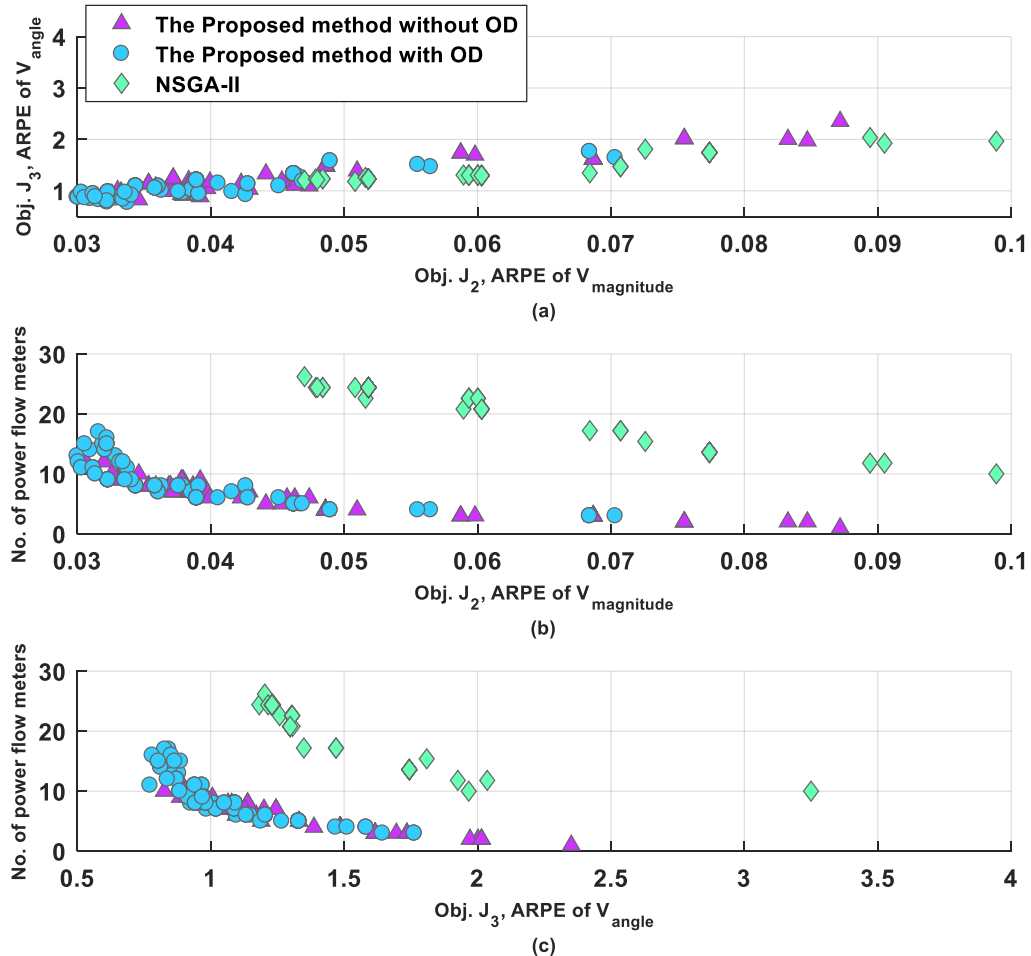


Fig. 4.11: Indian Practical 85-bus distribution system optimal Pareto-front plots:: 5% error in real measurements and 50% error in Pseudo measurements without DG (OD- Objective Discretization method)

Table 4.7: Indian Practical 85-bus distribution system: Optimal location of the power flow meters different measurement uncertainty without DG.

Metrological error (in %)	Algorithm	Position of PMs (Line numbers)	Number of power flow meters	Objective function values		
				J_1	J_2	J_3
1	Proposed algorithm with OD*	1, 10, 17, 24, 30, 57	6	7	0.0281	0.6552

	Proposed algorithm without OD*	1, 8, 9, 30, 57, 67	6	7	0.0286	0.7074
	NSGA-II [43]	1,6,7,18,23,33,35 ,56,67,69	10	11	0.0338	0.8526
	PSO-KH [73]	1, 13, 18, 26, 75, 79, 84	7	8	0.0385	1.1077
	EDA-IPM [75]	1,13,19,25,75,78, 84	7	8	0.0383	1.0952
	DP [38]	1, 13, 21, 32, 37, 47, 51, 54	8	9	0.0444	1.5213
	OOA [28]	1, 9,16, 43, 62, 69, 70, 72, 76	9	10	0.0579	1.2356
5	Proposed algorithm with OD*	1, 24,28,33,59,71	6	7	0.0451	0.9845
	Proposed algorithm without OD*	1, 8,17, 27, 32, 57	6	7	0.0499	1.1709
	NSGA-II [43]	1, 4, 6, 9, 26, 30, 49, 59, 63, 71, 80	11	12	0.0884	1.7494
	PSO-KH [73]	1, 16, 21, 24, 33, 69, 77, 79	8	9	0.0439	1.2855
	EDA-IPM [75]	1,12,20,43,50,68, 75, 83	8	9	0.0464	1.4298
	DP [38]	1, 7, 14, 19, 33, 39,42, 48, 53, 59, 61	11	12	0.0518	1.6239
	OOA [28]	1, 18, 21, 23, 34, 36,37, 61, 63, 75, 76	11	12	0.0466	1.3689

*OD - Objective Discretization method

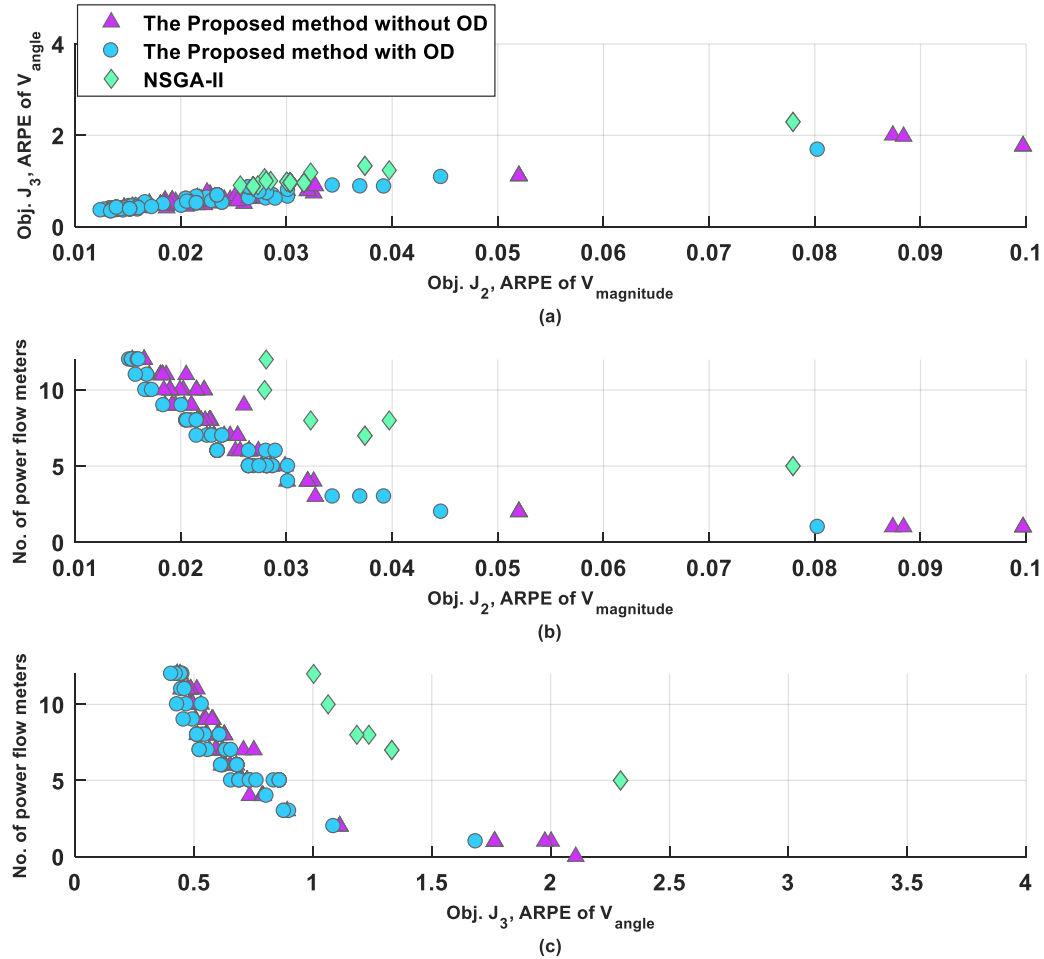


Fig. 4.12: Indian Practical 85-bus active distribution system optimal Pareto-front plots:
1% error in real measurements and 50% error in Pseudo measurements with DG Type-1 (P)
(OD- Objective Discretization method)

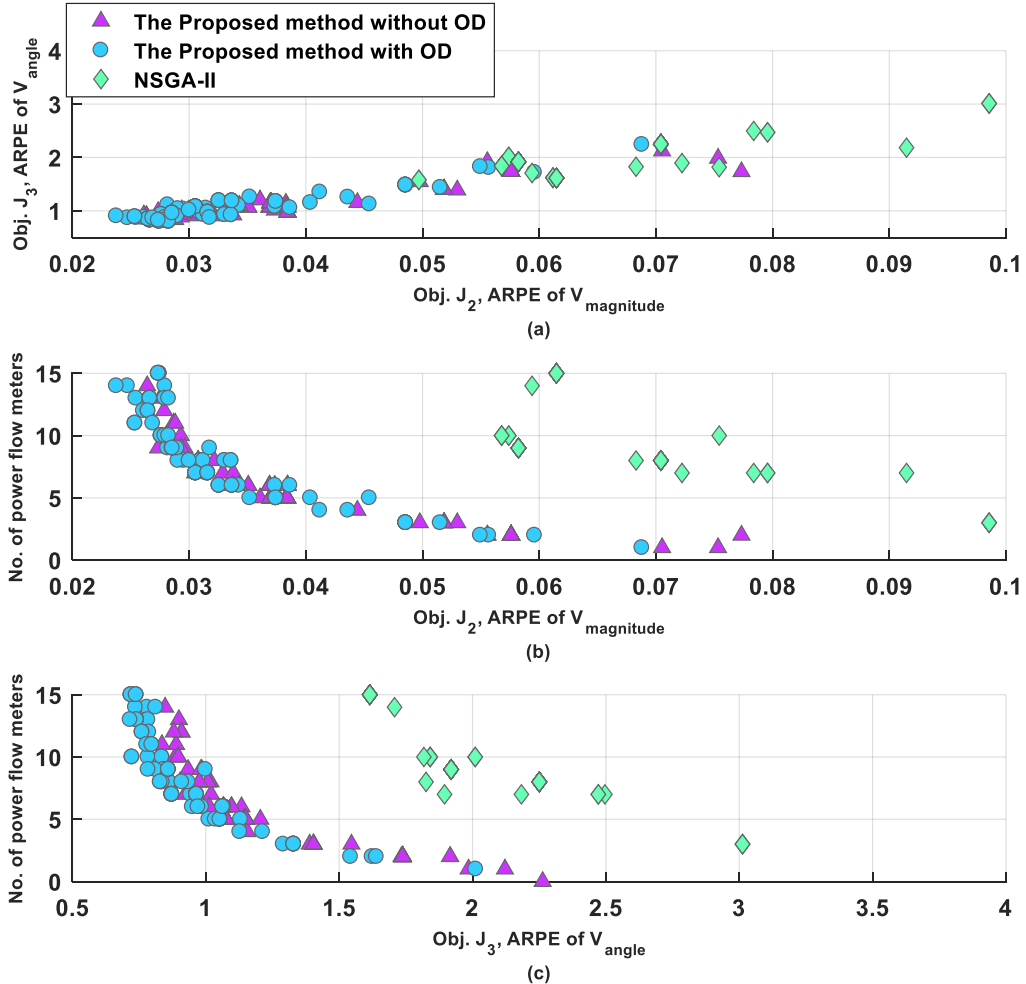


Fig. 4.13: Indian Practical 85-bus active distribution system optimal Pareto-front plots: 5% error in real measurements and 50% error in Pseudo measurements with DG Type-1 (P) (OD- Objective Discretization method)

Table 4.8: Indian Practical 85-bus distribution system: Optimal location of the power flow meters different measurement uncertainty with DG Type-1(P)

Metrological error (in %)	Algorithm	Position of PMs (Line numbers)	Number of power flow meters	Objective function values		
				J_1	J_2	J_3
1	Proposed algorithm with OD*	1, 18, 24, 56, 62	5	8	0.0265	0.6543

	Proposed algorithm without OD*	1, 7, 25, 29, 57	5	8	0.0276	0.6903
	NSGA-II [43]	1, 7 ,11, 24, 27, 31, 39, 67	8	11	0.0323	1.1849
	EDA-IPM [75]	1, 9, 23, 28, 44	5	8	0.0367	1.0473
	DP [38]	1,10,33,46, 58, 63,71,77, 79	9	12	0.0580	1.0967
	OOA [28]	1, 11, 14, 16, 32, 42, 54, 70	8	11	0.0574	1.0841
5	Proposed algorithm with OD*	1, 17,24, 33,57, 63	6	9	0.0326	0.9494
	Proposed algorithm without OD*	1, 17, 24, 29, 30, 56	6	9	0.0337	0.9728
	NSGA-II [43]	1,16,17,19,26,39, 46, 62, 77	9	12	0.0582	1.9197
	EDA-IPM [75]	1, 9, 17, 28, 42, 62, 79	7	10	0.0400	1.1001
	DP [38]	1,14,15,18,22,27, 47, 54, 72	9	12	0.6683	1.3053
	OOA [28]	1,31,46,48,58,62,65, 67, 77,78	10	13	0.6742	1.3053

*OD - Objective Discretization method

The proposed algorithm with objective discretization method for DG type-1 (P) case is evaluated with 1%, and 5% measurement error, and the optimal Pareto fronts are given in figs. 4.12 and 4.13, respectively. Table-4.8 presents the findings for DG type-1 (P). The proposed algorithm with and without the objective discretization, with 1% measurement error, both requires total 8 meters. On the other hand, NSGA-II, EDA-IPM, DP and OOA requires 11, 8, 12, and 11 meters, respectively. The average relative percentage error (ARPE) of voltage magnitude (J_2) and ARPE of voltage angle (J_3) for the proposed method with and without the objective discretization, are 0.0265%, 0.6543%, and 0.0276%, 0.6903%, respectively. On the other hand, for NSGA-II, EDA-IPM, DP and OOA the ARPE of voltage magnitude (J_2) and voltage angle (J_3) are 0.0323%, 0.0367%, 0.0580%, 0.0574% and 1.1849%, 1.0473%,

1.0967%, 1.0841%, respectively. When the proposed method with objective discretization is compared with the proposed method without objective discretization and EDA-IPM, requires the same number meters. Moreover, the proposed method with objective discretization outperforms in terms of average relative percentage error (ARPE) of voltage magnitude (J_2) and voltage angle (J_3) as shown in Table-4.8. Furthermore, in the case of a 5% measurement error, the proposed method with objective discretization outperforms all other methods in terms of solution quality as well as the number of meters required.

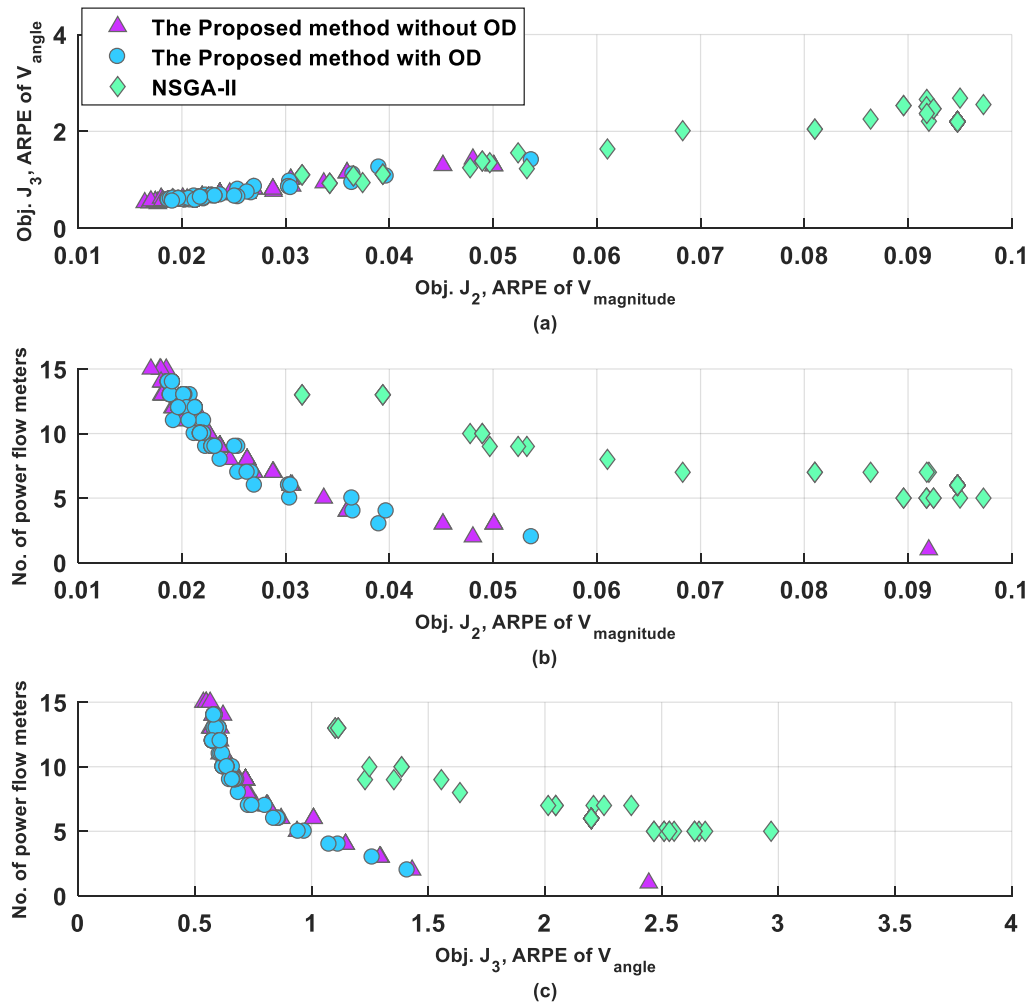


Fig. 4.14: Indian Practical 85-bus active distribution system optimal Pareto-front plots:
1% error in real measurements and 50% error in Pseudo measurements with DG Type-2 (P-jQ)
(OD- Objective Discretization method)

It has been noticed that when real measurement uncertainty increases, the meters required increases. It is worth noting that, when compared to passive network, active network voltage

magnitude and angle error are reduced. The reason for this is that the DG provides the active power to nearby loads, where power drawn from the main feeder is reduced. Therefore, the degree of error related to power flow measurement reduces. The proposed method is also verified for DG type-2 and type-3, and corresponding final Pareto fronts displayed in fig. 4.14, 4.15 and corresponding results are tabulated in Tables 4.9 and 4.10.

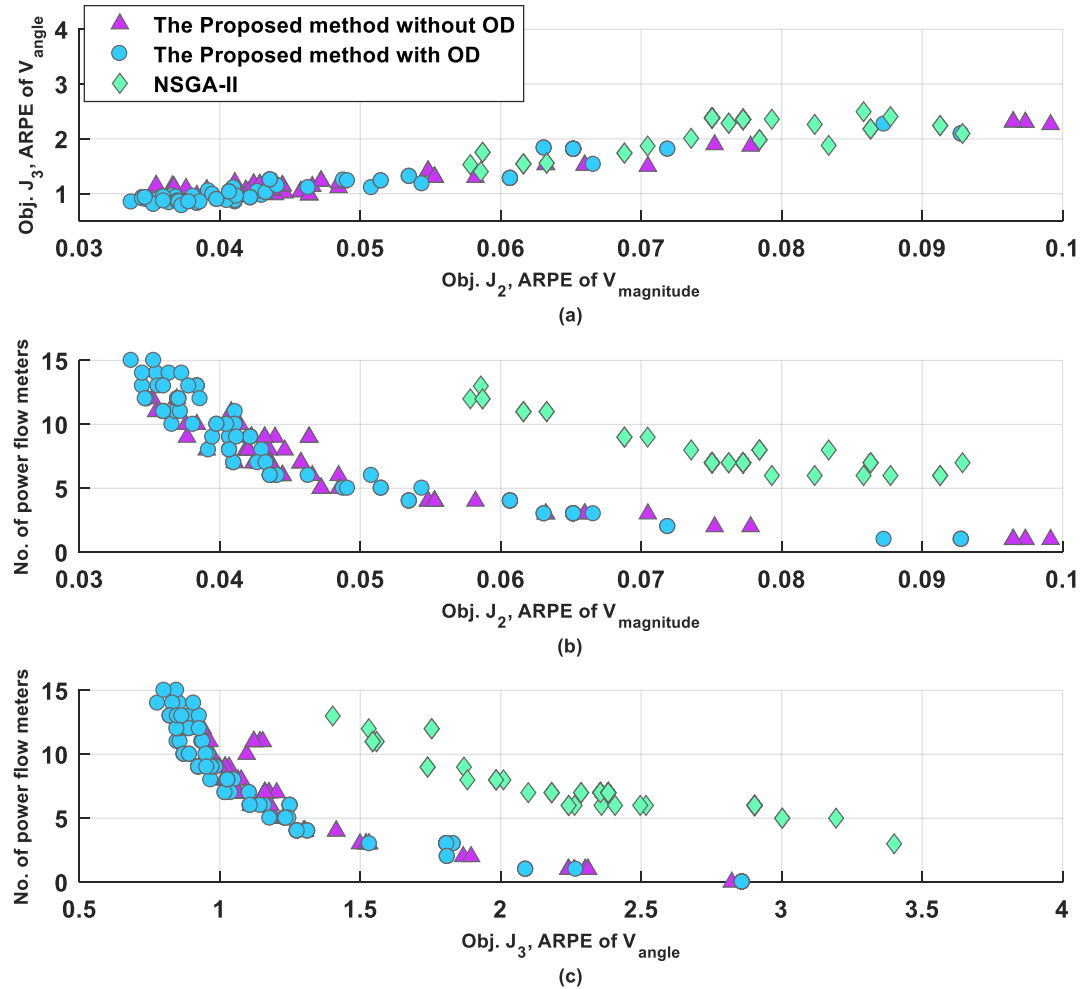


Fig. 4.15: Indian Practical 85-bus active distribution system optimal Pareto-front plots:
1% error in real measurements and 50% error in Pseudo measurements with DG Type-3 ($P+jQ$)
(OD- Objective Discretization method)

Table 4.9: Indian Practical 85-bus distribution system: Optimal location of the power flow meters with 1% measurement uncertainty for DG Type-2(P-jQ).

Algorithm	Position of PMs (Line numbers)	Number of power flow meters	Objective function values		
			J_1 Cost of meters (1 per unit device)	J_2 ARPE of voltage magnitude	J_3 ARPE of voltage angle
Proposed algorithm with OD*	1,17, 25, 31, 57, 63	6	9	0.0270	0.8380
Proposed algorithm without OD*	1, 17, 25, 30, 57, 65	6	9	0.0305	0.8697
NSGA-II [43]	1, 16, 19, 23, 27, 30, 49, 54, 67	9	12	0.0533	1.2292
EDA-IPM [75]	1, 17, 25, 29, 34, 58, 60	7	10	0.0386	1.1584
DP [38]	1, 23, 30, 37, 40, 62, 75	7	10	0.0408	1.3911
OOA [28]	1, 3, 9, 14, 20, 52, 54, 62, 69	9	12	0.0387	1.2929

*OD - Objective Discretization method

Table 4.10: Indian Practical 85-bus distribution system: Optimal location of the power flow meters with 1% measurement uncertainty for DG Type-3(P+jQ).

Algorithm	Position of PMs (Line numbers)	Number of power flow meters	Objective function values		
			J_1 Cost of meters (1 per unit device)	J_2 ARPE of voltage magnitude	J_3 ARPE of voltage angle
Proposed algorithm with OD*	1, 16, 17, 30, 59, 66	6	9	0.0436	1.1079
Proposed algorithm without OD*	1, 16, 17, 26, 29, 56	6	9	0.0440	1.1104
NSGA-II [43]	1, 23, 24, 50, 57, 62, 66, 70	8	11	0.0708	1.8956

EDA-IPM [75]	1, 23, 31, 49, 58, 59, 61	7	10	0.0500	1.1191
DP [38]	1, 18, 25, 35, 66, 70, 76, 82	8	11	0.0513	1.2059
OOA [28]	1, 14, 33, 37, 41, 65, 83, 84	8	11	0.0534	1.3162

*OD - Objective Discretization method

4.8 Summary

This work proposed a new MOEA using objective discretization and indicator-based approach, which is based on IGD-NS performance indicator. Because of combinatorial nature of meter placement problem, the objective space is discrete in nature. To enhance the performance of the proposed method, objective discretization method was adopted, with different granularity along the objectives, so that it enhances the search ability of MOEA and decreases the non-dominated solutions in population. IGD-NS indicator measures diversity and convergence of solution sets and guides the evolution process in MOEA. The indicator IGD-NS can reduce the non-dominated solutions with no contribution to the indicator value. As the performance of MOEA depends on the approximate Pareto front shape, the proposed method employed a reference point method, which adaptively updates the reference points to follow the Pareto front shape. Moreover, the proposed method improves the performance characteristics of MOEA, enhances search ability, provides uniformly distributed solutions on Pareto front, and follow the irregular Pareto front. In addition, the effect of meter placement on various categories of renewable sources is addressed.

In practical applications, a greater number of non-dominated solutions are required with a high degree of diversity. Most of MOEAs use population or external archive to store non-dominated solutions obtained in each generation. In general, only a limited number of diverse non-dominated solutions can be achieved in each generation, in most of population based MOEAs. Moreover, all the conventional MOEAs are designed based on fixed heuristic rules. Therefore, in evolution process these MOEAs may not adapt to the changes in evolutionary environment. However, the additional diverse solutions can be obtained by properly designing the reproduction operator in MOEA. Using machine learning model as reproduction operator, many diverse solutions can be generated directly as needed in the objective space. This provides the ability to learn the environment of evolutionary process by building the learning models from the candidate solutions of current generation. Therefore, chapter 5 proposes an inverse model based MOEAs for meter placement problem in active distribution system.

Chapter 5

Multi-Objective Meter Placement in Active Distribution System State Estimation using Inverse Modeling based on Multi-label Gaussian Process Classification Algorithm with Adaptive Reference Point Method

Published in

Bhanu Prasad Chintala, D. M. Vinod Kumar, “Multi-objective Meter placement in Active Distribution System State Estimation using Inverse Modelling based on Multi-label Gaussian Process Classification algorithm with Adaptive reference point method” **International Transactions on Electrical energy Systems**, Wiley, Vol. 31, No. 8, pp. 1-30, August 2021.

Chapter 5

Multi-Objective Meter Placement in Active Distribution System State Estimation using Inverse Modeling based on Multi-label Gaussian Process Classification Algorithm with Adaptive Reference Point Method

5.1 Introduction

The model based MOEAs are designed to replace the traditional operators such as selection, reproduction, and fitness evaluations with machine learning models. This provides the ability to learn the environment of evolutionary process by building the learning models from the candidate solutions of current generation. Candidate solutions of current generation in evolution process used as sample data for training of the models.

This chapter proposed an inverse model based multi-objective evolutionary algorithm with adaptive reference point method. In practical applications, a greater number of non-dominated solutions are required with a high degree of diversity. Using inverse model, many such solutions can be generated directly as needed in the objective space. Inverse model maps non-dominated solutions from objective space to decision space.

Most of the MOEAs, such as dominance-based, decomposition-based and indicator based MOEAs are designed based on developing the effective fitness calculation or selection process to solve the multi-objective optimization problems. Whereas the model based evolutionary algorithms focuses primarily on effective reproduction process, which explicitly improves the connectedness and regularity property [97] in distribution of Pareto solutions. The connectedness property improves the search efficiency of MOEA.

Inverse model estimates the conditional probability of decision variables, for given objective values. Meter cost and estimation error in voltage magnitude and angle are considered as objectives for the meter placement problem. The meter locations on each distribution network node, are represented as binary value. Therefore, decision space consists of combination of meters in binary variables. The objective space consists of integer values. The classification model is employed to map the integer value objective space to binary value decision space. The output consists of meter combinations represented as binary string, where meter locations belong to multiple labels simultaneously. Therefore, the proposed method uses the multi-label Gaussian Classification for inverse model [98]

The main contributions of this work, are as follows:

- i. A new inverse model-based multi-objective evolutionary algorithm with adaptive reference point method is proposed for meter placement in distribution system state estimation. Inverse model generates the additional non-dominated candidate solutions by sampling the objective distribution. It improves the search efficiency and diversity of Pareto front.
- ii. Meter placement is a combinatorial optimization problem consist of binary decision variables. Therefore, inverse model is realized by classification as it maps non-dominated solution from integer domain objective space to the binary domain decision space. Each meter location is represented as a label to model the binary string in decision space, as meter locations belong to multiple labels simultaneously. Therefore, inverse model is realized using multi-label Gaussian classification.
- iii. The combination of meter locations may not provide continuous non-dominated solutions in Pareto front. Consequently, discontinues Pareto front is formed. The performance of MOEA is affected by the shape of Pareto front. Therefore, adaptive reference point method is employed to follow the shape of the Pareto front.
- iv. Conflicting objectives such as minimizing the cost of metering infrastructure and error in state estimates is considered, and the inverse model based multi-objective framework is used to achieve an optimal meter placement solution in an active distribution network by considering effect of the measurement uncertainty and different types of renewable sources.

5.2 Problem Formulation:

The objectives considered for meter placement are : minimizing i) cost of measurement devices (J_1) ii) the average relative percentage error (ARPE) of voltage magnitude (J_2) and iii) the average relative percentage error (ARPE) of voltage angle (J_3). The objectives that are considered are described as follows:

$$\text{Min } J_1 = \sum_{i=1}^{n^l} C_{PM,i} \cdot U_{PM,i} + \sum_{j=1}^n C_{VMM,j} \cdot U_{VMM,j} \quad (5.1)$$

$$\text{Min } J_2 = \frac{1}{m} \sum_m \frac{1}{n} \left(\sum_{i=1}^n \frac{V_i^t - \hat{V}_i}{V_i^t} \right) \times 100 \quad (5.2)$$

$$\text{Min } J_3 = \frac{1}{m} \sum_m \frac{1}{n} \left(\sum_{i=1}^n \frac{\delta_i^t - \hat{\delta}_i}{\delta_i^t} \right) \times 100 \quad (5.3)$$

Subject to constraints of prespecified limits are considered as 1% and 5% of voltage magnitude and voltage angle relative deviation, respectively for 95% of simulated cases [30], the constraints are presented as follows:

$$g_1 = \left| \frac{V_i^t - \hat{V}_i}{V_i^t} \right| < 1\% \quad (5.4)$$

$$g_2 = \left| \frac{\delta_i^t - \hat{\delta}_i}{\delta_i^t} \right| < 5\% \quad (5.5)$$

Where n and n_l are the number of nodes and lines in distribution system, m is the number of Monte Carlo simulation cases, C_{PM} and C_{VMM} represents the relative normalized costs of power flow meters (PM) and voltage magnitude meter (VMM). The normalized cost of VMM and PM are considered to be the same per unit device cost for comparison purpose and normalized cost is assumed to be 1 unit per device. U_{PM} and U_{VMM} represents the locations of measurement devices as binary variables. When the device is placed at node or on line, then the meter location is represented as '1' and '0' otherwise. Where, g_1 and g_2 are inequality constraints of relative voltage magnitude and voltage angle error limits, V^t , \hat{V} , δ^t and $\hat{\delta}$ are the true value of voltage magnitude, estimated value of voltage magnitude, the true value of voltage angle, and estimated value of voltage angle respectively.

5.3 Methodology:

The proposed method uses inverse model based multi-objective evolutionary algorithm with adaptive reference point method. In practical applications, a greater number of non-dominated solutions are required with a high degree of diversity. Using inverse model, many such solutions can be generated directly as needed in the objective space. Inverse model maps non-dominated solutions from objective space to decision space.

Most of the MOEAs, such as dominance-based, decomposition-based and indicator based MOEAs are designed based on developing the effective fitness calculation or selection process to solve the multi-objective optimization problems. Whereas, the model based evolutionary algorithms focuses primarily on effective reproduction process, which explicitly improves the connectedness and regularity property [97] in distribution of Pareto solutions. The connectedness property improves the search efficiency of MOEA.

This model estimates the conditional probability of decision variables, for given objective values. Meter cost and estimation error in voltage magnitude and angle are considered as objectives for the meter placement problem. The meter locations on each distribution network node, are represented as binary value. Therefore, decision space consists of combination of

meters in binary variables. The objective space consists of integer values. The classification model is employed to map the integer value objective space to binary value decision space. The output consists of meter combinations represented as binary string, where meter locations belong to multiple labels simultaneously. Therefore, the proposed method uses the multi-label Gaussian Classification for inverse model [98].

The algorithm is divided into three stages for simplicity and better understanding. The stage-1 describes the multi-objective evolutionary algorithm using inverse model and stage-2 explains the proposed multi-objective evolutionary algorithm using inverse model with adaptive reference point method, stage-3 discusses the inverse model realized by Multi-label Gaussian Process Classification. The meter placement problem is basically a combinatorial optimization problem, as a large combination of possible solutions, makes the search space large and complex. Therefore, the objective space is irregular and discontinuous. As a consequence, the Pareto front is discontinuous. Therefore, the adaptive reference point method is employed to adjust the reference vectors according to the Pareto front solutions. Moreover, the adaptive reference point method improves search ability of the MOEA and enhances the performance.

The multi-objective evolutionary algorithm using inverse model (stage-1) comprises initialization, partition of population, selection, inverse model and reproduction phases.

- i. **Initialization:** Initially, the population with size 'N', is randomly generated with binary string, which represents the meter locations on each node or line of distribution system. The uniformly distributed reference points are generated using Systematic Sampling Approach (SSA) as follows:

$$N(D, M) = \binom{D + M - 1}{M - 1} \text{ for } D > 0 \quad (5.6)$$

Where D is the number of divisions along with each objective coordinate, and M is the number of objectives.

- ii. **Partition of Population:** Then the population is divided into K subpopulations. The proposed method divides population is based on objective space. On the other hand, division of population is done in reference space in most of decomposition based MOEAs. The partition of population is based on minimum acute angle method expressed as follows:

$$k_t = \operatorname{argmin}_{t=1,2,\dots,K} \frac{\vec{s}_t}{\|\vec{s}_t\|} \times \vec{v}_t \quad (5.7)$$

The solution \vec{S}_t is belongs to the t^{th} partition, when the acute angle between unit solution \vec{S}_t and weight vector \vec{v}_t is minimum, where $t = 1, 2, \dots, K$ and operator x gives the sine function values between unit solution \vec{S}_t and weight vector \vec{v}_t . Then non-dominated sorting and selection process are performed on the K subpopulations.

- iii. **Inverse Model:** Multi-label Gaussian classification is used to estimate the conditional probability of decision variables, for given objective variables. Gaussian Process is used widely for supervised learning. It gives information about the pattern of distribution over function, which is modelled in terms of mean and variance as a function of input variables [87]. The Pareto front solutions (objective) values are considered as input and the meter locations are considered as output labels in multi-label Gaussian classification. Each meter location is treated as a classification label. Therefore, multi-label classification is used for inverse model.

Random grouping method is employed before the inverse model, where multiple decision variables are randomly grouped together to be estimated as output using each objective through inverse model. In general, the random grouping method is used for handling the large scale optimization problems [99], [100]. It is difficult to estimate the m -input and n -output multivariate inverse model directly. This method reduces the number of inverse models required and also enhances the scalability of the algorithm. Using the random grouping technique, the m -by- n multivariate model can be decomposed into m -by- n univariate inverse models to estimate the distribution of conditional probability $P(Y|X)$. In the model, Y refers to output labels and X to input values. Let X be the collection of input variables and Y is the output labels. X is the set of instances of ‘ m ’ objective vales $\{x_1, x_2, \dots, x_i, \dots, x_m\}$ and Y is the class labels (meter locations) and $y_i \in \{0, 1\}$ represented by binary variables. Then the training set T is given by $\{(X_1, Y_1), (X_2, Y_2), \dots, (X_n, Y_n)\}$. If the output labels are independently sampled over the training set then the conditional probability can be expressed as

$$p(Y|X) = \prod_{i=1}^n p(y_i|x_i) \quad (5.8)$$

The above equation can be approximated using the random grouping method, and it introduces the additive Gaussian noise due to the decomposition from multivariate model to univariate model. Then the approximated expression can be as follows

$$p(Y|X) \approx \prod_{i=1}^n p(y_i|x_i) + \epsilon_{j,i} \quad (5.9)$$

Where $\epsilon_{j,i}$ is additive noise in the model and therefore, the above conditional probability can be estimated using Gaussian process classification.

To map the distribution of input variables, a latent function is used to quash the response to limit the interval in between [0,1]. The squashing function used is sigmoid function $\sigma(t)$, where it is defined as

$$\sigma(t) = \frac{1}{1+e^{-t}} \quad (5.10)$$

The classification model is represented with the conditional probability of output y for given sample input x as follows:

$$p(y = 1 | x) = \sigma(f(x)) \quad (5.11)$$

All the sample labels are generated independently, conditioned on latent function $f(x)$ for each training samples $i=1,2,\dots, n$. Then the joint probability is given by

$$p(y|f) = \prod_{i=1}^n p(y_i|f(x_i)) = \prod_{i=1}^n \sigma(y_i f_i) \quad (5.12)$$

The prediction probability over latent function f is given by Bayes' rule as follows:

$$p(f|x, y) = \frac{p(y|f)p(f|x)}{p(y|x)} \quad (5.13)$$

Then the marginal probability is given by

$$p(y|X) = \int p(y|f)p(f|x)df \quad (5.14)$$

Where the likelihood distribution $p(f|x)$ is non-Gaussian and makes the integration analytically intractable. Then, the solution is determined using Laplace approximation method [101].

The Gaussian Process can be applied over latent function $f(x)$ as the distribution in term of mean ($m(x)$) and variance ($K(x, x')$) as given below:

$$f(x) \sim Gp(m(x), K(x, x')) \quad (5.15)$$

where the covariance function K is given by

$$K = K^X(x, x') \otimes K_f \quad (5.16)$$

Where K^X is covariance between x and x' , and K_f gives the correlation among the labels and operator \otimes denotes Kronecker product. The K^X is calculated as:

$$K^X(x, x') = \sum_{x \in X, x' \in X'} \frac{1}{n_x n_{x'}} K_x(x, x')$$

where $K_x(x, x') = e^{-\frac{\|x-x'\|^2}{\delta^2}}$ (5.17)

Where $n_x, n_{x'}$ are dimensions of X and X' , δ is the width parameter, which is taken in between 1 to 2. Then the joint distribution can be written as

$$p(f|X, Y, K_f) = \mathcal{N}(f|m(x), K^X \otimes K_f) \quad (5.18)$$

Then the prediction probability over the test sample X_* can be given by the joint probability over $f(x), f(X_*)$, which are denoted as f, f_*

$$p(f_*, f | X, Y, X_*, K_f) = \mathcal{N} \left(\begin{bmatrix} f_* \\ f \end{bmatrix} \mid \begin{bmatrix} m(X_*) \\ m(X) \end{bmatrix}, \begin{bmatrix} K_{**} & K_* \\ K_*^T & K \end{bmatrix} \otimes K_f \right) \quad (5.19)$$

Where $K_{**} = K^X(X_*, X_*)$, $K_* = K^X(X_*, X)$. The distribution over latent function f_* is given by approximating the likelihood distribution using Laplace approximation [101] as

$$p(f_* | X, Y, f, X_*, K_f) = \mathcal{N} (f_* | (K_*^T K^{-1} \otimes I_f) \hat{f}, (K_{**} - K_*^T K^{-1} K_*) \otimes K_f + (K_*^T K^{-1} \otimes I_f) A^{-1} (K_*^T K^{-1} \otimes I_f)^T) \quad (5.20)$$

Where $\hat{f} = \text{argmax } p(f | X, Y, K_f)$ and $A = -\nabla \nabla \log p(f | X, Y, K_f) |_{f=\hat{f}}$, then the predicted output is given by

$$p(y_* = 1 | X, Y, X_*, K_f) = \int \sigma(f_*) p(f_* | X, Y, f, X_*, K_f) df_* \quad (5.21)$$

The above integral is analytically not computable, because of non-linearity of the latent function. Therefore, the approximation [102] is given by

$$p(y_* = 1 | X, Y, X_*, K_f) \approx \sigma(m / \sqrt{1 + \frac{\pi s^2}{8}}) \quad (5.22)$$

Where m and s are mean and variance of $p(f_* | X, Y, f, X_*, K_f)$ respectively.

The whole process is dependent on K_f , with the algorithm is divided into two steps as estimation step and maximization step. In estimation step, initially K_f is assumed to be unity matrix and then the mean \hat{f} is calculated. In maximization step for a given \hat{f} value from previous step, the value of K_f is updated. Once the both steps are within the specified tolerance levels the mean and variance of marginal probability over f_* is calculated, following which the predicted values are calculated for the test samples. The test inputs are uniformly generated within the interval of obj_j^{\min} to obj_j^{\max} . Where obj_j is j th objective value and $j=1,2,\dots,M$, and M is the number of objective values. The pseudo algorithm for multi-label Gaussian process classification is given in stage-3.

- iv. **Reproduction:** The new offspring population is generated by sampling from the inverse model. The mutation operation is performed on the new offspring population. Then the offspring population and old population are combined to form the next generation. The final optimal solution from the trade-off solutions is obtained using a min-max fuzzy method [88].

The algorithm in stage-1 performs better with regular Pareto fronts, while in case of irregular and discontinuous Pareto fronts, the performance deteriorates. This is due to the uniformly distributed reference points being unable to follow the approximate Pareto front. On the other hand, the meter placement is a combinatorial optimization problem, where a large combination of decision variables leads to discontinuous nondominated solutions on Pareto

front. The adaptive reference point method [94] is employed, to adjust the reference point to follow the irregular and discontinuous approximate Pareto front. This improves the performance of the MOEA. Stage-2 algorithm incorporates the adaptive reference point method to the stage-1 algorithm, which enhance the performance of the MOEA.

i. **Adaptive Reference Point Method:** There are two solution sets and two reference point sets are maintained separately for each generation. The solution sets consist of the current population (P) and the Archive population (A), while the reference sets consist uniformly generated reference point set (R) and adaptively adjusted reference point set (R') are maintained and updated for each generation. Initially, the Archive population (A) and adaptively adjusted reference point set (R') are copied from the current population (P) and uniformly generated reference point set (R) respectively.

The Archive population (A) and adaptively adjusted reference point set (R') are updated for each generation. First, the redundant and dominated solutions are deleted from the archive population (A). Then the reference points (R') are adjusted based on the Archive population (A), by selecting the minimum value of objective value with minimum angle criteria. The extreme end solutions on the Pareto front, are preserved to maintain the diversity of the population; this is done by adjusting the location of extreme solutions and their associated reference point locations. The minimum orthogonal projection of objective values and reference points to the product vector of ideal point (Z^*) and reference point ($\overrightarrow{Z^*r}$) are used to adjust the location of extreme end solutions on PF and their associated reference points, respectively. Then the contributing solutions, which are nearest to at least one reference point, are identified and copied into a new archive population(A'). The remaining new archive population (A') space is filled in by candidate solutions from A or A', until A' reaches the maximum size of a minimum of ($|R|, |A|$) size. The candidate solutions with a maximum of the minimum acute angle between two candidate solutions are selected for new archive population (A'). The reference points are adaptively updated according to the new archive population (A'). The closest reference points to the contributing solution are copied into adaptively adjusted reference points (R'). Then the remaining reference points of R' are filled with the reference points associated with candidate solutions from the new archive A' one by one until the minimum of ($|R|, |A'|$) size is reached. The selection of reference points to update R', is based on the maximum value of minimum acute angel between objective value in A' and the corresponding reference values in R'.

Then the reference points (R') are adjusted based on the current population (P), by selecting the minimum value of objective value with angle criteria.

5.4 Stage wise Process of the Proposed Algorithm:

Stage-1: The multi-objective evolutionary algorithm using inverse model

Step 1: Initialization:

The population (P) with population size 'N', is initialized randomly with meter locations as decision variables. The uniformly distributed reference points (R) are generated using Systematic Sampling Approach (SSA) [87].

Step 2: // Main loop//

While ("Stopping Criteria is not satisfied") do

Step-3: Population Partition:

The population is partitioned into K subpopulations using **minimum** acute angle method using (5.7). Then non-dominated sorting and selection is performed on the K subpopulations.

Step 4: for k = 1 to K

Inverse Model: the decision variables are grouped using random grouping method. then the objective space is mapped onto decision space using multi-label Gaussian classification as shown in stage-3. Then the inverse model is trained to get the estimated output distribution.

Step 5: End for

Reproduction:

The new offspring population (Q) is generated by sampling the estimated output distribution from the inverse model. Then the mutation operation is performed.

Step 6: Update the new generation:

The offspring population (Q) and population (P) are combined to form the next generation population.

End while

Stage-2: The multi-objective evolutionary algorithm using inverse model with adaptive reference point method

Step 1: **Initialization:** The population (P) with population size 'N', is initialized randomly with meter locations as decision variables. The uniformly distributed reference points (R) are generated using Systematic Sampling Approach (SSA). Initialize Archive population (A) and adaptive a reference point set (R'). copy the population (P), Reference point set (R) to the archive population (A) and adaptive reference point set (R') respectively.

Step 2: // Main loop//

While ("Stopping Criteria is not satisfied") do

Step-3: **Population Partition:** The population is partitioned into K subpopulations through **minimum** acute angle method using (5.7). Then non-dominated sorting and selection is performed on the K subpopulations.

Step 4: for k = 1 to K

Inverse Model: the decision variables are grouped using random grouping method. then the objective space is mapped onto decision space using multi-label Gaussian process classification as shown in stage-3. Then the inverse model is trained to get the estimated output distribution.

Step 5: **Reproduction:** The new offspring population (Q) is generated by sampling the estimated output distribution from the inverse model. Then the mutation operation is performed.

End for

// Reference point Adaptation method//

Step 6: // Normalize the current population (P), archive population (A) and reference point set

for i= 1 to M

// M is number of objectives //

$z_i^* = \min_{p \in P} f_i(p)$

// $f_i(p)$ are objective values belonging to population P //

$f_i(p) = f_i(p) - z_i^*, \forall p \in A \cup P$

$R_i^j = R_i^j * (z_i^{had} - z_i^*), \forall j \in \{1, \dots, |R|\}$

End for

Step 7: // Update Archive population (A) //

Step 8: Delete the redundant and dominated candidate solutions from ‘A’
 // adjust the location of a reference point set (R) to preserve the extreme end solutions in PF//
 Initialize the empty R'
For every r belongs to R

$$p = \operatorname{argmin}_{p \in A} \|F(p)\| \sin(\vec{z^*r}, F(p))$$

$$r'_i = \frac{r_i}{\|r_i\|} \cdot \|F(p)\| \cos(\vec{z^*r}, F(p)), \quad \forall i \in \{1, 2, \dots, M\}$$

$$R' \leftarrow R' \cup \{r'\}$$

End for

Step 9: // identify contributing solutions (A^{con}) in A//
 Initialize empty contributing solution A^{con} and archive population A'

$$A^{\text{con}} = \{p \in A \mid \exists r \in R: \text{dis}(r, F(p)) = \min_{q \in A} \text{dis}(r, F(q))\}$$

$$A' = A' \cup A^{\text{con}}$$

Step 10: // fill remaining space in A' from A and A' //
 //fill until the size less than minimum size of R or A//

While (size (A') < min(size(R), size(A))) **do**

$$A' = A' \cup (\operatorname{argmax}_{p \in (A \setminus A')} \min_{q \in A'} \arccos(F(p), F(q)))$$
End while

// identify the reference points near to the contributing solutions A^{con} and current population P//
 Identify the reference points which are nearest to the contributing solutions A^{con} copy them to R'

$$R' = R' \cup \{r \in R \mid \exists p \in A^{\text{con}} : \text{dis}(r, F(p)) = \min_{s \in R} \text{dis}(s, F(p))\}$$
Update the new generation:
 The offspring population (Q) and population (P) are combined to form the next generation population.

End while

Stage-3: Multi-label Gaussian process classification

//Training//

Step 1: **Input:** X, Y, K

Initialization: Initialize estimated latent function \hat{f} with unit vector of size testing sample output Y and initialize K_f as identity matrix with the size of number of labels ‘L’.

Step 2: **Estimation step:** for given K_f estimate the \hat{f} .

Step 3: Then apply logarithm for marginal likelihood function and calculate its value for estimated \hat{f} , and if the values are within the tolerance (t_0) then go to step 4 or else go to step 2.

Step 4: **Maximization step:** for a given \hat{f} from estimation step, update the K_f .

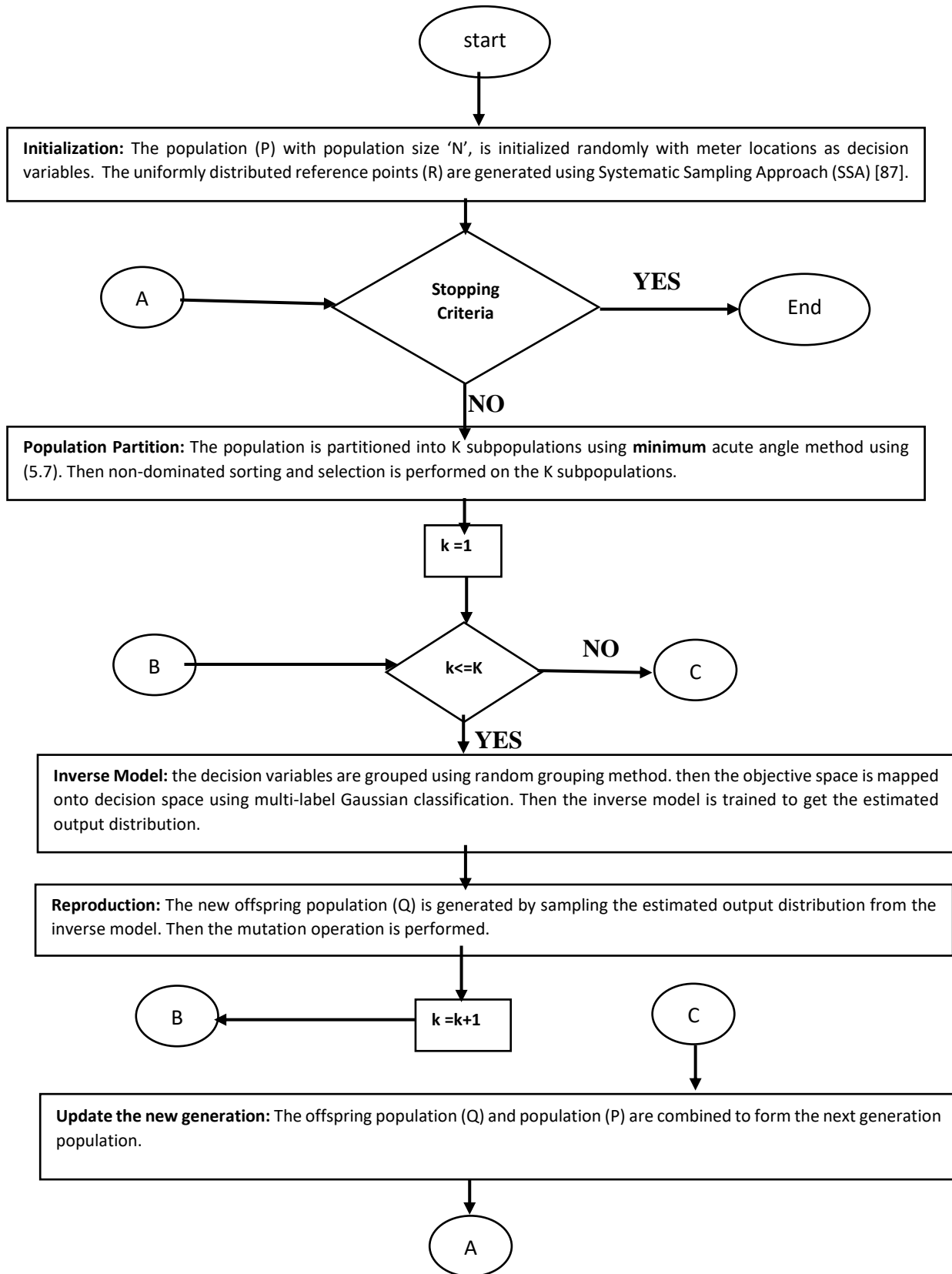
Step 5: if the difference between the two K_f values of consequent loops is smaller than tolerance (t_1) then go to next step 6 or else go to step 2.

//Testing//

Step 6: **Input:** X^* , X, Y, K, K_f , \hat{f}

Calculate the mean and variance.

Step 7: predict the output.

**Fig. 5.1:** Flowchart of the proposed algorithm.

5.5 Simulation and Test Conditions:

The BC-DSSE [16], [17] is supplied with substation measurements, virtual measurements, and pseudo-measurements, to obtain observable measurement set for the proposed method. For the proposed method, the following assumptions are considered:

- i. Voltage magnitude meter at the reference bus is treated as substation measurements. Substation measurements are provided with 1% accuracy. A power flow meter is placed at each DG for active distribution system. These measurements are considered as default measurements.
- ii. A small value of the standard deviation is supplied with virtual measurements, in the order of 10^{-8} .
- iii. The performance of the proposed algorithm is tested with large uncertainty in Pseudo measurements. The huge errors are considered with a maximum error of 50% in Pseudo measurements.
- iv. The power flow meters and voltage meters are supplied with 1% and 5% error with Gaussian distribution.

The objective values are obtained using Monte Carlo simulations under different measurement uncertainties and the following assumptions are considered

- i. Monte Carlo simulation is carried out with 1000 trials for different load conditions for 100 scenarios [37] with each measurement set in population.
- ii. The objectives of voltage magnitude error and voltage angle error are calculated and the constraint violation (5.6) and (5.7) is calculated for 95% simulation cases.

In addition, the parameters used for the proposed algorithm, MOEA/D [49], and NSGA-II [43] are shown in Table-5.1. The population size is considered to be 100, while the population size is determined on the basis of the weight vectors created from the Systematic Sampling Approach (SSA) for decomposition-based methods. For the proposed method, and MOEA/D, with three objectives, the population size is chosen is 91 after the Systematic Sampling Approach (SSA). For all the methods the maximum number of generations are taken as 50. Different Crossover and Mutation rates are tested and chosen Crossover rate (Pc) is 1.0, Mutation rate (Pm) is 0.05 for which it gives the better performance of the MOEA.

Table 5.1: Parameters of the proposed algorithm, MOEA/D/L, MOEA/D and NSGA-II

Algorithm	Control Parameters
The Proposed algorithm, MOEA/D [49]	Crossover rate (Pc)=1.0, Mutation rate (Pm)=0.05.
NSGA-II [43]	Population size =100, Crossover rate (Pc)=0.8, Mutation rate (Pm)=0.01.

5.6 Results and Discussions

The competence of proposed MOEA is verified on PG&E 69-bus distribution system and Indian Practical 85-bus distribution system. This work considered different types of scenarios, such as the impact of meter placement in passive as well as active distribution network have been investigated. Moreover, different types of renewable sources in active network are considered such as DG generating only active power to the network, DG generating active power and absorbing reactive power from the network, and DG generating both active and reactive power (Table-5.2). The distributed generation is assumed as dispatch-able and modelled as a stochastic variable. The details of distributed generation size, location, and types are given in Table-5.2. The DG locations on the distribution system, are at 50, 61 nodes on PG&E 69-bus distribution system, and at 45, 61 nodes on Indian Practical 85-bus distribution system, are decided based on optimal power loss and voltage deviation [75]. The proposed method is compared with MOEA based on decomposition (MOEA/D) [49], non-dominated sorting genetic algorithm (NSGA-II) [43], on existing multi-objective methods such as multi-objective hybrid estimation of distribution algorithm- interior point method (EDA-IPM) [75].

Table 5.2: Distributed generation size and locations

Test System	Bus Number	DG type and Capacity (MW) base value		
		Type-1 (P)	Type-2 (P+jQ)	Type-3 (P+jQ)
PG&E 69-bus Distribution System	50	0.180	0.180-j 0.087	0.180+j 0.087
	61	0.270	0.270-j 0.130	0.270+j 0.130
Indian Practical 85-bus Distribution System	45	0.277	0.235-j 0.145	0.235+j 0.145
	61	0.290	0.246-j 0.152	0.246+j 0.152

For all figs. 5.1 to 5.12 the repeating captions are specified as given here: **(a)** objective function- J_2 average relative percentage error (ARPE) of voltage magnitude Vs. objective function- J_3 average relative percentage error (ARPE) of voltage angle. **(b)** objective function- J_2 average relative percentage error (ARPE) of voltage magnitude Vs. the number of power flow meters **(c)** objective function- J_3 average relative percentage error (ARPE) of voltage angle Vs. the number of power flow meters.

5.6.1 PG&E 69-bus Distribution System

The proposed algorithm is tested on PG&E 69-bus distribution system [92], which has 21 zero bus injection nodes treated as virtual measurements, and a total real power load of 3.802 MW and one VMM, one power flow meter at substation and one power flow meter is placed at each DG, and these are considered as default measurements. Two renewable energy sources

are located on the 50th and 61th bus.

The proposed algorithm for meter placement problem is investigated with 1%, and 5% real measurement uncertainty. The results correspond to objective values and performance of state estimation without DG, as shown in Table-5.3. The obtained Pareto fronts obtained are shown in fig. 5.2 and 5.3 for 1%, and 5% real measurement uncertainty, respectively. The proposed algorithm with and without adaptive reference point method, with 1% accuracy of real measurements, requires 5 meters including the default measurements, whereas MOEA/D, and NSGA-II require 7 and 8 respectively. The average relative percentage error (ARPE) of voltage magnitude and ARPE of voltage angle for the proposed method with and without adaptive reference point method, are 0.0011%, 0.0012% and 0.3477%, 0.4725%, respectively. The ARE of voltage magnitude and voltage angle in percentage for MOEA/D and NSGA-II are 0.0019%, 0.0038% and 0.6025%, 1.6474%, respectively. The existing method in literature such as PSO-KH, EDA-IPM require 6 meters, the quality of the proposed method is far superior as shown in Table-5.3.

Similarly, with 5% real measurement uncertainty the proposed method shows superiority in terms of estimated error of voltage magnitude, angle and as well as the number of meters required.

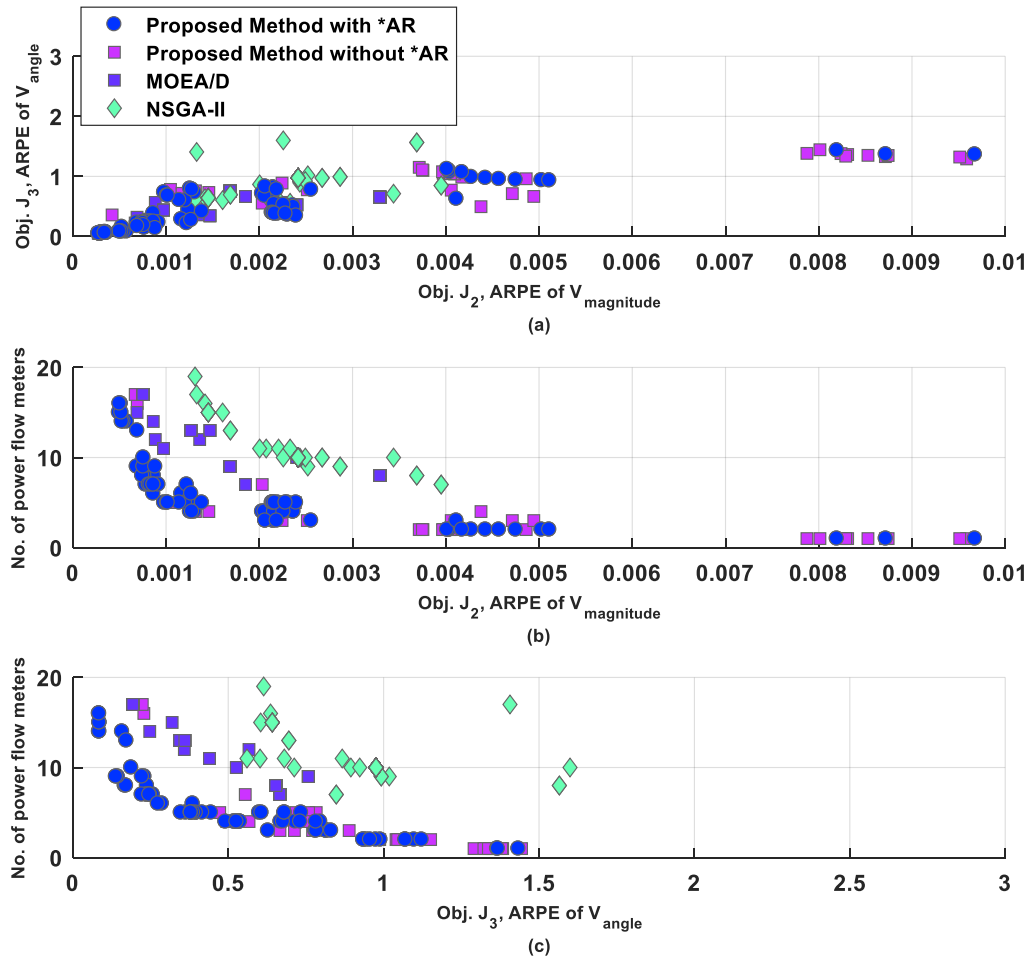


Fig. 5.2: PG&E 69-bus distribution system optimal Pareto-front plots: under 1% uncertainty in real measurements 50% uncertainty in Pseudo measurements for without DG (AR –Adaptive reference point method)

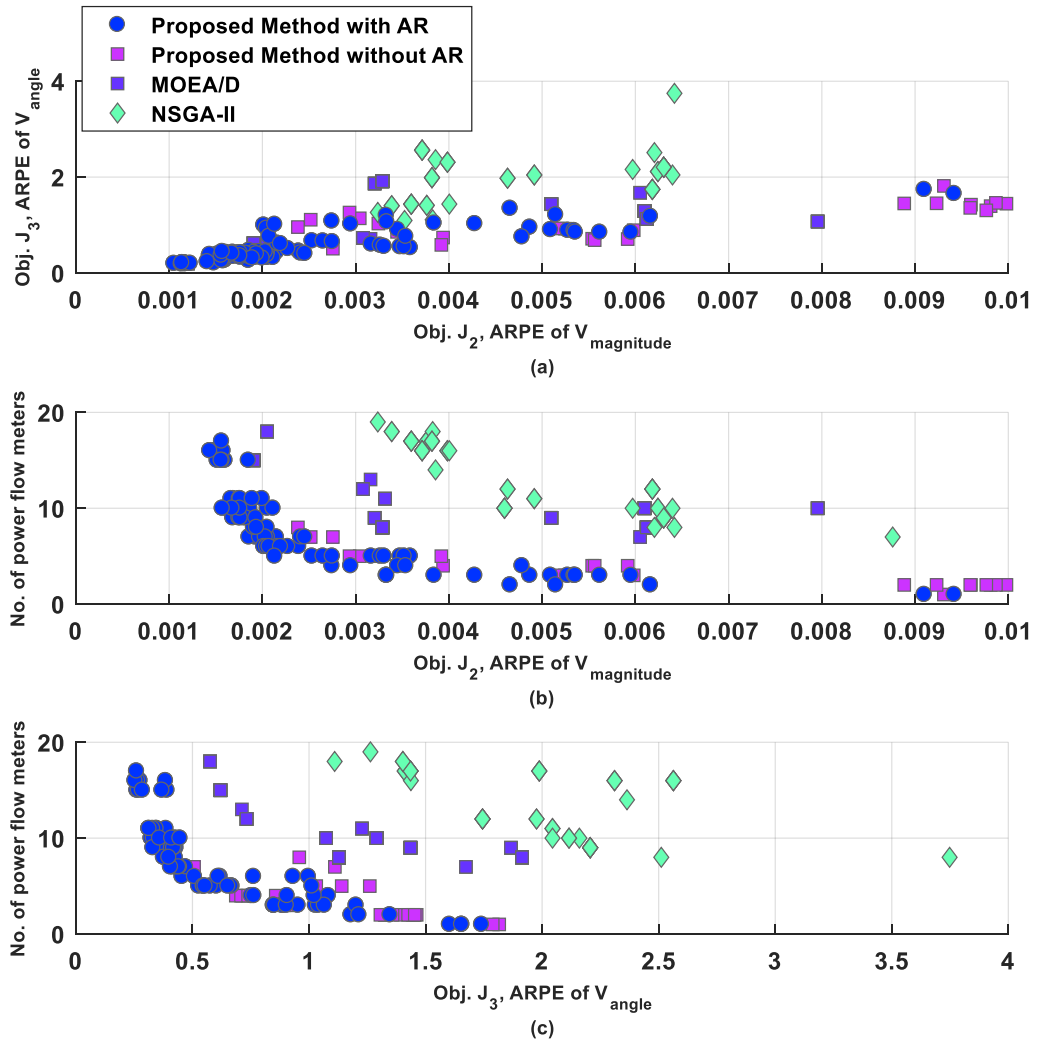


Fig. 5.3: PG&E 69-bus distribution system optimal Pareto-front plots: under 5% uncertainty in real measurements 50% uncertainty in Pseudo measurements for without DG (AR –Adaptive reference point method)

Table 5.3: P&G 69-bus distribution system: Optimal location of the power flow meters under different measurement uncertainty for without DG.

Metrological error (in %)	Algorithm	Location of power flow meters (Line numbers)	Number of power flow meters	Objective function values		
				J_1	J_2	J_3
1	Proposed algorithm with AR*	7, 10, 31, 42	4	5	0.0011	0.3477
	Proposed algorithm without AR*	4, 32, 45, 58	4	5	0.0012	0.4725
	MOEA/D [49]	6, 11, 28, 43, 53, 62	6	7	0.0019	0.6025
	NSGA-II [43]	4, 10, 11, 12, 42, 55, 68	7	8	0.0038	1.6474

	PSO-KH [73]	1, 7, 24, 54, 66	5	6	0.0028	0.4947
	EDA-IPM [75]	1, 3, 7, 24, 51	5	6	0.0025	0.4821
5	Proposed algorithm with AR*	10, 15, 29, 42, 46	5	6	0.0020	0.4555
	Proposed algorithm without AR*	15, 30, 32, 44, 48, 54	6	7	0.0025	0.5066
	MOEA/D [49]	1, 9, 13, 19, 30, 34, 47, 63	8	9	0.0032	1.2314
	NSGA-II [43]	1, 3, 8, 14, 29, 36, 39, 45, 53, 60, 63, 66	12	13	0.0049	1.7634
	PSO-KH [73]	1, 7, 14, 21, 28, 33, 49, 53, 61	9	10	0.0058	1.1491
	EDA-IPM [75]	1, 7, 14, 19, 28, 33, 47, 53, 61	9	10	0.0056	1.1273

(AR* - Adaptive Reference Point Method)

The proposed algorithm for meter placement problem in the active distribution system is investigated with 1%, and 5% real measurement uncertainty and the Pareto optimal plots are shown in figs. 5.4 to 5.5, respectively. The results of DG type-1 (P), are tabulated in Table-5.4. The proposed algorithm with and without adaptive reference point method, with 1% accuracy of real measurements, requires 8 meters including the default measurements at each DG and on the first line, whereas MOEA/D, NSGA-II, PSO-KH, and EDA-IPM requires 10, 12, 8 and 8 respectively. The average relative percentage error (ARPE) of voltage magnitude and ARPE of voltage angle for the proposed method is 0.0009%, 0.0012% and 0.3018%, 0.3366% respectively, whereas for MOEA/D, NSGA-II, PSO-KH and EDA-IPM the values are 0.0020%, 0.0044%, 0.0011%, 0.0018% and 0.3813%, 0.7954%, 0.2653%, 0.3125% respectively. As the proposed method shows superiority with the other algorithms. In the case of 5% real measurement uncertainty, when compared to other methods, the proposed method shows superiority in terms of estimated error of voltage magnitude, angle and as well as the number of meters required. Similarly, the proposed method is tested for DG type-2, type-3 and the optimal Pareto fronts are shown in figs. 5.6 and 5.7, respectively. The performance of all the algorithms is tabulated in Table 5.5 and 5.6 for DG type-2 and type-3, respectively.

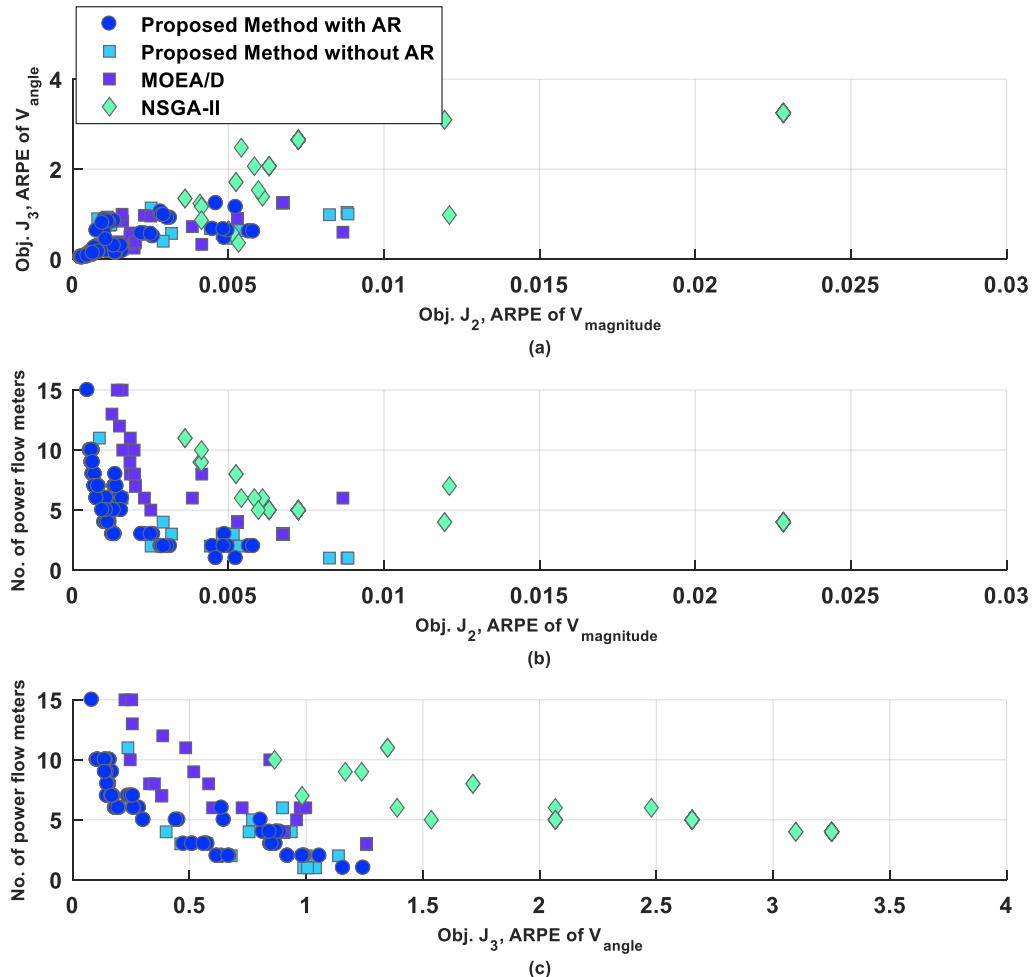


Fig. 5.4: PG&E 69-bus distribution system optimal Pareto-front plots: under 1% uncertainty in real measurements 50% uncertainty in Pseudo measurements with DG Type-1 (P) (AR –Adaptive reference point method)

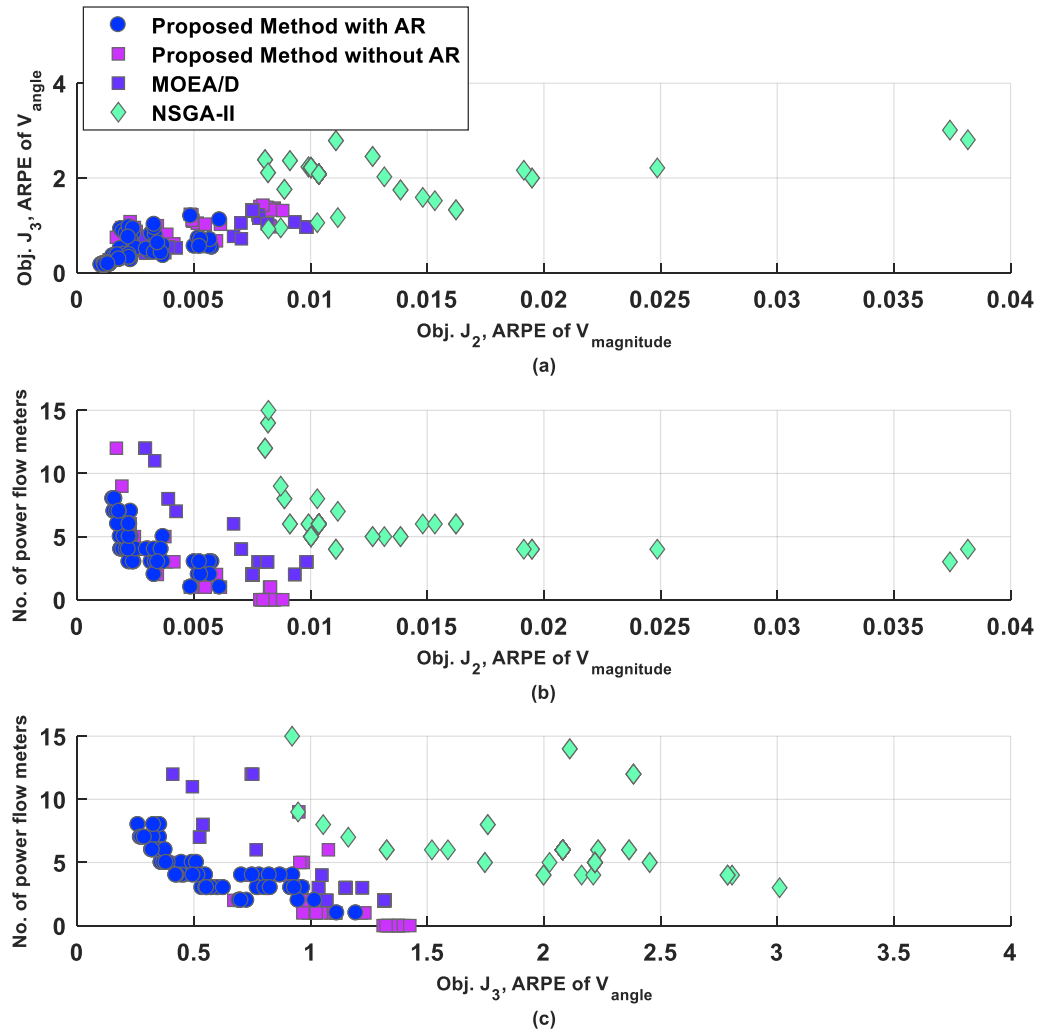


Fig. 5.5: PG&E 69-bus distribution system optimal Pareto-front plots: under 5% uncertainty in real measurements 50% uncertainty in Pseudo measurements with DG Type-1 (P) (AR –Adaptive reference point method).

Table 5.4: P&G 69-bus distribution system: Optimal location of the power flow meters under different measurement uncertainty for DG Type-1(P).

Metrological error (in %)	Algorithm	Location of Power flow meters (Line numbers)	Number of power flow meters	Objective function values		
				J_1	J_2	J_3
1	Proposed algorithm with AR*	14, 28, 32, 41, 57	5	8	0.0009	0.3018
	Proposed algorithm without AR*	12, 27, 32, 41, 57	5	8	0.0012	0.3366
	MOEA/D [49]	6, 14, 31, 33, 44, 45, 57	7	10	0.0020	0.3813
	NSGA-II [43]	9, 12, 18, 30, 41, 48, 52, 53, 60	9	12	0.0044	0.7954

	PSO-KH [73]	1, 49, 52, 59, 67	5	8	0.0011	0.2653
	EDA-IPM [75]	1, 49, 52, 60, 68	5	8	0.0018	0.3125
5	Proposed algorithm with AR*	9, 14, 28, 29, 44, 47	6	9	0.0017	0.3187
	Proposed algorithm without AR*	12, 13, 46, 55, 58, 60	6	9	0.0023	0.4321
	MOEA/D [49]	6, 10, 14, 16, 30, 43, 54	7	10	0.0042	0.5244
	NSGA-II [43]	8, 9, 15, 23, 30, 36, 43, 46, 58	9	12	0.0087	0.9465
	PSO-KH [73]	1, 3, 17, 25, 34, 42, 50, 63	8	11	0.0063	1.0587
	EDA-IPM [75]	1, 3, 17, 24, 33, 41, 50, 63	9	12	0.0051	1.1122

(AR* - Adaptive Reference Point Method)

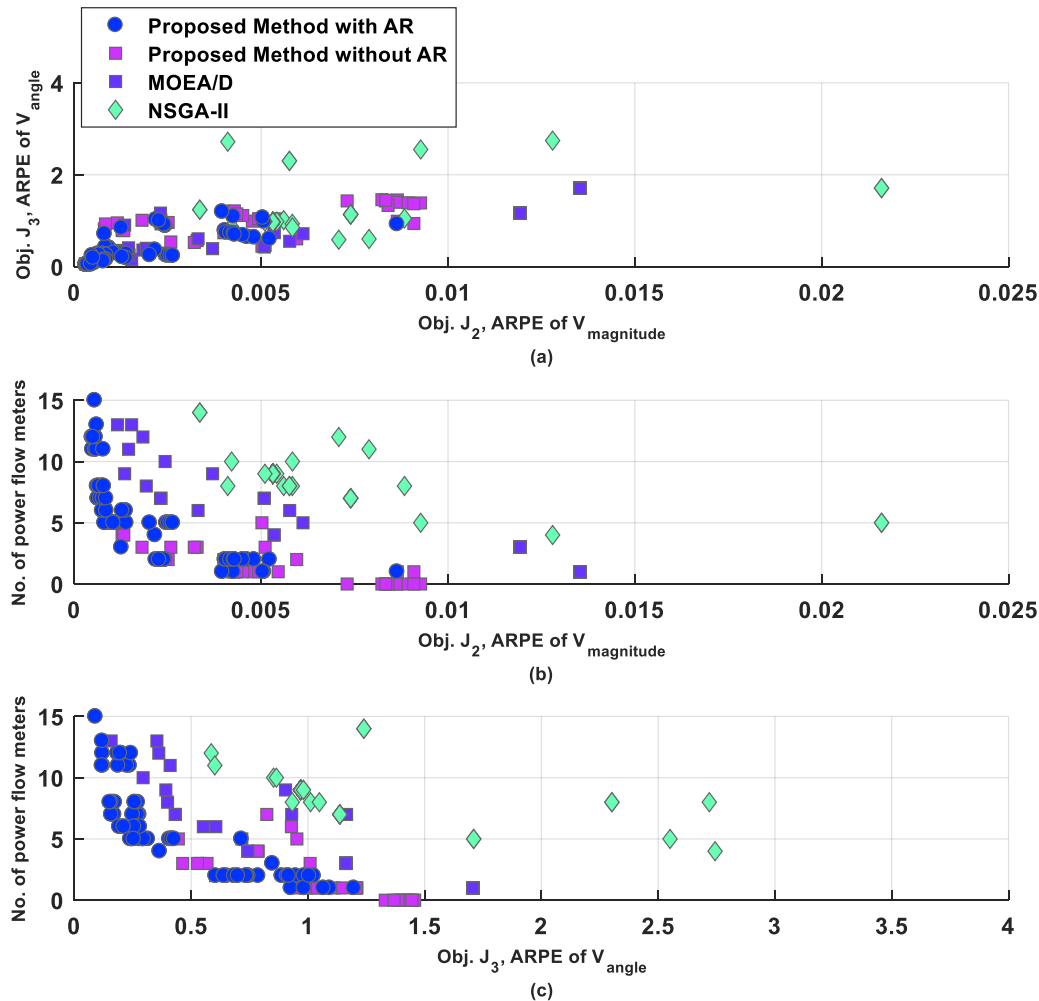


Fig. 5.6: PG&E 69-bus distribution system optimal Pareto-front plots: under 1% uncertainty in real measurements 50% uncertainty in Pseudo measurements with DG Type-2 (P-jQ) (AR –Adaptive reference point method).

Table 5.5: P&G 69-bus distribution system: Optimal location of the power flow meters with 1% measurement uncertainty for DG Type-2(P-jQ).

Algorithm	Location of Power flow meters (Line numbers)	Number of power flow meters	Objective function values		
			J_1	J_2	J_3
Cost of meters (1 per unit device)	ARPE of voltage magnitude	ARPE of voltage angle			
Proposed algorithm with AR*	6, 9, 28, 30, 42	5	8	0.0008	0.2399
Proposed algorithm without AR*	4, 5, 27, 29, 38	5	8	0.0013	0.2474
MOEA/D [49]	7, 13, 30, 40, 45, 57, 63, 68	8	11	0.0019	0.3991
NSGA-II [43]	7, 16, 21, 31, 37, 40, 44, 58	8	11	0.0064	0.8544
EDA-IPM [75]	1, 5, 24, 37, 42	5	8	0.0069	1.1807

(AR* - Adaptive Reference Point Method)

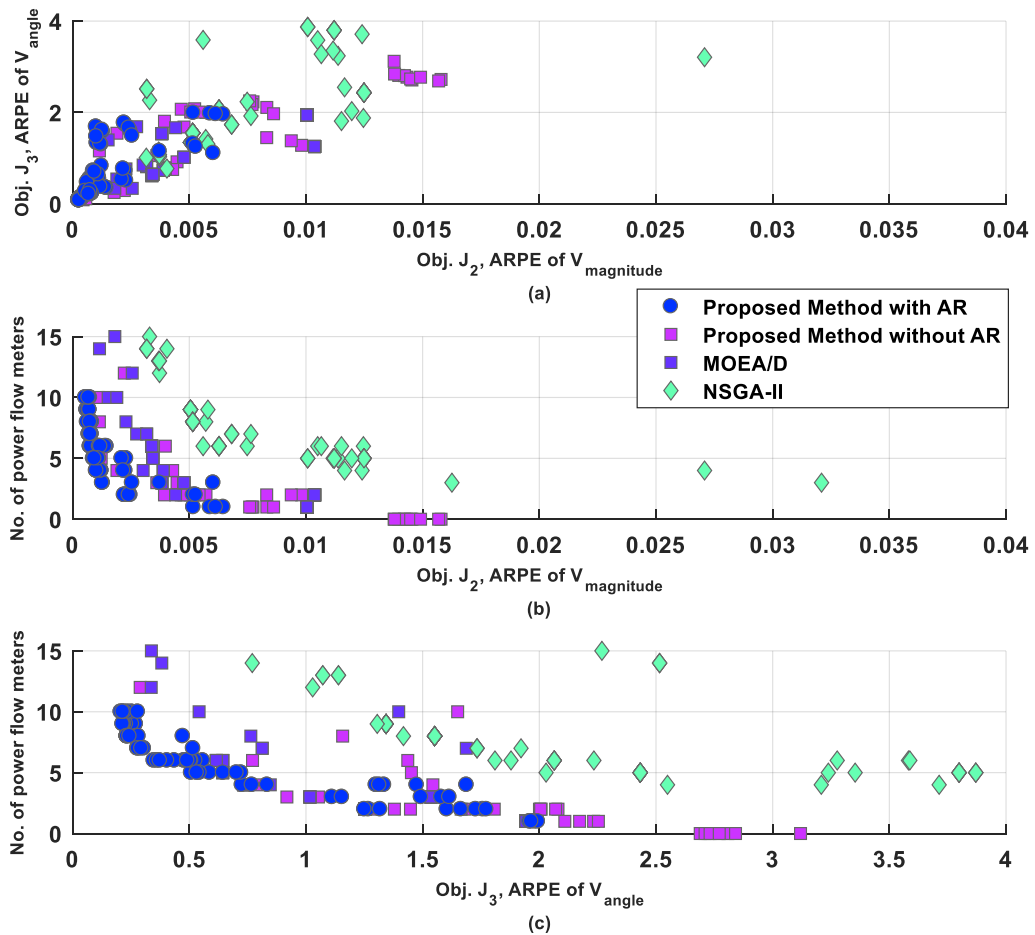


Fig. 5.7: PG&E 69-bus distribution system optimal Pareto-front plots: under 1% uncertainty in real measurements 50% uncertainty in Pseudo measurements with DG Type-3 (P+jQ) (AR –Adaptive reference point method).

Table 5.6: P&G 69-bus distribution system: Optimal location of the power flow meters with 1% measurement uncertainty for DG Type-3(P+jQ).

Algorithm	Location of Power flow meters (Line numbers)	Number of power flow meters	Objective function values		
			J_1	J_2	J_3
Proposed algorithm with AR*	8, 32, 42, 54	4	7	0.0010	0.7257
Proposed algorithm without AR*	6, 30, 37, 56	4	7	0.0011	0.7501
MOEA/D [49]	4, 11, 31, 42, 56	5	8	0.0034	0.6430
NSGA-II [43]	4, 9, 13, 22, 26, 29, 40, 55, 68	9	12	0.0039	1.2852
EDA-IPM [75]	1, 11, 32, 45, 51	5	8	0.0067	0.9864

(AR* - Adaptive Reference Point Method)

5.6.2 Indian Practical 85-bus distribution system

The proposed method has been investigated on Indian Practical 85-bus distribution system [93], which has 84 lines, 26 zero injection nodes, and a total load of real and reactive power of 2.574 MW and 2.622 MVAR respectively. The zero bus injections are modeled as virtual measurements, and one VMM at the slack bus, one power flow meter on the first line, and one power flow meter are placed at each DG, which is considered as default measurements.

The proposed algorithm is tested with 1%, and 5% real measurement uncertainty and the corresponding Pareto fronts are shown in figs. 5.8 and 5.9, respectively. The results correspond to objective values and performance of state estimation without DG, which are tabulated in Table-5.7. The proposed algorithm with and without adaptive reference point method, with 1% accuracy of real measurements, requires 7 meters including the default measurements, while MOEA/D, and NSGA-II require 10 and 11 respectively. The average relative percentage error (ARPE) of voltage magnitude and ARPE of voltage angle for the proposed method are 0.0278%, 0.0298% and 0.6894%, 0.7099% respectively. The ARPE of voltage magnitude and voltage angle for MOEA/D and NSGA-II are 0.0385%, 0.0338% and 1.2964%, 0.8526%, respectively. The existing methods in literature such as PSO-KH, EDA-IPM requires 8 meters, and ARPE of voltage magnitude and ARPE of voltage angle of 0.0385%, 0.0383% and 1.1737%, 1.0952%, respectively. The proposed method is superior in terms of objective value quality and number of meters when compared to all the methods as shown in Table-7. Similarly, with 5% real measurement uncertainty the proposed method shows superiority in terms of estimated error of voltage magnitude, angle and as well as the number of meters required. It is observed from the results that the number of meters required increases with an increase in uncertainty in real measurement.

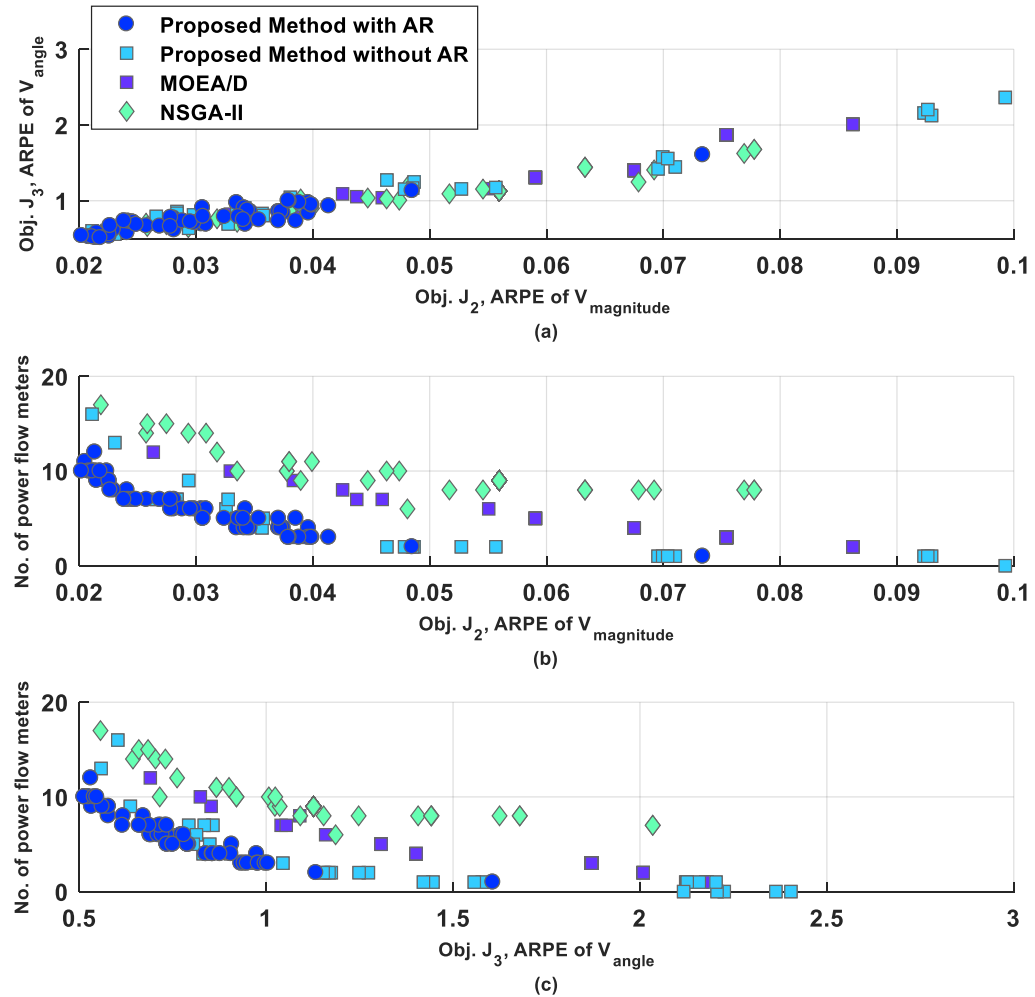


Fig. 5.8: Indian Practical 85-bus active distribution system optimal Pareto-front plots:
Real measurements with an accuracy of 1% and Pseudo measurements with an accuracy of 50% without DG (AR –Adaptive reference point method).

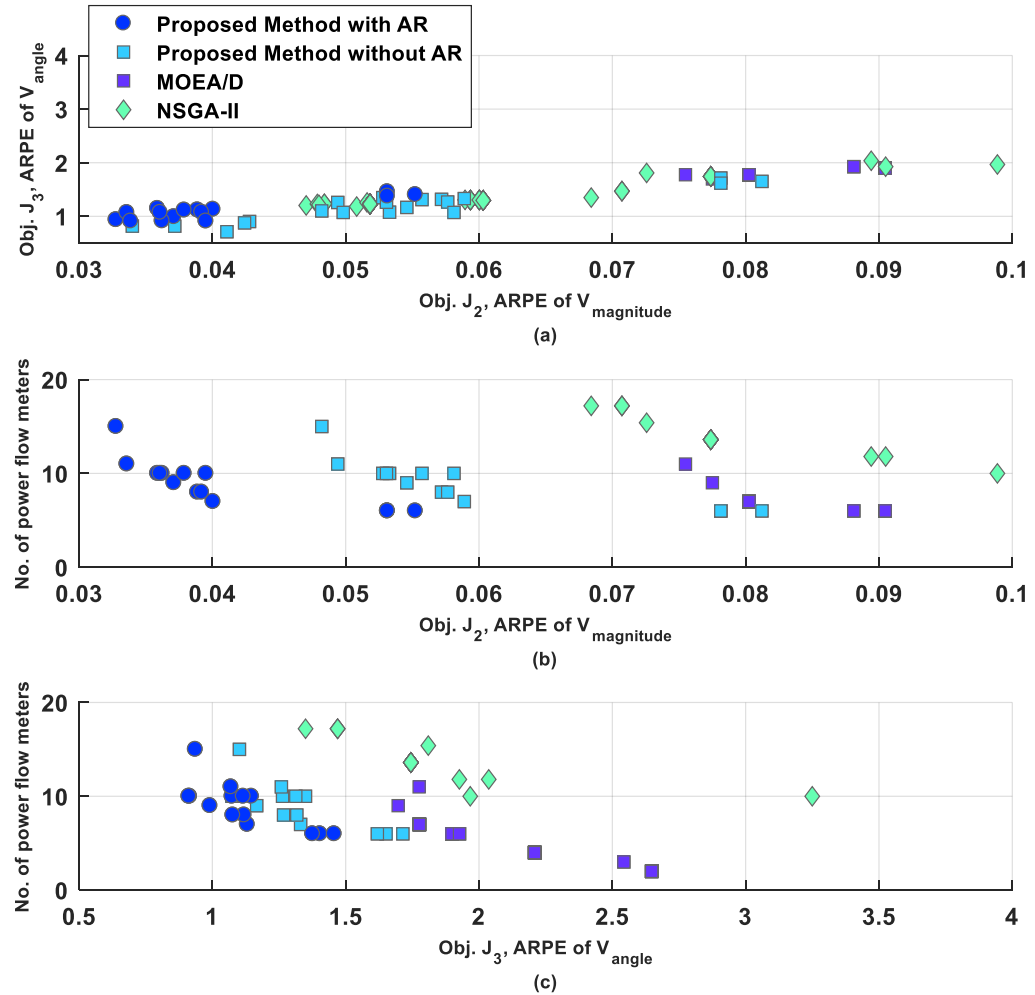


Fig. 5.9: Indian Practical 85-bus active distribution system optimal Pareto-front plots:
Real measurements with an accuracy of 5% and Pseudo measurements with an accuracy of 50% without DG (AR –Adaptive reference point method).

Table 5.7: Indian Practical 85-bus distribution system: Optimal location of the power flow meters under different measurement uncertainty for without DG.

Metrological error (in %)	Algorithm	Location of Power flow meters (Line numbers)	Number of power flow meters	Objective function values		
				J_1 Cost of meters (1 per unit device)	J_2 ARPE of voltage magnitude	J_3 ARPE of voltage angle
1	Proposed algorithm with AR*	8, 17, 24, 33, 56, 59	6	7	0.0278	0.6894
	Proposed algorithm without AR*	6, 7, 11, 28, 30, 59	6	7	0.0298	0.7099
	MOEA/D [49]	1,7, 16, 19, 27, 30, 47, 59, 72	9	10	0.0385	1.2964

	NSGA-II [43]	1,6, 7, 18, 23, 33, 35, 56, 67, 69	10	11	0.0338	0.8526
	PSO-KH [73]	1, 13, 18, 26, 75, 79, 84	7	8	0.0385	1.1737
	EDA-IPM [75]	1, 13, 19, 25, 75, 78, 84	7	8	0.0383	1.0952
5	Proposed algorithm with AR*	9, 16, 17, 24, 32, 56, 63	7	8	0.0351	0.9056
	Proposed algorithm without AR*	16, 17, 25, 32, 34, 59, 72	7	8	0.0413	1.2671
	MOEA/D [49]	1,6, 8, 26, 32, 44, 54, 55, 69, 74, 83	11	12	0.0783	1.7764
	NSGA-II [43]	1,4, 6, 9, 26, 30, 49, 59, 63, 71, 80	11	12	0.0884	1.7494
	PSO-KH [73]	1, 16, 21, 24, 33, 69, 77, 79	8	9	0.0439	1.2855
	EDA-IPM [75]	1, 12, 20, 43, 50, 68, 75, 83	8	9	0.0464	1.4298

(AR* - Adaptive Reference Point Method)

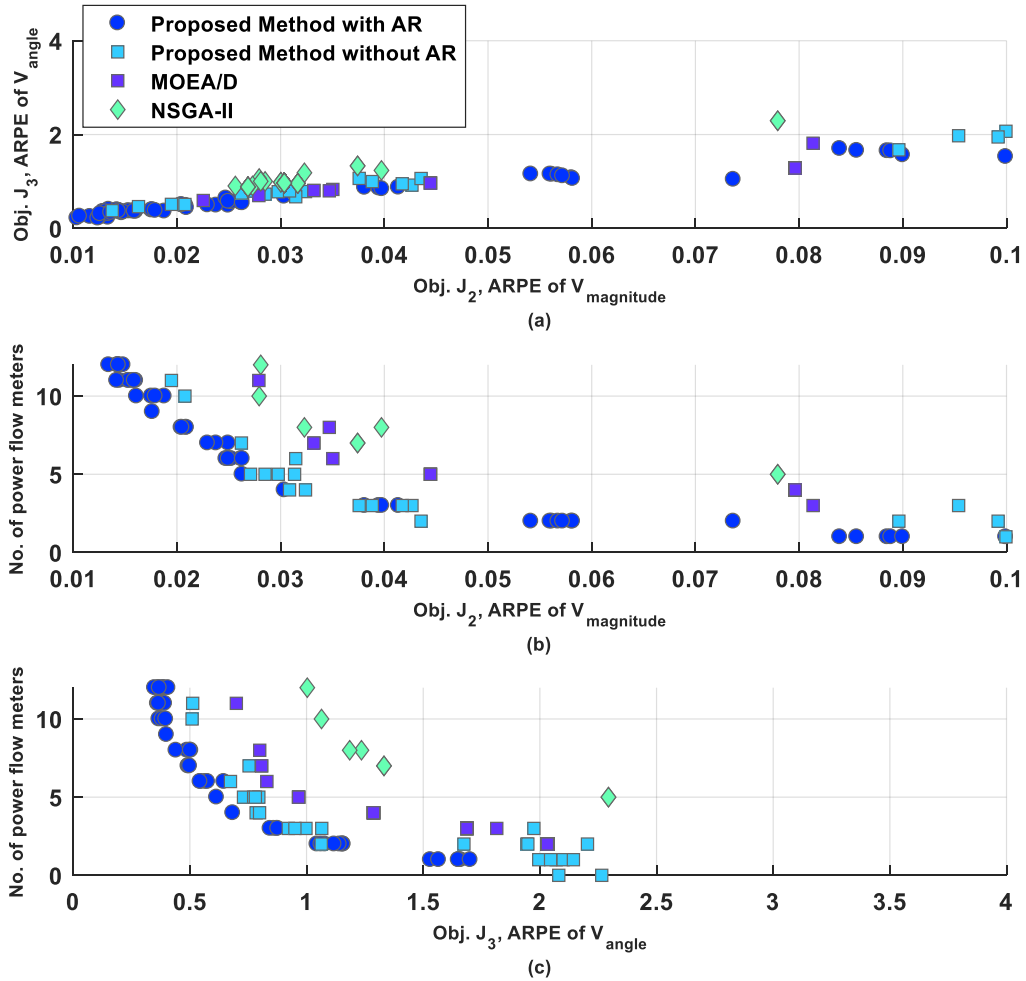


Fig. 5.10: Indian Practical 85-bus active distribution system optimal Pareto-front plots:
Real measurements with an accuracy of 1% and Pseudo measurements with an accuracy of 50% with DG Type-1 (P) (AR –Adaptive reference point method).

The proposed algorithm for meter placement problem in the active distribution system for DG type-1 is investigated with 1%, and 5% real measurement uncertainty and the Pareto optimal plots are shown in figs. 5.10 to 5.11, respectively. The results for DG type-1 (P), are tabulated in Table-5.8. The proposed algorithm with and without adaptive reference point method, with 1% accuracy of real measurements, requires 8 and 8 respectively, meters including the default measurements at each DG and on the first line, whereas MOEA/D, NSGA-II, PSO-KH, and EDA-IPM requires 9, 11, 8 and 8 respectively. The average relative percentage error (ARPE) of voltage magnitude and ARPE of voltage angle for the proposed method are 0.0263% and 0.6144%, respectively. Whereas, for MOEA/D, NSGA-II, PSO-KH

and EDA-IPM are 0.0323%, 0.0347%, 0.0347%, 0.0367% and 1.1407%, 1.1849%, 1.0013%, 1.0473% respectively. The proposed method is superior to the majority of algorithms already in use or available. In the case of 5% real measurement uncertainty, when compared to all the methods the proposed method shows superiority in terms of estimated error of voltage magnitude, angle and as well as the number of meters required. It is observed that the number of meters required increases with an increase in real measurement uncertainty.

Similarly, the proposed method is tested for DG type-2, type-3 and the optimal Pareto fronts are shown in fig. 5.12 and 5.13, respectively. The performance of all the algorithms is tabulated in Table 5.9 and 5.10 for DG type-2 and type-3, respectively.

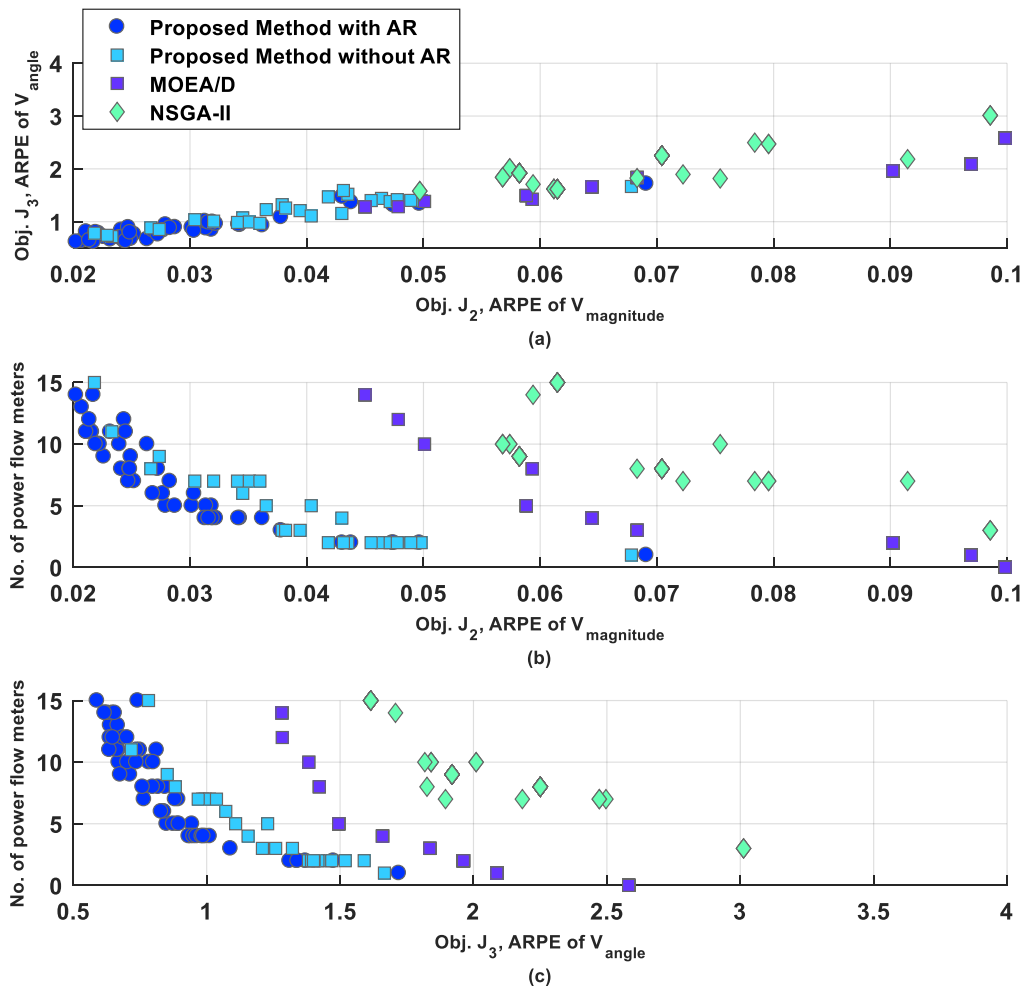


Fig. 5.11: Indian Practical 85-bus active distribution system optimal Pareto-front plots: Real measurements with an accuracy of 5% and Pseudo measurements with an accuracy of 50% with DG Type-1 (P) (AR –Adaptive reference point method).

Table 5.8: Indian Practical 85-bus distribution system: Optimal location of the power flow meters under different measurement uncertainty for with DG Type-1(P).

Metrological error (in %)	Algorithm	Location of Power flow meters (Line numbers)	Number of power flow meters	Objective function values		
				J ₁	J ₂	J ₃
1	Proposed algorithm with AR*	7, 10, 29, 47, 56	5	8	0.0263	0.6144
	Proposed algorithm without AR*	7, 11, 30, 56, 63	5	8	0.0271	0.7298
	MOEA/D [49]	3, 6, 24, 31, 69, 78	6	9	0.0389	1.1407
	NSGA-II [43]	4, 7, 11, 24, 27, 31, 39, 67	8	11	0.0323	1.1849
	PSO-KH [73]	1, 9, 27, 33, 44	5	8	0.0347	1.0013
	EDA-IPM [75]	1, 9, 23, 28, 44	5	8	0.0367	1.0473
5	Proposed algorithm with AR*	9, 16, 18, 24, 31, 57	6	9	0.0268	0.8289
	Proposed algorithm without AR*	7, 16, 31, 40, 57, 71	6	9	0.0345	1.0716
	MOEA/D [49]	13, 17, 25, 26, 66	5	8	0.0588	1.4948
	NSGA-II [43]	8, 16, 17, 19, 26, 39, 46, 62, 77	9	12	0.0582	1.9197
	PSO-KH [73]	1, 9, 19, 28, 46, 62, 79	7	10	0.0419	1.2124
	EDA-IPM [75]	1, 9, 17, 28, 42, 62, 79	7	10	0.0400	1.1001

(AR* - Adaptive Reference Point Method)

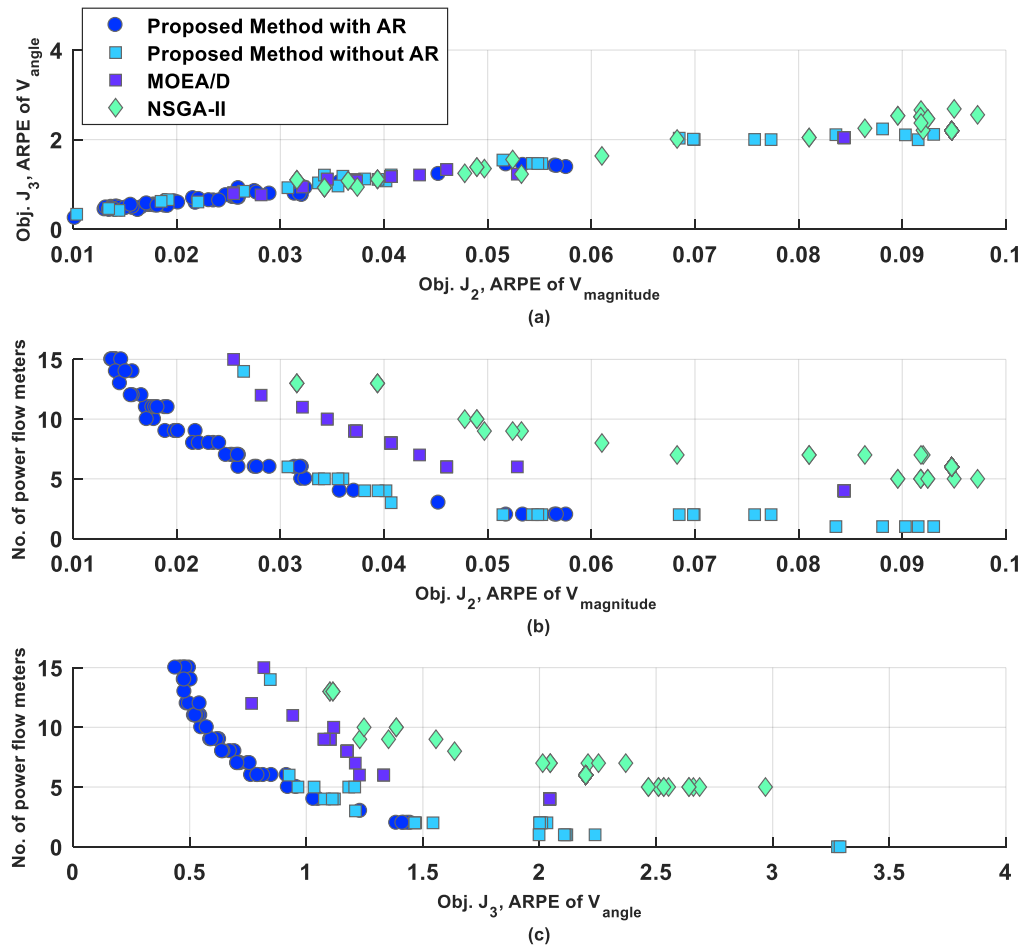


Fig. 5.12: Indian Practical 85-bus active distribution system optimal Pareto-front plots:
Real measurements with an accuracy of 1% and Pseudo measurements with an accuracy of 50% with DG Type-2 (P-jQ) (AR –Adaptive reference point method).

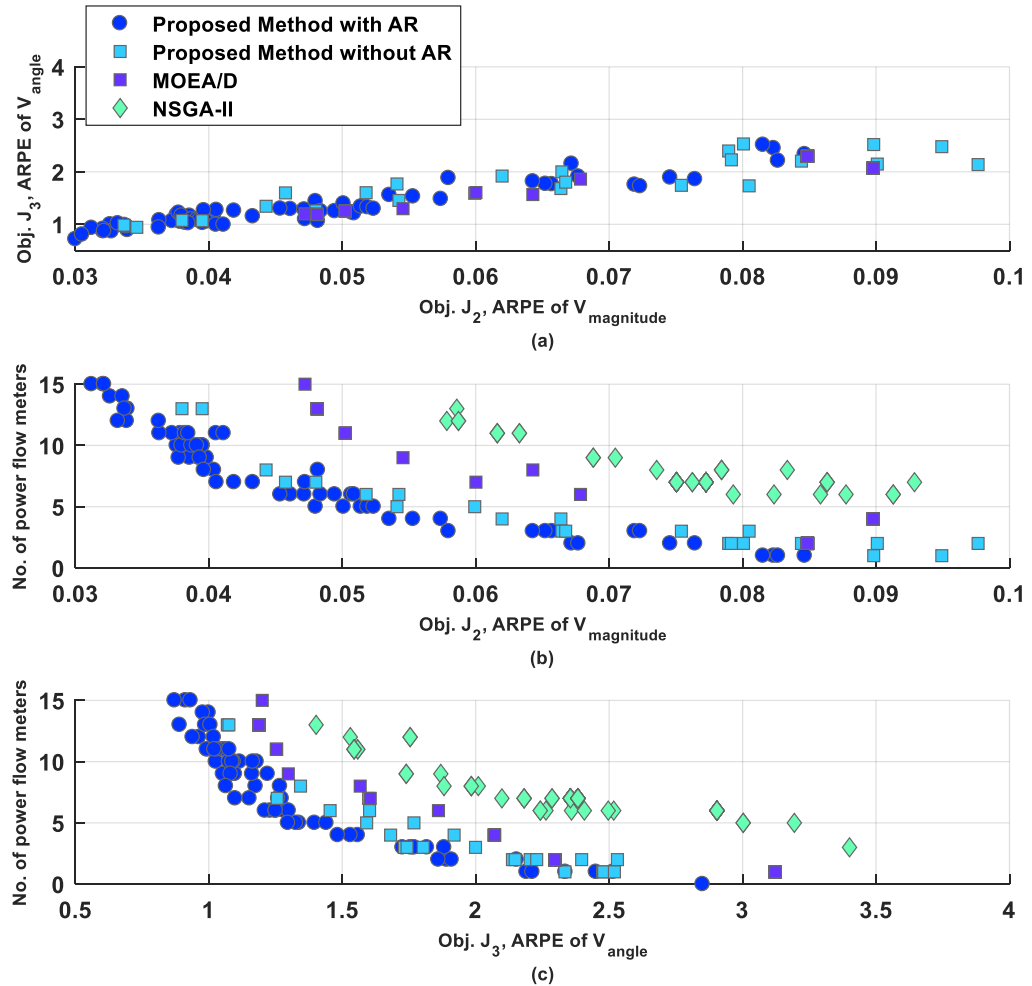


Fig. 5.13: Indian Practical 85-bus active distribution system optimal Pareto-front plots: Real measurements with an accuracy of 1% and Pseudo measurements with an accuracy of 50% with DG Type-3 (P+jQ) (AR –Adaptive reference point method).

Table 5.9: Indian Practical 85-bus distribution system: Optimal location of the power flow meters with 1% measurement uncertainty for with DG Type-2(P-jQ).

Algorithm	Location of Power flow meters (Line numbers)	Number of power flow meters	Objective function values		
			J_1 Cost of meters (1 per unit device)	J_2 ARPE of voltage magnitude	J_3 ARPE of voltage angle
Proposed algorithm with AR*	7, 8, 26, 57, 60	5	8	0.0320	0.9213
Proposed algorithm without AR*	5, 17, 24, 31, 59	5	8	0.0337	0.9642
MOEA/D [49]	3, 6, 23, 26, 29, 33, 38, 45, 57, 65, 83	11	14	0.0321	0.9418

NSGA-II [43]	13, 16, 19, 23, 27, 30, 49, 54, 67	9	12	0.0533	1.2292
EDA-IPM [75]	1, 17, 25, 29, 34, 58, 60	7	10	0.0386	1.1584

Table 5.10: Indian Practical 85-bus distribution system: Optimal location of the power flow meters with 1% measurement uncertainty for with DG Type-3 (P+jQ).

Algorithm	Location of Power flow meters(Line numbers)	Number of power flow meters	Objective function values		
			J₁ Cost of meters (1 per unit device)	J₂ ARPE of voltage magnitude	J₃ ARPE of voltage angle
Proposed algorithm with AR*	8, 15, 16, 17, 31, 59	6	9	0.0404	1.2104
Proposed algorithm without AR*	10, 16, 17, 26, 29, 56	6	9	0.0440	1.2204
MOEA/D [49]	5, 8, 14, 15, 16, 17, 32, 36, 67	9	12	0.0546	1.2980
NSGA-II [43]	6, 23, 24, 50, 57, 62, 66, 70	8	11	0.0708	1.8956
EDA-IPM [75]	1, 23, 31, 49, 58, 59, 61	7	10	0.0500	1.1191

(AR* - Adaptive Reference Point Method)

The inverse model reproduces the addition non-dominated solutions from the estimated conditional probability, which improves the search efficiency of MOEA. From the results it is evident that the proposed method out performs compared to other methods, in terms of estimated error of voltage magnitude, angle and number of meters required. When the Pareto fronts in figs. 5.2 to 5.13 are examined, the proposed method shows the evenly distributed diverse solutions on optimal Pareto front as compared to the proposed method without adaptive reference point method, MOEA/D and NSGA-II Pareto fronts. The discontinuities in Pareto fronts are clearly noticeable in all the plots from figs. 5.2 to 5.13. These discontinuities are due to the combinatorial nature of the meter placement problem, may not provide continuous values in objective space. When the shape of the Pareto front is irregular (disconnected, degenerated, and with sharp tails), uniformly distributed reference points in MOEA/D, unable to obtain the best approximation to Pareto front. As the reference points are adaptively adjusted in the proposed method, the distribution of reference points reflects the shape of the approximate optimal Pareto front and maintains evenly distributed non-dominated solutions on Pareto front. Moreover, the results obtained show the efficiency of the proposed algorithm in terms of estimated error of voltage magnitude, angle, minimum number of meters, diversity, and distribution of solutions on the Pareto front.

5.7 Summary

This work proposed a new inverse model based multi-objective evolutionary algorithm for meter placement in active distribution system state estimation. Inverse model maps the candidate solution in Pareto front from objective space to decision space. The decision space is a binary value string, which represents the meter locations and objective values are in integer domain. To map the binary space to integer domain, the inverse model is realized by multi-label Gaussian process classification. The inverse model is used as reproduction operator to generate additional candidate solutions from estimated distribution of conditional probability. The main benefit of inverse model is to generate samples that are directly belong in desired objective space and improved search efficiency of the evolutionary algorithm. As the meter placement problem is combinatorial optimization, the Pareto front is discontinuous. Therefore, the reference points are adjusted using adaptive reference point method, so that the reference points follow shape of the approximate Pareto front, which improves the performance of the proposed algorithm. The meter placement in an active distribution system is modelled as multi-objective problem of conflicting objectives such as the accuracy of state estimation and the cost of the meter configuration to achieve the optimal solution.

In distribution system, state estimation performance can be enhanced using the meter placement problem and it is handled in two ways using i) topological observability and ii) made numerically observable by adding Pseudo measurements. The second method, made numerically observable by adding Pseudo measurements, is widely used to formulate the meter placement problem in distribution system. The power injection measurements at all the nodes are modeled as Pseudo measurements, and these are fixed set of measurements considered in meter placement problem. The drawback with pseudo measurement based meter placement is the accuracy of state estimation suffers due to the huge error associated with Pseudo measurements. The minimum number of Pseudo measurements that are needed to be added to the measurement set is not addressed in the literature. Therefore, chapter 6 proposes a multi-objective meter placement in distribution system using numerical observability to find the minimum number of Pseudo measurements for given set of real measurements.

Chapter 6

Many Objective Meter Placement in Active Distribution System State Estimation based on Numerical Observability Method

Under review in

Bhanu Prasad Chintala, D. M. Vinod Kumar, “Many Objective Evolutionary Optimization for Meter Placement in Active Distribution System based on Numerical Observability”, **Applied Soft Computing**, Elsevier. [*Under Review*].

Chapter 6

Many Objective Meter Placement in Active Distribution System State Estimation based on Numerical Observability Method

6.1 Introduction

The distribution system contains a large number of nodes, to make the system observable, the measurement devices need to be installed almost at each node, which is economically not suitable. Therefore, meters need to be installed at appropriate locations optimally. The additional meters are required to improve the observability of the network and redundancy of measurements, which enhances the performance of state estimation. In distribution system, state estimation performance is upgraded using the meter placement problem and it is handled in literature in two ways using i) topological observability and ii) made numerically observable by adding Pseudo measurements. Using topological observability based meter placement, the total number of meters required is around one third of the number of nodes in distribution system. Whereas, using the pseudo measurement based meter placement method the number of meters required is very less than the topological observability based meter placement method. The advantage of a smaller number of meters is due to the additional Pseudo measurements that are supplied along with real measurements.

To improve the performance of state estimation, additional real measurements were added along with the fixed Pseudo measurements using the optimal meter placement method. The drawback with pseudo measurement based meter placement is the accuracy of state estimation suffers due to the huge error associated with Pseudo measurements. The minimum number of Pseudo measurements that are needed to be added to the measurement set is not addressed in the literature.

This chapter proposes many-objective evolutionary optimization for meter placement problem in an active distribution system based on numerical observability. In general, the Pseudo measurements are fixed, and all the node injections are modeled as Pseudo measurements. Whereas, with fixed Pseudo measurements, state estimation accuracy degrades, and the number of actual measurements required to achieve the desired state estimation accuracy rises. The evolutionary optimization process only selects combination of real measurements, without changing the fixed Pseudo measurements, so that the formulated objectives are optimized. For the first time, this work proposes the numerical observability to

select the minimum number of Pseudo measurements for a given set of real measurements, which satisfies the observability of the network. By choosing the minimum number of Pseudo measurements the accuracy of state estimation increases and the number of real measurements also reduces. The trade-off between distribution leve Phasor measurement units (D-PMUs) and intelligent electronic devices (IEDs) are considered to formulate the meter placement problem. When the objectives increase above three, then most of the multi-objectives fail to perform effectively, as the objective spaces increase. Therefore, many-objective evolutionary algorithms are utilized to overcome the issues with multiple objectives. A many-objective optimization is designed to handle the minimization of the number of meters of D-PMUs and IEDs along with minimization of root mean square errors of voltage magnitude and voltage angle as objectives. The meter placement problem is a combinatorial optimization, the decision space consists of the binary values which represent the meter locations and objective space in integer values. Therefore, to map the integer objective domain to the binary decision domain, a multi-label Gaussian process classifier as an inverse model generates the additional solution sets in the decision space. Therefore, a many-objective inverse model based evolutionary optimization is used to formulate meter placement problem in distribution system. The main contributions are as follows:

- i. For the first time, the numerical observability method is used to minimize the number of Pseudo measurements for a given set of real measurements, which are generated by evolutionary optimization.
- ii. An inverse model based many-objective evolutionary optimization is designed using four objectives as minimization of D-PMUs cost, minimization of IEDs cost, minimization of root means square errors of voltage magnitude and minimization of root mean square errors of voltage angle. Multi-label Gaussian process classification is used to map the objective space and binary decision space in the inverse model.
- iii. The trade-off between D-PMUs and IEDs are considered to formulate the meter placement problem.

6.2 Problem Formulation:

The many objective meter placement problem is designed using objectives: minimizing i) cost of D-PMUs (J_1) ii) cost of IEDs (J_2) and iii) the root mean square error of voltage

magnitude (J_3) and iv) the root mean square error of voltage angle (J_4). The objectives are mathematically represented as follows:

$$\min J_1 = \sum_{i=1}^n C_{D-PMU,i} \cdot P_{D-PMU,i} \quad (6.1)$$

$$\min J_2 = \sum_{i=1}^{nl} C_{IED,i} \cdot P_{IED,i} \quad (6.2)$$

$$\min J_3 = \frac{1}{m} \sum_{j=1}^m \sqrt{\frac{1}{n} \left(\sum_{i=1}^n (V_i^t - \hat{V}_i)^2 \right)} \quad (6.3)$$

$$\min J_4 = \frac{1}{m} \sum_{j=1}^m \sqrt{\frac{1}{n} \left(\sum_{i=1}^n (\delta_i^t - \hat{\delta}_i)^2 \right)} \quad (6.4)$$

Where C_{D-PMU} , C_{IED} are the cost of distribution level PMUs and IEDs respectively. The per-unit cost of D-PMU is considered as 0.3 and IED is considered as 0.6 [74], [103]. P_{D-PMU} , P_{IED} are the positions in binary values of D-PMUs and IEDs respectively. Whereas, V^t , δ^t are true values and \hat{V} , $\hat{\delta}$ are estimated values of states. The number of Monte Carlo Scenarios are denoted by m , the number of nodes and lines are denoted by n, nl .

6.3 Numerical Observability Method:

The numerical observability method is based Gram-Schmidt on orthogonalization approach of rows of Jacobian [104]. The numerical observability method determines the orthogonal basis of Jacobian matrix rows. If the number of vectors in the basis is equal to $(n-1)$, then the system is observable. The Gram-Schmidt process provides the linearly independent vectors $V = \text{span} \{v_1, v_2, \dots, v_n\}$ and the orthogonalization process is using the projections on linearly independent vectors which gives the projection of linearly independent vector V_i onto the row h_j in the Jacobian matrix. The projection operator is expressed as follows:

$$p(h_j) = (h_j \cdot V_i) V_i \quad (6.5)$$

The error of each projection is calculated, and based on the maximum error value of projection the next row is selected from the Jacobean matrix. In distribution system, Gain matrix is used for calculating the linearly dependent rows as the Gain matrix is symmetric matrix [83]. Then, the linearly independent vector is determined using the selected row. The error projection is evaluated as follows:

$$e_j = \|h_j - p(h_j)\| \quad (6.6)$$

The stopping criterion is based on the error of projection, if it is less than or equal to 10^{-7} , then the process is terminated. When the linearly independent vectors V consists of $(n-1)$ vectors

then the system is observable otherwise unobservable. if the system is unobservable for a given set of measurements, then the additional Pseudo measurements are determined by using previous linearly independent vectors V using the Gram-Schmidt process until it reaches the stopping criteria (projection error $\leq 10^{-7}$). The power injections are at each node with 50% error are modeled as Pseudo measurements and Jacobean is formulated with Pseudo measurements and projection of rows on linearly independent vectors is calculated, and projection errors are calculated to select the Pseudo measurements. This procedure gives the minimum number of Pseudo measurements for a given set of real measurements.

6.4 Many-Objective Evolutionary Optimization using Inverse Model:

The proposed method uses model based many-objective evolutionary optimization. The locations of measurements are represented with binary values, and the objectives are in integer values. Multi-label Gaussian Process classification [98] generates additional non-dominated solutions, which improves the diversity of the population. The inverse model is realized by Gaussian process classification by mapping the objective space to the meter location binary decision space. Then in the reproduction process, the offspring population is produced from the inverse model. The detailed algorithm is provided step by step as follows:

Step 1: Initialization: The initial population with meter locations of D-PMUs and IEDs is generated randomly. The Systematic Sampling Approach is used to create uniformly dispersed reference points [87].

Step 2: Numerical Observability Method: The power injections at all the nodes are modeled as Pseudo measurements. The real measurements (D-PMUs and IEDs) along with Pseudo measurements are supplied to the numerical observability to determine the minimal number of Pseudo measurements for a given set of real measurements.

Step 3: State Estimation: State estimation is evaluated for a given set of the substation measurements, virtual measurements, minimum set of Pseudo measurements, and real measurements. The state estimation is executed for the ‘m’ number of Monte Carlo simulations for different measurement errors.

Step 4: Partition of Population: The population is divided into K subpopulations using the minimum acute angle criteria and it expressed as follows:

$$k_t = \arg \min_{t=1,2,\dots,K} \frac{\vec{s}_t}{\|\vec{s}_t\|} \times \vec{v}_t \quad (6.7)$$

The candidate of population \vec{S}_t is added to partition t , when the acute angle between unit \vec{S}_t and reference vector \vec{v}_t is minimum, where $t = 1, 2, \dots, K$. Then non-dominated sorting is applied on the K subpopulations.

Step 5: Gaussian Process Classification based Inverse model: The multi-label Gaussian process classification is used to map the integer objective space to binary decision space [29]. The model involves of the estimation step and maximization step. The estimation step estimates the latent function for a given covariance function where the maximization step updates the covariance function for the estimated latent function.

Step 6: Reproduction: Samples from the inverse model are used to produce the additional offspring. The mutation operator is applied then the offspring and old population are combined to produces the next generation. Then, using the adaptive reference point method, the reference points are adaptively modified based on the new population to follow the discontinuous Pareto front [105]. Then the trade-off objective optimal value is selected using the fuzzy min-max method [88]. The flow chart of the proposed many-objective evolutionary method is given in fig. 6.1.

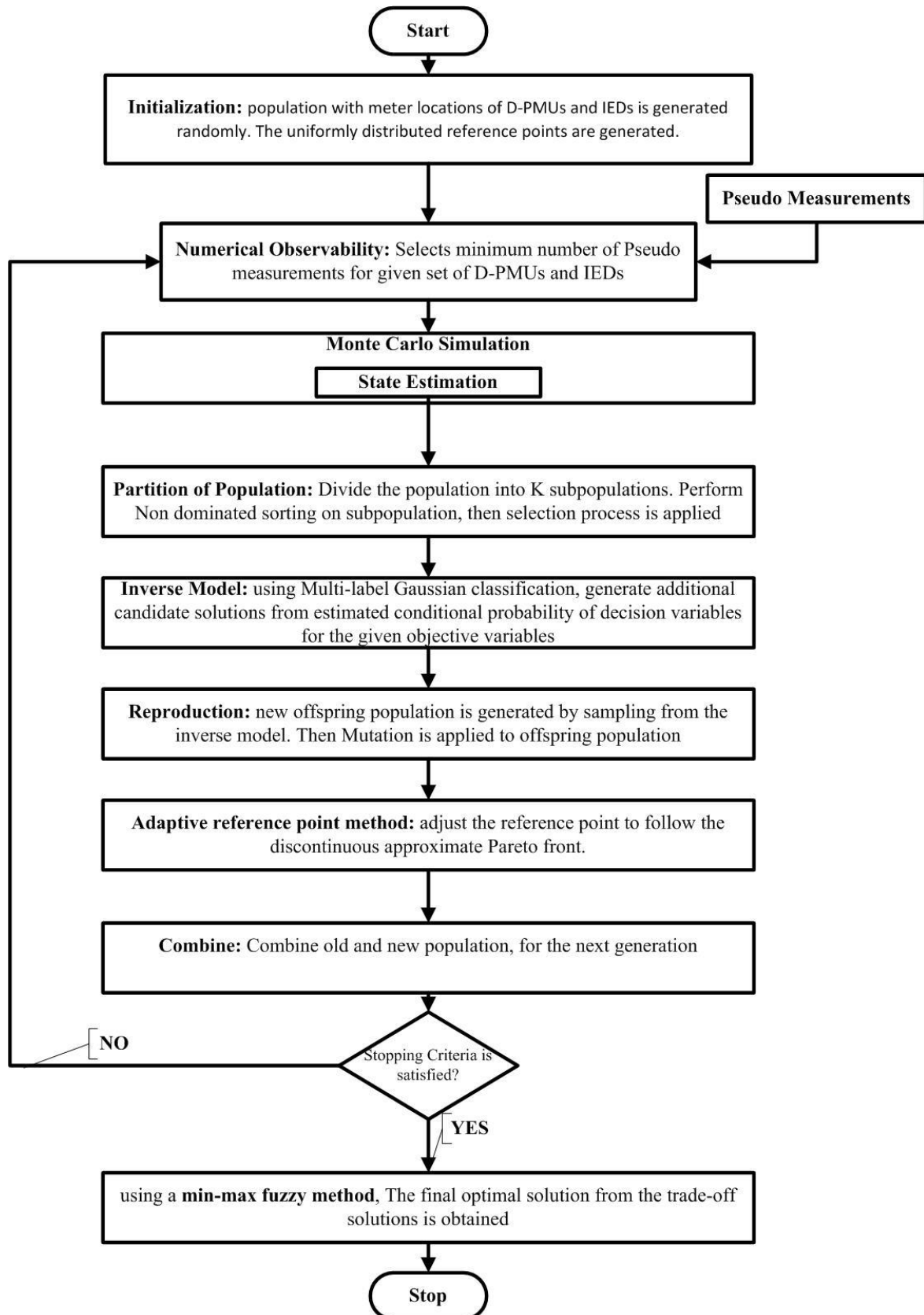


Fig. 6.1: Flow chart of the proposed numerical observability method based meter placement.

6.5 Simulation and Test Conditions:

Monte Carlo simulations are used to determine the objective values and constraint violations for different uncertainties of measurements. the Monte Carlo trials are considered as 1000 for 100 different network conditions [22]. The error percentage of different types of measurements are considered as follows:

Default measurements: Voltage measurement and power flow measurements at slack bus and first line are considered as default measurements. In active distribution system at each DG one power flow measurement is considered as the default measurement. The error is considered as 1%.

Virtual measurements: Zero bus injections are modeled as virtual measurements with 10^{-8} as the variance of measurement.

Real Measurement: D-PMUs and IEDs are placed using the proposed method with the percentage error is 1% and 5%.

Pseudo measurements: All the power injections at each node are modeled as Pseudo measurements with 50% error. The minimum set of Pseudo measurements are identified using numerical observability method.

6.6 Results and Discussion:

The proposed method is verified on PG&E 69-bus and Indian Practical 85-bus distribution test system and tested for 1% and 5% real measurement error accuracy. The effect of renewable energy sources is considered and modeled as DGs, which produces active power. The details of distributed generation locations and their base values are given in Table 6.1. These DG positions were chosen based on the least amount of power loss and voltage deviation [75].

Table 6.1: Distributed generation size and locations

Test System	Bus Number	DG base value (MW)
PG&E 69-bus Distribution System	50	0.180
	61	0.270
Indian Practical 85-bus Distribution System	45	0.277
	61	0.290

The proposed method is compared with EDA-IPM [75] and NSGA-II [75], both methods have considered PMUs and IEDs, and authors in EDA-IPM considered the cost of PMUs as 1 per unit and IEDs as 0.6 per unit. The PMU considered is not distribution level PMU (D-PMU). Therefore, the authors considered the cost of the PMU is 1 per unit. Whereas the proposed method considered D-PMUs with 0.3 per unit cost and IEDs with the same cost as 0.6 per unit.

In EDA-IPM and NSGA-II considered only three objectives, not considered the four objectives. To asses the performance of D-PMU a 1% Total Vector Error (TVE) is considred as per the IEEE synchrophasor standards (IEEE C37.118.1a-2014). The total vector error is defined as folows

$$Total\ Vector\ Error\ (TVE) = \frac{|\bar{X}_{measured} - \bar{X}_{Theoretical}|}{\bar{X}_{Theoretical}} \quad (6.8)$$

Where $\bar{X}_{measured}$ is the measured voltage from the D-PMU after state estimation and $\bar{X}_{Theoretical}$ is the theoretical voltage from load flow. The maximum total vector error for given D-PMUs are taken as the performance benchmark for given measurement set obtained from the proposed algorithm.

6.6.1 PG&E 69-bus Distribution System:

The proposed algorithm with numerical observability method and without numerical observability method is verified on PG&E 69-bus distribution system, the details of distribution system is given in [92]. The meter placement is evaluated for 1% and 5% of errors in real measurements. The Pareto fronts of different objectives are shown in figs. 6.2 and 6.3 correspond to the 1% and 5% errors with DG. For 1% error, the proposed algorithm with numerical observability shows superiority as it improves the accuracy of state estimates as objective J_3 (root mean square error of voltage magnitude) and objective J_4 (root mean square error of voltage angle) and the number of D-PMUs and IEDs. The proposed method with numerical observability requires 2 D-PMUs and 3 IEDs and having minimum state estimate error as J_3 equals $5.1892e^{-05}$ and J_4 equals $2.9641e^{-06}$ when compared to proposed method without numerical observability, EDA-IPM, and NSGA-II. Similarly, the same can be observed with 5% of error case. The results of with DG case are given in Table-6.2. The same hold with the without DG case for 1% and 5% errors, the Pareto fronts are given in figs. 6.4, 6.5, and results are tabulated in Table 6.3.

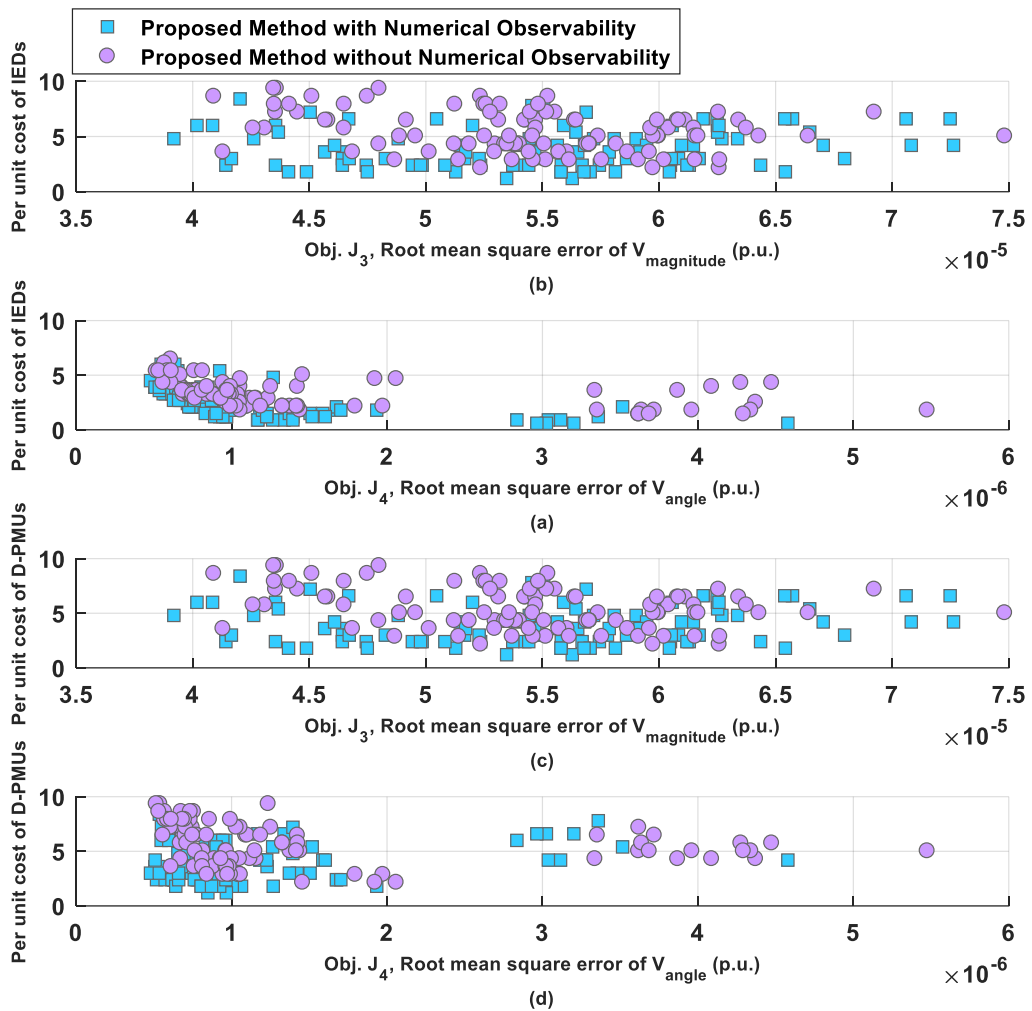


Fig. 6.2: PG&E 69-bus distribution system optimal Pareto-front plots: with 1% error in real measurements and Pseudo measurements with an accuracy of 50% with DG

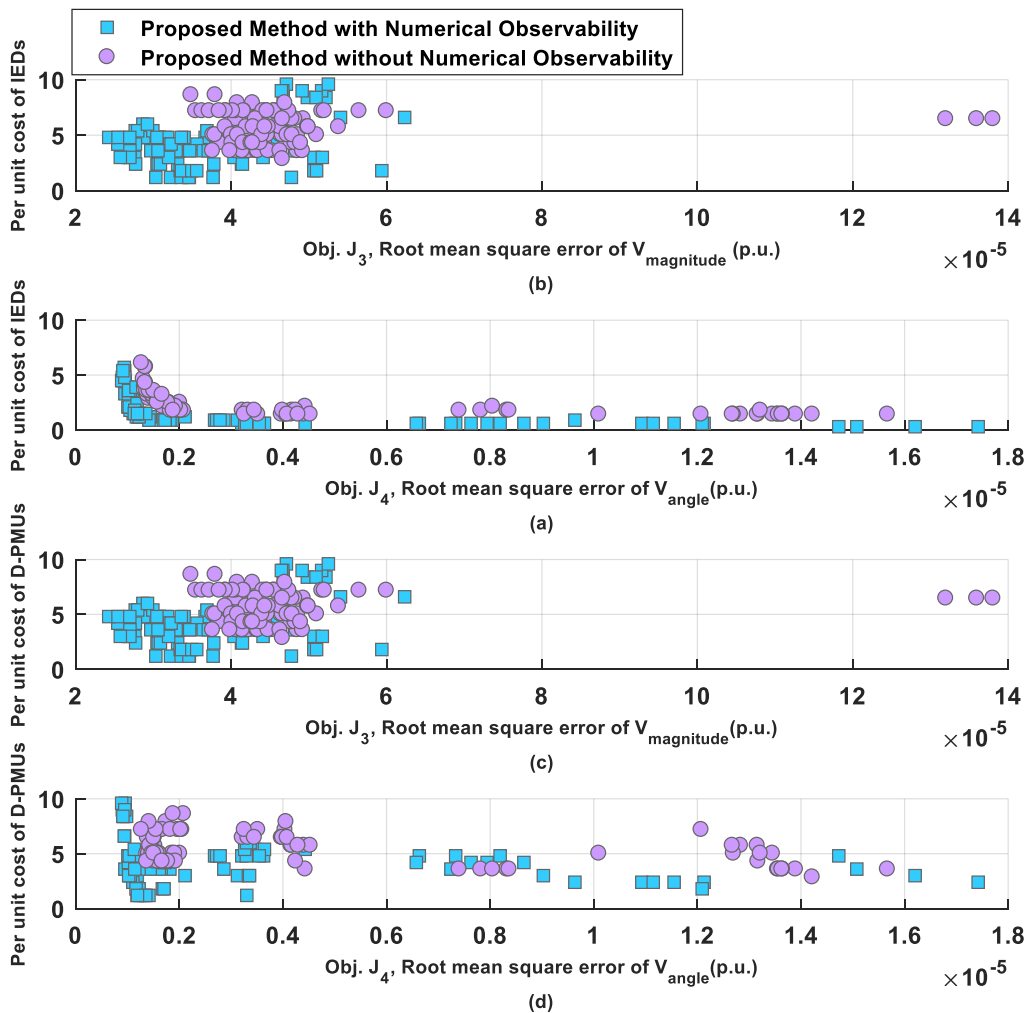


Fig. 6.3: PG&E 69-bus distribution system optimal Pareto-front plots: with 5% error in real measurements and Pseudo measurements with an accuracy of 50% with DG.

Table 6.2: PG&E 69-bus distribution system: Optimal location of the D-PMUs and IEDs under different measurement uncertainty for with DG

Measurem ent error (in %)	Algorithm	Location of D- PMUs (Node numbers)	Location of IEDs (Line numbers)	Objective function values				Maximum TVE
				J ₁ Per unit cost of D- PMUs	J ₂ Per unit cost of IEDs	J ₃ Root mean square error of Voltage magnitud e (in p.u.)	J ₄ Root mean square error of Voltage angle (in p.u.)	
1	Proposed algorithm with Numerical Observability	17, 29	47, 50, 60	0.6	1.8	5.1892e-05	2.9641e-06	0.001015
	Proposed algorithm	4, 17, 23, 29	14, 34, 41, 50, 56	1.2	3	5.9751e-05	3.6186e-06	0.003012

	without Numerical Observability							
	EDA-IPM [75]	27,62	1,2,4	2	1.8	0.0098	-	-
	NSGA-II [75]	21,27,34, 49,57	1,6,37	5	1.8	0.0129	-	-
5	Proposed algorithm with Numerical Observability	41, 55	3, 18, 25, 32, 48, 58, 64	0.6	4.8	2.5419e- 05	3.2065e-06	0.001952
	Proposed algorithm without Numerical Observability	12, 36, 43, 54	10,16, 22, 33, 41, 66, 68	1.2	4.8	3.7612e- 05	3.7129e-06	0.004107
	EDA-IPM [75]	27,67	1,2,3,8,25, 29,57,65	2	4.8	0.0152	-	-
	NSGA-II [75]	14,17,36, 44	1,7,9,13,14 ,17,31,32,3 9, 47,54,60,6 3	4	7.8	0.0182	-	-

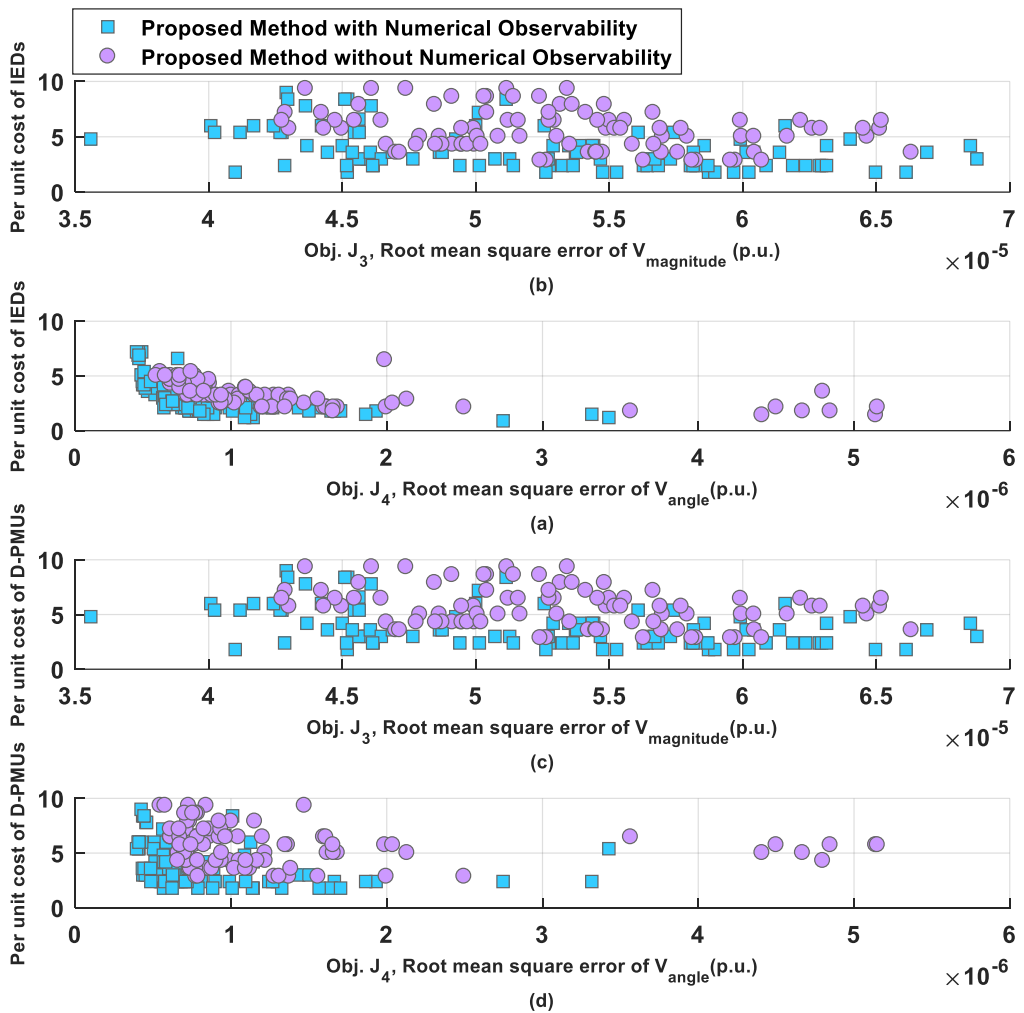


Fig. 6.4: PG&E 69-bus distribution system optimal Pareto-front plots: with 1% error in real measurements and Pseudo measurements with an accuracy of 50% without DG.

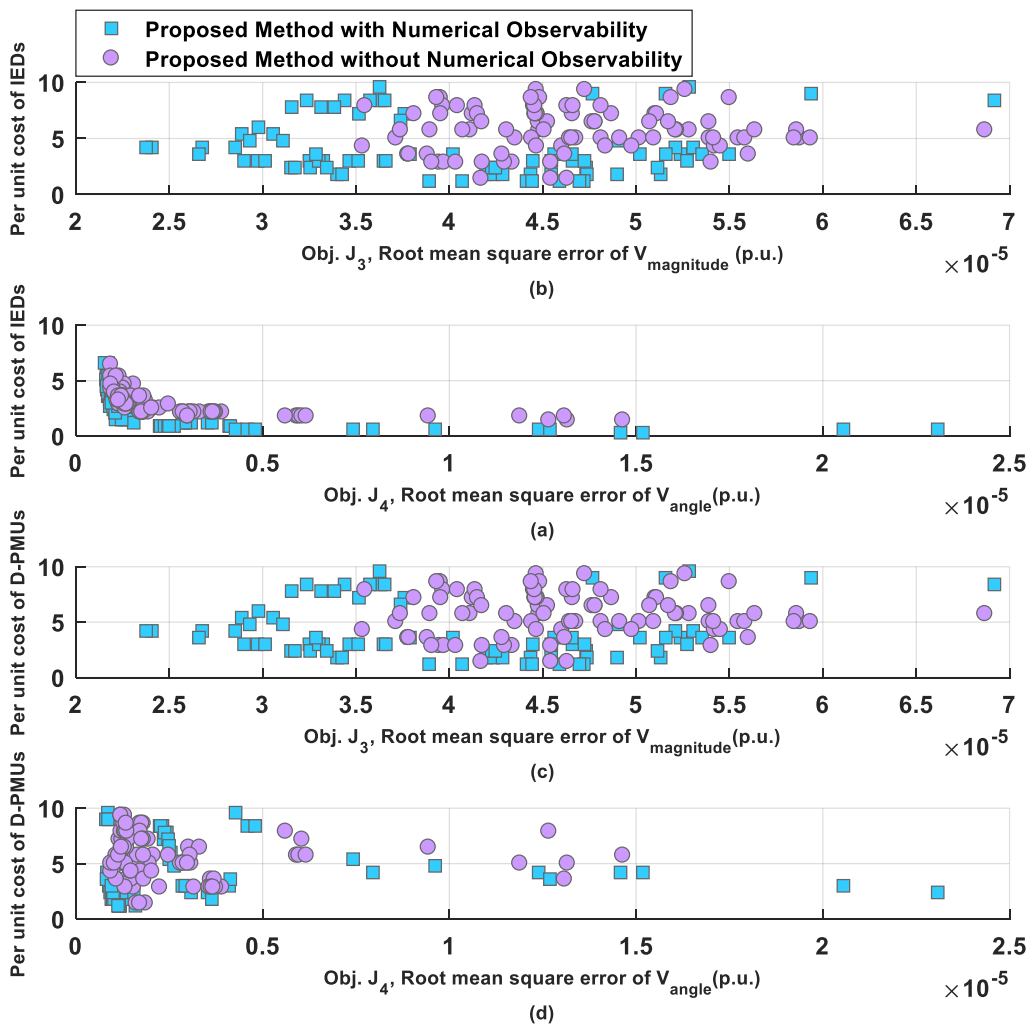


Fig. 6.5: PG&E 69-bus distribution system optimal Pareto-front plots: With 5% error in real measurements and Pseudo measurements with an accuracy of 50% without DG.

Table 6.3: PG&E 69-bus distribution system: Optimal location of the D-PMUs and IEDs under different measurement uncertainty for without DG.

Measureme nt error (in %)	Algorithm	Location of D- PMUs (Node numbers)	Locatio n of IEDs (Line number s)	Objective function values				Maximum TVE
				J ₁ Per unit cost of D-PMUs	J ₂ Per unit cost of IEDs	J ₃ Root mean square error of Voltage magnitude (in p.u.)	J ₄ Root mean square error of Voltage angle (in p.u.)	
1	Proposed algorithm with Numerical Observability	10, 13	38, 44, 61, 65	0.6	2.4	5.8139e-05	2.7467e-06	0.001148

	Proposed algorithm without Numerical Observability	4, 17, 23, 29	14, 34, 41, 56, 59	1.2	3	6.2604e-05	3.6742e-06	0.001840
5	Proposed algorithm with Numerical Observability	10, 16, 37, 54, 56	38, 44, 61, 65, 68	1.5	3	3.2505e-05	1.0601e-06	0.002114
	Proposed algorithm without Numerical Observability	6, 17, 25, 50, 53	4, 14, 17, 20, 46, 51	1.5	3.6	3.5477e-05	2.9895e-06	0.003015

6.6.2 Indian Practical 85-bus Distribution System:

The proposed method with and without numerical observability method is verified on Indian Practical 85-bus distribution system, the details of which can be found in [93]. The results of DG for 1% and 5% error case Pareto fronts are displayed in figs. 6.5 and 6.6 and the results are tabulated in Table-6.4. The obtained results show the effectiveness of the method using numerical observability method, as it produces fewer state estimate errors ($J_3 = 6.2508e^{-05}$ and $J_4 = 1.4338e^{-06}$) and a smaller number of meters required as compared to the proposed method without numerical observability method, EDA-IPM, and NSGA-II. Similarly, the same can be observed with 5% of error case. The without DG case is presented in Table 6.5 and the Pareto fronts are given in figs. 6.7 and 6.8.

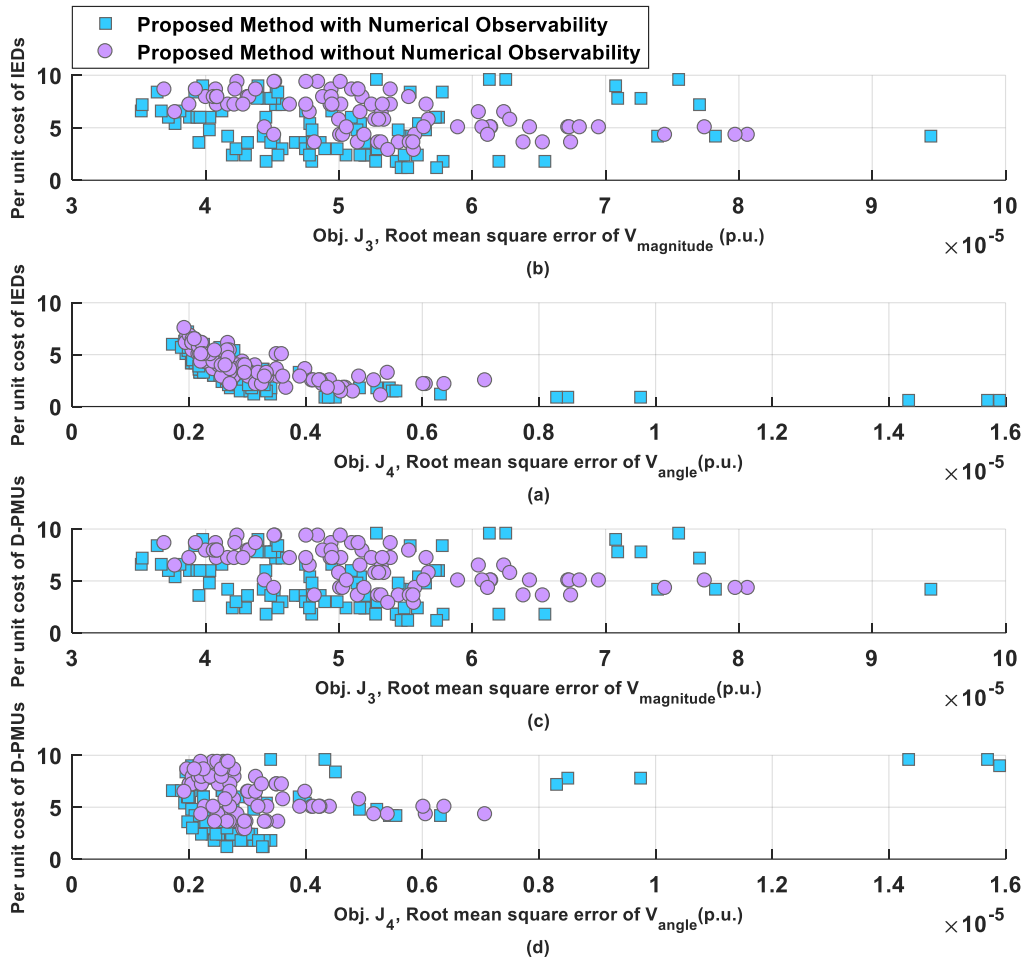


Fig. 6.6: Indian Practical 85-bus distribution system optimal Pareto-front plots: With 1% error in real measurements and Pseudo measurements with an accuracy of 50% with DG.

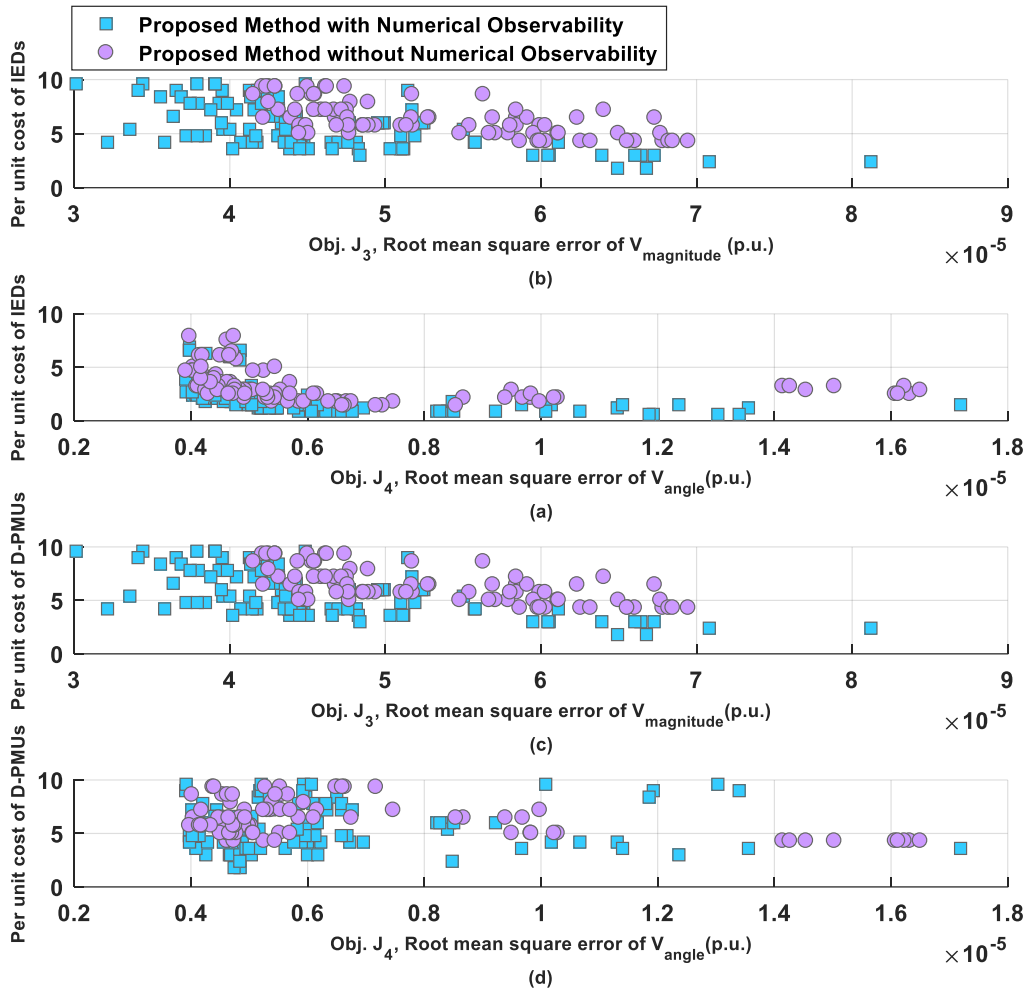


Fig. 6.7: Indian Practical 85-bus distribution system optimal Pareto-front plots: With 5% error in real measurements and Pseudo measurements with an accuracy of 50% with DG.

Table 6.4: Indian Practical 85-bus distribution system: Optimal location of the D-PMUs and IEDs with 1% measurement uncertainty for with DG.

Measurement error (in %)	Algorithm	Location of D-PMUs (Node numbers)	Location of IEDs (Line numbers)	Objective function values				Maximum TVE
				J ₁ Per unit cost of D-PMUs	J ₂ Per unit cost of IEDs	J ₃ Root mean square error of Voltage magnitude (in p.u.)	J ₄ Root mean square error of Voltage angle (in p.u.)	
1	Proposed algorithm with Numerical Observability	11, 77	18, 75, 82	0.6	1.8	6.2508e-05	1.4338e-06	0.003154
	Proposed algorithm	55, 73, 77	27, 75, 79, 82	0.9	2.4	8.0282e-05	5.2922e-06	0.005415

	without Numerical Observability							
	EDA-IPM [75]	42,71,78	1,2	3	1.2	0.0096	-	-
	NSGA-II [75]	72,76	1,8,14,43, 47,69	2	3.6	0.0136	-	-
5	Proposed algorithm with Numerical Observability	41, 55, 66, 82	24, 37, 49, 65, 84	1.2	3.0	3.2140e-05	5.1532e-06	0.004821
	Proposed algorithm without Numerical Observability	19, 26, 44, 60, 80	18, 26, 35, 40, 54, 75	1.5	3.6	4.1850e-05	5.3851e-06	0.005619
	EDA-IPM [75]	27, 42, 60, 62, 70, 75	1,3,5	6	1.8	0.0146	-	-
	NSGA-II [75]	39,52,61,6 5, 71,76, 79,82	1,3,5,6,34 ,37	8	3.6	0.0202	-	-

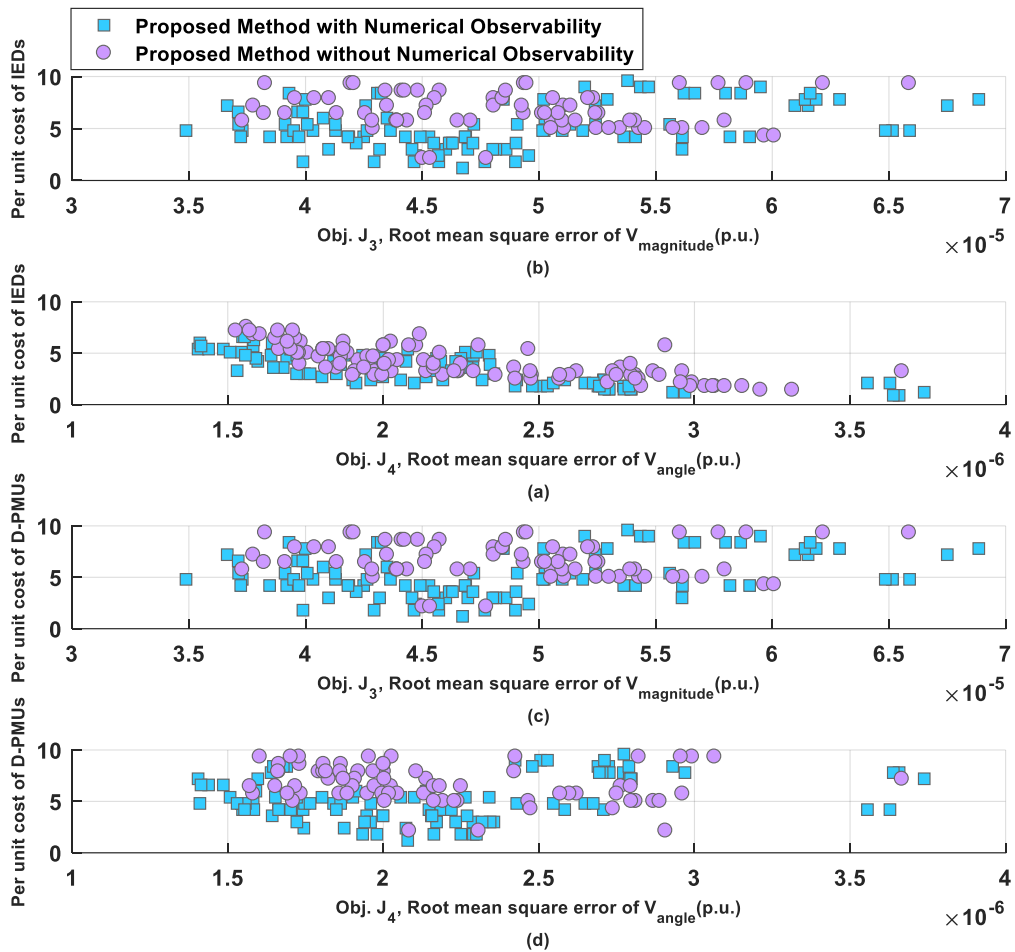


Fig. 6.8: Indian Practical 85-bus distribution system optimal Pareto-front plots: With 1% error in real measurements and Pseudo measurements with an accuracy of 50% without DG

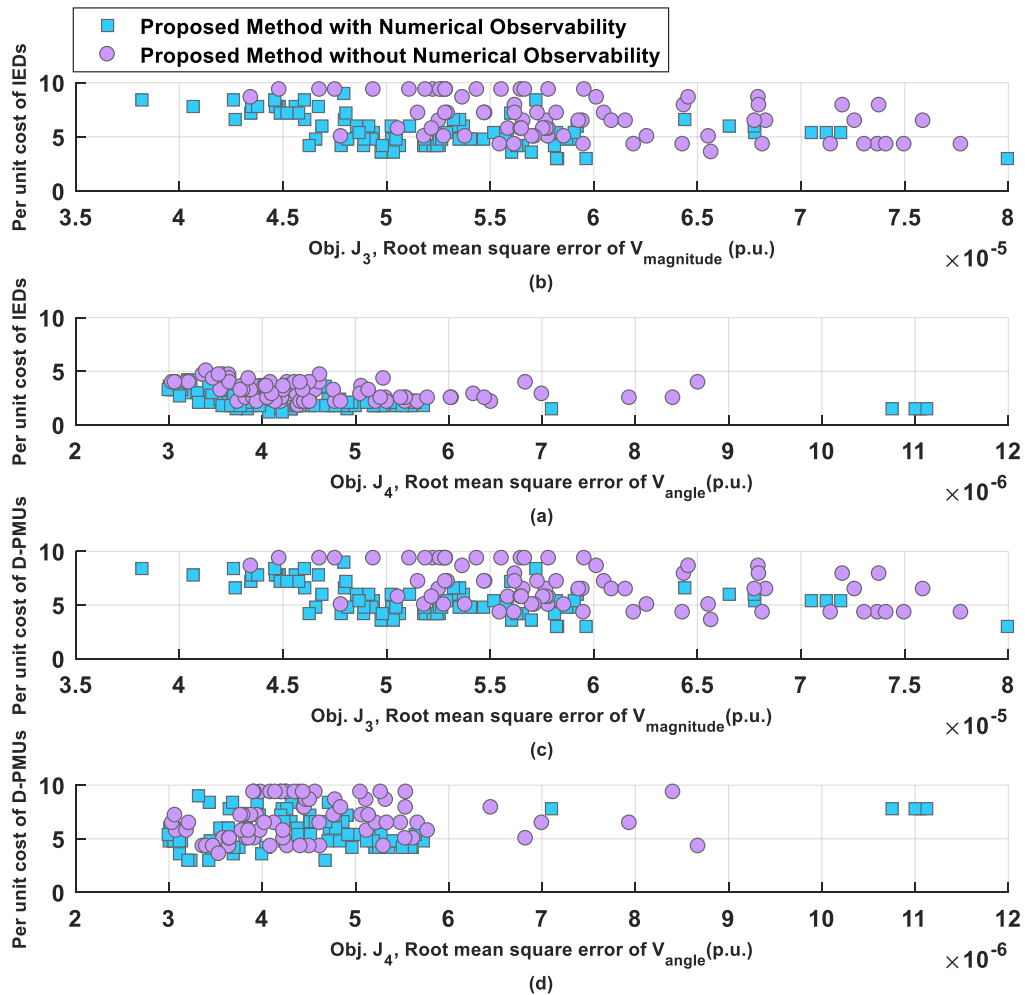


Fig. 6.9: Indian Practical 85-bus distribution system optimal Pareto-front plots: With 5% error in real measurements and Pseudo measurements with an accuracy of 50% without DG.

Table 6.5: Indian Practical 85-bus distribution system: Optimal location of the D-PMUs and IEDs under different measurement uncertainty for without DG.

Measurement error (in %)	Algorithm	Location of D-PMUs (Node numbers)	Location of IEDs (Line numbers)	Objective function values				Maximum TVE
				J ₁ Per unit cost of D-PMUs	J ₂ Per unit cost of IEDs	J ₃ Root mean square error of Voltage magnitude (in p.u.)	J ₄ Root mean square error of Voltage angle (in p.u.)	
1	Proposed algorithm with Numerical Observability	52, 71	35, 49, 55, 79	0.6	2.4	6.1882e-05	3.6390e-06	0.004105
	Proposed algorithm without	14, 51, 71	32, 49, 52, 55, 77	0.9	3.0	6.3180e-05	3.2118e-06	0.004817

	Numerical Observability							
5	Proposed algorithm with Numerical Observability	24, 44, 74, 83	38, 41, 54, 60, 69, 79, 82	1.2	4.2	3.9395e-05	4.0684e-06	0.005214
	Proposed algorithm without Numerical Observability	24, 32, 39, 74, 83	36, 49, 54, 60, 69, 74, 79, 82	1.5	4.8	4.0557e-05	4.3857e-06	0.006142

The obtained results show the proposed method with numerical observability improves the accuracy of state estimation. This is evident from objectives J_3 and J_4 when compared with all other methods. This in turn leads to reducing the number of meters required. The greater number of solutions crowded together can be found in all the Pareto front plots from fig. 6.2 to 6.9, which is due to the multi-label Gaussian process classification inverse model, which improved the diversity and search ability of the evolutionary algorithm.

6.7 The Comparision of Proposed Methods

This thesis proposed four multi-objective meter placement methods for distribution system state estimation. In chapter 3, Decomposition and Local dominace base MOEA with Binomial Distribution Mante Carlo simulations (DLD-MOEA-BDMC) method is proposed. In chapter 4 Indicator Based MOEA using Objective Discretization (IB-MOEA-OD) method is proposed and chapter 5 proposed a Model Based MOEA using Adaptive Reference point method (MB-MOEA-AR). All the three methods addresses the same objective functions: minimization of i) cost of measurement devices (J_1) ii) the average relative percentage error (ARPE) of voltage magnitude (J_2) and iii) the average relative percentage error (ARPE) of voltage angle (J_3). Whereas, in this chapter a inverse model based many-objective evolutionary algorithm is proposed with different objective functions. Therefore, results of first three proposed methods are summarised as follows:

6.7.1 PG&E 69-bus Distribution System

For PG&E 69-bus distribution system, without DG case the proposed IB-MOEA-OD gives the better results as compared to others, whereas in contrary in with DG (Type-1, Type-2, and Type 3) cases the proposed MB-MOEA-AR provides better results in most of the cases. The results without DG case is presented in Table 6.6. DG type-1, DG type-2 and DG type-3 cases are tabulated in Tables 6.7, 6.8, and 6.9, respectively.

Table 6.6: PG&E 69-bus distribution system: Summary of different proposed algorithms: Optimal location of the power flow meters under different metrological errors for without DG

Metrological error (in %)	Algorithm	Location of Power flow meters (Line numbers)	Number of power flow meters	Objective function values		
				J_1	J_2	J_3
1	Proposed DLD-MOEA-BDMC algorithm (chapter 3)	1,5,13,30,54	5	6	0.0014	0.4547
	Proposed IB-MOEA-OD algorithm (chapter 4)	1, 13, 32, 43, 55	5	6	0.0008	0.2641
	Proposed IM-MOEA-AR algorithm (chapter 5)	7, 10, 31, 42	4	5	0.0011	0.3477
5	Proposed DLD-MOEA-BDMC algorithm (chapter 3)	1,9,13, 26, 31, 46, 60	7	8	0.0023	0.6288
	Proposed IB-MOEA-OD algorithm (chapter 4)	1, 15, 29, 40, 47, 56	6	7	0.0020	0.3458
	Proposed IM-MOEA-AR algorithm (chapter 5)	10, 15, 29, 42, 46	5	6	0.0020	0.4555

Table 6.7: PG&E 69-bus distribution system: Summary of different proposed algorithms: Optimal location of the power flow meters under different metrological errors with DG Type-1(P)

Metrological error (in %)	Algorithm	Location of Power flow meters(Line numbers)	Number of power flow meters	Objective function values		
				J_1	J_2	J_3
1	Proposed IB-MOEA-OD algorithm (chapter 4)	1, 13, 30, 41, 56	5	8	0.0011	0.3122
	Proposed IM-MOEA-AR algorithm (chapter 5)	14, 28, 32, 41, 57	5	8	0.0009	0.3018
5	Proposed IB-MOEA-OD algorithm (chapter 4)	1, 14, 32, 42, 47, 55	6	9	0.0017	0.4698
	Proposed IM-MOEA-AR algorithm (chapter 5)	9, 14, 28, 29, 44, 47	6	9	0.0017	0.3187

Table 6.8: PG&E 69-bus distribution system: Summary of different proposed algorithms: Optimal location of the power flow meters with 1% measurement uncertainty with DG Type-2(P-jQ).

Algorithm	Location of Power flow meters(Line numbers)	Number of power flow meters	Objective function values		
			J_1	J_2	J_3
Proposed IB-MOEA-OD algorithm (chapter 4)	1, 14, 29, 41, 55	5	8	0.0014	0.3800
Proposed IM-MOEA-AR algorithm	6, 9, 28, 30, 42	5	8	0.0008	0.2399

(chapter 5)					
-------------	--	--	--	--	--

Table 6.9: PG&E 69-bus distribution system: Summary of different proposed algorithms: Optimal location of the power flow meters with 1% measurement uncertainty with DG Type-3(P+jQ).

Algorithm	Location of Power flow meters(Line numbers)	Number of power flow meters	Objective function values		
			J_1 Cost of meters (1 per unit device)	J_2 ARPE of voltage magnitude	J_3 ARPE of voltage angle
Proposed IB-MOEA-OD algorithm (chapter 4)	1, 13, 31, 40, 58	5	8	0.0012	0.5714
Proposed IM-MOEA-AR algorithm (chapter 5)	8, 32, 42, 54	4	7	0.0010	0.7257

6.7.2 Indian Practical 85-bus Distribution System

For Indian Practical 85-bus distribution system, with and without DG cases the proposed MB-MOEA-AR gives the better results in most of the cases as compared to others. The results without DG case is presented in Table 6.10. DG type-1, DG type-2 and DG type-3 cases are tabulated in Tables 6.11, 6.12, and 6.13, respectively.

Table 6.10: Indian Practical 85-bus distribution system: Summary of different proposed algorithms: Optimal location of the power flow meters under different metrological errors without DG

Metrological error (in %)	Algorithm	Location of Power flow meters (Line numbers)	Number of power flow meters	Objective function values		
				J_1 Cost of meters (1 per unit device)	J_2 ARPE of voltage magnitude	J_3 ARPE of voltage angle
1	Proposed DLD-MOEA-BDMC algorithm	1,6,11,26,30,63	6	7	0.0337	0.7153

	(chapter 3)					
	Proposed IB-MOEA-OD algorithm (chapter 4)	1, 10,17, 24,30,57	6	7	0.0281	0.6552
	Proposed IM-MOEA-AR algorithm (chapter 5)	8, 17, 24, 33, 56, 59	6	7	0.0278	0.6894
5	Proposed DLD-MOEA-BDMC algorithm (chapter 3)	1,7, 26, 32, 39, 45, 57, 79, 84	9	10	0.0492	1.4288
	Proposed IB-MOEA-OD algorithm (chapter 4)	1, 24,28,33,59,71	6	7	0.0451	0.9845
	Proposed IM-MOEA-AR algorithm (chapter 5)	9, 16, 17, 24, 32, 56, 63	7	8	0.0351	0.9056

Table 6.11: Indian Practical 85-bus distribution system: Summary of different proposed algorithms: Optimal location of the power flow meters different measurement uncertainty with DG Type-1(P)

Metrological error (in %)	Algorithm	Position of PMs (Line numbers)	Number of power flow meters	Objective function values		
				J ₁ Cost of meters (1 per unit device)	J ₂ ARPE of voltage magnitude	J ₃ ARPE of voltage angle
1	Proposed IB-MOEA-OD algorithm (chapter 4)	1, 18, 24, 56, 62	5	8	0.0265	0.6543
	Proposed IM-MOEA-AR algorithm (chapter 5)	7, 10, 29, 47, 56	5	8	0.0263	0.6144

5	Proposed IB- MOEA-OD algorithm (chapter 4)	1, 17, 24, 33, 57, 63	6	9	0.0326	0.9494
	Proposed IM- MOEA-AR algorithm (chapter 5)	9, 16, 18, 24, 31, 57	6	9	0.0268	0.8289

Table 6.12: Indian Practical 85-bus distribution system: Summary of different proposed algorithms: Optimal location of the power flow meters with 1% measurement uncertainty for DG Type-2(P-jQ).

Algorithm	Position of PMs (Line numbers)	Number of power flow meters	Objective function values		
			J₁ Cost of meters (1 per unit device)	J₂ ARPE of voltage magnitude	J₃ ARPE of voltage angle
Proposed IB- MOEA-OD algorithm (chapter 4)	1, 17, 25, 31, 57, 63	6	9	0.0270	0.8380
Proposed IM- MOEA-AR algorithm (chapter 5)	7, 8, 26, 57, 60	5	8	0.0320	0.9213

Table 6.13: Indian Practical 85-bus distribution system: Summary of different proposed algorithms: Optimal location of the power flow meters with 1% measurement uncertainty for DG Type-3(P+jQ).

Algorithm	Position of PMs (Line numbers)	Number of power flow meters	Objective function values		
			J₁ Cost of meters (1 per unit device)	J₂ ARPE of voltage magnitude	J₃ Cost of meters (1 per unit device)
Proposed IB- MOEA-OD algorithm (chapter 4)	1, 16, 17, 30, 59, 66	6	9	0.0436	1.1079

Proposed IM- MOEA-AR algorithm (chapter 5)	8, 15, 16, 17, 31, 59	6	9	0.0404	1.2104
--	-----------------------	---	---	--------	--------

6.8 Summary

A many objective meter placement using numerical observability method is proposed for distribution system state estimation. In general, all the power injections are modeled as Pseudo measurements. A fixed number of Pseudo measurements deteriorates the accuracy of state estimation. Therefore, the minimum number of Pseudo measurements is determined using the numerical observability method for a given combination of real measurements. This approach improves the performance of meter placement by decreasing the state estimation errors and decreases the number of real measurements required. An inverse model-based many-objective evolutionary optimization is used to formulate meter placement, which maps the integer objective space to discrete decision space and produces combination of meter locations based on the inverse model, which is realized using multi-label Gaussian process classification. This improves the search ability of evolutionary optimization and provides diverse solutions in population. The effectiveness of the proposed method is tested for the active and passive distribution networks and with different measurement uncertainties.

Chapter 7

Conclusions

Chapter 7

Conclusions

7.1 General

In this thesis, an optimal meter placement of meters such as power flow meters, distribution level Phasor measurement units (D-PMUs) and intelligent electronic devices (IEDs) for active distribution system state estimation has been investigated using new multi-objective evolutionary algorithms. This thesis explores the new multi-objective frameworks such as decomposition based multi-objective evolutionary algorithms (MOEAs), indicator based MOEAs and model based MOEAs and their application in meter placement problem. Furthermore, optimal allocation of meters are obtained for passive and active distribution networks under various operating scenarios. This chapter presents the important findings proposed in this thesis and discusses future extensions of the proposed research work.

7.2 Summary of Important Findings:

This research work inspects the multi-objective meter placement problem and addresses the issues with combinatorial optimization, discrete and discontinuous Pareto fronts, population initialization using Binomial distribution-based Monte Carlo trails, search ability and diversity issues as well as reducing the Pseudo measurements using numerical observability method are addressed. The following conclusions are arrived from the research work carried out and reported in previous chapters of this thesis.

- i. An optimal meter placement in distribution system state estimation using a new hybrid multi-objective evolutionary algorithm based on decomposition and local dominance is proposed.
 - Minimizing the cost of measurement devices, average relative percentage error of voltage magnitude and average relative percentage error of voltage angle are the three objectives, that are considered to model the multi-objective meter placement problem.
 - The hybridization of decomposition and dominance techniques improved the convergence and diversity of solutions in the Pareto front.
 - As the meter placement is a combinatorial optimization problem, the population of the proposed algorithm is initialized using the Binomial distribution-based Monte Carlo method, which improved the diversity of Pareto front. Diversity improvement is the main goal of the Binomial distribution-based Monte Carlo method and also improves the convergence.

- The results of the proposed method are compared with multi-objective evolutionary algorithm based on decomposition (MOEA/D), Non-dominated sorting genetic algorithm-II (NSGA-II) and with multi-objective hybrid particle swarm optimization-krill herd algorithm (PSO-KH), multi-objective hybrid estimation of distribution algorithm- interior point method (EDA-IPM) and demonstrated on PG&E 69-bus distribution system and Indian Practical 85-bus distribution system.

ii. A new indicator based MOEA using objective discretization method is proposed to find the optimal locations of power flow meter in active distribution system in presence of various types of DGs.

- As the meter placement problem is a combinatorial nature, the objective space is discrete. Therefore, to enhance the performance of the proposed method, objective discretization method was adopted, with different granularity along the objectives, so that it enhances the search ability of MOEA and decreases the non-dominated solutions in population.
- MOEA is an indicator-based method with inverted generational distance indicator, including non-contributing solution detection (IGD-NS), which measures diversity and convergence of solution sets and guides the evolution process. The indicator IGD-NS can reduce the non-dominated solutions with no contribution to the indicator value.
- As the performance of MOEA depends on the approximate Pareto front shape, the proposed method employed a reference point method, which adaptively updates the reference points to follow the Pareto front shape.
- Moreover, the proposed method improves the performance characteristics of MOEA, enhances search ability, provides uniformly distributed solutions on Pareto front, and follow the irregular Pareto front.
- The versatility of the proposed method is demonstrated on PG&E 69-bus distribution system and on Indian Practical 85-bus distribution system. The results obtained are demonstrate the superiority of the proposed method over NSGA-II and other methods such as with multi-objective hybrid PSO Krill herd algorithm (PSO-KH), multi-objective hybrid estimation of distribution algorithm- interior point method (EDA-IPM), dynamic programming (DP) and ordinal optimization algorithm (OOA).

iii. A new inverse model based multi-objective evolutionary algorithm is proposed for meter placement in active distribution system state estimation.

- Inverse model maps the candidate solution in Pareto front from objective space to decision space. The decision space is a binary value string, which represents the meter locations and objective values are in integer domain. To map the binary space to integer domain, the inverse model is realized by multi-label Gaussian classification.
- The inverse model is used as reproduction operator to generate additional candidate solutions from estimated distribution of conditional probability. The main benefit of inverse model is to generate samples that are directly belong in desired objective space and improved search efficiency of the evolutionary algorithm.
- As the meter placement problem is combinatorial optimization, the Pareto front is discontinuous. Therefore, the reference points are adjusted using adaptive reference point method, so that the reference points follow shape of the approximate Pareto front, which improves the performance of the proposed algorithm.
- The meter placement in an active distribution system is modelled as multi-objective problem of conflicting objectives such as the accuracy of state estimation and the cost of the meter configuration to achieve the optimal solution.

iv. A many objective meter placement using numerical observability is proposed for an active distribution system.

- In general, the power injections are modelled as Pseudo measurements. A fixed number of Pseudo measurements deteriorates the accuracy of state estimation. Therefore, The minimum number of Pseudo measurements is determined using the numerical observability for a given combination of real measurements. This approach improves the performance of meter placement by decreasing the state estimation errors and decreases the number of real measurements required.
- An inverse model-based many-objective evolutionary optimization is used to formulate meter placement problem, which maps the integer objective space to discrete decision space and produces combination meter locations based on the model realized using multi-label Gaussian process classification. This improves the search ability of evolutionary optimization and provides diverse solutions in population.
- The meter placement problem is designed as many-objective evolutionary optimization with four objectives as i) cost of D-PMUs, ii) cost of IEDs, iii) root mean square error of voltage magnitude, iv) and root mean square error of voltage angle.

- The impact of distributed generation, as well as various real measurement uncertainties, are taken into account in order to validate the proposed method, which is tested using the PG&E 69-bus and Indian Practical 85-bus distribution test systems.

7.3 Scope of the Future Work

The research work in future can be extended on the following aspects:

- The meter placement can be extended for formulating robust meter placement to handle meter malfunctions and measurement tampering aspects to enhance the security in cyber-physical systems.
- Big data, data analytics techniques and machine learning methods can be utilised to model the multi-objective framework design to adopt the problem specific and computationally complex problems like meter placement problem.
- The meter placement can be extended to multi-level decentralized distribution system state estimation study in smart grid environment. Since only a limited number of real-time measurements are present at primary and secondary distribution network and distributed generation sites, load estimates at unmeasured buses remote from substation need to provide satisfactory state estimation results. The proposed algorithm can be applied in either grid connected mode or island mode and can effectively identify the breakerstatus errors at substations and feeders.
- Further, the meter placement problem can take into account the system contingencies such as phasor failures, the PMU losses and the branch outage under the influence of distributed generation.

References

- [1]. A. Abur and A. Gomez-Exposito, *Power System State Estimation. Theory and Implementation*. Marcel Dekker, New York, 2004.
- [2]. F. C. Scheppe and J. Wildes, "Power system static state estimation, Part I: Exact Model," *IEEE Trans. on Power Apparatus and Systems*, Vol. 89, No. 1, Jan. 1970.
- [3]. A. Monticelli, "Electric power system state estimation," in *Proceedings of the IEEE*, Vol. 88, No. 2, pp. 262-282, Feb. 2000.
- [4]. A. Monticelli, *State estimation in electric power systems: a generalized approach*. Springer Science and Business Media, 1999.
- [5]. L. Mili, M. Cheniae, and P. Rousseeuw, "Robust state estimation of electric power systems," *IEEE Trans. Circuits Syst. I, Fundam. Theory Appl.* , Vol. 41, No. 5, pp. 349–358, May 1994.
- [6]. M. Gol and A. Abur, "LAV based robust state estimation for systems measured by PMUs," *IEEE Trans. Smart Grid*, Vol. 5, No. 4, pp. 1808–1814, Jul. 2014.
- [7]. M. E. Baran, J. Zhu, and A. W. Kelley, "Meter placement for real-time monitoring of distribution feeders," *IEEE Trans. Power Syst.*, Vol. 11, No. 1, pp. 332-337, 1996.
- [8]. M. E. Baran and A. W. Kelley, "State estimation for real-time monitoring of distribution systems," *IEEE Trans. Power Syst.*, Vol. 9, No. 3, pp. 1601–1609, Aug. 1994.
- [9]. C. N. Lu, J. H. Tang, and W. H. E. Liu, "Distribution system state estimation," *IEEE Trans. Power Syst.*, Vol. 10, No. 1, pp. 229–240, Feb. 1995.
- [10]. D. A. Haughton and G. T. Heydt, "A linear state estimation formulation for smart distribution systems," *IEEE Trans. Power Syst.*, Vol. 28, No. 2, pp. 1187–1195, May 2013.
- [11]. Y. Deng, Y. He, and B. Zhang, "A branch-estimation-based state estimation method for radial distribution systems," *IEEE Trans. Power Del.*, Vol. 17, No. 4, pp. 1057–1062, Oct. 2002.

- [12]. M. E. Baran and A. W. Kelley, “A branch-current-based state estimation method for distribution systems,” *IEEE Trans. Power Syst.*, Vol. 10, No. 1, pp. 483–491, Feb. 1995.
- [13]. W. M. Lin, J. H. Teng, and S. J. Chen, “A highly efficient algorithm in treating current measurements for the branch-current-based distribution state estimation,” *IEEE Trans. Power Del.*, Vol. 16, No. 4, pp. 433–439, Jul. 2001.
- [14]. J. H. Teng, “Using voltage measurements to improve the results of branch-current-based state estimators for distribution systems,” *IEEE Proceedings-Generation, Transmission and Distribution*, Vol. 149, No. 6, pp. 667–672, Nov. 2002.
- [15]. M. E. Baran, J. Jung, and T. E. McDermott, “Including voltage measurements in branch current state estimation for distribution systems,” In *IEEE Power and Energy Society General Meeting*, pp. 1–5, Jul. 2009.
- [16]. H. Wang and N. N. Schulz, “A revised branch current-based distribution system state estimation algorithm and meter placement impact,” *IEEE Trans. Power Syst.*, Vol. 19, No. 1, pp. 207–213, Feb. 2004.
- [17]. M. Pau, P. A. Pegoraro, and S. Sulis, “Efficient branch-current-based distribution system state estimation including synchronized measurements,” *IEEE Trans. Instrum. Meas.*, Vol. 62, No. 9, pp. 2419–2429, Sep. 2013.
- [18]. M. Pau, P. A. Pegoraro, and S. Sulis, “Branch current state estimator for distribution system based on synchronized measurements,” in *Proc. IEEE Int. Workshop AMPS*, pp. 53–58, Sep. 2012.
- [19]. Lin W.M. and Teng J.H., ‘State estimation for distribution systems with zero injection constraints’, *IEEE Trans. Power Syst.*, Vol. 11, No. 1, pp. 518–524, 1996.
- [20]. Rodrigo Z. Fanucchi, Michel Bessani, Marcos H.M. Camillo, Anderson da S. Soares, and João B.A. Stochastic indexes for power distribution systems resilience analysis, *IET Gener. Transm. Distrib.*, Vol. 13, No. 12, pp. 2507-2516, 2019.
- [21]. A. Angioni, T. Schlsser, F. Ponci, and A. Monti, “Impact of Pseudo measurements from new power profiles on state estimation in low voltage grids,” *IEEE Trans. Instrum. Meas.*, Vol. 65, No. 1, pp. 70–77, Jan 2016.

[22]. V. A. Evangelopoulos, P. S. Georgilakis, and N. D. Hatziaargyriou, “Optimal operation of smart distribution networks: A review of models, methods and future research”, *Electr. Power Syst. Res.*, Vol. 14, No. 12, pp. 95–106, 2016.

[23]. Rishabh Verma and Vaskar Sarkar, “Active distribution network load flow analysis through non-repetitive FBS iterations with integrated DG and transformer modelling”, *IET Gener. Transm. Distrib.*, Vol. 13, No. 4, pp. 478-484, 2019.

[24]. Wei-Min Lin and Jen-Hao Teng, "State estimation for distribution systems with zero-injection constraints," in *IEEE Transactions on Power Systems*, Vol. 11, No. 1, pp. 518-524, Feb. 1996.

[25]. K. Li, “State Estimation for Power Distribution System and Measurement Impacts,” *IEEE Trans. Power Syst.*, Vol. 11, No. 2, pp. 911–916, 1996.

[26]. R. A. Jabr, B. C. Pal, and R. Singh, “Choice of estimator for distribution system state estimation,” *IET Gener. Transm. Distrib.*, Vol. 3, No. 7, pp. 666–678, 2009.

[27]. Muscas, C., Pilo, F., Pisano, G., Sara S., ‘Optimal allocation of multichannel measurement devices for distribution state estimation’, *IEEE Trans. Instrum. Meas.*, Vol. 58, No. 6, pp. 1929–1937, 2009.

[28]. Sing, R., Pal, B.C., Jabr, R.A., and Richard B. Vinter, ‘Meter placement for distribution system state estimation: an ordinal optimization approach’, *IEEE Trans. Power Syst.*, Vol. 26, No. 4, pp. 2328–2335, 2011.

[29]. Kapil Chauhan and Ranjana Sodhi, "A Comparative Analysis of μ PMU Placement for Active Distribution Network's Observability", 8th International Conference on Power Systems (ICPS), 2019, Jaipur, India.

[30]. R. Singh, B. C. Pal, and R. B. Vinter, “Measurement placement in distribution system state estimation,” *IEEE Trans. Power Syst.*, Vol. 24, No. 2, pp. 668–675, 2009.

[31]. Kaveh Dehghanpour, Zhaoyu Wang, Jianhui Wang, Yuxuan Yuan, and Fankun Bu, A Survey on State Estimation Techniques and Challenges in Smart Distribution Systems , *IEEE Transactions on Smart Grid*, Vol. 10, No. 2, pp. 2312 – 2322, 2019.

[32]. Fiaz Ahmad, Akhtar Rasool, Emre Ozsoy, S. Rajasekar, Asif Sabanovic, and Meltem Elitas, Distribution system state estimation-A step towards smart grid , *Renewable and Sustainable Energy Reviews*, Vol. 81, No. 1, pp. 2659–2671, 2018.

[33]. Sachidananda Prasad and D. M. Vinod Kumar, "Distribution System State Estimation: A bibliographical Survey," 2017 14th IEEE India Council International Conference (INDICON), pp. 1-6, 2017.

[34]. Junqi Liu, Junjie Tang, Ferdinanda Ponci, Antonello Monti, Carlo Muscas, and Paolo Attilio Pegoraro, "Trade-offs in PMU deployment for state estimation in active distribution grids", IEEE Trans. Smart Grid, Vol. 3, No. 2, pp. 915–924, 2012.

[35]. Shafiu, A., Jenkins, N., and Strbac, G., "Measurement location for state estimation of distribution networks with generation", IEE Proc.-Gener. Transm. Distrib., Vol. 152, No. 2, pp. 240–246, 2005.

[36]. Junqi Liu, Junjie Tang, Ferdinanda Ponci, Antonello Monti, Carlo Muscas, and Paolo Attilio Pegoraro, "Trade-offs in PMU deployment for state estimation in active distribution grids", IEEE Trans. Smart Grid, Vol. 3, No. 2, pp. 915–924, 2012.

[37]. Pau, M., Pegoraro, P.A., and Sulis, S., "Efficient branch-current-based distribution system state estimation including synchronized measurement", IEEE Trans. Instrum. Meas., Vol. 62, No. 9, pp. 2419–2429, 2013.

[38]. Pegoraro P.A., and Sulis S., "Robustness-oriented meter placement for distribution system state estimation in presence of network parameter uncertainty", IEEE Trans. Instrum. Meas., Vol. 62, No. 5, pp. 954–962, 2013.

[39]. Damavandi M.G., Krishnamurthy V., and Marti J.R., "Robust meter placement for state estimation in active distribution systems", IEEE Trans. Smart Grid, Vol. 6, No. 4, pp. 1972–1982, 2015.

[40]. Xiaoshuang Chen, Jin Lin, Can Wan, Yonghua Song, Shi You, Yi Zong, Wanfang Guo, and Yuanxi Li, "Optimal meter placement for distribution network state estimation: a circuit representation-based MILP approach", IEEE Trans. Power Syst., Vol. 31, No. 6, pp. 4357–4370, 2016.

[41]. Marler, R.T. and Arora, J.S., "The weighted sum method for multi-objective optimization: new insights", Structural and multidisciplinary optimization, Vol. 41, No. 6, pp.853-862, 2010.

[42]. A. Trivedi, D. Srinivasan, K. Sanyal and A. Ghosh, "A Survey of Multi-objective Evolutionary Algorithms Based on Decomposition," in IEEE Transactions on Evolutionary Computation, Vol. 21, No. 3, pp. 440-462, June 2017.

[43]. K. Deb, A. Pratap, S. Agarwal, and T. Meyarivan, "A fast and elitist multi objective genetic algorithm: NSGA-II", *IEEE Transactions on Evolutionary Computation*, Vol. 6, No. 2, pp. 182–197, 2002.

[44]. V. J. Amuso and J. Enslin, "The Strength Pareto Evolutionary Algorithm 2 (SPEA2) applied to simultaneous multi- mission waveform design," *2007 International Waveform Diversity and Design Conference*, pp. 407-417, 2007.

[45]. David W. Corne, Nick R. Jerram, Joshua D. Knowles, and Martin J. Oates. " PESA-II: region-based selection in evolutionary multiobjective optimization", In *Proceedings of the 3rd Annual Conference on Genetic and Evolutionary Computation (GECCO'01)*, Morgan Kaufmann Publishers Inc., San Francisco, CA, USA, 283–290, 2001.

[46]. K. Li, K. Deb, Q. Zhang, and S. Kwong, "An evolutionary many-objective optimization algorithm based on dominance and decomposition," *IEEE Trans. Evolutionary Computation*, Vol. 19, No. 5, pp. 694–716, 2015.

[47]. S. Yang, M. Li, X. Liu and J. Zheng, "A Grid-Based Evolutionary Algorithm for Many-Objective Optimization," in *IEEE Transactions on Evolutionary Computation*, Vol. 17, No. 5, pp. 721-736, Oct. 2013.

[48]. X. Zhang, Y. Tian and Y. Jin, "A Knee Point-Driven Evolutionary Algorithm for Many-Objective Optimization," in *IEEE Transactions on Evolutionary Computation*, Vol. 19, No. 6, pp. 761-776, Dec. 2015.

[49]. Q. Zhang and H. Li, "MOEA/D: A Multiobjective Evolutionary Algorithm Based on Decomposition," in *IEEE Transactions on Evolutionary Computation*, Vol. 11, No. 6, pp. 712-731, Dec. 2007.

[50]. Gu, F., Liu, H.L. and Tan, K.C., "A multiobjective evolutionary algorithm using dynamic weight design method", *International Journal of Innovative Computing, Information and Control*, Vo. 8, No. 5 (B), pp.3677-3688, 2012.

[51]. Liu, L., Lu, J. and Yang, S., "Many-objective optimization of antenna arrays using an improved multiple-single-objective pareto sampling algorithm", *IEEE Antennas and Wireless Propagation Letters*, Vol. 11, No. 1, pp.399-402, 2012.,

[52]. H. Ishibuchi and T. Murata, "Multi-objective genetic local search algorithm," Proceedings of IEEE International Conference on Evolutionary Computation, pp. 119-124, 1996.

[53]. H. Ishibuchi, Y. Setoguchi, H. Masuda, and Y. Nojima, "Performance of decomposition-based many-objective algorithms strongly depends on Pareto front shapes", IEEE Trans. E Comput., Vol. 21, No. 2, pp. 169–190, 2017.

[54]. Zitzler, E., Laumanns, M. and Bleuler, S., "A tutorial on evolutionary multiobjective optimization", Metaheuristics for multiobjective optimisation, Vol. 535, No. 1, pp.3-37, 2004.

[55]. A. Menchaca-Mendez and C. A. C. Coello, "GDE-MOEA: A new MOEA based on the generational distance indicator and ϵ -dominance," 2015 IEEE Congress on Evolutionary Computation (CEC), pp. 947-955, 2015.

[56]. S. Jiang, J. Zhang, Y. Ong, A. N. Zhang and P. S. Tan, "A Simple and Fast Hypervolume Indicator-Based Multiobjective Evolutionary Algorithm," in IEEE Transactions on Cybernetics, Vol. 45, No. 10, pp. 2202-2213, Oct. 2015.

[57]. R. Hernández Gómez, C.A. Coello Coello,"Improved metaheuristic based on the R2 indicator for many-objective optimization," Proceedings of the 2015 on Genetic and Evolutionary Computation Conference-Gecco'15, ACM Press, New York, USA pp. 679-686, 2015.

[58]. Y. Liu, J. Wei, X. Li and M. Li, "Generational Distance Indicator-Based Evolutionary Algorithm With an Improved Niching Method for Many-Objective Optimization Problems," in IEEE Access, Vol. 7, No. 1, pp. 63881-63891, 2019.

[59]. A. Zhou, Y. Jin, Q. Zhang, B. Sendhoff, and E. Tsang, combining model-based and genetics-based offspring generation for multi-objective optimization using a convergence criterion, in Proc. IEEE Congr. E Comput., Vancouver, BC, Canada, pp. 892–899, 2006.

[60]. L. While, P. Hingston, L. Barone, and S. Huband, A faster algorithm for calculating hypervolume, IEEE Trans. E Comput., Vol. 10, No. 1, pp. 29–38, 2006.

[61]. D. Brockhoff, T. Wagner, and H. Trautmann, "On the properties of the R2 indicator," in Proc. 14th Annu. Conf. Genet. Evol. Comput., Philadelphia, PA, USA, pp. 465–472, 2012.

[62]. O. Schütze, X. Esquivel, A. Lara, and C. A. C. Coello, "Using the averaged Hausdorff distance as a performance measure in evolutionary multiobjective optimization," *IEEE Trans. Evol. Comput.*, Vol. 16, No. 4, pp. 504–522, Aug. 2012.

[63]. H. Wang, Y. Jin, and X. Yao, "Diversity assessment in many-objective optimization," *IEEE Trans. Cybern.*, Vol. 47, No. 6, pp. 1510–1522, Jun. 2017.

[64]. Laumanns, M. and Ocenasek, J., September. Bayesian optimization algorithms for multi-objective optimization. In *International Conference on Parallel Problem Solving from Nature*, Springer, Berlin, Heidelberg, pp. 298-307, 2002.

[65]. Lozano, J.A., Larrañaga, P., Inza, I. and Bengoetxea, E. eds., *Towards a new evolutionary computation: advances on estimation of distribution algorithms*, Vol. 192, No. 1, pp. 1510–1522, 2006, Springer.

[66]. Tianping Chen and Hong Chen, "Approximation capability to functions of several variables, nonlinear functionals, and operators by radial basis function neural networks," in *IEEE Transactions on Neural Networks*, Vol. 6, No. 4, pp. 904-910, July 1995.

[67]. H. K. Singh, T. Ray and W. Smith, "Surrogate assisted Simulated Annealing (SASA) for constrained multi-objective optimization," *IEEE Congress on Evolutionary Computation*, pp. 1-8, 2010.

[68]. S. B. Gee, K. C. Tan and C. Alippi, "Solving Multiobjective Optimization Problems in Unknown Dynamic Environments: An Inverse Modeling Approach," in *IEEE Transactions on Cybernetics*, Vol. 47, No. 12, pp. 4223-4234, Dec. 2017.

[69]. Y. Tian, X. Zhang, R. Cheng, C. He and Y. Jin, "Guiding Evolutionary Multiobjective Optimization With Generic Front Modeling," in *IEEE Transactions on Cybernetics*, Vol. 50, No. 3, pp. 1106-1119, March 2020.

[70]. D. Lim, Y. Jin, Y. Ong and B. Sendhoff, "Generalizing Surrogate-Assisted Evolutionary Computation," in *IEEE Transactions on Evolutionary Computation*, Vol. 14, No. 3, pp. 329-355, June 2010.

[71]. Cheng, R., He, C., Jin, Y. and Yao, X., "Model-based evolutionary algorithms: a short survey", *Complex and Intelligent Systems*, Vol. 4, No. 4, pp.283-292, 2018.

[72]. Hisao Ishibuchi, Noritaka Tsukamoto and Yusuke Nojima, "Evolutionary many-objective optimization: A short review," *2008 IEEE Congress on Evolutionary*

Computation (IEEE World Congress on Computational Intelligence), pp. 2419-2426, 2008.

- [73]. Sachidananda Prasad and D M Vinod Kumar, "Optimal Allocation of Measurement Devices for Distribution State Estimation Using Multi objective Hybrid PSO–Krill Herd Algorithm", IEEE Trans. Instrum. Meas., Vol. 66, No. 8, pp. 2022-2035, 2017.
- [74]. Sachidananda Prasad and D M Vinod Kumar, "Trade-offs in PMU and IED Deployment for Active Distribution State Estimation Using Multi-Objective Evolutionary Algorithm", IEEE Trans. Instrum. Meas., Vol. 67, No. 6, pp. 1298- 1307, 2018.
- [75]. Sachidananda Prasad and D M Vinod Kumar, "Multi-objective hybrid estimation of distribution algorithm-interior point method-based meter placement for active distribution state estimation", IET Generation, Transmission and Distribution, Vol. 12, No. 3, pp. 767-779, 2018.
- [76]. Sachidananda Prasad and D M Vinod Kumar, "Robust meter placement for active distribution state estimation using a new multi-objective optimisation model", IET Science, Measurement and Technology, Vol. 12, NO. 8, pp. 1047- 1057, 2018.
- [77]. R. C. Purshouse and P. J. Fleming, On the evolutionary optimization of many conflicting objectives, IEEE Trans. E Comput., Vol. 11, No. 6, pp. 770–784, 2007.
- [78]. H. Ishibuchi, H. Masuda and Y. Nojima, "Pareto Fronts of Many-Objective Degenerate Test Problems," in IEEE Transactions on Evolutionary Computation, Vol. 20, No. 5, pp. 807-813, Oct. 2016.
- [79]. M. Li, S. Yang, and X. Liu, Pareto or non-Pareto: Bi-criterion evolution in multiobjective optimization, IEEE Trans. E Comput., Vol. 20, No. 5, pp. 645–665, 2016.
- [80]. Weiyu Chen, Hisao Ishibuchi, Ke Shang, Effects of Discretization of Decision and Objective Spaces on the Performance of Evolutionary Multi- objective Optimization Algorithms, IEEE Symposium Series on Computational Intelligence (SSCI), Xiamen, China, 2019.
- [81]. Hisao Ishibuchi, Masakazu Yamane and Yusuke Nojima, Difficulty in Evolutionary Multiobjective Optimization of Discrete Objective Functions with Different Granularities, lecture notes in Computer science 7811: Evolutionary multi-criterion optimization, Springer, pp. 230-245, Berlin, 2013.

[82]. F. Schmidt, M.C. de Almeida, "A theoretical framework for qualitative problems in power system state estimation", *Electric Power Systems Research*, Vol. 154, No. 1, pp. 528–537, 2018.

[83]. Ratmir Gelagaev, Pieter Vermeyen, Joos Vandewalle, and Johan Driesen, "Numerical Observability Analysis of Distribution Systems", *Proceedings of 14th International Conference on Harmonics and Quality of Power – ICHQP*, 2010.

[84]. Y. Nan, K. Shang, H. Ishibuchi and L. He, "Reverse Strategy for Non-Dominated Archiving," in *IEEE Access*, Vol. 8, No. 1, pp. 119458-119469, 2020.

[85]. Kapil Chauhan and Ranjana Sodhi, "Placement of Distribution-Level Phasor Measurements for Topological Observability and Monitoring of Active Distribution Networks", *IEEE Trans. Instrum. Meas.*, Vol. 69, No. 6, pp. 3451-3460, 2019.

[86]. Y Zhang and Y Li, "A many-objective Evolutionary Algorithm Based on Decomposition and Local Dominance", *arXiv preprint arXiv:1807.10275*, 2018.

[87]. I. Das and J. E. Dennis, "Normal-boundary intersection: A new method for generating Pareto optimal points in multicriteria optimization problems," *SIAM J. Optim.*, Vol. 8, No. 3, pp. 631–657, 1998.

[88]. S. Kayalvizhi and D. M. Vinod Kumar, "Dispatchable DG planning in distribution networks considering costs," in *Proc. IEEE Int. Conf. Recent Develop. Control, Autom. Power Eng.* 2016.

[89]. J Han, M He, and X Wang, "Improvement of Differential Evolution Multiobjective Optimization Algorithm Based on Decomposition", *Journal of Physics: Conference Series*, 2019.

[90]. Peter A. N. Bosman and Dirk Thierens, "The balance between proximity and diversity in multi-objective evolutionary algorithms", *IEEE Trans. Evol. Comput.*, Vol. 7, No. 2, pp. 174-188, 2003.

[91]. R. Singh, B. C. Pal, and R. A. Jabr, "Distribution system state estimation through Gaussian mixture model of the load as pseudo-measurement," *IET Gener. Transm. Distrib.*, Vol. 4, No. 1, pp. 50-59, 2010.

[92]. Saver J.S. and Das D., "Impact of network reconfiguration on loss allocation of radial distribution systems", *IEEE Trans. Power Deliv.*, Vol. 22, No. 4, pp. 2473–2480, 2007.

[93]. D. Das, D. P. Kothari, and A. Kalam, “Simple and efficient method for load flow solution of radial distribution networks,” *Int. J. Electr. Power Energy Syst.*, Vol. 17, No. 5, pp. 335–346, 1995.

[94]. Ye Tian, Ran Cheng, Xingyi Zhang, Fan Cheng, and Yaochu jin, “An indicator-based multi-objective evolutionary algorithm with reference point adaption for better versatility” , *IEEE Trans. E Comput.*, Vol. 22, No. 4, pp. 609-622, 2018.

[95]. R. Cheng, Y. Jin, M. Olhofer, and B. Sendhoff, “A reference vector guided evolutionary algorithm for many-objective optimization”, *IEEE Trans. E Comput.*, Vol. 20, No. 5, pp. 773–791, 2016.

[96]. X. Zhang, Y. Tian, R. Cheng, and Y. Jin, “An efficient approach to nondominated sorting for evolutionary multi-objective optimization” , *IEEE Trans. E Comput.*, Vol. 19, No. 2, pp. 201–213, 2015.

[97]. Y. Jin and B. Sendhoff, “Connectedness, regularity and the success of local search in evolutionary multi-objective optimization,” in *Proceedings of the IEEE Congress on Evolutionary Computation*, Vol. 3, No. 1, pp. 1910–1917, 2003.

[98]. Jianjun He, Hong Gu and Zhelong Wang, Multi-instance multi-label learning based on Gaussian with application to visual mobile robot navigation , *Journal of Information Sciences*, Vol. 190, No. 2, pp. 162–177, 2012.

[99]. X. Li and X. Yao, “Cooperatively coevolving particle swarms for large scale optimization,” *IEEE Transactions on Evolutionary Computation*, Vol. 16, No. 2, pp. 210–224, 2012.

[100]. Z. Yang, K. Tang, and X. Yao, “Large scale evolutionary optimization using cooperative coevolution,” *Information Sciences*, Vol. 178, No. 15, pp. 2985–2999, 2008.

[101]. C. Rasmussen and K. Williams, *Gaussian for Machine Learning*, MIT press, 2006.

[102]. P. Maragakis, F. Ritort, C. Bustamante, M. Karplus and G. Crooks, Bayesian estimates of free energies from nonequilibrium work data in the presence of instrument noise, *Journal of Chemical Physics*, pp. 129-137,2008.

[103]. Bogdan Pinte, Michael Quinlan, and Karl Reinhard, "Low Voltage Micro-Phasor Measurement Unit", *IEEE Power and Energy Conference at Illinois (PECI)*, Champaign, IL, USA, 2015.

[104]. Henar Herrero and Cristina Solares, "A Greedy Algorithm for Observability Analysis", *IEEE Transactions on Power Systems*, Vol. 35, no. 2, pp. 1638 - 1641, March

2020.

[105]. Ye Tian, Ran Cheng, Xingyi Zhang, Fan Cheng, and Yaochu Jin, "An Indicator-Based Multiobjective Evolutionary Algorithm With Reference Point Adaptation for Better Versatility", *IEEE Transactions on Evolutionary Computation*, Vol. 22, No. 4, pp. 609 - 622, 2018.

Appendix-A

PG&E 69-bus distribution system data

Number of buses: 69

Number of lines: 68

Bus voltage: 12.66kV

Total active power load: 3.80MW

Total reactive power load: 2.69 MW

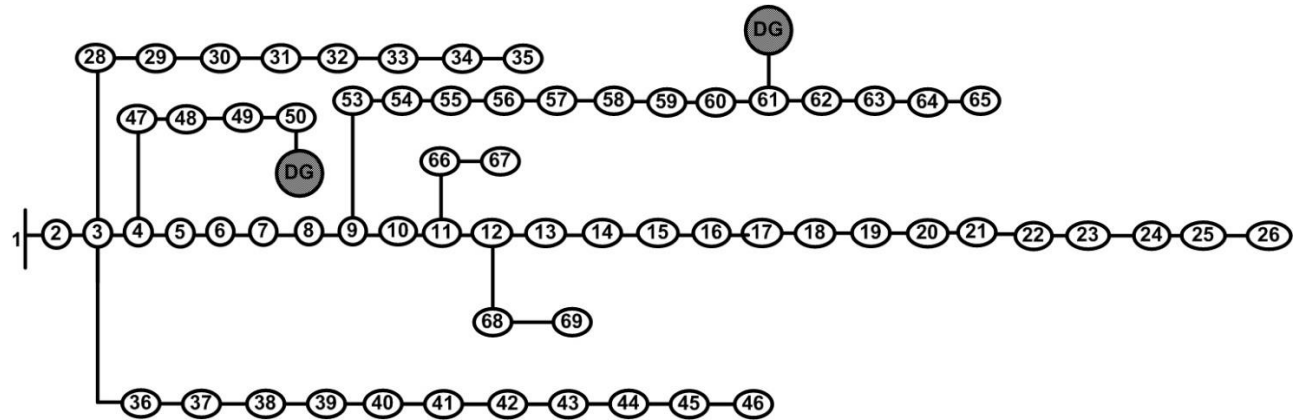


Fig. A.1: Single-line diagram of PG&E 69-bus system

Table A.1: Line data of PG&E 69-bus distribution system

Line No.	From	To	R (in pu)	X (in pu)
1	1	2	3.12E-06	7.49E-06
2	2	3	3.12E-06	7.49E-06
3	3	4	9.36E-06	2.25E-05
4	4	5	0.00016	0.00018
5	5	6	0.00228	0.00116
6	6	7	0.00238	0.00121
7	7	8	0.00058	0.00029
8	8	9	0.00031	0.00016
9	9	10	0.00511	0.00169
10	10	11	0.00117	0.00039
11	11	12	0.00444	0.00147
12	12	13	0.00643	0.00212
13	13	14	0.00651	0.00215
14	14	15	0.0066	0.00218
15	15	16	0.00123	0.00041
16	16	17	0.00234	0.00077

17	17	18	2.93E-05	9.98E-06
18	18	19	0.00204	0.00068
19	19	20	0.00131	0.00043
20	20	21	0.00213	0.0007
21	21	22	8.73E-05	2.87E-05
22	22	23	0.00099	0.00033
23	23	24	0.00216	0.00071
24	24	25	0.00467	0.00154
25	25	26	0.00193	0.00064
26	26	27	0.00108	0.00036
27	3	28	2.75E-05	6.74E-05
28	28	29	0.0004	0.00098
29	29	30	0.00248	0.00082
30	30	31	0.00044	0.00015
31	31	32	0.00219	0.00072
32	32	33	0.00524	0.00176
33	33	34	0.01066	0.00352
34	34	35	0.0092	0.00304
35	3	36	2.75E-05	6.74E-05
36	36	37	0.0004	0.00098
37	37	38	0.00066	0.00077
38	38	39	0.00019	0.00022
39	39	40	1.12E-05	1.31E-05
40	40	41	0.00454	0.00531
41	41	42	0.00193	0.00226
42	42	43	0.00026	0.0003
43	43	44	5.74E-05	7.24E-05
44	44	45	0.00068	0.00086
45	45	46	5.62E-06	7.49E-06
46	4	47	2.12E-05	5.24E-05
47	47	48	0.00053	0.0013
48	48	49	0.00181	0.00442
49	49	50	0.00051	0.00126
50	8	51	0.00058	0.0003
51	51	52	0.00207	0.0007
52	9	53	0.00109	0.00055
53	53	54	0.00127	0.00065
54	54	55	0.00177	0.0009
55	55	56	0.00176	0.00089
56	56	57	0.00992	0.00333
57	57	58	0.00489	0.00164
58	58	59	0.0019	0.00063
59	59	60	0.00241	0.00073

60	60	61	0.00317	0.00161
61	61	62	0.00061	0.00031
62	62	63	0.00091	0.00046
63	63	64	0.00443	0.00226
64	64	65	0.0065	0.00331
65	11	66	0.00126	0.00038
66	66	67	2.93E-05	8.73E-06
67	12	68	0.00461	0.00153
68	68	69	2.93E-05	9.98E-06

Table A.2: Load data of PG&E 69-bus distribution system

Bus No.	P (in pu)	Q (in pu)
1	0	0
2	0	0
3	0	0
4	0	0
5	0	0
6	0.0026	0.0022
7	0.0404	0.03
8	0.075	0.054
9	0.03	0.022
10	0.028	0.019
11	0.145	0.104
12	0.145	0.104
13	0.008	0.0055
14	0.008	0.0055
15	0	0
16	0.0455	0.03
17	0.06	0.035
18	0.06	0.035
19	0	0
20	0.001	0.0006
21	0.114	0.081
22	0.0053	0.0035
23	0	0
24	0.028	0.02
25	0	0
26	0.014	0.01
27	0.014	0.01
28	0.026	0.0186
29	0.026	0.0186

30	0	0
31	0	0
32	0	0
33	0.014	0.01
34	0.0195	0.014
35	0.006	0.004
36	0.026	0.0186
37	0.026	0.0186
38	0	0
39	0.024	0.017
40	0.024	0.017
41	0.0012	0.001
42	0	0
43	0.006	0.0043
44	0	0
45	0.0392	0.0263
46	0.0392	0.0263
47	0	0
48	0.079	0.0564
49	0.3847	0.2745
50	0.3847	0.2745
51	0.0405	0.0283
52	0.0036	0.0027
53	0.0043	0.0035
54	0.0264	0.019
55	0.024	0.0172
56	0	0
57	0	0
58	0	0
59	0.1	0.072
60	0	0
61	1.244	0.888
62	0.032	0.023
63	0	0
64	0.227	0.162
65	0.059	0.042
66	0.018	0.013
67	0.018	0.013
68	0.028	0.02
69	0.028	0.02

Appendix-B

Indian Practical 85-bus distribution system data

Number of buses: 85

Number of lines: 84

Bus voltage: 11kV

Total active power load: 2.5708MW

Total reactive power load: 2.6218 MW

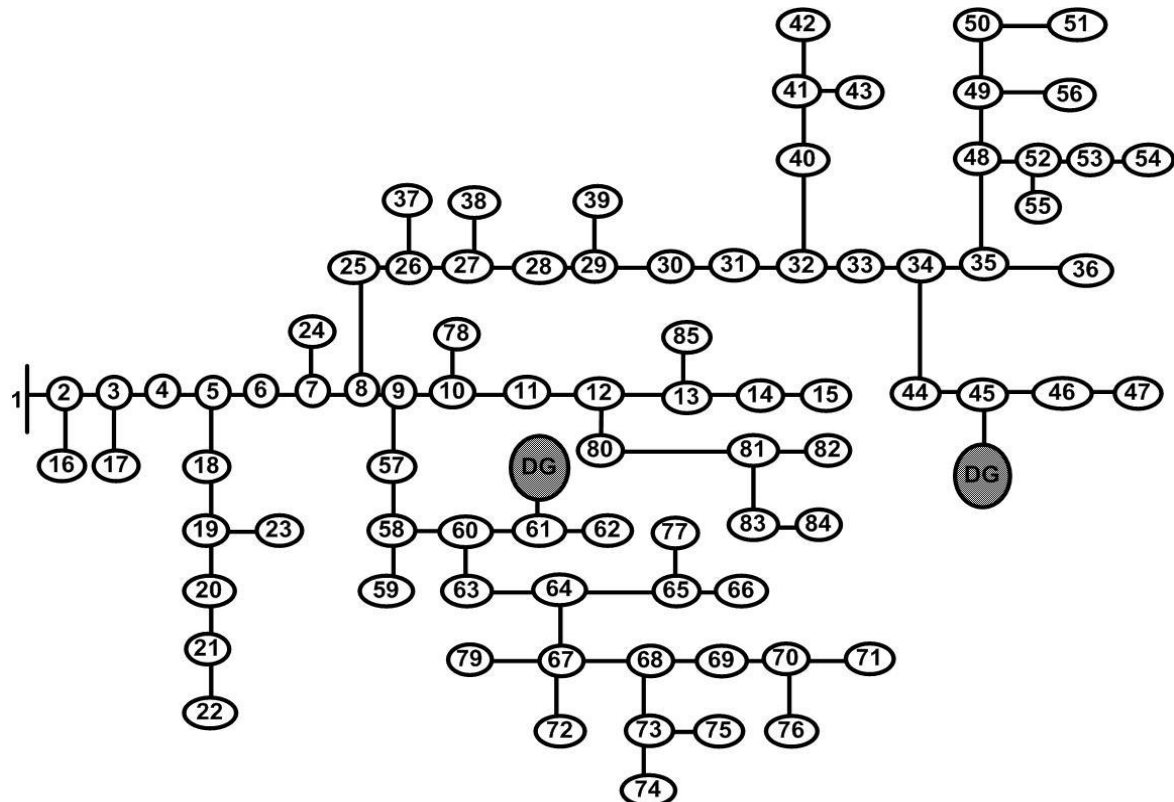


Fig. B.1: Single-line diagram of Indian Practical 85-bus distribution system

Table B.1: Line data of Indian Practical 85-bus distribution system

Line No.	From	To	R (in pu)	X (in pu)
1	1	2	0.0009	0.0006
2	2	3	0.0013	0.0009
3	3	4	0.0018	0.0012
4	4	5	0.0009	0.0006
5	5	6	0.0036	0.0025
6	6	7	0.0022	0.0015
7	7	8	0.0099	0.0068
8	8	9	0.0009	0.0006
9	9	10	0.0049	0.0034

10	10	11	0.0045	0.0031
11	11	12	0.0045	0.0031
12	12	13	0.0049	0.0034
13	13	14	0.0022	0.0015
14	14	15	0.0027	0.0018
15	2	16	0.006	0.0025
16	3	17	0.0038	0.0016
17	5	18	0.0068	0.0028
18	18	19	0.0053	0.0022
19	19	20	0.0038	0.0016
20	20	21	0.0068	0.0028
21	21	22	0.0128	0.0053
22	19	23	0.0015	0.0006
23	7	24	0.0075	0.0031
24	8	25	0.0038	0.0016
25	25	26	0.003	0.0012
26	26	27	0.0045	0.0019
27	27	28	0.0023	0.0009
28	28	29	0.0045	0.0019
29	29	30	0.0045	0.0019
30	30	31	0.0023	0.0009
31	31	32	0.0015	0.0006
32	32	33	0.0015	0.0006
33	33	34	0.0068	0.0028
34	34	35	0.0053	0.0022
35	35	36	0.0015	0.0006
36	26	37	0.003	0.0012
37	27	38	0.0083	0.0034
38	29	39	0.0045	0.0019
39	32	40	0.0038	0.0016
40	40	41	0.0083	0.0034
41	41	42	0.0023	0.0009
42	41	43	0.0038	0.0016
43	34	44	0.0083	0.0034
44	44	45	0.0075	0.0031
45	45	46	0.0075	0.0031
46	46	47	0.0045	0.0019
47	35	48	0.0053	0.0022
48	48	49	0.0015	0.0006
49	49	50	0.003	0.0012
50	50	51	0.0038	0.0016
51	48	52	0.0113	0.0047
52	52	53	0.0038	0.0016

53	53	54	0.0045	0.0019
54	52	55	0.0045	0.0019
55	49	56	0.0045	0.0019
56	9	57	0.0023	0.0009
57	57	58	0.0068	0.0028
58	58	59	0.0015	0.0006
59	58	60	0.0045	0.0019
60	60	61	0.006	0.0025
61	61	62	0.0083	0.0034
62	60	63	0.0015	0.0006
63	63	64	0.006	0.0025
64	64	65	0.0015	0.0006
65	65	66	0.0015	0.0006
66	64	67	0.0038	0.0016
67	67	68	0.0075	0.0031
68	68	69	0.009	0.0037
69	69	70	0.0038	0.0016
70	70	71	0.0045	0.0019
71	67	72	0.0015	0.0006
72	68	73	0.0098	0.0041
73	73	74	0.0023	0.0009
74	73	75	0.0083	0.0034
75	70	76	0.0045	0.0019
76	65	77	0.0008	0.0003
77	10	78	0.0053	0.0022
78	67	79	0.0045	0.0019
79	12	80	0.006	0.0025
80	80	81	0.003	0.0012
81	81	82	0.0008	0.0003
82	81	83	0.009	0.0037
83	83	84	0.0083	0.0034
84	13	85	0.0068	0.0028

Table B.2: Load data of Indian Practical 85-bus distribution system

Bus No.	P (in pu)	Q (in pu)
1	0	0
2	0	0
3	0	0
4	0.056	0.0571
5	0	0
6	0.0353	0.036
7	0	0
8	0.0353	0.036

9	0	0
10	0	0
11	0.056	0.0571
12	0	0
13	0	0
14	0.0353	0.036
15	0.0353	0.036
16	0.0353	0.036
17	0.112	0.1143
18	0.056	0.0571
19	0.056	0.0571
20	0.0353	0.036
21	0.0353	0.036
22	0.0353	0.036
23	0.056	0.0571
24	0.0353	0.036
25	0.0353	0.036
26	0.056	0.0571
27	0	0
28	0.056	0.0571
29	0	0
30	0.0353	0.036
31	0.0353	0.036
32	0	0
33	0.014	0.0143
34	0	0
35	0	0
36	0.0353	0.036
37	0.056	0.0571
38	0.056	0.0571
39	0.056	0.0571
40	0.0353	0.036
41	0	0
42	0.0353	0.036
43	0.0353	0.036
44	0.0353	0.036
45	0.0353	0.036
46	0.0353	0.036
47	0.014	0.0143
48	0	0
49	0	0
50	0.0363	0.037
51	0.056	0.0571

52	0	0
53	0.0353	0.036
54	0.056	0.0571
55	0.056	0.0571
56	0.014	0.0143
57	0.056	0.0571
58	0	0
59	0.056	0.0571
60	0	0
61	0.112	0.1143
62	0.056	0.0571
63	0.014	0.0143
64	0	0
65	0	0
66	0.056	0.0571
67	0	0
68	0	0
69	0.056	0.0571
70	0	0
71	0.0353	0.036
72	0.056	0.0571
73	0	0
74	0.056	0.0571
75	0.0353	0.036
76	0.056	0.0571
77	0.014	0.0143
78	0.056	0.0571
79	0.0353	0.036
80	0.056	0.0571
81	0	0
82	0.056	0.0571
83	0.0353	0.036
84	0.014	0.0143
85	0.0353	0.036

PUBLICATIONS

Journals Published:

1. **Bhanu Prasad Chintala**, D. M. Vinod Kumar, “Multi-Objective Hybrid Decomposition and Local Dominance based Meter Placement for Distribution System State Estimation” **IET Generation, Transmission and Distribution**, Vol. 14, No. 20, pp. 4416-4425, September 2020.
2. **Bhanu Prasad Chintala**, D. M. Vinod Kumar, “Meter placement in active distribution system state estimation using indicator based multi-objective evolutionary algorithm with adaptive reference point method”, accepted for publication in **Journal of Institution of Engineers (India): Series-B**, Springer Nature.
3. **Bhanu Prasad Chintala**, D. M. Vinod Kumar, “Multi-objective Meter placement in Active Distribution System State Estimation using Inverse Modelling based on Multi-label Gaussian Process Classification algorithm with Adaptive reference point method” **International Transactions on Electrical energy Systems**, Wiley, Vol. 31, No. 8, pp. 1-30, August 2021.

Journals Communicated:

1. **Bhanu Prasad Chintala**, D. M. Vinod Kumar, “Many Objective Evolutionary Optimization for Meter Placement in Active Distribution System based on Numerical Observability”, **Applied Soft Computing**, Elsevier. [*Under Review*].

Curriculum-Vitae

Name: Bhanu Prasad Chintala
Date of Birth: 03-August-1987
Gender: Male
Contact Number: +91-9908301796
Email Id: bhanuxlnt@gmail.com

Academic Qualifications:

Program	Institution	CGPA / Percentage	Year of completion
M. Tech (Power Systems Engineering)	NIT Warangal	8.1	2015
B.Tech. (Electrical and Electronics Engineering)	ATRI, JNTU Hyderabad	63%	2008